

**DISSERTATION**

submitted

to the

Combined Faculty for Mathematics and Computer Science

of the

**Ruperto Carola University of Heidelberg, Germany,**

for the degree of

Doctor of Natural Sciences

Put forward by

**Kevin Stein**

born in:

Schwetzingen, Germany

Oral Examination:



Experimental and Computational  
Stability Analysis:  
from Slackline Athletes to  
Persons with Schizophrenia

Advisors: Prof. Dr. Katja Mombaur  
Prof. Dr. Dr. Thomas Fuchs



---

## **Zusammenfassung:**

Menschen bewegen sich seit Jahrtausenden auf der Erde, jedoch haben wir immer noch nicht genau verstanden wie sie dabei Balance halten. Sie meistern Balanceaufgaben entweder indem sie Ausgleichsbewegungen durchführen oder erlernen eine spezifische, stabile Bewegung. In dieser Arbeit analysieren wir statische und dynamische Balance basierend auf Ganzkörperbewegungserfassung. Wir haben dazu einen Test für Statische Balance entwickelt und Balancieren auf der Slackline sowie den Seiltänzerang (Tandem Walk) als Balanceaufgabe verwendet. In zwei Studien haben wir Bewegungsdaten von über 60 Teilnehmern erfasst.

In der ersten Studie haben wir Balancieren auf der Slackline analysiert mit dem Ziel Balance Indikatoren und Messvariablen für Slackline Expertise zu entwickeln. Wir haben dazu Anfänger, die noch nie auf einer Slackline balanciert haben und professionelle Slackliner verglichen. Alle Teilnehmer haben ebenfalls den Statischen Balance Test absolviert. Hier zeigten Slackline Profis durchgehend sehr gute Balance, wohingegen die Anfängergruppe stark variierte. Dementsprechend wurde die Anfänger Gruppe in balanceerfahren und balanceunerfahren geteilt. Basierend auf über 300 Aufnahmen von 20 Teilnehmern haben wir 30 Balance Indikatoren definiert und ausgewertet. Wir konnten zeigen, dass man normalisierter Drehimpuls und Schwerpunktbeschleunigung verwenden kann um Stabilität und die schwere von Ausgleichsbewegungen zu quantifizieren. Des weiteren fanden wir eindeutige Unterschiede in der Körperhaltung und Bewegungsstrategie. Diese ermöglichen trainierten Slacklinern eine aufrechten Körperposition zu halten. Sie zeigten bessere Bewegungskoordination, geringere Beschleunigung am Standfuß durch die Slackline und angepasste Nachgiebigkeit im Standbein.

In der Balancestudie des "Schizophrenia and the Moving Body" Projekts von Lily Martin haben wir die Balancefähigkeiten einer Experimentalgruppe, bestehend aus Menschen mit Schizophrenie und einer gesunden Kontrollgruppe verglichen. Alle Teilnehmer haben den Statischen Balance Test und zweimal den Seiltänzerang, einmal mit offenen und einmal mit geschlossenen Augen, durchgeführt. Anwendung der Balance Indikatoren hat gezeigt, dass die Experimentalgruppe Defizite in statischer und dynamischer Balance hat. Während dem Seiltänzerang zeigten sie signifikant höhere Werte für normalisierten Drehimpuls und Schwerpunktsbeschleunigung und benötigten mehr Ausfallschritte um Balance zu halten. Ein Vergleich der Balancestrategien beider Gruppen zeigt, dass ein Teil der Kontrollgruppe die Balanceaufgabe durch Armbewegung erfolgreich meistert, wohingegen Teilnehmer aus der Experimentalgruppe ausschließlich Ausgleichsschritte nutzen und kaum Armeinsatz zeigen.

In einer Zusammenfassung der beiden Studien haben wir Bewegungsdaten aller Teilnehmer verglichen. Dabei zeigte sich, dass wir seitliche Center of Pressure Schwingungsdistanz und vor-zurück Schwingungsgeschwindigkeit als geeignete Parameter zur Quantifizierung von statischen Balancefähigkeiten verwenden können. Anschließend haben wir den Seiltänzerang zum Laufen auf der Slackline mithilfe der Balanceindikatoren verglichen. Erfahrene Slackliner sind in der Lage viele Indikatoren auf Werte, wie wir sie beim einfacheren Seiltänzerang finden, zu reduzieren. Lediglich normalisierter Drehimpuls in der Frontalebene und seitliche Schwerpunktbeschleunigung sind erhöht. Die Slackline spezifische Bewegungsstrategie findet sich bei keinem der anderen Teilnehmer.

Im letzten Teil dieser Arbeit haben wir einen Kontaktsensor für die Slackline entwickelt mit dem man zuverlässig die Interaktion zwischen dem Probanden und der Slackline messen kann. Auf diesen Daten basierend haben wir ein Kontaktmodell entworfen und damit innerhalb eines Optimalsteuerungsproblems einen Sprung auf der Slackline rekonstruiert.



---

**Abstract:**

Humans have walked the earth for more than 200,000 years, yet it is not fully understood how this is achieved in stable and robust manner. In this work we analyzed human balancing during static and dynamic balance tasks based on motion capture data. A balancing task requires the subject to either constantly perform recovery movements or to learn an inherently stable and robust motion specific to the task. We designed a static balance test and analyzed dynamic balance during slackline balancing and the tandem walk test. We gathered data from over 60 participants in two studies.

In the first study, we analyzed slackline balancing with the goal to define balance performance indicators and measures for slackline expertise. We compared beginners that had never balanced on a slackline before to professional slackline athletes. All participants also performed the static balance test. We found that trained slackliners balance very well in the static balance test, whereas the beginner group showed a larger variance in the time they managed to balance. Therefore, we divided the beginner group into balance-experienced and balance-inexperienced according to this test. Based on over 300 balancing trials on the slackline of 20 participants we defined and evaluated over 30 balance metrics. Normalized angular momentum and Center of Mass acceleration allow us to quantify stability and amount of recovery movements. Posture and movement was similar for the beginner groups, whereas professional slackliners have adapted a different pose and strategy that allows them to consistently maintain a horizontal head orientation and upright posture. We found that their hand movement is more coordinated, their stance foot less accelerated by the slackline and their stance leg more compliant.

In the balance study of the "Schizophrenia and the Moving Body" project by Lily Martin, we compared the balance capabilities of an experimental group consisting of persons with schizophrenia to a healthy control group. Participants performed the static balance test and twice the tandem walk, once with eyes open and once with eyes closed. Applying the balance indicators showed deficits in static and dynamic balance of the experimental group when compared to the control group. They had significantly larger values for normalized angular momentum and Center of Mass acceleration and took significantly more recovery steps to maintain balance. When analyzing the strategy employed by the two groups, we found that the control group successfully used their arms to balance and place correct steps, whereas the experimental group mainly relied on recovery steps and did not involve the arms.

We combined and analyzed data from all participants of both studies. For static balance we found that sideways Center of Pressure sway distance and front-back sway velocity are the most suitable parameters to quantify balance capabilities. We then compared flat ground tandem walking to slackline walking based on the balance performance indicators. Professional slackline athletes are able to reduce many performance indicators to the values regular tandem walking. The only show larger normalized angular momentum in the frontal plane and increased sideways Center of Mass acceleration, which are both a direct consequence of the instability introduced by the slackline. Further, we found that their pose and movement strategy is specific to slackline balancing and not used by other participants neither in tandem walking nor slackline walking of beginners.

In the last part of this thesis we prototyped a pressure sensor for the slackline and showed that we can reliably measure Center of Pressure data during slackline balancing. Based on the findings we developed a specific contact interaction model. We used this contact model inside an optimal control problem formulation to perform a fully dynamic reconstruction of slackline jumping.



---

## **Acknowledgments:**

The research of this thesis was conducted at the research group Optimization, Robotics and Biomechanics (ORB) at the Interdisciplinary Center for Scientific Computing (IWR) and the Faculty of Mathematics and Computer Science at Heidelberg University. Funding by the Carl Zeiss Foundation within the "Heidelberg Center for Motion Research" is gratefully acknowledged. I want to thank the Heidelberg Graduate School Mathematical and Computational Methods for the Sciences (HGS MathComp) for financially supporting my conference publications and attendance. Further I want to thank the Baden-Württemberg Ministry of Science, Research and the Arts and Ruprecht-Karls-Universität Heidelberg for additional funding for open access publications. I also want to thank the Simulation and Optimization research group of the IWR at Heidelberg University for giving me the possibility to work with MUSCOD-II.

First of all, I want to thank Prof. Dr. Katja Mombaur for having me join her group 'Optimization, Robotics and Biomechanics', five years ago. I enjoyed carrying out my Master's and PhD thesis under her supervision. It has been an adventurous journey full of productive research, great discussions and fun experiments. I want to thank her for all the support, the flexibility, all the feedback on my publications and this thesis and the financial support for conference trips. I felt always welcome and appreciated, even during the snowboard balance experiment.

I want to thank my co-supervisor Prof. Dr. Dr. Thomas Fuchs for his interdisciplinary input to my work and for taking on the challenge to combine slackline balancing and research on schizophrenia.

Finally, I want to thank all the anonymous participants in the research studies and everyone who made this work possible.

I want to thank all my colleagues and friends who helped me throughout this project. Lily for the great collaboration and having me join her research project. Alex for always having an open ear and being available when help was needed. Matt for his scientific input and great ping pong training. Liz for the company during my runs and the fun game nights. My office mates Anna Lena for sharing her MUSCOD expertise and Jonas for his coding skills. Yue for inviting me on the interesting trip to India and her great support when I first joined ORB. Amartya for all the great ping pong sessions. Basti for being patient zero in my experiments. Giorgos and Peter for all the coffee. Felix and Moni for the great company on our Toronto trip. All the Hiwi's that helped with the experiments and data labeling. Thanks to Gabriel, Elif, Eric, Stephan, Klaus, Tobias and especially to Qiao, Rasmus, Lukas and Felix, who turned out to be great climbing buddies.

Many thanks to Den for proofreading and correcting my English and for being there throughout the last four years.

Also, thanks Mum, thanks Dad and thanks to my brother!



# Contents

	<b>Page</b>
<b>I Introduction and Motivation</b>	<b>5</b>
<b>1 Balance and Stability in Human Movement</b>	<b>7</b>
1.1 Sensing of Movement in Humans . . . . .	7
1.2 Mechanical Stability Criteria . . . . .	8
1.3 Assessment of Balance . . . . .	11
1.3.1 Clinical Balance Assessment . . . . .	11
1.3.2 Balance Tasks in this Work . . . . .	15
1.4 Research Questions . . . . .	16
<b>2 Schizophrenia</b>	<b>19</b>
2.1 Symptoms and Assessment . . . . .	19
2.1.1 Positive and Negative Syndrome Scale . . . . .	19
2.1.2 Motor Control - Neurological Soft Signs . . . . .	20
2.2 Research on Causes and Treatments . . . . .	20
2.2.1 The Embodiment Approach: Schizophrenia as Disembodiment . . . . .	21
2.2.2 The research project "Schizophrenia and the Moving Body" . . . . .	21
2.3 Research Questions . . . . .	23
<b>II Human Movement Analysis</b>	<b>25</b>
<b>3 Measuring Human Motion</b>	<b>27</b>
3.1 Marker-based Motion Capture - Qualisys . . . . .	27
3.1.1 Marker Set . . . . .	29
3.2 IMU-based Motion Capture - Xsens . . . . .	32
3.3 Pre-Study System Comparison . . . . .	35
3.4 Force and Pressure Measurements . . . . .	41
3.4.1 Force Plates . . . . .	41
3.4.2 Pressure-Sensitive Insoles . . . . .	42
<b>4 Modeling of Human Movement</b>	<b>43</b>
4.1 Subject Specific Modeling . . . . .	44
4.2 Kinematics and Dynamics . . . . .	47
<b>5 Reconstruction of Motion</b>	<b>51</b>
5.1 Inverse Kinematic Reconstruction . . . . .	51

5.2	Optimal Control Based Motion Analysis . . . . .	54
5.3	Comparison of the two Methods . . . . .	58
<b>III</b>	<b>Analysis of Static and Dynamic Balance</b>	<b>59</b>
<b>6</b>	<b>Static Balance Test</b>	<b>61</b>
6.1	Balance Test Protocol . . . . .	62
6.2	Visual Evaluation . . . . .	63
6.3	Center of Pressure Sway Analysis . . . . .	64
6.4	Choice of Parameters for Center of Pressure (CoP) sway analysis . . . . .	67
<b>7</b>	<b>The Slackline Study</b>	<b>71</b>
7.1	Protocol . . . . .	72
7.2	Static Balance Test, Subject Grouping and Overview . . . . .	74
7.3	Evaluation and Performance Indicators . . . . .	77
7.4	Single Leg Balancing . . . . .	84
7.4.1	Time and Overview . . . . .	84
7.4.2	Movement and Strategy . . . . .	85
7.4.3	Slackline Interaction . . . . .	91
7.4.4	Summary . . . . .	95
7.5	Slackline Walking . . . . .	97
7.5.1	Time and Overview . . . . .	97
7.5.2	Movement and Strategy . . . . .	98
7.5.3	Summary . . . . .	102
7.6	Comparison Between Stable and Unstable Balancing . . . . .	106
7.7	Discussion . . . . .	109
<b>8</b>	<b>Static and Dynamic Balance in Schizophrenia Patients</b>	<b>111</b>
8.1	Motion Capture Protocol . . . . .	112
8.2	Static Stability Evaluation . . . . .	113
8.2.1	Success Rate and Time in Balance . . . . .	113
8.2.2	Center of Pressure Sway Analysis . . . . .	117
8.2.3	Difference Between Eyes Open and Eyes Closed Condition . . . . .	122
8.2.4	Summary of Static Balance Analysis . . . . .	123
8.3	Performance Indicators for Tandem Walking . . . . .	124
8.4	Dynamic Stability Analysis . . . . .	128
8.4.1	Quality of Task Execution . . . . .	128
8.4.2	Dynamic Balance Capabilities . . . . .	131
8.4.3	Balance Strategy . . . . .	135
8.4.4	Summary and Discussion of Dynamic Balance . . . . .	140
8.5	Correlation with Medication and Positive and Negative Syndrome Scale (PANSS)	143
8.6	Discussion . . . . .	145

<b>9</b>	<b>Interstudy comparison of Balance Metrics</b>	<b>147</b>
9.1	Balance Performance in the Balance Test . . . . .	148
9.2	Comparison of Tandem and Slackline Walking . . . . .	151
9.3	Summary and Discussion . . . . .	158
<b>IV</b>	<b>Technical and Computational Studies of Slackline Motions</b>	<b>159</b>
<b>10</b>	<b>Towards a first contact interaction measurement on the slackline</b>	<b>161</b>
10.1	Validation of the Sensor Matrix . . . . .	163
10.1.1	Validation with Force Plates . . . . .	163
10.1.2	Measurements on the Slackline . . . . .	165
10.2	Foot Contact Analysis and Modeling . . . . .	167
10.2.1	Slackline Contact Modeling . . . . .	168
<b>11</b>	<b>Whole Body Dynamic Analysis of Challenging Slackline Jumping</b>	<b>169</b>
11.1	Optimal Control Problem Formulation . . . . .	171
11.2	Method Comparison . . . . .	173
11.2.1	Fitting Error . . . . .	173
11.2.2	Dynamics Analysis . . . . .	175
11.3	Slackline Spring Model . . . . .	182
11.3.1	Stiffness Estimation . . . . .	182
11.3.2	Interaction Analysis . . . . .	184
11.4	Discussion . . . . .	186
<b>12</b>	<b>Summary and Outlook</b>	<b>187</b>
<b>A</b>	<b>Appendix</b>	<b>191</b>
A.1	List of Figures . . . . .	191
A.2	List of Tables . . . . .	193
A.3	List of Acronyms . . . . .	194
A.4	Code . . . . .	195
<b>B</b>	<b>Bibliography</b>	<b>201</b>



## Overview and Organization

**Balance** describes the general ability to control posture independently of constraints imposed by the environment or the type of movement. While the term balance is often used in the context of difficult situations, such as tightrope walking or riding a unicycle, balance is inherent to any kind of locomotion and summarizes stability, robustness against perturbations and the ability to perform task specific recovery motions. Humans are able to learn nearly impossible balance tasks efficiently and with few mistakes. It is yet to be fully understood how humans maintain balance.

**Schizophrenia** is a serious psychiatric disorder with an estimated 20 million cases globally [1]. It affects a persons thoughts, feelings and behaviors. Positive symptoms include hallucinations, delusion and hostility [2]. Even though effective treatment exists for positive symptoms, there is still no treatment for negative symptoms, which make up a lot of the burden of the people. Negative symptoms of schizophrenia are, for example, social withdrawal, decreased emotional expression and lack of spontaneity [3]. They also seem to be connected to movement and it has been shown that movement therapy is able to reduce negative symptoms significantly [4]. The connection between schizophrenia, movement and balance in particular, is subject of current research and this thesis.

## Objectives

The thesis was carried out at the Heidelberg Center for Motion Research (HCMR) [5] with funding by the Carl Zeiss Foundation under supervision of Prof. Katja Mombaur and Prof. Thomas Fuchs. The overall objective was to investigate balance in different subject groups during standing, tandem walking and slackline balancing. We based this work on state-of-the-art motion capture equipment including marker and IMU-based motion capture, force plate measurements and pressure-sensitive insoles. The data was evaluated using subject specific rigid multi-body modeling, inverse kinematic fitting and optimal control.

Slackline balancing was investigated using different methodologies: first, we proposed and evaluated stability metrics and parameters to define slackline expertise based on a motion capture study including balance experienced slackline athletes and balance inexperienced beginners. Second, we prototyped a pressure and force sensor in collaboration with the Heidelberg Innovation Lab [6] and measured the contact interaction between the athlete and the slackline. Third, we developed a contact model based on the sensor measurement and employed it inside an optimal control framework to perform a dynamic reconstruction of slackline balancing and jumping.

Motion capture assessment of persons with schizophrenia was done in collaboration with Lily Martin within the research project "Schizophrenia and the Moving Body" [7]. This further included the Center for Psychosocial Medicine and was supervised by Prof. Thomas Fuchs. The objective was to assist data recording, to revise the lab protocol and to define suitable balance tasks. We analyzed the balance data using the stability metrics developed for slackline balancing and defined more task specific parameters.

## **Contributions**

Contributions presented in this PhD thesis can be grouped into theoretical study design for balance assessment, implementation and automation of the respective evaluation pipelines and more in-depth analysis of slackline balancing.

### **Study design and data collection**

The work of this thesis included planning and realization of two motion capture studies and data collection of more than 70 participants in total. The first study aims to evaluate human balancing on the slackline by comparing balance-inexperienced beginners, sportive balance-experienced beginners and professional slackline athletes. This included evaluation of the available measurement equipment in a pre-study, and recruitment and assessment of 20 subjects from the Heidelberg region. The motion capture study of the "Schizophrenia and the Moving Body" project was designed and planned by Lily Martin and revised in collaboration [7]. It included the assessment of than 50 participants recruited by Lily Martin. We collected movement data of persons with schizophrenia and a control group. Among other tasks, we recorded static balancing and the tandem walk balance test to obtain a comprehensive picture that can also be related to the slackline study.

### **Implementation of a motion analysis pipeline for balance tasks**

We implemented and automated an analysis pipeline for static balancing on force plates and dynamic balance during tandem walking and slackline balancing. Force plate data was evaluated using more than 20 balance metrics following the state of the literature. Motion capture data was evaluated based on a subject-specific rigid body model and inverse kinematics fitting. We defined and computed more than 30 performance indicators for dynamic balance capabilities and compared groups statistically. We further formulated hypotheses related to schizophrenia and investigated the data accordingly.

### **Slackline Contact Measurements and Modeling**

We measured the interaction between the subject and the slackline using sensor insoles and a pressure sensor that was mounted on the slackline. We evaluated the agreement of the two methods and compared both devices against state-of-the-art force plates on level ground. Based on the measurements, we developed a slackline specific contact model that describes the interaction between the contact foot and the slackline.

## **Optimization-based Whole-body Dynamic Analysis of Slackline Jumping**

We collected motion capture data of challenging slackline jumping with rotations around the vertical axis. Based on the contact model derived from the sensor measurement we formulated an optimal control problem that allows us to compute a dynamic reconstruction of the jumping motion.

## **Outline and Organization of the Thesis**

The thesis is divided into four parts: introduction and motivation, methodology of human movement analysis, balance analysis studies and more detailed technical and computational analysis of slackline motions.

### **Introduction**

We explain balance and stability in human movement in Chapter 1 and schizophrenia and how it affects human movement in Chapter 2. In Chapter 3 we introduce the motion capture equipment available. In a pre-study we compared a marker based system to an IMU-based system for the two walking tasks we aim to analyze.

### **Methodology, Modeling and Evaluation**

The evaluation pipeline for the motion capture data is explained in Chapter 4 and 5. We present general and subject specific rigid body modeling as well as kinematics and dynamics computations and how movement can be reconstructed employing the rigid body models and motion capture data. Two reconstruction algorithms are presented and the specific advantages and disadvantages elaborated.

### **Motion Capture Studies**

In Chapter 6 we introduce several balance performance indicators for static balance and discuss how we can use them to evaluate stability in static balance. The Slackline study with the study protocol, evaluation and all results is presented in Chapter 7. We evaluate single leg balancing and walking separately. In Chapter 8 we present the evaluation of the balance tasks of the study "Schizophrenia and the Moving Body". An overview and comparison of both studies is done Chapter 9.

### **Slackline Contact Model and Optimization Based Analysis**

The interaction between the subject and the slackline is measured in Chapter 10 and a slackline specific contact model is designed. A dynamic analysis of challenging slackline jumping, using said contact model is performed in Chapter 11.



## **Part I**

### **Introduction and Motivation**



# 1 Balance and Stability in Human Movement

Humans have walked the earth for more than 200,000 years, yet it is not fully understood how this is achieved [8]. Stability, robustness and perturbation recovery play an important role in several research fields. Engineers build walking robots [9–11], biologists investigate the interaction between senses related to balance [12], doctors and psychologists research the impact of different diseases and aging on balance capabilities [13, 14] and biomechanists constantly analyze new motions and wonder why humans do not fall [15, 16].

In this work, we follow the terminology of Mombaur and Vallery [17] and define stability as the inherent property of a motion to persist under small perturbations. We consider a movement as stable and a subject as stable and in balance if the motion is performed as intended and there are no visible interruptions needed to regain posture. The robustness of a movement quantifies how large the perturbations can become before a recovery movement is required. A balancing task requires the subject to either constantly perform recovery movements or to learn an inherently stable and robust motion specific to the task.

## 1.1 Sensing of Movement in Humans

The perception of balance, movement and spatial orientation is mainly based on three sensory systems: the vestibular system, the visual system and proprioception [18, 19]. Information from at least two of the systems is required to maintain stability. Humans are still able to stand upright with eyes closed or to walk on stilts where proprioception is limited. In the Romberg Test [20] participants are required to maintain balance with eyes closed. If they show large postural sway or fall, it is concluded, that their proprioception or vestibular system is impaired. Alcohol or substance abuse leads to fall due to incorrect visual information and disturbed vestibular sensing [21].

### Vestibular System

The vestibular system is located in the inner ear and consists of 5 organs [22]. The three semicircular canals, which detect rotational movement in three directions and the utricle and saccule which detect linear movement in vertical and horizontal direction. Inertia effects when moving the head cause fluid movement in the semicircular canals. The inner walls of the vestibular organs are populated by sensory hair cells that are able to sense the direction of this fluid flow inside the canals. Bending of the hair leads to opening or closing of transduction channels for potassium causing the connected synapse to fire. The vestibular system is closely linked to the visual system by the Vestibulo-Ocular Reflex (VOR) that coordinates eye movement. The synaptic signals from the hair cells in the semicircular canals are directly exciting the eye muscles in order to stabilize retinal images during head rotation. Other reflexes let us maintain a horizontal head position or even activate leg and trunk muscles to maintain an upright posture and balance. Their pathways, and in what way the vestibular system is involved, are far from understood.

### **Visual**

Visual perception can be divided into focal and ambient vision [23]. Focal vision involving the central part of the retina allows for motion perception and object recognition. Ambient or peripheral vision recognizes general movement in the scene and is dominant in perception of self-motion and postural control [24]. In case of redundant or contradictory information, the visual input is considered more important than the information from proprioception and the vestibular system [25].

### **Proprioception**

Proprioception describes the sensation of body position and movement [26]. Although visual observation and tactile sensing can give a sense of the current body posture, proprioception is mainly based on mechanosensory neurons located within muscles, tendons and joints. Neurons on the muscle spindle fire when the muscle changes in length. The golgi tendon organs recognize the tendon load and encode the muscle force. Joint receptors realize when joints reach a certain threshold, often functioning as limit detectors. The most important function of proprioception is to stabilize human posture and protect the body from joint overloading or unhealthy configurations. One example is reflex-based control of agonist and antagonist muscles to protect the muscle from excessive force or from moving the joint beyond the limit. In locomotion proprioception, feedback allows for adjustment of timing and amplitude of muscle activity and robustness of the motor output.

## **1.2 Mechanical Stability Criteria**

In classical mechanics one can formulate various criteria to stabilize a mechanical system against gravitational pull. In the following section we present balance criteria found in the literature for stability in locomotion.

### **Support Polygon**

Many criteria are developed around the concept of the support polygon. It describes the smallest convex area on the ground that includes all contact points between the subject and the floor. When standing on one foot, it is exactly the foot area, when standing on both feet it includes the area of both feet and the area between them.

### **Static Stability**

Static stability is given when the ground projection of the Center of Mass (CoM) is located inside the support polygon and has relatively small velocity or zero velocity [27]. It is the reason why static objects, like tables, do not tilt. Humans are able to stand in statically stable state. We are also able to explain stability in certain animal and robotic locomotion. A 6-legged robot, for example can always maintain three legs on the ground in alternating mode, the so-called tripod gait. With this gait, the CoM ground projection is always inside the support polygon. The distance between the CoM ground projection to the edge of the support polygon is used as a measure of how stable a subject is during tasks [28]. Advanced locomotion is usually not statically stable. Humans shift their CoM way beyond their feet area and support area during regular walking. The concept of the support polygon becomes invalid for running as there are phases without ground contact.

### Center of Pressure and Zero Moment Point

The pressure distribution along the sole of the foot can be summarized in one vector by integrating over the area, the Ground Reaction Forces (GRF). The position of the GRF is the CoP and the length represents the total force. During walking, the CoP moves from the heel to the front of the foot and then again to the heel of the other foot when taking a step. It is always inside the support polygon. In humanoid robotics Vukobratovic introduced the Zero Moment Point (ZMP) [29]. The ZMP is the point on the floor in which the sum of the torques produced by gravity and inertial forces about the horizontal axis is zero. This point coincides with the CoP for non sliding contacts and when it is located inside the support polygon. It enabled quasi dynamic gait for humanoid robots [30]. The resulting gait, however, does not appear very human-like and robots tend to walk with very bent knees, almost in a half squatting position. The limitations of this stability concept are reached when the ZMP is located outside the support polygon. The CoP remains at the edge and the subject inevitably starts to rotate about that point. ZMP based robot control therefore aims to maintain the ZMP well inside the support polygon. For situations where the ZMP is close to the edge, one can not predict if a subject is still stable [31]. It is a momentary analysis and not able to tell whether there will be a fall or a stabilization. Situations with a slipping or moving contact, such as skiing or skate boarding are also beyond the model assumptions.

### Capture Point

The Capture Point (CP) [32] or Extrapolated Center of Mass (xCoM) [33] is the point where a simple bipedal model could step to come to a full stop. It provides possible foot placement during recovery movements in unbalanced situations. For higher velocities a larger number of steps can be required. Engelsberger et al. [34] showed that it is possible to generate locomotion by always stepping slightly short of the CP. Experimental evidence for this was found for example by McAndrew-Young et al. [35]. Lugade et al. [36] found that elderly participants step closer to the CP, suggesting different stability margins during gait. For more complex multi body systems the CP can be extended to a larger capture region when taking the angular momentum and inertia into account and when allowing for all possible motions of the system.

### Virtual Pivot Point

The Virtual Pivot Point (VPP) was defined by Maus et al. [37] and can be found in bipedal walking of humans and chickens. When tracing the direction of the GRF over the gait cycle they found, that the force vectors coincide in one point above the CoM. This results in a self-stabilizing effect on the mechanical system, given that a hanging pendulum is inherently stable. It is suggested that the VPP can be used to make predictions on human balance [38].

### Angular Momentum

The angular momentum about the CoM, often referred to as centroidal momentum, is considered an important quantity of stability. Despite the constant cyclic movement of the feet in the sagittal plane during walking or running, there should not be any other sources of angular momentum during locomotion, as the goal is to maintain an upright posture. Arms and legs move with a phase shift of  $180^\circ$  and cancel out the resulting overall angular momentum around the vertical axis.

There is no intrinsic way to counteract rotations of the upper body in the frontal plane during gait. Any large value of angular momentum in this plane clearly indicates recovery movements and instability. Therefore minimization of angular momentum is often used as objective function to generate stable locomotion [39].

### **Zero Rate of Change of Angular Momentum**

The point of Zero Rate of Change of Angular Momentum (ZRAM) was introduced by Goswami et al. [40]. It is the point where the GRF would need to act to achieve a zero change in angular momentum. It can be computed by following the direction of the GRF vector from the CoM position until it intersects with the contact plane. Always stepping on this point would result in a constant angular momentum. In context of minimization of the angular momentum around the CoM during locomotion it is often considered as a stability criterion.

### **Definition of Stability and Orbital Stability in the Sense of Lyapunov**

The stability criteria presented so far are limited by the assumption that the contact with the environment is fixed and that the criteria has to be fulfilled at every instance of the movement. Stability in the sense of Lyapunov is a more general approach that considers the movement trajectory or movement cycle, in case of a repeating motion. It analyzes the effect of a perturbation on the continuation of the movement. A solution of a non-autonomous, explicitly time-dependent system  $x(t)$  is stable if small perturbations of the trajectory result in perturbed trajectories that always stay in a finite neighborhood of the original trajectory [41, 42]. A solution is called asymptotically stable if the perturbed trajectory converges back towards the unperturbed solution for  $t \rightarrow \infty$ .

For a non time-dependent system, e.g. a cyclic motion, orbital stability and orbital asymptotic stability can be defined. They follow the same definition, except that time and phase shifts (orbital shifts) of the motion may occur. The system is still considered stable. In the case of walking, for example, a perturbation may lead to an early or delayed step and the subsequent movement cycle continues as originally intended. This definition of stability has successfully been applied to create passive-dynamic robots without sensors or motors that can walk down slopes, or more dynamic robots with few motors and sensors that provide feedback [43].

In any case a, very accurate model that includes all feedback and control loops as well as environment interaction is required to compute the system's reaction to a perturbation. While this is possible for smaller mechanical systems, computational effort becomes too high for systems with many Degrees of Freedom (DoF) [44, 45].

## 1.3 Assessment of Balance

### 1.3.1 Clinical Balance Assessment

Humans apply different strategies to maintain balance depending on the amount of perturbation [46, 47]. For static stance, small perturbations are stabilized employing the so-called ankle strategy using the ankle joints. With larger perturbations the knee (knee-strategy) and hip (hip-strategy) joints become involved. The role of the arms is often neglected for static stance [48]. If the perturbation is significantly larger, a recovery step is taken and specific arm movement becomes important [49].

Clinical assessment and training of balance is manifold. Many tests try to evaluate if the subject is stable during a movement and what balance strategies are applied. Balance performance is an important measure of locomotion training in rehabilitation, for example, after stroke or sports injury [50, 51]. In aging studies balance performance is discussed as an indicator for risk of falling. The level of frailty and required assistance is often defined using standardized clinical balance assessment [52, 53]. The effect of a certain condition on human balance is part of ongoing research. Results of these balance tests have been related to stroke [50, 51], to aging [54], to sports [55] and to schizophrenia [56, 57]. In their review, Ruhe et al. [58] compared over 100 studies, that connected lower back pain and CoP sway. Qiu et al. tried to distinguish between age, fear of falling and fall history based on CoP measurements [59].

The evaluation of balance tasks can be divided into instrumented and non-instrumented (visual) analysis. Instrumented tests can be based on CoP measurements or sensors attached to a balance platform. Visual analysis can be a subjective impression or a point rating scale. Sometimes simply the time a person was able to maintain balance or whether the task was performed successfully is used as a measure for balance performance. The following tasks are established in the literature to assess balance in different situations.

#### **Balance Error Scoring System**

This test was developed by the sports medicine research laboratory at the University of North Carolina [60]. It consists of three standing tasks that are performed with eyes closed for 20 s, once on regular surface and on a deformable foam block. The subject stands with in parallel stance, single leg stance on the non dominant leg and tandem stance with the feet in line and the dominant leg in front. For all tasks, the participant is asked to maintain the hands at the hips. The tasks are evaluated based on the amount of occurring recovery movements. Each of the following movements is counted as one error point: removing the hands from the pelvis, opening the eyes, taking a step, large hip tilt (abduction), lifting of a foot and leaving the balance position for longer than 20 s. The score per task is limited to 10 points. Norm data of different age groups is available in the literature [61]. A significant drop in balance performance is found for elderly older than 50 years and in athletes after concussion.

### **Functional Reach Test**

In the functional reach test, the participant is asked to stand upright and reach out in front as far as possible without losing balance or rotating the upper body around the vertical axis. A modified version of this test can also be performed whilst sitting. The test aims to define stability limits in elderly and Parkinson patients. Duncan et al. [62] found prediction validity for falling in male participants above the age of 70. Norm values exist for Parkinson patients in the early stages [63].

### **Star Excursion Balance Test**

Similar to the functional reach test, the Star Excursion Balance test relies on reaching movements, in this case, with the foot. The participant stands on one foot with hands at the pelvis. Around the stance foot, there are eight positions/directions marked on a circle in 45° steps. The subject has to reach with the free leg as far as possible in each of the directions without touching the floor or taking the hands off the pelvis. The test is mainly used with younger participants after injury of the knee or lower extremities to evaluate the recovery process.

### **Berg Scale**

The Berg Scale was one of the first standardized test to assess balance capabilities in elderly during static positions and sit-to-stand and stand-to-sit movements [54]. It consists of 14 tasks, including standing with eyes open and closed, reaching, getting up and sitting down on different chairs and performing rotations around the vertical axis. A score is assigned to each task on a scale from 0-4. Norm values are published for elderly [64] and Parkinson patients [65].

### **Get-up & Go and Timed Get-up & Go**

The Get-up and Go test aims to evaluate balance in elderly and persons with impaired balance capabilities in every day life situations [66]. During the task the subject has to stand up from a chair, walk 3 m, turn around, walk back and sit down again. This is evaluated on a scale from 0-5. To overcome the subjectivity of this rating, the Timed Get-up and Go test was introduced [67]. A person that does not need assistance in every day life should be able to perform the test in under 10 s while persons depending on help might need 30 s and longer. This can be also be used to evaluate the effectiveness of support equipment like walkers, rollators or exoskeletons.

### **Balance Test - Rehabilitation (GGT-Reha)**

This balance test is split into static balance, dynamic balance and static balance under constrained conditions and mainly designed for participants with neurological diseases in rehabilitation and physiotherapy [68]. The static tests include the same tasks as the Balance Error Scoring System, with eyes open and closed on flat ground and on a deformable surface. The dynamic part includes different walking tasks such as walking forward, backward and sideways, walking on a line with freely chosen step length, and the tandem walk. All tasks are evaluated on a 0-4 scale.

### **Tandem Walk (Seiltänzerengang)**

During the tandem walk, the subject has to place one foot directly in front of the other one with the heel and toes in contact. The tandem walk is a widely applied test of dynamic stability and is similar to walking on a line or on a balance beam in gymnastics. A successful tandem walk test requires a certain distance or number of steps without additional sideways stepping or falling. It is used as part of the field sobriety test by the police to determine if somebody is intoxicated with alcohol or other drugs [69]. Neurologists use it to diagnose ataxia or the posterior vermal split syndrome [70, 71]. Lark et al. [72] found differences in balance for elderly subjects using the tandem walk. Cohen et al. [73] suggested it as a fast screening method for peripheral neuropathy.

### **Balance Evaluation System Test**

This test includes 36 different situations that are grouped into six sub assessments: Biomechanical Constraints, Stability Limits/Verticality, Anticipatory Postural Adjustments, Postural Responses, Sensory Orientation and Stability in Gait [74]. Many of the tasks have been borrowed from existing clinical tests, already mentioned above, like the functional reach test or the timed up and go test. Each task is rated on a scale from 0-3.

### **Instrumented Assessment**

Instrumented balance testing, visual feedback and gamification have gained relevance in balance analysis and training in the past years. Force plates are commonly used by many studies and record the CoP position during static balance tasks to evaluate additional data next to the balance scores [75]. Instrumented treadmills can also record the CoP during walking and running [76]. In fall prevention, treadmills can introduce sudden changes in gait velocity or sideways disturbances [77]. Balance platforms, such as the Wii balance board, allow and record the tilt of the stance foot. They have been used to investigate balance after stroke [78, 79].

### **Limitations**

There are clear limitations to non-instrumented balance tests that rely on a subjective balance score. The result of the test clearly depends on the scientist. For comparability and consistent evaluation, the rating should be done by more than one person and by the same persons for all trials throughout one study. Comparing results between studies can be difficult, since there is only few norm databases, which again are composed of many studies including different subjective ratings.

Furthermore, a uniform understanding of the task by all participants is required, to avoid bias towards certain perturbation recovery actions. If instructions between studies are different, some subjects might tend to use their hands to keep balance, while others maintain them on the pelvis and take a step instead. Depending on the test, the rating for these two actions might be different. In most tests, the tasks are performed only once, leading to only a small sample for each participant. A person might fail 9 out of 10 times and still end up succeeding in the test.

On the other hand, all tests aim to capture the current state of balance capabilities and try to avoid learning effects throughout the assessment. The trade-off between learning the task and recording a larger number of trials for each participants limits conclusive data acquisition. Moreover, most clinical tests are designed for elderly or rehabilitation. They aim to find balance deficits or track progress towards expected balance capabilities. Rarely do they value, or even measure, especially good balancing skills. If participants manage to perform all tasks flawlessly, no further insight can be obtained from visual evaluation. Instrumented assessment allows for a more objective and in depth view. A wider range of data can be recorded and numeric results allow comparison on a broader spectrum.

Collection of CoP data is well established, however, the duration of the recording is a matter of discussion. Depending on the study one finds analysis of a few seconds up until several minutes [80]. Evaluation of the data is not standardized either. In their review Yamamoto et al. [81] suggested 73 parameters that can be computed from the data. For most of the parameters it is not clear whether they are related to good or bad balance. Many studies only discuss the difference between groups with respect to the parameters without further generalization.

Another limitation is the conclusion that can be derived from balance assessment in context of neurological diseases. As introduced earlier, there are at least three senses involved in balance. Fitness, mental focus during the task, age and level of task specific balance training play an important role to the outcome. It is reasonable to find relationships between balance capabilities and a given disease that influence human sensing; however, stating a diagnosis based on a balance test result seems ambiguous. When analyzing especially good balance capabilities there are also limitations. Balance training can be very task specific. Many sports require and train balance in fast movements that can not be reproduced in a standard balance test. Also, the generalization to static balance and the task that can be measured is different for every sport [55, 82, 83]. How static balance can be used as a predictor for balance performance in a balance sport that has not been performed by the subject yet is rarely investigated.

### 1.3.2 Balance Tasks in this Work

We base the analysis of balance on three task of increasing difficulty: a static balance test, the tandem walk test and slackline balancing.

#### Static Balance Test

The static balance assessment is based on the clinical rehabilitation test (GGT-Reha) and we decided on the following three balance tasks: parallel stance, single leg stance and tandem stance. Each one will be performed with eyes open and eyes closed and with the hands remaining at the pelvis. Single leg stance and tandem stance are performed twice, once for each leg. The test should take no longer than 10 min and leave enough time for other data acquisition. We record movement data for visual evaluation and CoP data.

#### Tandem Walk

For dynamic balance we chose the tandem walk test. Participants perform the tandem walk twice, once with eyes open and once with eyes closed. The task is well established in the literature, however a more in-depth analysis using the proposed methodology of this work is yet to be done [84, 85].

#### Slackline Balancing

Slackline balancing is a sport where the athlete tries to maintain balance on an elastic ribbon band that is mounted between two anchor points as can be seen in Figure 1.1. Walking on a slackline is very similar to the tandem walk, but unlike on flat surface the slackline can swing both sideways and vertically, which increases the difficulty of maintaining an upright position. The restoring forces always point towards the straight line defined by the two anchor points [86, 87]. As can be seen in Figure 1.1, the subject stands well above the anchor points, thus the VPP is below the CoM and does not provide stabilization, but makes the system intrinsically unstable.

The length of slacklines ranges between a couple meters for beginners up to a few hundred meters in case of the Guinness World Record [88]. They are used for posture and strength training in rehabilitation, as recreational sport in parks, to assist balance training in other sports or as so-called high lines in context of extreme sports. The training effects on posture, neuromuscular performance and other balance tasks has been well studied [89, 90]. Keller et al. found improved postural control and reduced h-reflexes [91]. These reflexes are responsible for the shaking knee movement a beginner experiences when trying to stand on a long slackline for the first time.

Different to the static balance test, where several evaluations are established in the literature, little research can be found on to the question how to evaluate slackline balance performance. Kodama et al. [92] compared one beginner and one expert and found differences in hand coordination and less knee and CoM variability. Serrien et al. [93, 94] employed self-organizing maps to analyze and compared kinematic motion capture before and after a 6 weeks training intervention. They found that the balance coordination pattern changed significantly by means of increased range of motion and decreased velocity in joints.



**Figure 1.1:** Slackline balancing.

## 1.4 Research Questions

### **What criteria can we use to evaluate balance based on motion capture data?**

Mechanical balance performance indicators that evaluate tandem walking and slackline balancing based on motion capture data have yet to be established in the literature. We aim to find balance metrics that are able to measure slackline balance expertise and aim to apply them also to tandem walking.

### **What biomechanical implications do these balance metrics have?**

Balance can be evaluated from different viewpoints. First, we can analyze how well the balance task is fulfilled by a subject. This can be succeeding or falling, but also measures of balance control. One can imagine that someone balancing calmly has better stability and better adjusted recovery movements than somebody with wild arm motions, even when they manage to balance for the same amount of time. Second, they can hint towards a certain skill that allows the subject to perform the task. This can be, for example, faster reactions or better movement coordination. A balance-experienced participant might do small recovery movements early compared to a beginner that performs large movements shortly before a fall is inevitable. Third, the balance metric can represent the difficulty of the task itself, independent of skill level. This can, for example, be some sort of variability. Regular walking repeats the same movement, whereas walking on a slackline might require different step length or timing for every step.

### **Can we measure the training level of balance?**

Subjects vary in their static balance skills. It is assumed, that this correlates with the amount and type of sport they perform on a daily basis. Thompson et al. [55] found differences in balance performance between soccer athletes and non-athletes. Bressel et al. [82] found differences in static and dynamic balance skills between soccer, gymnastic and basketball athletes. A slackline specific literature review by Donath et al. [95] found that slackline training has a large effect on dynamic balance and only a small effect on static balance. Based on these findings, we want to use the static balance test to differentiate between "balance-experienced" and "balance-inexperienced" and find a measure for the balance training level. We also want to investigate if experienced slackline athletes outperform the beginner group in the static balance test.

### **How do static balance and balancing on a slackline relate?**

The effect of slackline training on other static and dynamic balance tasks has been well studied [90, 95]. It was found that slackline training over a longer time period has only a small effect on the result of a static balance test. However, predictors that enable us to foresee if a subject will be good at slackline balancing are yet to be found. We hypothesize that, if we split the beginner group, that has never done slackline balancing, according to the results of the balance test, we will find significant differences in their slackline performance. We expect to find a high correlation between the static balance test and the time a beginner subject is able to balance on the slackline during the first balancing session. If this is the case, we can deepen our analysis of slackline balance strategies and compare three groups: balance inexperienced beginners, balance experienced beginners and professionals.

### **How does removing the visual input effect the different groups during static balance?**

Keeping balance with eyes closed is more difficult, since the visual feedback is not available and the subject has to rely on proprioception and the vestibular system [20]. Teng et al. [56] showed that patients with diagnosed schizophrenia have difficulties to maintain balance in conflicting sensory conditions. Thompson et al. [55] showed that sportive athletes succeed at a higher rate in the eyes closed condition. The Romberg test [20] attributes better proprioception to persons that pass the balance test with eyes closed. Correlation between the eyes closed static balance test and slackline balance performance would indicate that better proprioception is beneficial.



## 2 Schizophrenia

Schizophrenia is a chronic and severe mental disorder that affects about 20 million people worldwide [1]. Distortions in thinking, emotions, perception, language and behavior are characteristic for the disease [3]. Persons with schizophrenia are 2-3 times more likely to die earlier than the general population. The average potential life loss is estimated at approximately 28 years in the US [96, 97].

### 2.1 Symptoms and Assessment

Symptoms of schizophrenia are manifold [98]. Following the ICD-10 classification [99], persons with schizophrenia often experience hallucinations, such as hearing voices or seeing things that are not there. They suffer from delusions and can be fixed in false beliefs or suspicions. They exhibit abnormal behavior such as wandering aimlessly, mumbling or laughing to themselves. Speech and use of language can be disorganized and incoherent. Emotions might be disturbed, leading to apathy and disconnection between expressed emotions and body language or facial expressions. Motor control can be abnormal, leading to repetitive movement, restlessness or stiffness.

In general, symptoms can be grouped into positive and negative symptoms. Positive symptoms are additional experiences or behavioral patterns that are not present in healthy subjects. Negative symptoms represent reduction and impairment compared to healthy subjects.

#### 2.1.1 Positive and Negative Syndrome Scale

The PANSS introduced by Kay et al. [2] aims to standardize the assessment of symptoms in schizophrenia. The scale contains 30 items rated from 1 to 7 representing, absent, minimal, mild, moderate, moderate-severe, severe or extreme symptoms. Items are grouped into positive scale, negative scale and the general psychopathology scale. The positive scale contains the positive symptoms delusion, conceptual disorganization, hallucinatory behavior, excitement, grandiosity, suspiciousness and hostility.

The negative scale includes the following negative symptoms: blunt affect, emotional withdrawal, poor rapport, passive-apathetic social withdrawal, difficulty in abstract thinking, lack of spontaneity and flow of conversation and stereotyped thinking. The general scale contains somatic concern, anxiety, guilt feelings, tension, mannerism and posturing, depression, motor retardation, uncooperativeness, unusual thought content, disorientation, poor attention, lack of judgment and insight, disturbance of volition, poor impulse control, preoccupation and active social avoidance.

### 2.1.2 Motor Control - Neurological Soft Signs

The Heidelberg Scale of Neurological Soft Signs (NSS) was developed by Schröder et al. [100]. It consists of 16 tasks that aim to reliably quantify minor neurological abnormalities. They are grouped into the following five subscores: Motor Coordination, Sensory Integration, Complex Motor Tasks, Right/Left and Spatial Orientation and Hard Signs. Each task is evaluated on a scale from 0 - 3, with score 0 representing no abnormalities and 1 to 3 representing a (large) difference from the desired task execution.

Buchanan and Heinrichs [101] found higher scores in persons with schizophrenia than in non-psychiatric controls supporting the hypothesis that also motor control is affected by the disease. Fritze et al. [102] investigated if NSS is modulated by current antipsychotic dosage and found no significant effect. Hirjak et al. [103] investigated the connection between NSS and multimodal imaging. Their overview of current research suggests that NSS are related to structural and functional changes in the thalamo-cortical network and basal ganglia.

## 2.2 Research on Causes and Treatments

The exact causes of schizophrenia are yet to be understood. The biopsychosocial model looks at the interaction between biology, social environment and psychology as the main factors for health and disease development [104]. Current research states that genetics play a key role. The heritability is estimated to be 79 % [105]. While the general population has a lifetime risk of approximately 0.33 % to 0.75 % to suffer from schizophrenia, it was found that first degree relatives of somebody with schizophrenia have a 6.9 % risk to develop the disease [106, 107]. Concordance rate in identical twins of affected people is between 33 % and 40 %. For dizygotic twins it is around 7 % [105, 108]. Furthermore, schizophrenia has been linked to differences in brain development [109] and changes in level of the neurotransmitters dopamine and serotonin [110].

Many studies used functional brain imaging to detect differences in brain growth and abnormalities in certain brain areas and tried to link them to schizophrenia [111–113]. From the social perspective, stress and drug abuse can trigger schizophrenia in a person that are already at risk [114]. Treatment focuses on the use of antipsychotics against positive symptoms. They block dopamine and serotonin receptors in the brain, however, side effects are common and treatment response heterogeneous [115].

Effects on negative symptoms are mixed and finding an effective drug treating negative symptoms reliably is ongoing research [116, 117]. More recent approaches try to analyze the whole body and do not treat schizophrenia solely as a brain disease [4, 118].

### **2.2.1 The Embodiment Approach: Schizophrenia as Disembodiment**

The embodiment approach understands schizophrenia as a disturbance of the embodied self, so-called disembodiment [119]. The relation between the self of a person and their body is disrupted and the sense of self is weak or lost (depersonalization), resulting in a feeling of disconnection between self and body. Implicit and automatic body functioning is not taken for granted and emotions are not represented in body language [120]. The other way around, the understanding of sensory input coming from the body may be insufficient and the resulting motor control that relies on feedback is impaired. Everyday actions and body movements become fragmented. Disconnection to the own body results in disconnection to society and impaired sense of others.

Due to the disturbed self perception, understanding emotions of others becomes increasingly challenging and response to the social environment becomes arbitrary. Embodied Therapies, such as dance and movement therapy or body psychotherapy, target movement and body experience in order to change emotion and behavior and have shown success in reducing negative symptoms [4, 121].

### **2.2.2 The research project "Schizophrenia and the Moving Body"**

The "Schizophrenia and the Moving Body Project" [7] by Lily Martin and supervised by Prof. Dr. Dr. Thomas Fuchs, aims to find schizophrenia-specific movement markers in gait, balance and specific coordination tasks, aspiring to find experimental support of the embodiment approach. The project included phenomenological interviews, clinical assessment at the center for psychological medicine as well as motion data recording at HCMR.

The following tasks were recorded: regular walking, a static balance test, tandem walking with eyes open and eyes closed and a star jump. Thanks to fruitful collaboration in subject recruitment and data assessment between Lily Martin and the author of this thesis, a part of the data resulting from the project could be analyzed in the course of this thesis. These are the measurements of the static balance test and the tandem walk of persons with schizophrenia and healthy controls.

#### **Persons with schizophrenia (Experimental Group)**

All patients participated in an Examination of Self-Experience (EASE) interview [122] and assessment of NSS [100] as well as PANSS [2] and Extrapyrarnidal symptoms (EPS) (side effects of medication). Further, extended demographic data was collected. Participants were recruited by Lily Martin from the Center for Psychosocial Medicine in Heidelberg based on the following criteria:

### **Inclusion:**

- Ability to consent disorder (ICD 10 F20-29)
- Age between 18 and 60 years old
- Diagnosis of a schizophrenia spectrum
- Stable medication for at least 2 weeks prior to assessment

### **Exclusion:**

- Phase of acute psychosis (ICD 10 F23)
- Visual disabilities
- Catonic type of schizophrenia (ICD 10 20.2)
- Alcohol or substance abuse
- History of brain trauma, neurological diseases or heavy fractures
- IQ < 70
- Visible Tremor
- SAS score above 4 (Parkinsonoid)
- Language barriers

### **Healthy Comparison Subjects (Control Group)**

Healthy control subjects were recruited from the Heidelberg region. Clinical assessment only included NSS and demographic data. Control group participants had to fulfill the following requirements:

### **Inclusion:**

- Ability to consent
- Matched Body Mass Index (BMI) to the patient group
- Age between 18 and 60 years old

### **Exclusion:**

- History of psychosis, schizophrenia or depression
- Visible Tremor
- History of psychosis or schizophrenia in first degree relatives
- Visual disabilities
- History of brain trauma, neurological diseases or heavy fractures
- Alcohol or substance abuse
- IQ < 70
- Language barriers

## 2.3 Research Questions

Based on the motion capture recordings of the static balance test and the tandem walk we aim to investigate the following hypothesis by comparing the healthy control group to the experimental group consisting of persons with schizophrenia.

### **Static Balance:**

We want to confirm the literature, by showing that persons with schizophrenia show static balance deficits [56, 57]. We expect them to fail the static balance test at a higher rate and balance for a shorter time. We aim to find differences in CoP sway parameters when comparing successful trials. This can be related to balance impairment.

### **Visual Condition During Static Stance**

We expect loss of visual information to have a larger effect on the experimental group. The control group may be able to balance with eyes closed whereas the experimental group is expected to fall more often. Change in CoP sway parameters is expected to be larger for the experimental group.

### **Dynamic Balance**

Jeon et al. [70], showed that persons with schizophrenia fail the tandem walk at a higher rate by means of successful steps, distance without falling and walking speed. We expect to find differences for balance metrics found in slackline balancing that show that the experimental group has balance deficits even for successful tandem walk tests.

### **Visual Condition During Tandem Walk**

We expect loss of visual information to have a larger effect on the experimental group. The control group may be able to pass the tandem walk test with eyes closed whereas the experimental group is expected to fail the test more often.

### **Balance Strategy and Adaptability**

Good balance capabilities imply the correct choice of strategy for a given balance task. We hypothesize that the experimental group does not adjust their balance strategy to the eyes closed task. We expect to find a larger change of behavior in the control group.

### **Connection between Symptom load and Movement Parameters**

We are able to quantify symptoms using PANSS and medication using Olanzapine Equivalents (OPZ). We hypothesize that there are connections between different balance parameters, the medication and the PANSS score.



## **Part II**

# **Human Movement Analysis**



### 3 Measuring Human Motion

The assessment of human movement is manifold. We can collect kinematic data such as joint angles or segment positions [123, 124], measure muscle activation by means of EMG data [125], and record interaction forces using force plates. Eye-tracking systems are able to capture the subjects' gaze [126] and pressure sensitive insoles can measure the pressure distribution inside the shoes. Out of the many options available, we decided to base this work on kinematic data and force plate measurements to record the CoP position during balancing tasks.

The two motion capture systems available at HCMR for this work were: the marker-based system Qualisys [123] with the Qualisys Track Manager software (QTM, Version 2018.1) and the Inertial Measurement Unit (IMU) based system Xsens [124] with the MVN Analyze 2019 software. We describe and compare the two systems in the following sections. In the last section, we present two options for measuring GRF (Section 3.4).

#### 3.1 Marker-based Motion Capture - Qualisys

Marker-based motion capture systems employ multiple cameras that record the position of markers placed on the object of interest. They can be divided into active and passive systems, depending on the kind of markers they use. Active markers are usually LED's that actively send out light. Each marker emits a different frequency and can therefore be uniquely recognized by the cameras. Passive, retro-reflective, markers reflect the light of a flash that is part of the cameras. They do not rely on a power supply, are cheaper and their placement more versatile. On the downside, they need to be identified (labeled) either by an algorithm or manually by the user, since they are not distinguishable for the cameras. In either case, each marker has to be observed by at least two cameras for a 3D position reconstruction. The volume where the fields of view of the cameras overlap and a marker recording is possible is called the capture volume.



**Figure 3.1:** The motion capture equipment. The retro-reflective markers are shown at the left, one of the Qualisys Oqus 510 cameras in the middle and the calibration kit at the right.

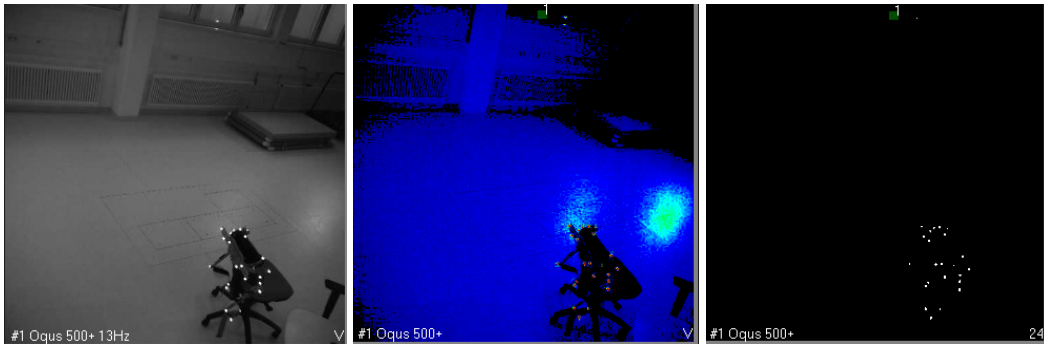


**Figure 3.2:** The three video mods of the Qualisys Oqus 500 cameras: regular gray scale video is shown at the left. The infrared intensity as a heat map is shown in the middle. Markers can be seen as red dots that reflect the light well. In marker mode (right), a binary and circularity filter are applied. The number of recognized markers is shown at the lower right.

In this work, we used the Qualisys motion capture system together with passive markers. All recordings were done with 8 Oqus 500+ cameras and 14 mm spherical markers. The position of each camera is determined during a calibration procedure. Hereby, four markers on a rectangular frame are placed in the center of the capture volume to define the coordinate system. Two markers of known distance are then moved around the capture volume until all cameras record a sufficient number of frames with all six calibration markers visible.

The exact position and orientation of each camera is reconstructed from the calibration data. Figure 3.1 shows the retro-reflective markers, a Qualisys Qqus 510 camera with the infrared flash, and the calibration kit. Each cameras has three different video modes: regular video, infrared intensity and marker mode. They are shown in Figure 3.2. The Oqus 500 cameras are able to record the infrared intensity at a frequency of 150 Hz and with a resolution of 4 mega pixel. For marker recognition, the intensity image is converted into binary format applying a threshold. Afterwards a circularity filter is applied. A minimum number of connected pixels is required for the circular area to be a considered as a marker.

Figure 3.3 shows how the 3d position of each marker in space is estimated from the 2d images. The quality of the calibration and exact knowledge on the camera position is crucial to the reconstruction accuracy. Based on a good calibration, QTM (Qualisys Track Manager), the software of Qualisys, is able to reconstruct the marker position with sub-millimeter accuracy.

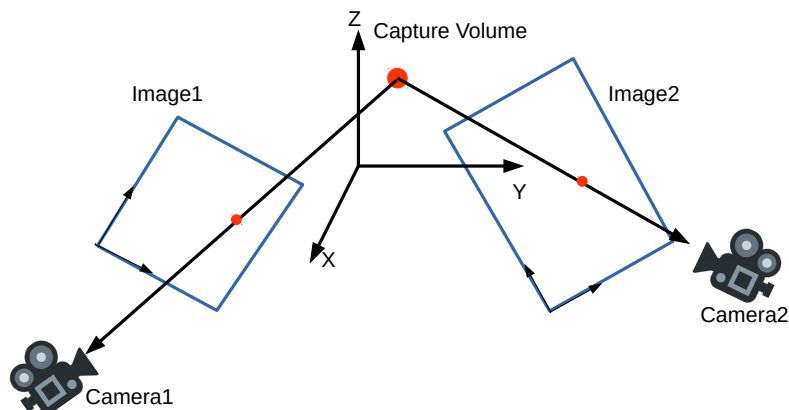


**Figure 3.3:** Each marker needs to be recognized by at least two cameras to reconstruct the 3d position in space. Knowledge of the exact camera position relative to the capture volumes coordinate system is crucial for an accurate measurement.

There are several ways to infer human kinematics from marker position measurements. In this work we used three different approaches, which are described in more detail in the respective sections.

- Direct computation of position and orientation of an individual segment from marker data for each frame (Section 3.3)
- Estimation of the whole body pose and all joint angles for each recorded frame individually (Section 5.1)
- Optimization of the whole motion as one large scale optimization problem (Section 5.2)

In each case the exact placement of markers depends on the type of evaluation planned. Each situation, subject and movement has influence on the so-called marker set and might require a different, individualized solution. Their development is task specific and ongoing research [127–129]. For this work an existing marker set was modified to better capture slackline balancing (Section 3.1.1).

### 3.1.1 Marker Set

All subjects were equipped with 49 retro-reflective markers following the marker set by Leardini et al. [128]. Markers are placed on prominent points, so-called bone or skeletal landmarks, directly on the skin of the subject. The goal of the marker set as a whole is to represent the subjects biomechanical model and enable us to record and reconstruct the movement of the underlying skeleton. Bone landmarks are chosen for different criteria: First, they should be reliably palpable for all subjects and be located directly under the skin. Muscle tissue or subcutaneous fat on top of the bones can cause movement artifacts that compromise the measurement.

Second, they should allow us to estimate the biomechanic model properties of the subject by means of joint center positions or segment lengths. Locations at the distal or proximal end of a bone or what later will be modeled as a segment are preferable. The same bone landmarks were used for all subjects. The marker set consists of 45 dynamic and 6 static markers. Figure 3.4 and 3.5 show the marker placement of all markers on the subject and the according bone landmarks. Names and descriptions are taken from the *Color Atlas of Skeletal Landmark Definitions* by Serge van Sint Jan [130]. Right-side markers are shown in green, left-side markers in blue and central markers in orange. Static markers are yellow and are only recorded during the static trial, before the actual measurement. 29 markers are located on the upper body. These are seven markers on each arm, four on the pelvis, six on the spine and two on the thorax. Three markers are placed on the head.

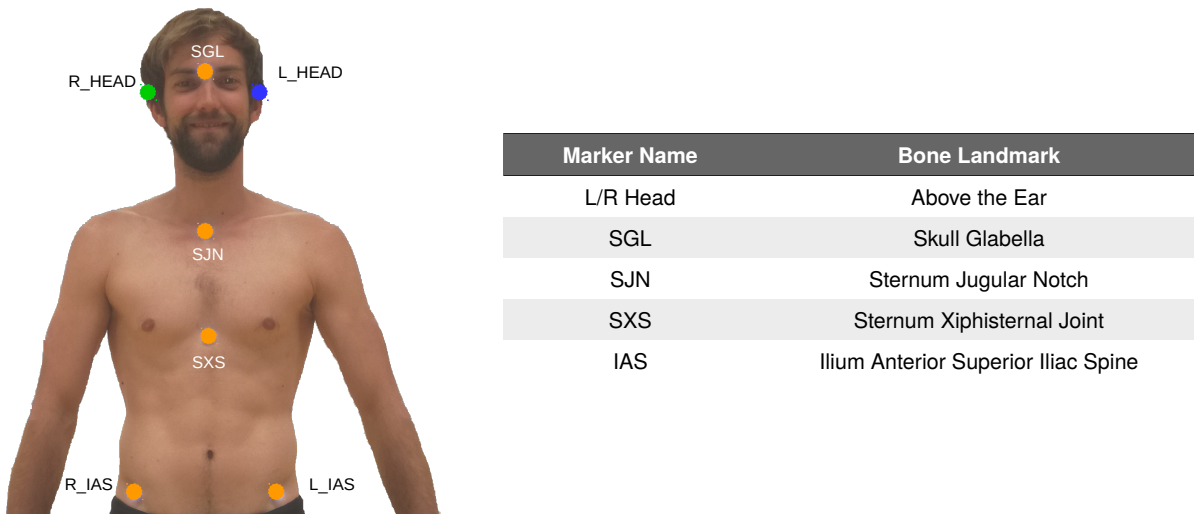


**Figure 3.4:** The front of the upper body part of the marker set.

For slackline balancing, the original marker set from Leardini et al. [128] was extended by two markers on the medial Epicondyle of the Humerus for better upper arm orientation and shoulder angle tracking. For a stretched elbow the four markers SAE, HUM, HLE and USP can all be in a straight line. In this case additional tracking information is necessary as the lower and upper arm rotation become interchangeable. They are shown in red. These markers were not used for the tandem walk experiments as they would fall off during natural walking and often be occluded.

22 markers are located on the lower body. Six markers at the foot and ankle, four markers at the knee and one marker at the thigh. Four of these are static makers that are placed on the medial side of the legs to estimate the knee and ankle distance and joint centers. Two static markers are placed centrally on the feet to estimate the sagittal rotation axis. They are removed after the static trial recording since they hinder free movement during walking, are often occluded and tend to fall off. The foot static markers are redundant in the evaluation and very close to the FM1 markers. They are removed to improve the automatic marker detection.

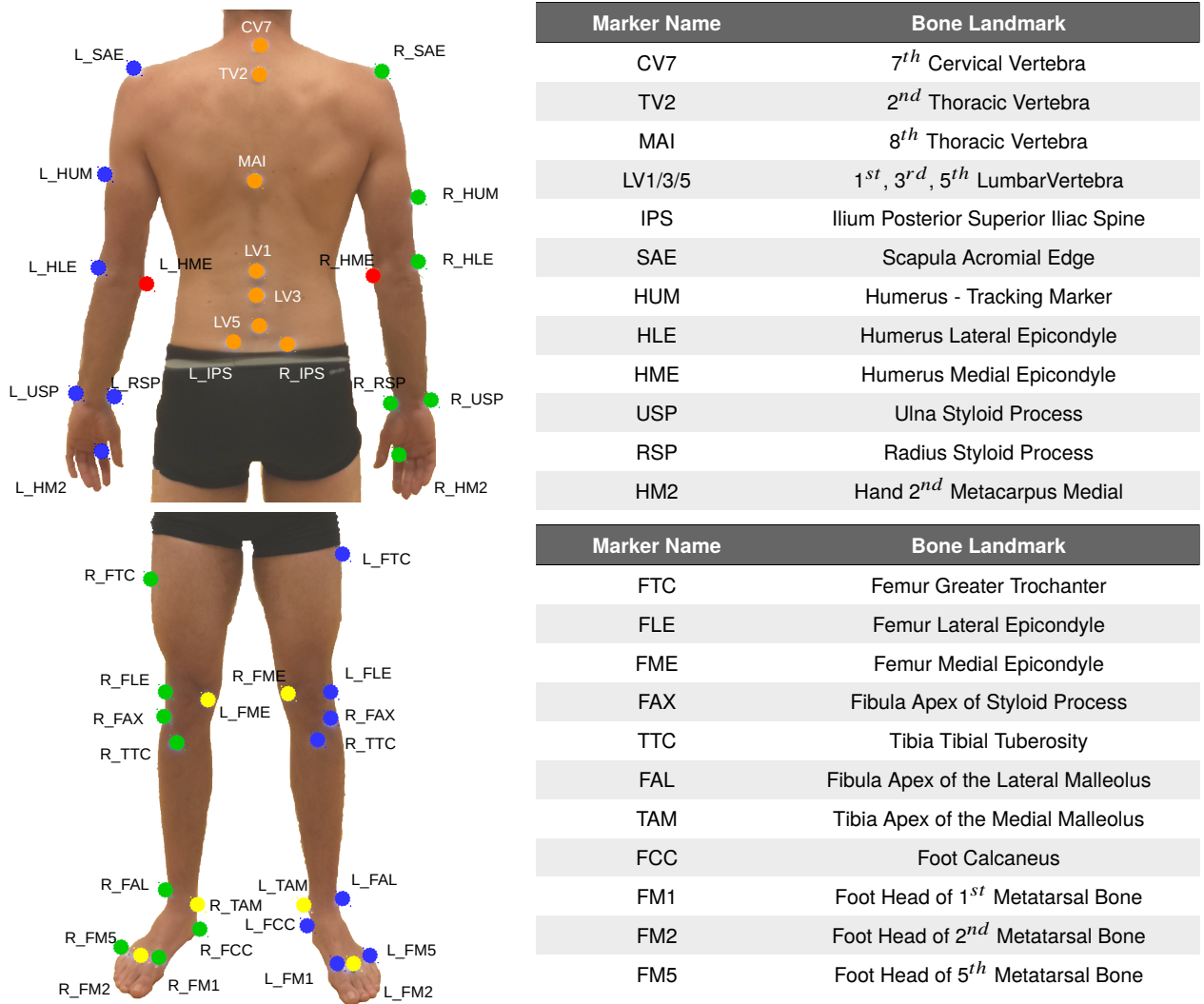
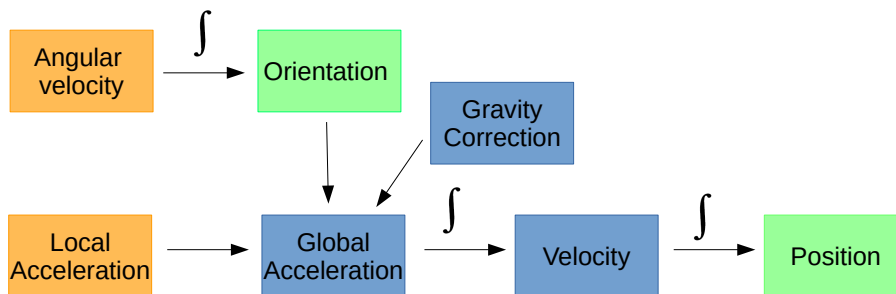


Figure 3.5: Top: The back part of the marker set. Bottom: All leg markers

### 3.2 IMU-based Motion Capture - Xsens

#### Inertial Measurement Unit

An IMU is able to measure angular velocity and linear acceleration in 3D space. By integrating these measurements over time one can compute the position and orientation of the sensors as described in Figure 3.6. Each integration leads to an unknown integration constant. Physically speaking, these are the initial orientation, the initial velocity and the initial position of the sensor. They have to be determined by a calibration beforehand. As the measurement values are prone to noise, the error of the position and orientation estimate grows over time. This is known as IMU sensor drift. Modern sensors and algorithms correct this drift by applying various filters and taking additional sensor measurements, like magnetic field or air pressure, into account.



**Figure 3.6:** IMU's measure angular velocity and linear acceleration (orange). By integrating the measurement values over time, the orientation and position of the sensor can be computed. The initial position, orientation and velocity have to be calibrated beforehand.

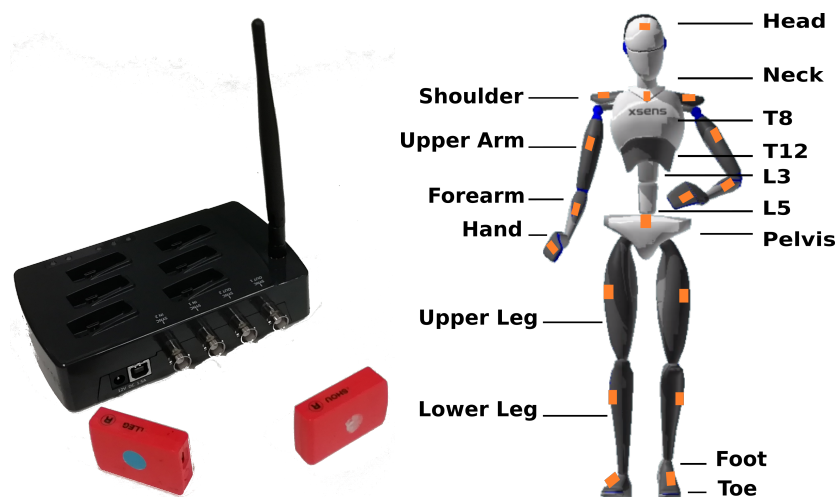


**Figure 3.7:** The Xsens model. 17 IMU sensors are placed on the different segments (orange). Segment dimensions have to be measured beforehand.

### Xsens

The Xsens motion capture system is based on three components: the IMU's sensors, a biomechanical model of the subject and a contact model of the interaction with the external world [131]. The sensor data comes from up to 18 IMU's. 17 of them are placed on the different segments of the subject and one IMU can be used to track an additional object. Each IMU contains a 3d gyroscopes, a 3d accelerometers and a 3d magnetometers. They perform measurements at a sampling rate of 1 kHz. The data is already processed on the sensor before being transmitted to the receiving station at a rate of 60 Hz. Figure 3.7 shows a sensor, the Xsens Avinda receiving station and the placement of the sensors as orange boxes on the subject.

### Biomechanical Model

The biomechanical model of the subject consists of 23 segments connected via rotational joints. The dimensions of the model are determined by body measurements of the subject. They are listed in Table 3.1. The sensor data is mapped to the according segments of the model and the kinematic restrictions taken into consideration. All joints can only rotate and segments have to stay connected at all times.

Body Measurement	Description
Body Height	Subject height
Foot Length	Length of the feet
Arm Span	Distance between middle fingers in T-pose
Ankle Height	Ground to distal tip of lateral malleolus
Hip Height	Ground to bony prominence of greater trochanter
Hip Width	Right to left anterior superior iliac spine
Knee Height	Ground to lateral epicondyle on the femor
Shoulder Width	Right to left acromial edge
Shoulder Height	Ground to C7 spinal process
Extra Sole Height	Additional thickness of soles, if wearing shoes

**Table 3.1:** The biomechanical model of Xsens is based on various body measurements of the subject. These have to be measured before the measurement or can be estimated from the subject's height.

#### **Contact Model - Scenarios**

The third part of the Xsens motion capture software is the contact model. Since there is no possibility to determine the absolute position of the subject in space using only IMU sensors, Xsens has developed an interaction model with the external environment to estimate which segment is in contact. Each segment has several points, that can establish contacts.

A contact is fixed with respect to the environment and does not move, hence the whole model is fixed in space. This counteracts the linear part of the IMU sensor drift. The segment is still able to rotate around this contact point. Multiple segments can be in contact, but only one point per segment. The user can choose between four scenarios.<sup>1</sup> Each scenario represents a different heuristic on where contacts can occur.

- **Single Level:** All contacts are at the same height, namely floor level.
- **Multi Level:** Contact height may vary, e.g. when climbing stairs.
- **No Level:** The subject will remain fixed in space, e.g. when walking on a treadmill. The pelvis segment will remain at a preset height.
- **Soft Floor:** Feet will slightly decrease in height, during the time between the feet contacting the ground and leaving it, e.g. grass, or soft carpet.

The scenario can be changed after the recording and the data can be reprocessed under the new constraints. As indicated above, each IMU needs to be calibrated, since they can not measure the initial position, orientation and velocity. The calibration procedure of Xsens works as follows: The subject assumes a standing, neutral pose (N-pose). Both arms have to be aligned with the upper body with thumbs facing forward. After this pose is held for about 5 s, the subject is required to walk forward for approximately 5 m, turn around and walk back to the start.

According to Xsens this performs a mapping of the magnetic field to further reduce drift [132]. The N-pose is crucial for the motion reconstruction quality, since deviations from this pose will be present as offset in all measurement data. The system needs to be re-calibrated in case one of the sensor positions changes. All computations are done by MVN Analyze software in a black-box fashion. User-defined evaluation of the sensor data is limited to the choice of the scenario and to defining and editing contact points.

---

<sup>1</sup>A fifth scenario was added after the completion of this research in MVN Analyze 2019.3.

### 3.3 Pre-Study System Comparison

Table 3.2 summarizes the advantages and disadvantages of the two systems. Crucial differences are highlighted in yellow and green, with green being the preferred choice. They require similar effort in subject preparation time. With Xsens, the subject can wear a comfortable sports outfit and shoes, while the markers of Qualisys are placed directly on the skin. This requires either tight fitting shirts and pants or, preferably, no T-shirt.

The two main differences in data acquisition are the calibration and the capture volume. The capture volume of Qualisys needs to be calibrated once, before the measurement and is limited in space. Xsens, on the other hand, can be used without restrictions, but needs to be calibrated by the subjects themselves. "Creating a good calibration is of utmost importance in order to ensure accurate results" [132]. This might be hard to achieve for a first-time user and has to be repeated after a certain measurement time.

The resulting data of the two systems is fundamentally different. Qualisys results in 3d positions of markers at a high accuracy and frequency. All evaluation is left to the user and additional software. This requires further, specific knowledge, but also allows for customization. Correct marker placement is key to reliable and comparable measurements. Xsens does everything for the user in a black-box fashion. The full motion of a biomechanical model is reconstructed including all kinematics. However, the result depends on accurate body measurements, a good calibration and the chosen scenario. Reprocessing the recorded data in another scenario changes the result.

	Qualisys	Xsens
Preparation Time	20 - 30 Minutes	15 Minutes
Marker/Sensor Placement	Directly on the skin	On top of regular cloth
Calibration	Done once beforehand	Done by the subject, multiple times
Measurement Time	no limit	3hrs Battery
Capture Volume	restricted	unrestricted
Measurement Results	Marker positions	Reconstructed, processed kinematics
Accuracy of Measurement	Millimeters	Centimeters / few Degrees
Sources of Error	Correct Marker Placement	Correct Body Dimensions, Proper N-Pose during Calibration, Results vary with Scenario

**Table 3.2:** Comparison of the two motion capture systems. Important differences are highlighted with the preferred option in green.

In the following pre-study we wanted to investigate the usability of Xsens for slackline balancing. The results of this study have been published in [133]. Xsens would allow us to perform outdoor measurements with larger slackline setups. There is no matching reconstruction scenario for the case of slackline balancing. Xsens assumes fixed contact points in all scenarios. This is not the case on the slackline as the feet are able to move in vertical and sideways direction. We equipped one subject with both motion capture systems as shown in Figure 3.8. We used all 17 sensors as shown in Figure 3.7 and placed the markers according to Section 3.1.1.

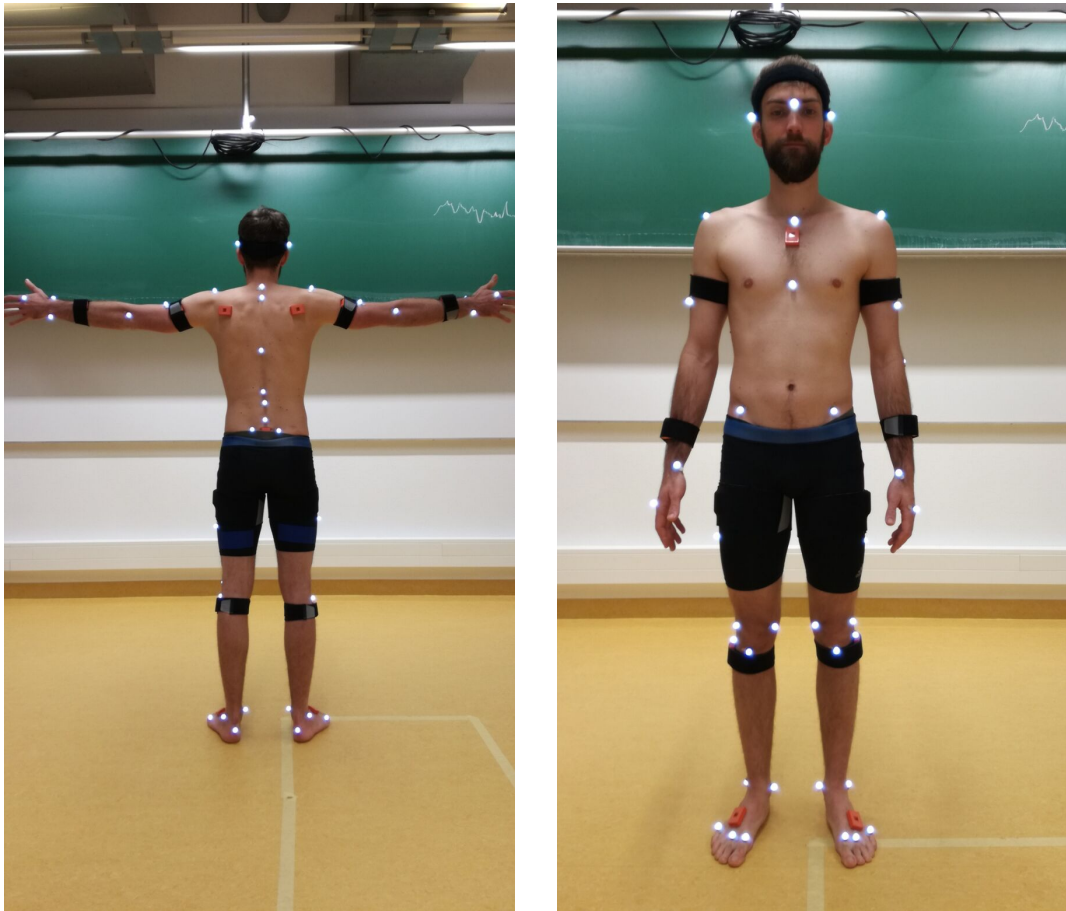


**Figure 3.8:** The subject with markers and Xsens IMU sensors. Markers were placed according to the marker set in Section 3.1.1. IMU sensor placement follows the Xsens Manual [132].

Both systems were physically synchronized using a trigger signal to start both measurements at the same time. We recorded single leg balancing with both legs and walking up and down the slackline. The same measurements were taken for standing and tandem walking on a regular surface. We reconstructed absolute position  $\vec{x}$  and orientation  $\mathbf{R}$  of hands, feet, pelvis and the head with respect to the lab frame. We used a subject-specific model of each segment as described in Section 4.1 and fitted it to the marker data as described in Section 5.1. For Xsens, the data was reprocessed in the single and multi level scenario to investigate which scenario is more suitable for the task.

The Qualisys marker data was processed as described in Section 5.1. Measurements were cut to the time on the actual task. Coordinate systems were aligned using affine transformations between the two coordinate systems and maximization of correlation. Temporal offsets due to reaction time of the software were corrected. For positions we computed the norm of the 3d position vector difference. For orientations the rotation matrix of one system was multiplied with the transposed of the other system. We convert this matrix into a vector of three Euler angles and take the norm of this vector as orientation deviation. In case both systems measure the same orientation this results in the unity matrix. All Euler angles would then be zero.

Results were converted into cm and °. Table 3.3 shows the mean position and rotation deviation for all measurements. The left value is for the single level, the right for the multi level reprocessing option. The results for each segment are shown in the top two groups and the summary for the four conditions at the bottom. Deviations are similar for standing on the slackline and the level ground conditions. This level of accuracy is also reported in the literature [134]. Slackline walking, however shows larger deviations.

	Feet		Hands	
	$\vec{x}$ [cm]	$\mathbf{R}$ [°]	$\vec{x}$ [cm]	$\mathbf{R}$ [°]
Slackline				
Standing	3.9 / 3.8	5.8 / 5.5	8.8 / 8.7	8.7 / 8.7
Walking	10.1 / 10.6	8.7 / 8.5	14.1 / 14.0	10.6 / 10.6
Ground				
Standing	4.1 / 4.6	6.1 / 6.4	11.6 / 11.8	13.9 / 14.4
Walking	6.0 / 6.6	5.6 / 5.6	9.5 / 9.8	8.2 / 8.3
	Head		Pelvis	
	$\vec{x}$ [cm]	$\mathbf{R}$ [°]	$\vec{x}$ [cm]	$\mathbf{R}$ [°]
Slackline				
Standing	3.3 / 3.3	3.0 / 2.9	2.9 / 2.2	3.9 / 3.5
Walking	10.2 / 10.9	3.9 / 4.1	10.2 / 10.7	3.8 / 4.2
Ground				
Standing	5.0 / 4.7	2.8 / 2.0	2.6 / 2.4	3.5 / 2.9
Walking	6.5 / 7.2	3.4 / 3.2	6.2 / 6.8	4.6 / 4.5
	Standing		Walking	
	$\vec{x}$ [cm]	$\mathbf{R}$ [°]	$\vec{x}$ [cm]	$\mathbf{R}$ [°]
Slackline	4.7 / 4.5	5.4 / 5.2	11.2 / 11.6	6.8 / 6.9
Ground	5.8 / 5.8	6.6 / 6.4	7.1 / 7.6	5.5 / 5.4

**Table 3.3:** The table shows the measurement difference for position  $\vec{x}$  and orientation  $\mathbf{R}$  between Qualisys and Xsens for the different segments and a summary of the four cases. The data was reprocessed in the single level (left) and the multi level scenario (right).

During all experiments of this work, contact forces will only act on the feet. A precise reconstruction of the foot position is crucial to many parts of the evaluation. We later want to analyze the foot acceleration due to the slackline or the CoM projection into the foot frame. Figure 3.9 shows the height of the foot contact during walking. On the left we see walking on a slackline and on the right on flat ground. Slacklines lower towards the middle and are higher at the anchor points. The red position, measured with the marker system, reflects this geometry, while the two reconstructions of Xsens (green and blue) both fix a certain height for the contact to happen. For level ground walking this is not an issue and all three curves coincide nicely.

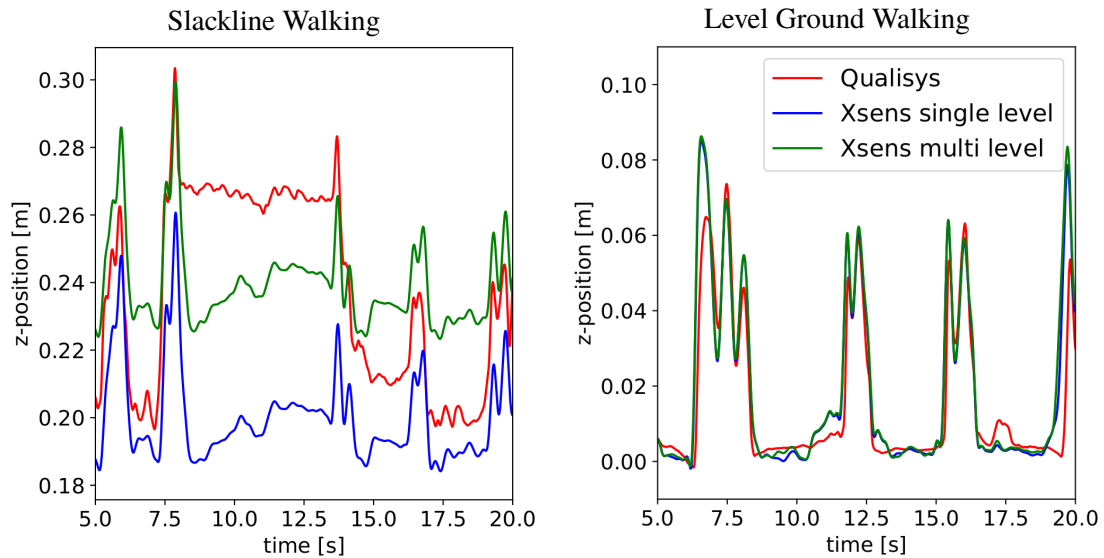


**Figure 3.9:** The plot shows the height of the foot during walking on a slackline (left) and on flat ground (right). In both cases, Xsens reconstructs the contact at the same level and the slope of the slackline is not resolved.

We look at the contact foot in more detail in Figure 3.10, this time for single leg balancing. Again, we plotted the slackline case on the left and the regular floor on the right. The upper row shows the sideways and the lower row the vertical direction. Both systems correctly resolve flat ground standing. From the marker measurement, we see that the slackline allows movement in both directions in the range of 4 cm. Vertical movement is rhythmical with a constant frequency, whereas sideways movement happens at multiple frequencies with different amplitudes. Xsens is not able to reproduce any of the sideways movement and the foot is locked to the contact. This is better for the vertical direction where Xsens is able to measure the movement, but not to its full extent. The resolved amplitude of the oscillation is approximately 50%.

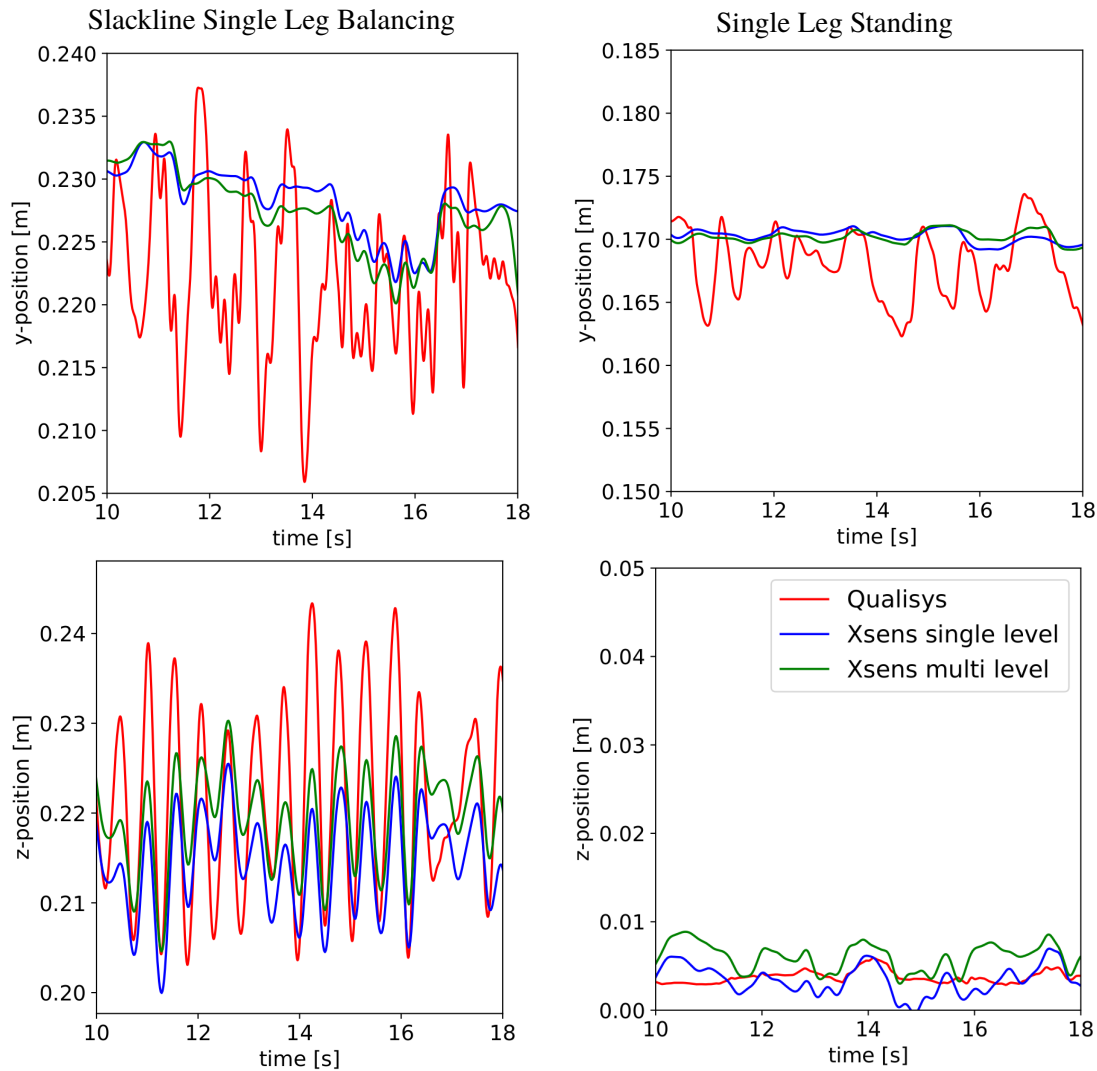


**Figure 3.10:** Foot position for standing on a slackline (left) and on flat ground (right). Xsens is not able to capture the full amplitude in the up and down direction (lower left plot) and does not reconstruct any sideways movement (upper left plot). For standing on flat ground the contact position is more accurate.

Further we analyzed the foot placement during tandem walking. The task requires the feet to be placed precisely in front of one another. We later intend to evaluate the stepping precision as a measure of balance capabilities and therefore need an accurate measurement. The result for a forward and backward tandem walk is shown in Figure 3.11. We plotted the horizontal position of the same foot during the task and see that the Xsens reconstruction drifts over time. In walking direction  $x$ , we find differences in step length with an accumulated error of  $\approx 10$  cm after 10 s and 5 steps. In sideways direction, the Qualisys measurement shows that the foot was placed on the  $y$  axis of the lab coordinate system as required by the task. The Xsens measurement, again, shows a drift of 6 cm after 15 s and 7 steps.

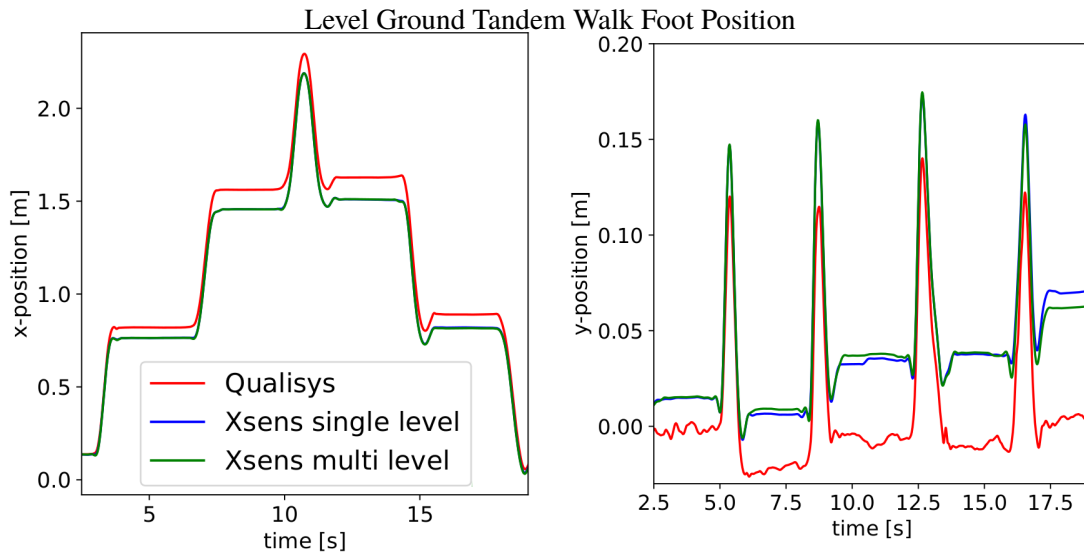


**Figure 3.11:** The plot shows the horizontal foot position on flat ground (right) during tandem walking. In both cases, the Xsens reconstruction shows drift in the contact position with respect to the marker based system.

Summarizing, we opted for marker-based motion capturing for all our studies for the following reasons:

- Xsens does not measure the slackline movement correctly.
- The contact model is not designed for moving contacts - no valid scenario.
- Xsens' accuracy highly depends on the calibration.
- The calibration has to be done (multiple times) by the subject.
- Achieved accuracy was not sufficient for precise evaluation.
- Accurate marker positions allow for customized evaluation that is not bound to a black-box reconstruction algorithm

### 3.4 Force and Pressure Measurements

#### 3.4.1 Force Plates

Interaction forces with the environment are fundamental to understanding human locomotion [27]. The measurement of ground reaction forces is part of many gait analysis protocols and enables us to compute joint torques or assess stability parameters [55, 135]. At the time being, there were two commercial systems available: two Bertec *FP4060\*08\*2000* force plates [136] and Moticon Pressure Insoles [137]. Prototyping a system that measures the pressure distribution during slackline balancing was part also of this work and is further described in Chapter 10. Figure 3.12 shows a schematic of a force plate. One force sensor is located in each corner of the measuring area. They measure the force in all three directions. From the sensor data the position  $\mathbf{p}$ , the total force  $\mathbf{F}$  and the moment  $\mathbf{M}$  are computed as described in Bertec patent description [136] and Equation 3.1.

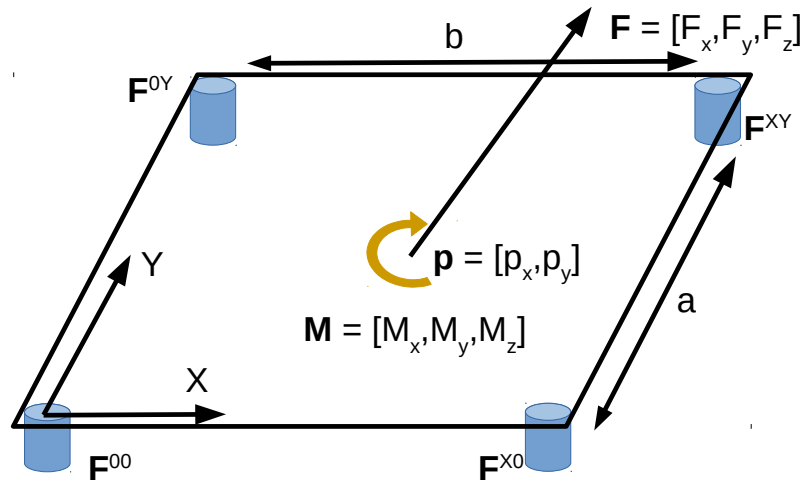


**Figure 3.12:** Schematic of a force plate. The position  $\mathbf{p}$ , the total force  $\mathbf{F}$  and the moment  $\mathbf{M}$  can be computed from the individual data with the formulae at the bottom.

$$\begin{aligned}
 \mathbf{F} &= \mathbf{F}^{00} + \mathbf{F}^{X0} + \mathbf{F}^{0Y} + \mathbf{F}^{XY} & (3.1) \\
 M_x &= \frac{b}{2} * (-F_z^{00} + F_z^{X0} - F_z^{0Y} + F_z^{XY}) \\
 M_y &= \frac{a}{2} * (F_z^{00} + F_z^{X0} - F_z^{0Y} - F_z^{XY}) \\
 M_z &= \frac{b}{2} * (F_x^{00} - F_x^{X0} + F_x^{0Y} - F_x^{XY}) \\
 &\quad + \frac{a}{2} * (-F_y^{00} - F_y^{X0} + F_y^{0Y} + F_y^{XY}) \\
 p_x &= -M_y / F_z \\
 p_y &= M_x / F_z
 \end{aligned}$$

### 3.4.2 Pressure-Sensitive Insoles

Pressure-sensitive insoles measure the entire pressure distribution at the foot. Moticon (Moticon GmbH, Munich, Germany) insoles consist of 13 individual sensors that cover approximately 50% of the sole area [138]. The sensor layout is shown at the left of Figure 3.13. Each sensor measures the local pressure in  $\text{N}/\text{m}^2$ . The pressure distribution of the whole foot area is estimated by a black-box algorithm and the total force computed as integral over the area. The CoP  $\vec{p}$  is computed directly from the sensor measurements [27]:

$$\mathbf{p} = \frac{1}{\sum_n v_i} \sum_{i=0}^n v_i * \mathbf{s}_i \quad (3.2)$$

where  $\mathbf{s}_i$  is the sensor position,  $v_i$  is the pressure measurement of sensor  $i$ . The resulting CoP position has good agreement with force plate measurements, however the computed GRF show deviations of up to 30% [138]. The area in which the CoP can be measured is also restricted by the sensor layout. If the whole pressure is measured by one sensor, the CoP would be located at the middle of the sensor. Standing on the edge of the shoe, for example, can not be measured accurately.

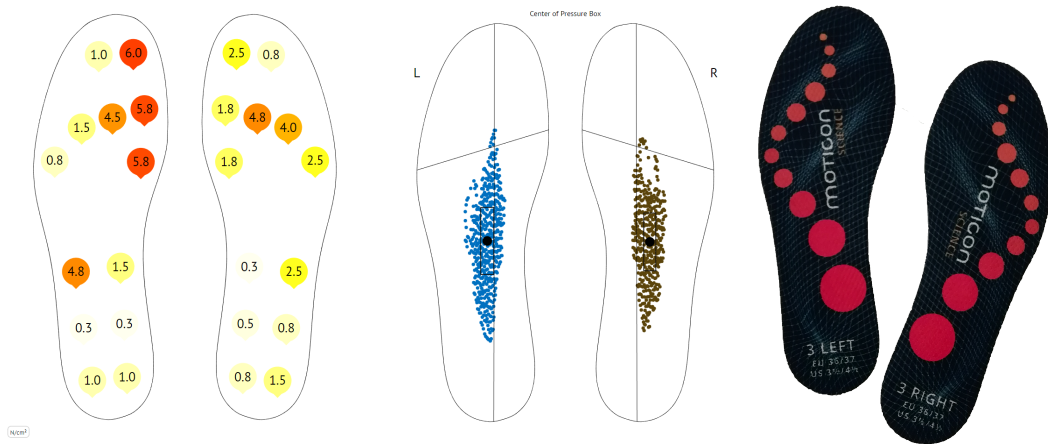
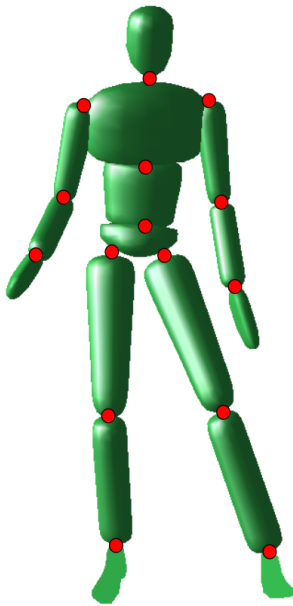


**Figure 3.13:** Moticon Pressure Soles. The sensor layout is shown at the left. Each sensor measures the local pressure. An example measurement with the CoP position is shown in the middle and a pair of the Insole3 model at the right.

## 4 Modeling of Human Movement

We analyze human movement and motion capture data based on rigid body models. Such a model consists of several bodies that are connected by joints, resulting in a kinematic tree. A generic model of a human is shown in Figure 4.1. It consists of 16 bodies, 15 joints and is based on the anthropomorphic data by de Leva [139]. Each joint has specific ways it allows the child body to move with respect to the parent body, so-called DoF. In this work, we use rotational and translational joints with up to 3 DoF.

The pelvis body is the first body of the model and "attached" to the lab frame via a so-called floating base, which allows to model translational and rotational movement in 3D space. The arms, the legs and the trunk consist of three rigid bodies each. Head and neck are modeled as a single body. Each body is described by the following quantities: dimensions, mass, inertia and the relative CoM position. These quantities are subject-specific and will be derived based on literature from the static marker recording as follows.



Body	Parent	Joint Name
Pelvis	Lab Frame	Floating Base
Middle Trunk	Pelvis	Lumbar Spine
Upper Trunk	Middle Trunk	Thorax Spine
Head	Upper Trunk	Neck
Upper Arm	Upper Trunk	Shoulder
Fore Arm	Upper Arm	Elbow
Hand	Fore Arm	Wrist
Thigh	Pelvis	Hip
Shank	Thigh	Knee
Foot	Shanke	Ankle

**Figure 4.1:** Left: A generic rigid body model of a human. Joints are visualized in red. Right: Table with the kinematic tree of the model.

## 4.1 Subject Specific Modeling

### Segments

In context of modeling human subjects, we now refer to all bodies, that represent parts of the body as *Segments*. The length of each segment and the joint center locations are estimated from the static trial recording and the measured subject height based on the work by Leardini et al.[128], Cappozzo et al. [129] and Rab et al. [127]. Table 4.1 shows the proximal and distal landmarks of each segment. Since there are no markers at the very end of the feet and hands, the segment length is estimated with a scaling factor from the distance between the proximal and the most distal marker. We use a factor of 2 for the hands and a factor of 1.2 for the feet.

Body / Segment Name	Proximal Marker / Landmark	Distal Marker / Landmark
Pelvis	Hip Joint Center	LV5
Middle Trunk	LV5	MAI
Upper Trunk	MAI	CV7
Head	CV7	Subject Height
Upper Arm	Shoulder Joint Center	HLE
Fore Arm	HLE	USP
Hand	USP	2 * HM2
Thigh	Hip Joint Center	FLE
Shank	FLE	FAL
Foot	FCC	1.2 * FM1

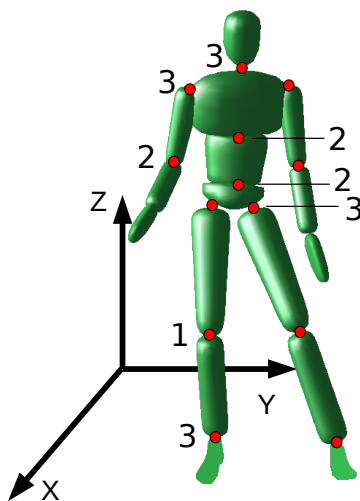
**Table 4.1:** Definition of segment lengths following Leardini et al.[128], Cappozzo et al. [129] and Rab et al. [127]. The table shows the proximal and distal landmarks for each segment. Hands are scaled by a factor of 2 and feet are scaled by factor of 1.2, since no markers are placed at the very end of the segment.

### Joint Center Locations

All segments are connected via rotational joints. The positions of the joint centers are defined as described in Table 4.2. The floating base is located at the Pelvis segment between the hip joint centers. We see that many joints are directly located at the midpoint between two markers. These are the wrists, elbows, knees and ankles following the definitions by Leardini et al.[128] and Cappozzo et al. [129]. The spinal joints are located on top of the midpoint between the two posterior iliac markers and on top of each other at the height of the LV5, MAI and CV7 markers. The hip joints are estimated following the pelvis model by Bell et al. [140]. Shoulder joints follow the definition by Rab et al. [127]. Code snippets for segment length and joint center location computation from the static trial can be found in the Appendix A.4.

Joint Name	Horizontal Location [X-Y Plane]	Vertical Location [Z-Direction]
Floating Base	Midpoint between Hip Joint Centers	
Lumbar Spine	Midpoint between IPS and IAS	LV5
Thorax Spine	Midpoint between IPS and IAS	MAI
Neck	Midpoint between IPS and IAS	CV7
Shoulder	SAE	0.17* SAE Distance below SAE
Elbow	Midpoint between HLE and HME	
Wrist	Midpoint between RSP and USP	
Hip	Midpoint between IPS and IAS +/- 0.36 * IAS Distance	0.3 * IAS Distance below IAS
Knee	Midpoint between FLE and FME	
Ankle	Midpoint between FAL and TAM	

**Table 4.2:** Definition of joint center locations in the horizontal plane and vertical direction.



Joint	Degrees of Freedom
3D Floating Base	TX, TY, TZ, RX, RY, RZ
Lumbar Spine	RY, RZ
Thorax Spine	RX, RY
Neck	RX, RY, RZ
Shoulder	RX, RY, RZ
Elbow	RY, RZ
Wrist	Fixed
Hip	RX, RY, RZ
Knee	RY
Ankle	RX, RY, RZ

**Figure 4.2:** The model with the location of the joints, the number DoF and the coordinate system. The table shows the rotation axes of each joint and order of rotation.

### Degrees of Freedom (DoF)

Figure 4.2 shows the model with the number of DoF per joint and their locations. The table shows all rotation axes of each joint (RX, RY, RZ) following the coordinate system of the model: the X-axis points along the sagittal plane to the front, the Y-axis perpendicular in the other horizontal direction and the Z-axis in the vertical direction. Neck, shoulder, hip and ankle joints are modeled as spherical joints with 3 DoF. Lumbar, thorax and elbow joint have 2 DoF each and the knee joints only have one rotational axis. A 6 DoF floating base with three translational DoF is attached to the Pelvis segment. It allows for translational movement in all three direction (TX, TY, TZ) and rotation around all axes.

### Dynamic Segment Properties

The dynamic properties of each segment are taken from Pablo de Leva's *Adjustments to Zatsiorsky-Seluyanov's segment inertia parameters* [139]. These are the CoM position relative to the segment length, the radius of gyration and the relative segment mass. The absolute CoM position is computed using the subject-specific segment length. The mass is linearly scaled with the length of the segment. The total mass of the model is adjusted to the measured mass of the subject. From the segment length  $l$ , mass  $m$  and radii of gyration  $r_i$ , the segments inertia  $\mathbf{I}$  is computed using

$$I_{ii} = m * (r_i * l)^2 \quad \text{for } i = [x, y, z] \quad (4.1)$$

Evaluation of the static trial and subject-specific modeling was automatized and implemented in Python and results in a Lua-model. The final model and the static trial are shown in Figure 4.3. Joint center locations are shown in white. Virtual markers are placed on the model.

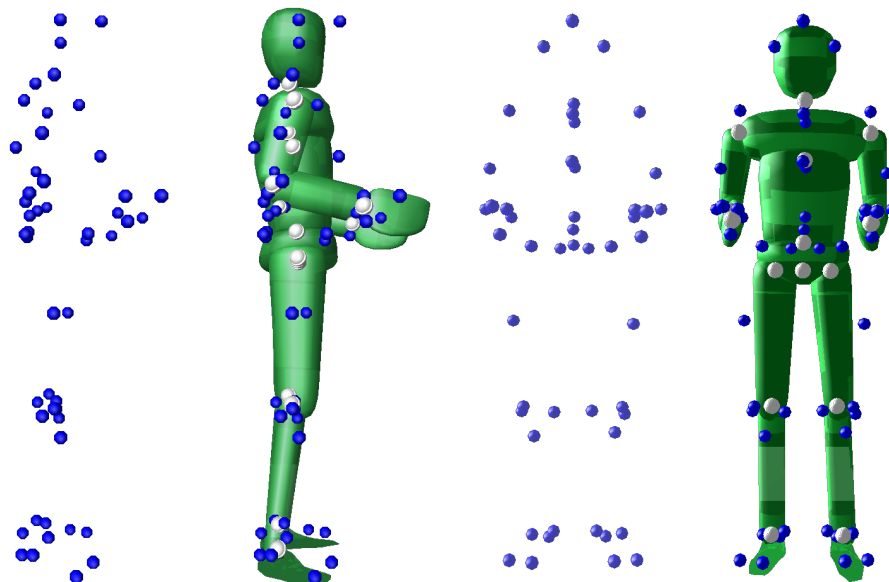


**Figure 4.3:** The static marker recording and the subject-specific model. Joint centers are shown in white.

## 4.2 Kinematics and Dynamics

### Kinematics

The state of a rigid body system with  $n_{dof}$  DoF is described using generalized coordinates  $\mathbf{q}$ , generalized velocities  $\dot{\mathbf{q}}$  and generalized accelerations  $\ddot{\mathbf{q}}$  [141]. Kinematics describe the relation between the model state and the position  $\mathbf{r}$ , velocity  $\dot{\mathbf{r}}$  and acceleration  $\ddot{\mathbf{r}}$  of body  $i$  in lab space. We define forward kinematics as:

$$(\mathbf{r}, \dot{\mathbf{r}}, \ddot{\mathbf{r}})_i = FK(\mathbf{q}, \dot{\mathbf{q}}, \ddot{\mathbf{q}}, i) \quad (4.2)$$

Computation of forward kinematics is well defined and there always exists a unique solutions. This is different for inverse kinematic, where different joint configurations can lead to the same body position:

$$(\mathbf{q}, \dot{\mathbf{q}}, \ddot{\mathbf{q}}) = IK(\mathbf{r}, \dot{\mathbf{r}}, \ddot{\mathbf{r}})_i \quad (4.3)$$

The reconstruction of the human movement from marker measurements is a typical inverse kinematics problem and will be discussed in more detail in Chapter 5.

### Dynamics

The dynamics describe the relation between the state of the rigid body system and all forces that can act on the system. Inverse dynamics computes the joint torques  $\tau$  for a known state:

$$\tau = ID(\mathbf{q}, \dot{\mathbf{q}}, \ddot{\mathbf{q}}) \quad (4.4)$$

Forward dynamics computes the joint acceleration for know position, velocity and torque:

$$\ddot{\mathbf{q}} = FD(\mathbf{q}, \dot{\mathbf{q}}, \tau) \quad (4.5)$$

The dynamics of a rigid body system can be described by the following equation [142]:

$$\mathbf{H}(\mathbf{q})\ddot{\mathbf{q}} + \mathbf{C}(\mathbf{q}, \dot{\mathbf{q}}) = \tau \quad (4.6)$$

where the matrix  $\mathbf{H}(\mathbf{q}) \in \mathbb{R}^{n_{dof} \times n_{dof}}$  is the generalized inertia matrix that is constructed from the current joint angles of the model, the inertia and the CoM positions of each segment.  $\mathbf{C}(\mathbf{q}, \dot{\mathbf{q}}) \in \mathbb{R}^{n_{dof}}$  is the generalized bias force (e.g. gravity or the Coriolis force) and  $\tau$  are the generalized forces applied at the joints. This equation holds when the model is in the air where no contacts to the environment exist and no external forces are applied. The rigid body model is not subject to an external constraint.

### Forced-based Contact Modeling

In this formulation we consider the contact as an external force acting on the rigid body system. This is, for example, the case when standing on a slackline. The contact interaction consists of contact forces  $\mathbf{F}$  and contact torques  $\mathbf{M}$  at a contact point  $\mathbf{p}$ . For simplicity we summarize the external forces in  $\mathbf{F}_{ext} = [\mathbf{M}, \mathbf{F}]$ . We can compute the generalized forces  $\tau_c$  resulting from an external force using:

$$\tau_c = \mathbf{G}(\mathbf{q}, \mathbf{p})^T \begin{bmatrix} \mathbf{M} \\ \mathbf{F} \end{bmatrix} = \mathbf{G}(\mathbf{q}, \mathbf{p})^T \mathbf{F}_{ext} \quad (4.7)$$

where  $\mathbf{G}(\mathbf{q}, \mathbf{p})$  is the 6D Jacobian for a point on a body that when multiplied with  $\dot{\mathbf{q}}$  gives a 6-D vector that has the global angular velocity as the first three entries and the global linear velocity as the last three entries. With external contact forces Equation 4.6 becomes:

$$\mathbf{H}(\mathbf{q})\ddot{\mathbf{q}} + \mathbf{C}(\mathbf{q}, \dot{\mathbf{q}}) = \boldsymbol{\tau} + \sum_{\text{contacts}} \boldsymbol{\tau}_c \quad (4.8)$$

### Constraint-based Contact Modeling

When a contact is established, the model is fixed in space with respect to the environment and constraint by a given contact point. In this formulation we assume a stationary, non-slipping, contact meaning that the position of the contact point is fixed in space. An additional constraint to Equation 4.6 is necessary:

$$\mathbf{H}(\mathbf{q})\ddot{\mathbf{q}} + \mathbf{C}(\mathbf{q}, \dot{\mathbf{q}}) = \boldsymbol{\tau} + \mathbf{G}(\mathbf{q})^T \boldsymbol{\lambda} \quad (4.9)$$

$$\mathbf{g}(\mathbf{q}) = \mathbf{0} \quad (4.10)$$

$$(4.11)$$

where  $\mathbf{g}(\mathbf{q})$  is a function that computes the distance of the contact point to its desired position.  $\mathbf{G}(\mathbf{q}) = \frac{\partial}{\partial \mathbf{q}} \mathbf{g}(\mathbf{q})$  is the contact Jacobian and  $\boldsymbol{\lambda}$  is the contact force. By differentiating the position constraints twice we find:

$$\mathbf{G}(\mathbf{q})\ddot{\mathbf{q}} + \dot{\mathbf{G}}(\mathbf{q})\dot{\mathbf{q}} = \boldsymbol{\gamma}(\mathbf{q}, \dot{\mathbf{q}}) = \mathbf{0} \quad (4.12)$$

Combining Equation 4.9 and 4.12 allows us to write the dynamics equations as a linear system:

$$\begin{bmatrix} \mathbf{H}(\mathbf{q}) & \mathbf{G}(\mathbf{q})^T \\ \mathbf{G}(\mathbf{q}) & 0 \end{bmatrix} \begin{bmatrix} \ddot{\mathbf{q}} \\ -\boldsymbol{\lambda} \end{bmatrix} = \begin{bmatrix} \boldsymbol{\tau} - \mathbf{C}(\mathbf{q}, \dot{\mathbf{q}}) \\ -\boldsymbol{\gamma}(\mathbf{q}, \dot{\mathbf{q}}) \end{bmatrix} \quad (4.13)$$

In case of non redundant constraints  $\mathbf{g}(\mathbf{q})$  this system is solvable for  $\ddot{\mathbf{q}}$  and  $\boldsymbol{\lambda}$ . To ensure that Equation 4.9 and Equation 4.13 are equivalent, the invariants of the constraints need to be fulfilled at the beginning of the contact:

$$\mathbf{g}(\mathbf{q}) = \mathbf{0} \quad (4.14)$$

$$\mathbf{G}(\mathbf{q})\dot{\mathbf{q}} = \mathbf{0} \quad (4.15)$$

In other words, the contact position needs to be reached by the system before Equation 4.13 is applied. The contact velocity needs to be zero, since the resulting contact acceleration will be zero.

### Impacts

The transition from a system without contacts to a system with a contact that is fixed with respect to the environment produces a discontinuity in the generalized velocity variables from  $\dot{\mathbf{q}}^-$  before the collision to  $\dot{\mathbf{q}}^+$  after the collision. This change can be computed using:

$$\begin{bmatrix} \mathbf{H}(\mathbf{q}) & \mathbf{G}(\mathbf{q}, \mathbf{p})^T \\ \mathbf{G}(\mathbf{q}, \mathbf{p}) & 0 \end{bmatrix} \begin{bmatrix} \dot{\mathbf{q}}^+ \\ -\boldsymbol{\Lambda} \end{bmatrix} = \begin{bmatrix} \mathbf{H}(\mathbf{q})\dot{\mathbf{q}}^- \\ -\mathbf{e}\mathbf{G}(\mathbf{q}, \mathbf{p})\dot{\mathbf{q}}^- \end{bmatrix} \quad (4.16)$$

where  $\boldsymbol{\Lambda}$  is the contact impulse. The upper part of Equation 4.16 describes the change of momentum of the system due to the collision. In the lower part the variable  $\mathbf{e}$  describes the corresponding velocity of the contact after the contact is established. We assume a perfect inelastic collision and a fixed contact, which means  $\mathbf{e} = 0$ .

### **Implementation**

For all computations we used the Rigid Body Dynamics Library (RBDL) [142]. Forward kinematic functions are called `CalcBodyToBaseCoordinates`, `CalcBodyWorldOrientation`, `CalcPointVelocity` and `CalcPointAcceleration`. Forward dynamics is implemented under the `ForwardDynamics` function. The contact Jacobian is computed using the `CalcPointJacobian6D` function. The exact recursive implementation is described in [141].



## 5 Reconstruction of Motion

There are several ways to reconstruct the underlying motion from marker motion capture data. Some kinematic data can directly be computed from the markers. The position of a segment, for example, can be defined as the mean of the markers attached to it. Joint angles can be computed from three markers, if the central marker coincides with the joint axes. The two approaches used in this work are based on the subject-specific rigid body model. Inverse kinematics computes the joint angles for a given frame of the measurement. Optimal control allows us to compute the whole joint angle trajectory for an entire motion.

### 5.1 Inverse Kinematic Reconstruction

With the kinematic model of the subject at hand, we want to reconstruct the pose for a given marker measurement. The computation of joint angles can be formulated as a least-squares optimization problem:

$$\min_{\mathbf{q}} \sum_{i=1}^{n_m} \|\mathbf{m}_i(\mathbf{q}) - \mathbf{m}_i^*\|^2 \quad (5.1)$$

where  $\mathbf{m}_i(\mathbf{q})$  is the position of the virtual marker  $i$  on the model given the joint angles  $\mathbf{q}$ . The measured reference position of the marker is denoted with  $\mathbf{m}_i^*$ . Both are given in the lab coordinate system. The optimization takes all  $n_m$  markers into account. As derived in Section 3.1.1 these are 45 for slackline measurements and 43 for the walking trials. The software tool Puppeteer by Martin Felis [143] employs an iterative Levenberg-Marquardt algorithm [144] to solve Equation 5.1. It defines the total error as the vector of all position differences:

$$\mathbf{e}(\mathbf{q}) = \begin{bmatrix} m_{1x}(\mathbf{q}) - m_{1x}^* \\ m_{1y}(\mathbf{q}) - m_{1y}^* \\ m_{1z}(\mathbf{q}) - m_{1z}^* \\ m_{2x}(\mathbf{q}) - m_{2x}^* \\ \vdots \\ m_{n_m z}(\mathbf{q}) - m_{n_m z}^* \end{bmatrix} \quad (5.2)$$

In each iteration of the algorithm it computes the change in joint angles  $\dot{\mathbf{q}}$  that reduces the residual vector  $\mathbf{e}$ . With  $\mathbf{J}$  being the matrix of all point Jacobians stacked, we define

$$\mathbf{r} \equiv \mathbf{e} - \mathbf{J}\dot{\mathbf{q}} \quad (5.3)$$

and minimize  $\mathbf{r}^2$ . Regarding the fact that rotational joints have the same configuration after a rotation about  $2\pi$  or  $360^\circ$ , we see that the system is highly redundant and that there are multiple solutions to this equation. Further, there are redundant configurations, already for a single three DoF joint that lead to the same orientation.

A unique solution is not always guaranteed when computing joint angles for a specific orientation. Another issue are singularities, where the Jacobian matrix does not have full rank. This happens when two rotational axis of a kinematic chain are in a parallel configuration and rotation of either would result in the same movement in task space. To introduce numerical robustness towards redundancies and singularities, a damping factor is added and the square of the joint velocity is minimized as well. We are looking for the minimum change in angles that leads to a solution. Summarizing, the cost function of the optimization is the following:

$$E(\mathbf{q}) = \frac{1}{2} \mathbf{r}^T \mathbf{r} + \frac{\lambda}{2} \dot{\mathbf{q}}^T \dot{\mathbf{q}} \quad (5.4)$$

where  $\lambda$  is the damping factor. We compute the derivative of Equation (5.4) with respect to  $\dot{\mathbf{q}}$  and set it to zero:

$$\begin{aligned} \frac{\partial E(\dot{\mathbf{q}})}{\partial \dot{\mathbf{q}}} &= \frac{\partial}{\partial \dot{\mathbf{q}}} \left[ \frac{1}{2} (\mathbf{e} - \mathbf{J}\dot{\mathbf{q}})^T (\mathbf{e} - \mathbf{J}\dot{\mathbf{q}}) + \frac{\lambda}{2} \dot{\mathbf{q}}^T \dot{\mathbf{q}} \right] \\ &= -\mathbf{J}^T \mathbf{e} + (\mathbf{J}^T \mathbf{J} + \lambda \mathbf{E}) \dot{\mathbf{q}} \\ &\stackrel{!}{=} 0 \end{aligned} \quad (5.5)$$

where  $\mathbf{E}$  is an identity matrix of the same size as  $\mathbf{J}^T \mathbf{J}$ . Solving for  $\dot{\mathbf{q}}$  leads to:

$$\dot{\mathbf{q}} = (\mathbf{J}^T \mathbf{J} + \lambda \mathbf{E})^{-1} \mathbf{J}^T \mathbf{e} \quad (5.6)$$

Additionally to the standard Levenberg-Marquardt algorithm, Sugihara proposed to add another weighting matrix proportional to  $\mathbf{e}$  to improve the convergence rate and add more robustness against singularities [145]:

$$W_{jj} = \frac{1}{2} (\mathbf{J}^T \mathbf{e})_j^2 \quad \text{for } j = 1 \dots 3n_m \quad (5.7)$$

Therefore, the update rule from step  $k$  to  $k + 1$  is:

$$\mathbf{q}_{k+1} = \mathbf{q}_k + (\mathbf{J}(\mathbf{q}_k)^T \mathbf{J}(\mathbf{q}_k) + \lambda \mathbf{E} + \mathbf{W}(\mathbf{q}_k))^{-1} \mathbf{J}(\mathbf{q}_k)^T \mathbf{e}(\mathbf{q}_k) \quad (5.8)$$

For each iteration, the Jacobian and residual vector are computed from the joint angles of the previous iteration. In Puppeteer the damping factor  $\lambda = 10^{-3}$ . The computation has two convergence criteria and one stopping criterion. Convergence is achieved if the desired position is reached ( $\|\mathbf{e}\| < 10^{-6}$ ) or if the step size per iteration is smaller than  $10^{-6}$ . This is the case when the model can not perfectly reproduce all marker positions. The algorithm then converges to the closest possible solution. In any case, the number of iterations is limited. We set the parameter of Puppeteer for the maximum number of iterations to  $max_{itter} = 1000$ .

There are several points to keep in mind when analyzing motion capture data based on inverse kinematics fitting.

- An initial guess  $\mathbf{q}_0$  is required. The solution strongly depends on  $\mathbf{q}_0$ .
- Convergence to local minima is possible due to the step size criterion and damping factor.
- Each frame is evaluated individually.

The computed joint configuration of the previous frame can be used to initialize the algorithm for the next frame, however, jumps in joint angles might still occur when initializing with a local minimum solution. Results from all frames are combined into the joint angle trajectory of the whole motion.

A common procedure is to apply filtering to smoothen the result and to account for the frame-by-frame based evaluation [146]. We applied a 5<sup>th</sup>-order Butterworth filter with a cutoff frequency of 9 Hz. There is no common agreement on the filter frequency. Winter suggests 6 Hz [27] for walking motions, but higher frequencies should be used for faster movements. Joint velocities and accelerations were computed using numerical differentiation. The resulting data represents the measured kinematics and is widely used for motion analysis [147]. The analysis method does not depend on the length of the marker recording or number of frames.

Further analysis beyond kinematic data requires additional measurements, such as interaction forces and a dynamic model of the subject like the one describes in Chapter 4. The overall CoM position, for example, depends on the mass and individual CoM position of each segment. The evaluation of angular momentum requires the individual segment inertia. The computation of joint torques requires knowledge of all external forces acting on the subject. In any case, there are various sources for error. Joint angles are derived on a frame-by-frame basis, the model is only an estimation of the actual mass distribution of the subject, and joint velocities and accelerations are derived through numeric differentiation.

All these factors combined can lead to physical inconsistencies. Nonetheless, we can perform a meaningful analysis, based on this approach. It is used in Chapter 7 and 8. An example, where a higher accuracy is required and the shortcomings are obvious, is in context of a slackline jumping motion in Chapter 11.

## 5.2 Optimal Control Based Motion Analysis

In the following section we describe how we can employ optimal control to reconstruct human movement from marker motion capture data. The key difference to the approach in Section 5.1 is that the optimization is carried out simultaneously over the whole motion and not just for single frames. The solution of the Optimal Control Problem (OCP) is therefore time consistent.

Additionally, the OCP framework allows us to formulate constraints that have to be respected by the resulting motion. These can be Newton's Equations of Motion (EoM), external contacts and physical limitations such as joint limits. In the following least-squares cost function we minimize the distance between the positions  $\mathbf{m}_i$  of the virtual markers on the model and the  $n_m$  recorded marker trajectories  $\mathbf{m}_i^*$  over the time  $t \in [0, T]$  of the motion. In the following we present a multi phase OCP formulation with  $n_{ph}$  phases:

$$\min_{\mathbf{x}, \mathbf{u}, \mathbf{p}} \sum_{i=0}^{n_{ph}-1} \int_{t_{i-1}}^{t_i} \sum_{i=0}^{n_m-1} \|\mathbf{m}_i(\mathbf{q}(t)) - \mathbf{m}_i^*(t)\|^2 dt \quad (5.9a)$$

subject to:

$$\dot{\mathbf{x}}(t) = f_i(t, \mathbf{x}(t), \mathbf{u}(t), \mathbf{p}) \quad (5.9b)$$

$$\mathbf{x}(t_{i+1}^+) = h_i(\mathbf{x}(t_{i+1}^-), \mathbf{p}) \quad (5.9c)$$

$$\mathbf{g}(t, \mathbf{x}(t), \mathbf{u}(t), \mathbf{p}) \geq 0 \quad (5.9d)$$

$$\mathbf{r}^{eq}(\mathbf{x}(0), \dots, \mathbf{x}(t_f), \mathbf{p}) = 0 \quad (5.9e)$$

$$\mathbf{r}^{ineq}(\mathbf{x}(0), \dots, \mathbf{x}(t_f), \mathbf{p}) \geq 0 \quad (5.9f)$$

The system is modeled with time dependent states  $\mathbf{x}(t)$  and free parameters  $\mathbf{p}$  that are fixed in time. The goal of the optimization is to find controls  $\mathbf{u}(t)$  such that the objective function is minimized. For human movement reconstruction, we define the state vector  $\mathbf{x} = [\mathbf{q}, \dot{\mathbf{q}}]$  as the joint angles and joint velocities. To implement a forward dynamics simulation we define the control vector as the acting joint torques  $\boldsymbol{\tau}$ .

The right hand side  $\dot{\mathbf{x}}(\cdot) = f(\cdot)$  is an Ordinary Differential Equations (ODE) that depend on the states, parameters and controls. We reformulate the EoM derived in Section 4.2 as first order differential equations and define the right hand side as  $\dot{\mathbf{x}} = [\dot{\mathbf{q}}, FD(\mathbf{x}, \mathbf{u})]$ , using the Forward Dynamics of the rigid body system. An OCP can be formulated with different phases, where each phase is subject to a different right hand side function. Multiple phases are necessary in the case that the motion includes contacts that are established or released.

The function  $h$  hereby describes the state change between consecutive phases. This can be the impact dynamics described in Equation 4.16. A physical contact can be implemented as a set of constraints, such that the position of a given segment is reached at the end of a phase. During the contact phase, the contact forces are modeled as inequality constraints. A ground contact force, for example, can only act unidirectionally and therefore contact forces need to be larger than zero.

Limitations on the joint angle, velocity, accelerations and torques can be formulated as boundary constraints  $r(\cdot)$ . A more general multi phase OCP objective function can be found, for example, in [148] and looks as follows:

$$\min_{\mathbf{x}, \mathbf{u}, \mathbf{p}, T} \sum_{i=0}^{n_{ph}-1} \int_{t_{i-1}}^{t_i} \phi_{L_i}(t, \mathbf{x}(t), \mathbf{u}(t), \mathbf{p}) dt + \sum_{i=0}^{n_{ph}-1} \phi_{M_i}(t_i, \mathbf{x}(t_i), \mathbf{p}) \quad (5.10)$$

Here, we distinguish between Lagrange and Mayer-type objective functions. The Lagrange function is integrated along a time horizon, while the Mayer function is evaluated at one point in time. Additionally, the time  $T$  of the motion can also be a free optimization parameter. The table below describes all variables of the OCP and their use in human movement reconstruction.

Variable	Description	Possible use for Movement Reconstruction
$\mathbf{x}$	States of the System	Joint angles, velocities, acceleration
$\mathbf{u}$	Controls	Joint Torques
$\mathbf{p}$	Parameters	Optimize for Model Parameters
$\phi_L$	Lagrange-Type Objective Function	Tracking of Marker Position, Regularization
$\phi_M$	Mayer-Type Objective Function	Minimize Movement Time
$i$	Phase Index	Different Contacts
$n_{ph}$	The number of phases	Implementation of different Dynamics
$t_i$	The time of each phase $t \in [0, T]$	Optimize Movement Timing
$t_i^+$	Beginning time of phase $i$	
$t_i^-$	End time of phase $i$	
$f_i$	System Dynamics (State Derivative)	Implement Equations of Motion
$h_i$	Transition function between Phases	Formulate Impact Dynamics
$g$	Path Constraints	Limit Joint Angles, Velocities, Torques
$r$	Point Constraints	Constraint Contact Points and Forces

There are three ways for solving nonlinear OCP in the literature: dynamic programming, indirect methods and direct methods. In this work we used the software package MUSCOD-II [149, 150] which uses the direct multiple shooting method developed by Bock et al. [151]. This approach discretizes the states and controls with respect to time. The result is a large but structured Nonlinear Program (NLP) which is solved by the Sequential Quadratic Programming (SQP) method.

### Control Discretization

Each phase  $i$  is divided into  $m_i$  subintervals:

$$I_{i,j} := [t_{i,j}, t_{i,j+1}], \quad j \in \{0, 1, \dots, m_i - 1\} \quad (5.11)$$

with intermediate time points  $t_{i,j}$ . The controls  $\mathbf{u}_i$  are defined by a piecewise approximation  $\hat{\mathbf{u}}$  on this grid.

$$\hat{\mathbf{u}}_i(t) := \boldsymbol{\varphi}_{i,j}(t, \boldsymbol{\rho}_{i,j}), \quad t \in I_{i,j}, \quad j = 0, 1, \dots, m_i - 1 \quad (5.12)$$

with the basis function  $\varphi(\cdot)$  of the approximation. In MUSCOD-II, they can be constant, linear, linear continuous or cubic. Continuity can be enforced either overall or only during each phase. The number of parameters  $\rho_{i,j}$  depends on the type of function. Piecewise constant approximation requires one parameter per multiple shooting interval, linear approximation two and so on. Higher polynomials are possible but mainly increase the problem complexity.

### State Discretization

For simplicity, we assume the same discretization for the states and controls. Theoretically, this is not required, however it is implemented this way in MUSCOD-II. For each interval the states are handled as Initial Value Problem (IVP). This approach is also known as multiple shooting. We define the initial value of phase  $i$  and multiple-shooting interval  $j$  as  $\mathbf{x}(t_{i,j}) = \mathbf{X}_{i,j}$  and parameterize the states as:

$$\dot{\mathbf{x}} = \mathbf{f}_i(t, \mathbf{x}, \boldsymbol{\varphi}(t, \boldsymbol{\rho}_{i,j})) \quad (5.13)$$

The IVP is solved for all shooting intervals simultaneously. To obtain a continuous solution, continuity conditions are enforced at all shooting nodes.

$$\mathbf{x}(t_{i,j+1}, \mathbf{X}_{i,j}, \boldsymbol{\rho}_{i,j}) - \mathbf{X}_{i,j+1} = 0 \quad \text{for } j = 0, 1, \dots, m_i - 1 \quad (5.14)$$

that ensure that the end point of each multiple shooting interval is equal to the starting point of the next.

### Resulting Discretized Optimal Control Problem

The continuous path constraints of Equation 5.9d are evaluated on each shooting node.

$$\mathbf{g}(\mathbf{X}_{i,j}, \boldsymbol{\rho}_{i,j}, \mathbf{p}) \geq 0 \quad \text{for } j = 0, 1, \dots, m_i - 1 \quad (5.15)$$

For constant and linear approximation of the controls, their boundaries are also respected between the shooting nodes, however, upper and lower bounds of the states might be violated between shooting nodes. Therefore one has to choose the multiple shooting intervals close enough to avoid this. To simplify the notation, we define the vector  $\mathbf{y}$  with all discretized multiple shooting variables:

$$\mathbf{y} := (\mathbf{X}_{i,j}, \boldsymbol{\rho}_{i,j}, \mathbf{p}) \quad (5.16)$$

and formulate the discretized objective function  $F(\mathbf{y})$ .

All equality constraints, including the continuity constraints from Equation 5.14 are formulated as  $G(\mathbf{y})$  and all inequality constraints as  $R(\mathbf{y})$ . The discretized optimal control problem can then be written as a finite high dimensional NLP.

$$\min_{\mathbf{y}} F(\mathbf{y}) \quad (5.17a)$$

subject to:

$$G(\mathbf{y}) = 0 \quad (5.17b)$$

$$R(\mathbf{y}) \geq 0 \quad (5.17c)$$

### Sequential Quadratic Programming (SQP)

In MUSCOD-II this problem is solved using SQP. Starting from an initial guess  $\mathbf{y}_0$  the SQP algorithm iterates

$$\mathbf{y}_{k+1} = \mathbf{y}_k + \alpha_k \Delta \mathbf{y}_k \quad (5.18)$$

with a step direction  $\Delta \mathbf{y}_k$  and step length  $\alpha_k$ .  $\alpha_k$  is adjusted according to various line search strategies. In each iteration  $k$  the the SQP algorithm solves a Quadratic Programming (QP) subproblem to find  $\Delta \mathbf{y}_k$ .

$$\min_{\Delta \mathbf{y}_k \in \Omega} \nabla F(\mathbf{y}_k) \Delta \mathbf{y}_k + \frac{1}{2} \Delta \mathbf{y}_k^T \mathbf{H}_k \Delta \mathbf{y}_k \quad (5.19a)$$

subject to:

$$G(\mathbf{y}_k) + \nabla_{\mathbf{y}} G(\mathbf{y}_k)^T \Delta \mathbf{y}_k = 0 \quad (5.19b)$$

$$R(\mathbf{y}_k) + \nabla_{\mathbf{y}} R(\mathbf{y}_k)^T \Delta \mathbf{y}_k \geq 0 \quad (5.19c)$$

where  $\nabla_{\mathbf{y}} G(\mathbf{y}_k)$  and  $\nabla_{\mathbf{y}} R(\mathbf{y}_k)$  are the Jacobians and  $\mathbf{H}_k$  is the approximated Hessian of the Lagrange function. Using an exact Hessian matrix can become computationally expensive and is therefore avoided. A bounded trust region  $\Omega \in \mathbb{R}^n$  has to be specified to have a well defined QP. In unconstrained cases, the SQP method corresponds to Newton's method for finding a point where the gradient vanishes. Under constraints, the method is equivalent to applying Newton's method to the Karush-Kuhn-Tucker (KKT), first order optimality conditions of the problem.

### 5.3 Comparison of the two Methods

Table 5.1 summarizes the two proposed approaches and highlights the crucial differences. Inverse kinematics can be applied to any kind of marker measurement provided a kinematic model. In this work we analyze large movement data sets based on this method in Chapter 7, 8 and 9. Optimal control requires a problem specific formulation that describes the different phases of the motion and their dynamics. It allows us to compute time consistent physical quantities such as the joint torques and interaction forces. The OCP-based analysis is computation-heavy and limited to a few seconds of motion due to numeric complexity. We used the OCP approach in Chapter 11 to analyze slackline jumping. In this context we compared the two methods and their results.

	Inverse Kinematics	Optimal Control
Formulation	General	Problem Specific
Approach	Frame-by-Frame	Whole Motion Optimization
Computation Time	Approximately 10 fps	Possibly days
Motion Length	Indefinitely	Few seconds per optimization problem
Kinematics	Unconstrained least squares fit	Kinematic constraints
Model-based evaluation	Inconsistent	Newton's Equations of Motion
External Forces	×	Part of problem formulation
Time Consistent	×	✓

**Table 5.1:** Comparison of the two motion reconstruction approaches. Important differences are highlighted with the preferred option in green. We see the advantages of the OCP formulation. On the downside, it requires a specific formulation for each motion, loads of computation time and can not be applied to longer recordings in a single optimization.

## **Part III**

# **Analysis of Static and Dynamic Balance**



## 6 Static Balance Test

In this chapter we present the protocol of the static balance test and the different ways to evaluate the data. The test is performed by all participants of both studies following the same protocol. We discuss the following questions:

- What parameters are there in the literature to evaluate static balancing?
- How do these parameters relate to balance?
- Are the parameters correlated or do they contain new information?

We want to use the results of this literature review to compare static balance of all participants. In the slackline study we intend to divide the beginner group into a balance-experienced and a balance-inexperienced subgroup. In the "Schizophrenia and the Moving Body" study we compare static balance capabilities of persons with schizophrenia and a control group to analyze if balance is impaired.

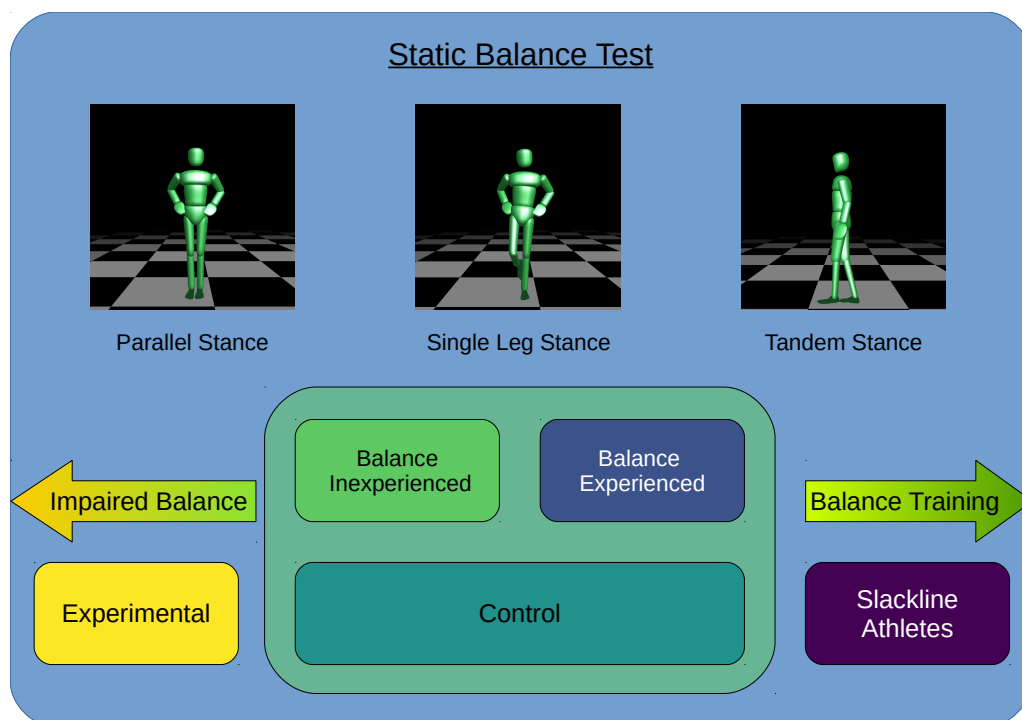


**Figure 6.1:** Overview of the Static Balance Test. All participants perform the three different tasks, once with eyes open and once with eyes closed and for both leg configurations. We want to investigate the effect of balance training and schizophrenia on static balance.

## 6.1 Balance Test Protocol

The static balance test consists of five individual tasks as visualized in Figure 6.1. The following balance situations were performed in sequence:

- **Parallel Stance:** Standing on both feet, with the feet close together.
- **Single Leg Stance:** Standing on one foot. One trial for each foot.
- **Tandem Stance:** Standing with the feet aligned. The heel of one foot is in touch with the toes of the other. One trial for each foot in front.

Subjects performed parallel stance once, the tandem once for each leg in front and single leg stance once on each leg. The total time for each task was 1 min. After 30 s participants were instructed to close their eyes and balance for another 30 s. They were instructed to maintain their hands on the pelvis and remain in the pose for as long as possible.

A step or arm movement should only occur to prevent severe falling. In case of a fall during the eyes open situation, subjects were asked to reassume the pose and continue balancing. If they fell after closing their eyes we continued with the next task. A 30 s break was given between each balancing task. For single leg balancing and the tandem stance, the (leading) foot for the first trial was chosen at random and switched for the second trial.

We used Bertec *FP4060\*08\*2000* force plates and recorded the GRF and CoP position at a rate of 900 Hz as described in Section 3.4. Tape marks were placed on the force plates to ensure the correct alignment and positioning of the feet. The Anterior-Posterior (AP) direction was aligned with the X axis of the lab coordinate system and the Medial-Lateral (ML) direction with the Y axis.

Subjects started outside the force plate, walked into the position at their own speed and placed the hands on the pelvis when they were stable. The recording was then started. After 60 s participants were instructed to step off the force plate and the recording was stopped.

## 6.2 Visual Evaluation

Evaluation of static balancing can be either done based on visual observations or by analysis of force plate data [75, 152]. Table 6.1 lists possible outcomes of static balancing and a scoring system, similar to what Berg et al. [54] or Ribeiro et al. [153] suggest. However, simply applying this rating has several pitfalls and requires a uniform understanding of the task by all participants. For example, when giving the instructions to stay in balance for as long as possible, some participants might still use their hands early and thus manage well (Score: 2), while others keep their hands at the pelvis and step off the force plate close to the end of the trial (Score: 5).

Following up on this thought, we find that the scoring does not see a difference between failing at the beginning or at the end of the trial. Hence, only the following two visual evaluations were considered as they are coherent with the given instructions: success vs. fall and, in case, that a subject failed, the time in balance.

Outcome / Recovery Movement	Balance Score
Stable throughout the task	0
Sliding movement of the stance foot	1
Arms were taken off the pelvis	2
One Step after which balance was regained	3
Multiple steps	4
Stepping off the force plate	5

**Table 6.1:** Possible outcomes of a balance task and respective balance scores as it is suggested and used in the literature [140].

### Success Rate

This is a binomial metric answering the question whether the subject succeeded to maintain balance for the full duration of the balance task. Everything other than a balance score of 0 according to Table 6.1 is considered a fall. This interpretation should be also clear to every participant. The main goal is to maintain balance without falling or performing a recovery movement.

### Time in Balance

We record the time, when the subject failed to maintain balance and performed a recovery movement. This gives more insight in the actual balance capabilities of the group, as the metric is able to differentiate between trials that fail at the very beginning and those that fail close to the end. Again, it should be made clear to all participants that they have to maintain balance for as long as possible and we treat every balance recovery movement in a uniform way by stopping the balance time.

### 6.3 Center of Pressure Sway Analysis

Since visual evaluation is not able to analyze successful trials in more detail, we rely on force plate data to do so. The analysis of CoP sway as a measure for balance performance is widely used in the literature. So-called stabilometric parameters aim to summarize the CoP trajectory into a single value. These are then used for statistical group comparison. There is a great number of different parameters in the literature.

Prieto et al. [154] proposed and evaluated more than 20 stabilometric parameters in 1996. 20 years later, Yamamoto et al. [81] used 73 parameters in their analysis. In many cases it is not obvious how the parameters are related to good or bad balance, as discussed by Raymakers et al. [75].

#### CoP Trajectory Conventions:

The force plate measurement consists of  $N$  data points with X and Y coordinates of the CoP. They represent the AP and ML direction in the lab coordinate system. We transformed the measurement from the lab frame  $O$  into the local frame by subtracting the trajectory mean from all data points and define:

$$AP[n] = AP_O[n] - \overline{AP} \quad (6.1)$$

$$ML[n] = ML_O[n] - \overline{ML} \quad (6.2)$$

Additionally, Resultant Distance (RD) is defined as the absolute 2D distance from the mean:

$$RD[n] = \sqrt{AP[n]^2 + ML[n]^2} \quad (6.3)$$

Further evaluation is based on these three trajectories, the number of measurement points  $N$  and the total time of the measurement  $T$ . In the following we present the proposed parameters by Prieto et al. [154] and discuss which ones are reasonable. They can be divided into distance, area and frequency measures.

#### Distance Measures

All proposed distance measures are summarized in Table 6.2. They are the Mean Absolute Distance (MDIST), the Standard Deviation of the Trajectory (RDIST), the Total Excursion (TOTEX) and the Mean Velocity (MVEL). MDIST and RDIST are very similar and highly correlated parameters [154]. We added the RATIO parameter to relate AP and ML distance measures. We assume that good balance control keeps the CoM close to the center, resulting in low sway distance values. The same is true for TOTEX and MVEL. Good balance control should result in a low velocity and a small excursion path. The only difference between MVEL and TOTEX is the normalization to the time of the measurement. The range does only depend on two points of the trajectory and is highly sensitive to a single balance movement.

Name	Description	Variable [X]	Formula
MDIST	Mean Absolute Distance	ML, AP, RD	$1/N \sum  X $
RDIST	Root Mean Square Distance	ML, AP, RD	$\sqrt{1/N \sum X^2}$
RATIO	Ratio between AP and ML RDIST		$RDIST_{ML}/RDIST_{AP}$
TOTEX	Total Excursion		$\sum_{n=1}^{N-1} [(AP[n+1] - AP[n])^2 + (ML[n+1] - ML[n])^2]^{\frac{1}{2}}$
TOTEX (AP/ML)	AP/ ML Excursion	ML, AP	$\sum_{n=1}^{N-1}  (X[n+1] - X[n]) $
MVEL	Mean Velocity	ML, AP, RD	$TOTEX_{ML,AP}/T$
Range	Total Range	ML, AP, RD	$Max(X) - Min(X)$

**Table 6.2:** CoP distance measures that summarize the CoP trajectory in a single parameter.

### Area Measures

Area measures try to estimate the area that encloses 95% of the CoP path. This can be either done by a circle or an ellipse. A larger sway area is interpreted as worse balance control. The circular area *Area - CC* is defined as:

$$Area - CC = \pi * (MDIST + 1.645 * s_{RD}) \quad (6.4)$$

$$s_{RD} = \sqrt{RDIST^2 - MDIST^2}$$

using the standard deviation of the resultant distance  $s_{RD}$ . The ellipse *Area - CE* is computed with the standard deviation  $s_{ML/AP}$  and the covariance  $c_{MLAP}$  between the AP and ML direction:

$$Area - CE = 6 * \pi * (s_{AP}^2 s_{ML}^2 - c_{MLAP}^2)^{\frac{1}{2}} \quad (6.5)$$

This elliptic area estimation should be more accurate since there are two fitting parameters instead of only one in the circle case. The area parameters are obviously highly correlated to the RDIST values. It is expected that the analysis is more conclusive when look at the RDIST values for ML and AP direction individually, rather than looking at their squared product.

### Hybrid Measures

Hybrid measures are defined by putting many of the before mentioned parameters into relation to each other. The sway area *Area-SW* can be interpreted as the product of MVEL and MDIST:

$$Area - SW = \frac{1}{2T} \sum_{n=1}^{N-1} [(AP[n+1] - AP[n])^2 + (ML[n+1] - ML[n])^2]^{\frac{1}{2}} \quad (6.6)$$

We expect good balance control to result in lower velocity and close distance to the center and therefore a small value for the sway area.

The Mean Frequency (MFREQ) is defined as the ratio between the mean velocity and the mean distance. It is the frequency at which the CoP trajectory would oscillate if it was perfectly harmonic.

$$MFREQ = \frac{MVEL}{2\pi MDIST} \quad (6.7)$$

Again, this can be defined for the ML, AP and RD trajectory. Since we assume small velocity and small distance values it is unclear if a small or large value for the mean frequency is to be expected or if this actually could be constant.

The Fractal Dimension (FD) compares the area against the excursion path. In other words, how much of the area is covered by the trajectory. Again, the area can either be defined using the diameter of a circle or of an ellipse.

$$FD = \log(N)/\log(Nd/TOTEX) \quad \text{with} \quad (6.8)$$

$$d_{FD-CC} = 2(MDIST + 1.645s_{RD}) \quad \text{or} \quad (6.9)$$

$$d_{FD-CE} = 24 * (s_{AP}^2 s_{ML}^2 - c_{MLAP}^2)^{\frac{1}{2}} \quad (6.10)$$

### Frequency Measures

Frequency measures analyze the power spectrum of the CoP trajectories when performing a fast Fourier transform [155, 156]. We considered the parameters presented in Table 6.3. The relation of these frequency measures to balance is not clear, however they are computed and compared in many scenarios in the literature [157, 158].

Name	Description	Variable
Power	Integrated Area of the Power Spectrum	ML, AP, RD
50% Frequency	Median frequency below which 50 % of the power is found	ML, AP, RD
95% Frequency	Frequency below which 95 % of the power is found	ML, AP, RD
CoP Frequency	Weighted Mean of the AP and ML 50% Frequency by Power	

**Table 6.3:** CoP frequency measures.

### Normalization to Body Factors

Chiari et al. [159] investigated the correlation of these parameters with respect to body factors such as height, weight, stance angle and foot size. They found correlation between distance parameters and subject height. Looking at the inverted pendulum model [80, 160] in Figure 6.2 and Equation 6.11, we see that the CoP position is in first order equivalent to the CoM ground projection. The angle  $\varphi$  relates the height of the CoM to the CoP. Movement of the CoM during the balance task results in the CoP trajectory that is visualized in the support polygon. We conclude, that normalization of CoP data by subject height is plausible when assuming that balance control is also related to tilt by means of the angle  $\varphi$ .

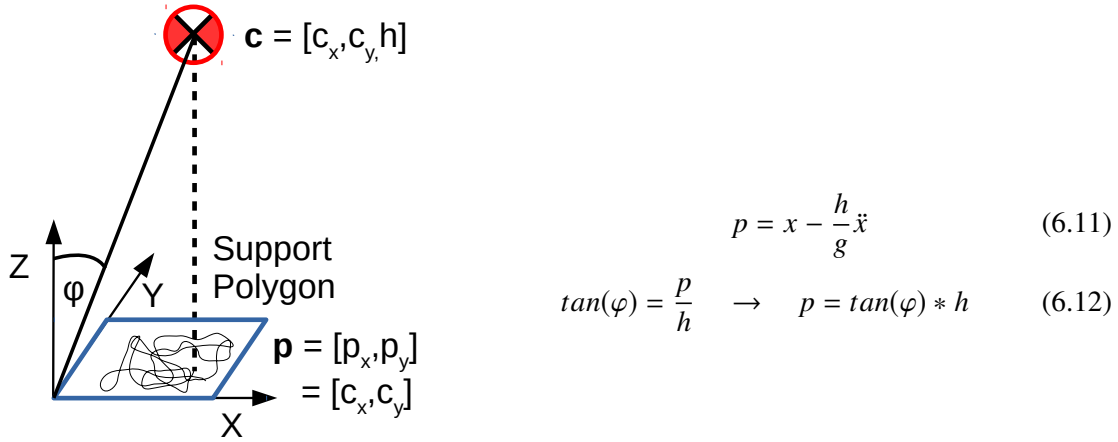


**Figure 6.2:** The inverted pendulum model. The CoP is in first order equivalent to the CoM ground projection.

## 6.4 Choice of Parameters for CoP sway analysis

All parameters presented above are based on the same two trajectories. We therefore expect many of them to convey redundant information. In the following we decide which ones to use for the group comparison and which ones to dismiss. We used all measurements that were obtained during the two motion capture studies and evaluated data from 66 participants and more than 400 successful balance tasks of 30 s each.

Figure 6.3 shows four correlation plots between the different measures. We used Pearson's correlation  $r$  [161]. The top row compares distance and frequency measures for AP (left) and ML direction (right). Clustering of two groups is evident, the first group being all distance measures and the second group being most of the frequency measures. The only exception is the Power metric, which, though being a frequency measure, is highly correlated with the distance metrics. MVEL is highly correlated with distance measures and less correlated with frequency measures. The same findings hold for the RD trajectory in the lower left plot. Additionally, area measures correlate with distance measures and FD correlates with frequency measures. The Ratio metric is not correlated to any other measure.

The lower right plot shows significant correlation between AP and ML distance measures and little correlation between frequency measures. However, correlation is not as high as for parameters computed from the same trajectory. We therefore conclude that additional information can be found by analyzing AP and ML trajectories separately and that focusing on one direction is not sufficient. In conclusion, we decide to evaluate the following parameters: RDIST, MVEL, RATIO and MFREQ. From another perspective we can say that RDIST summarizes amplitude of the trajectory, MVEL the amplitude of the derivative and MFREQ the ratio between the two. We evaluated them for the AP and ML trajectory individually and discard the RD trajectory.

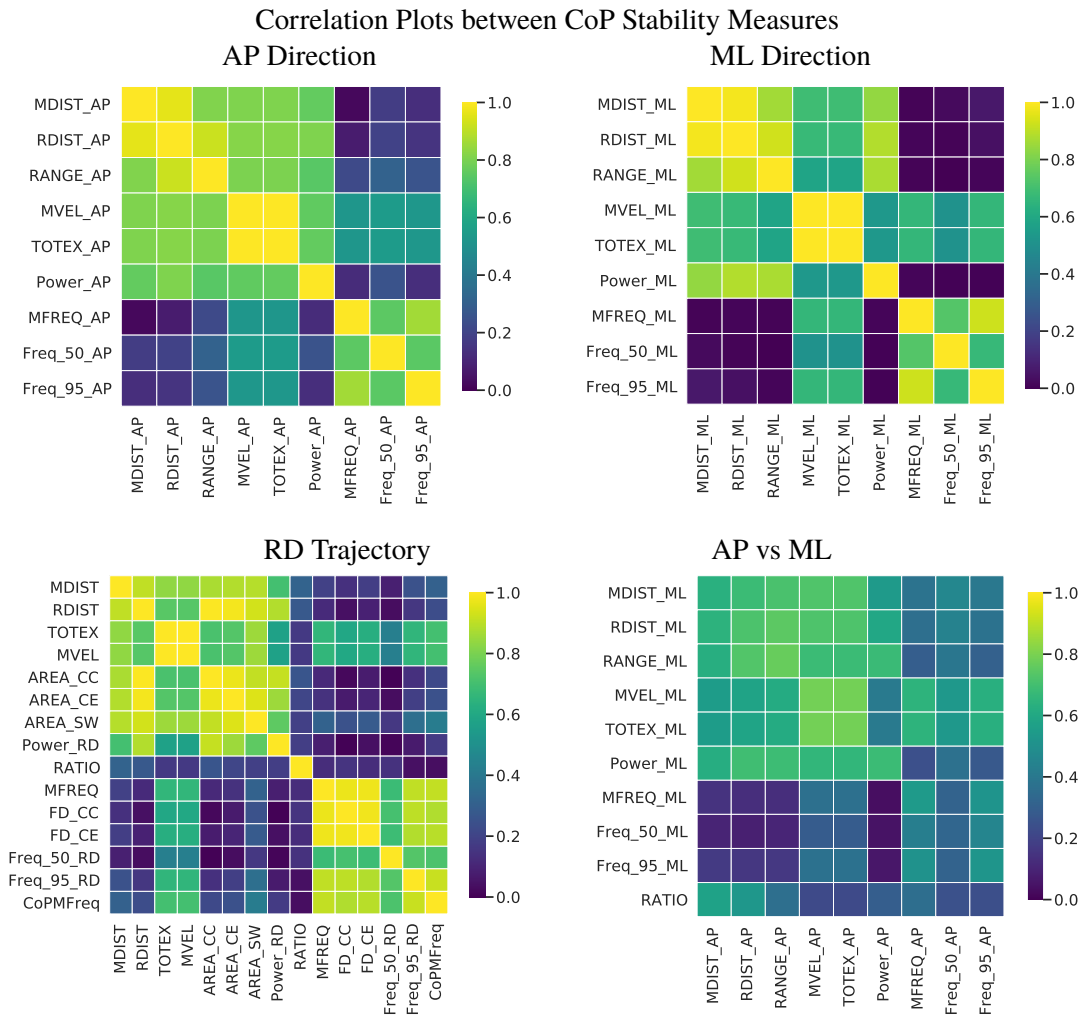


**Figure 6.3:** Correlation between stability metrics for all measured static balance tests in this work. The top row compares distance measures and frequency measures. The left bottom plot compares metrics based on the RD trajectory. At the bottom right we see the correlation between that AP and ML measures.

Figure 6.4 shows four example trajectories as they were measured during the studies. All measurements last 30 s. Parameters that we plan to evaluate are computed for the respective measurement. We want to illustrate how the parameters represent and summarize the visible features of the trajectories. The RDIST bounding box is shown in yellow. The upper row shows measurements with similar MFREQ, however there are significant differences in RDIST and MVEL. The lower left plot shows a low MFREQ due to low MVEL. The trajectory is comparably short. In the lower right plot, a measurement with a low RATIO parameter is shown. The CoP trajectory mainly moves in ML direction and only shows half the RDIST in AP direction.

Sample Measurements to demonstrate CoP parameters

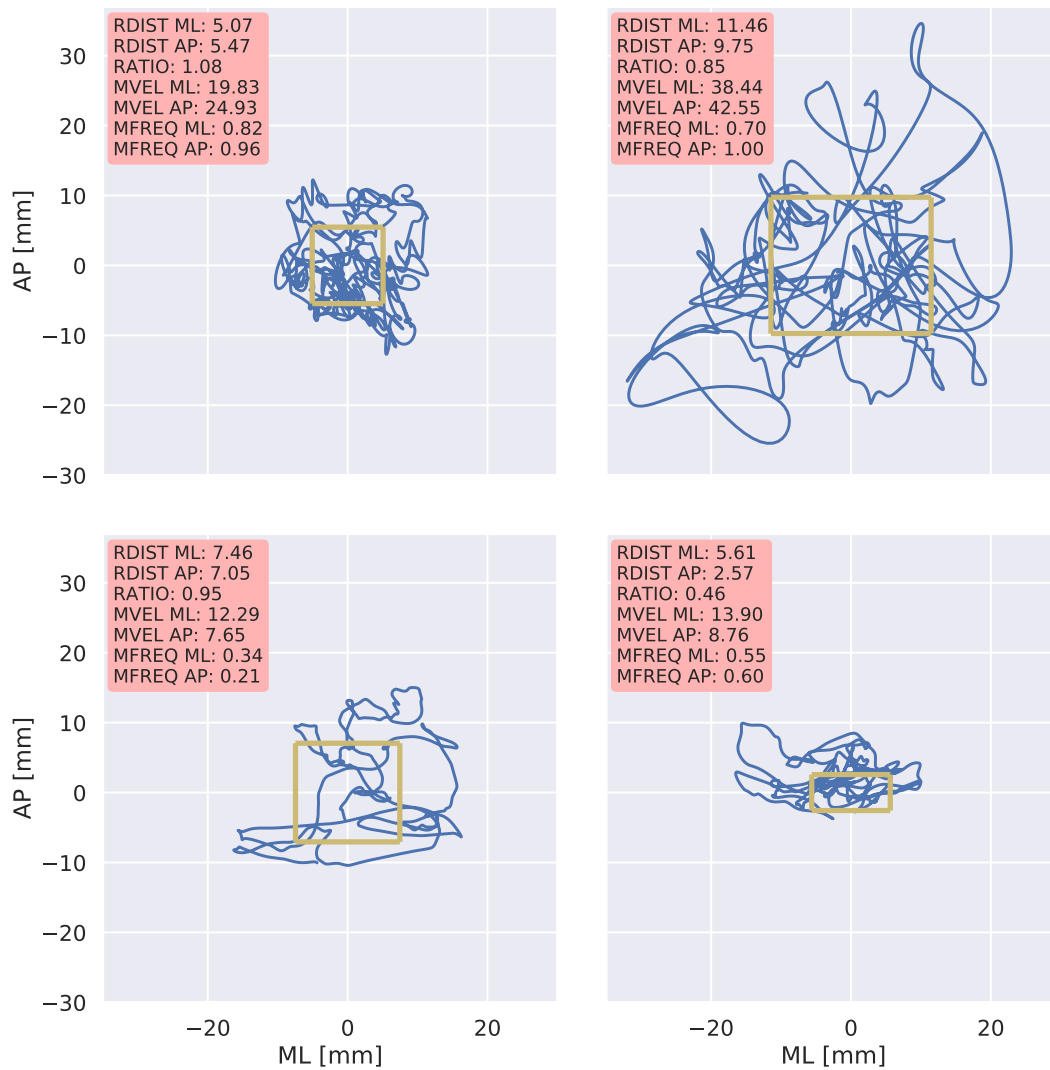


**Figure 6.4:** Sample measurements and evaluation. Four measurements are plotted and the proposed parameters evaluated. Extreme cases were chosen to visualize how geometric properties are translated into values. The yellow box represents the sway distance (RDIST) in both directions.



## 7 The Slackline Study

In the Slackline Study we analyze and compare slackline balancing of subjects with different experience levels. Participants were chosen from different ends of the performance spectrum. They were either practicing slackline balancing regularly or had no experience at all. Those without balance experience were further divide according to their experience in balance related tasks. We recruited one group that did practice balance and coordination related sports such as yoga or wingsun and another group that was either less sportive or doing strength related sport. However, we did not base the grouping on this criteria but had all subjects perform the static balance test to determine their static balancing skills. The test was evaluated by means of success rate and time in balance.

We recorded a total of 6 professional slackliners and 14 beginners. Six participants were female, 14 were male. Age was between 18 and 32 years. Weight was  $72 \pm 11$  kg, height  $1.76 \pm 0.09$  m and BMI  $23 \pm 2$  kg/m<sup>2</sup>. We describe the data acquisition protocol in Section 7.1. The evaluation and results of the balance test are described in Section 1.3.2. We define and propose performance indicators for slackline balancing in Section 7.3. We first analyze successful slackline balancing for single leg balancing and walking in Section 7.4. In Section 7.6 we evaluate the time shortly before falling. A preliminary study with fewer participants and a subset of the suggested performance indicators has been published in [133].

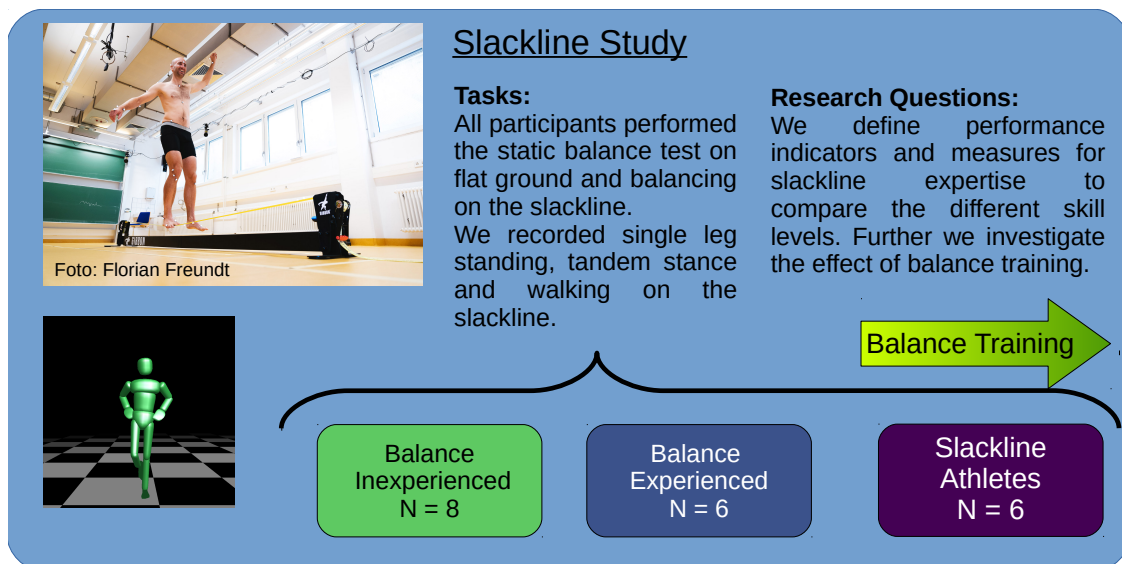
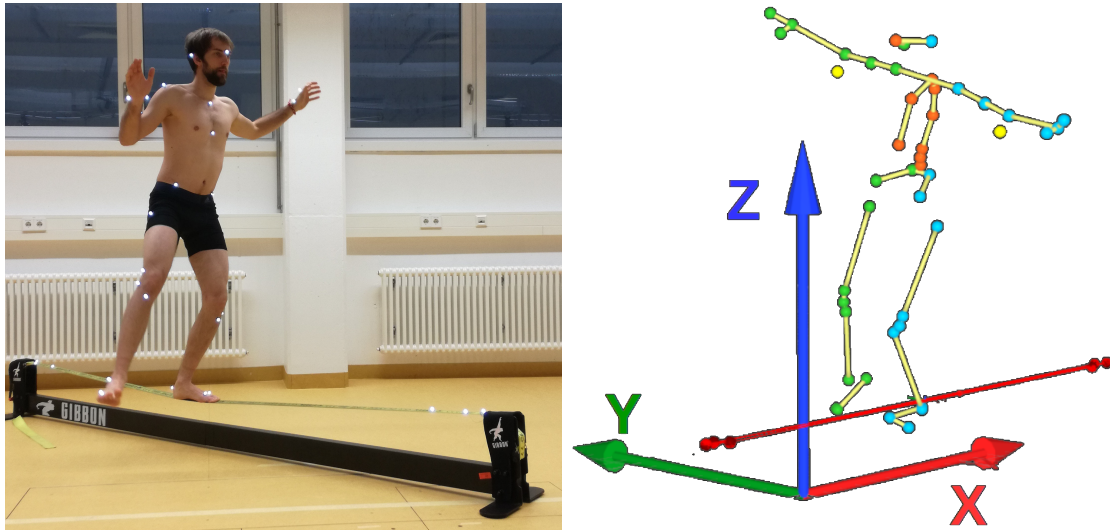


Figure 7.1: Overview of the Slackline Study

## 7.1 Protocol

The study protocol can be divided into three parts: the preparation of the subject, the balance test and the slackline balancing. The slackline motion capture experiments were approved by the ethics committee of the Faculty of Behavioral and Cultural Studies of Heidelberg University according to the Helsinki Declaration (AZ Mom 2016 1/2-A1, 2016 with amendment 2019). Written informed consent was obtained from all subjects before the measurements.



**Figure 7.2:** The setup of the Slackline Study and a motion capture recording with the coordinate system.

### Subject Preparation

All subjects were prepared with the marker set described in Section 3.1.1. The height and weight was measured and a static trial recorded. Afterwards the static markers were removed.

### Balance Test

The balance test was instructed and recorded following the protocol in Section 6.1.

### Slackline Balancing

After the balance test, slackline balancing was recorded. The slackline was installed using the Gibbon Slackrack 300 (ID Sports GmbH, Gibbon Slacklines, Stuttgart, Germany) as shown in Figure 7.2. The slackline was 3 m in length, 5 cm in width and mounted 31 cm above the ground. The motions were recorded using the marker-based motion capture system Qualisys introduced in Section 3.1 consisting of 8 Oqus 500 cameras at a frame rate of 150 Hz.

The following three tasks were recorded:

- **Single Leg Balancing:** Balancing on one foot in the middle of the slackline, left and right foot interchanging
- **Tandem Stance Balancing:** Balancing on both feet in the middle of the slackline, leading foot interchanging
- **Walking:** Beginning at one end of the slackline and walking to the other end. Then walking backwards to the start, going back and forth.

Subjects were asked to perform the task and maintain balance for as long as possible. After falling, the same task was repeated after a short break. For single leg balancing the stance leg was alternated after each trial. Up to 10 trials were recorded for each task and then switched to the next task. A 5 min break was given after each task was performed once and then the whole protocol was repeated a second time.

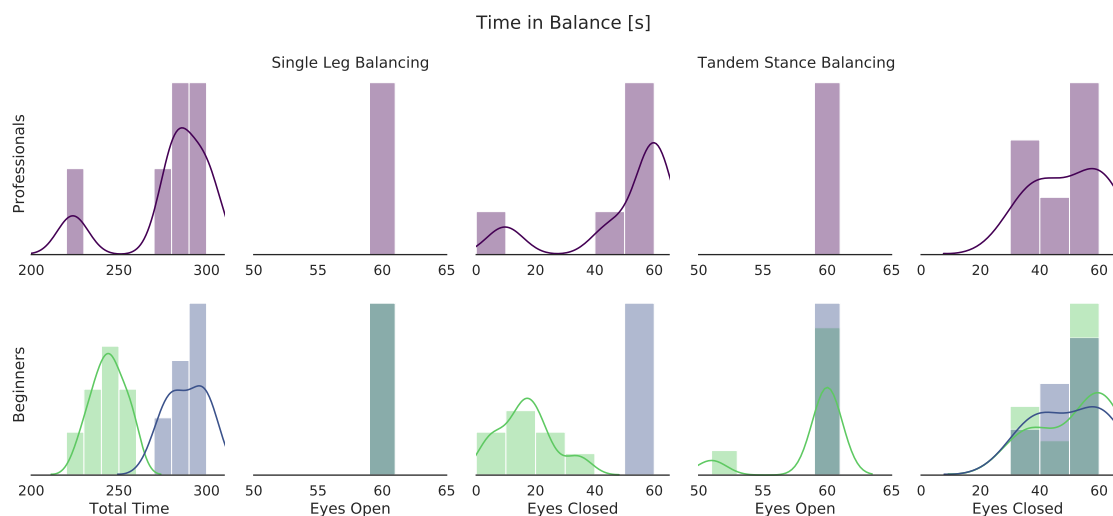


**Figure 7.3:** The Gibbon Slack Rack 300.

## 7.2 Static Balance Test, Subject Grouping and Overview

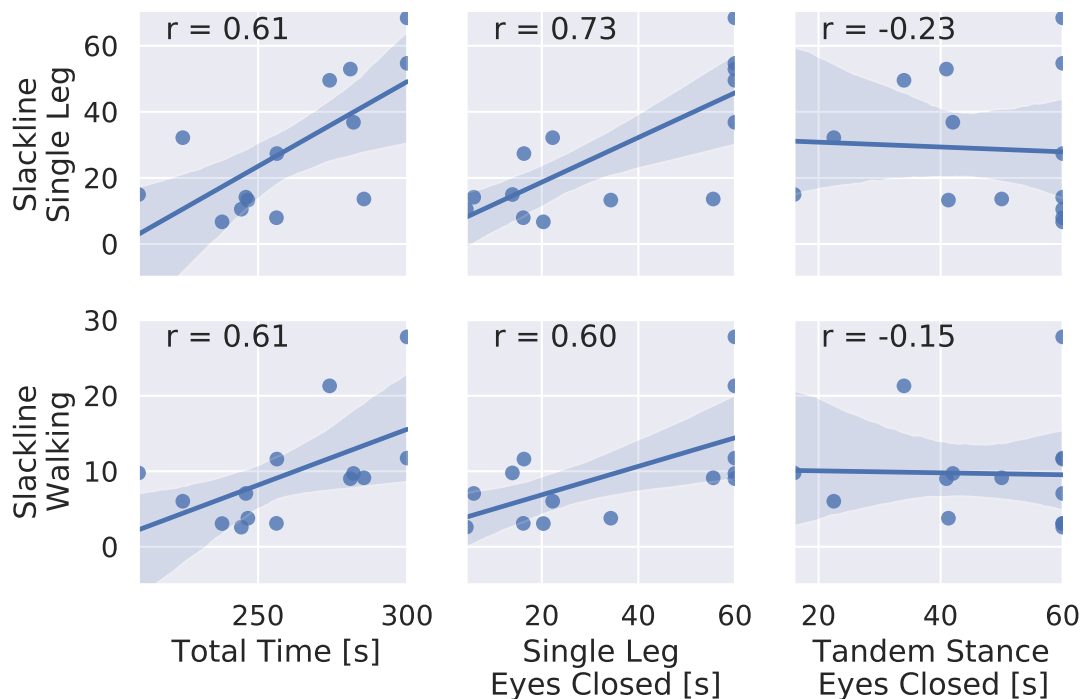
In this section we briefly describe the results of the balance test and the subject grouping that we derived. We aim to find a simple metric that represents static balance capabilities and allows us to divide the 14 beginner subjects into two subgroups. Further analysis of force plate data and comparison with the participants of the "Schizophrenia and the Moving Body" study is shown in Chapter 9. For now, all balance trials are evaluated by means of success rate and time in balance as defined in Section 1.3.2.

Figure 7.4 shows histograms of the time in balance for professional slackliners at the top and for beginners at the bottom. The summed time of all 5 tasks and the eyes open and eyes closed scenario is shown at the left. A maximum of 300 s could be achieved. The right four plots show the summed time in balance for single leg balancing and tandem stance with eyes open and eyes closed. Beginners and professional slackliners show similar distributions for tandem stance and single leg stance with eyes open. Differences between the groups are found for single leg stance with eyes closed. Only one subject of the professional group fell two times, but  $\approx 50\%$  of the beginners failed to maintain balance. This difference is also visible in the total time. Following the data, we define a threshold of 260 s to divide the beginners into six balance-experienced (sportive) beginners and eight balance-inexperienced beginners.



**Figure 7.4:** Histogram of time in balance during the static balance test for all participants of the slackline study. Professionals are shown at the top, beginners at the bottom. A threshold of 260 s of total balance time was chosen to divide the beginner group at the bottom. Inexperienced beginners are shown in light green, balance-experienced beginners in blue.

Figure 7.5 shows the average time in balance on the slackline for single leg balancing and walking plotted against the times in balance during the static balance test. We see large correlation ( $r > 0.6$ ) for the total time and the single leg case with eyes closed for both slackline tasks. This supports the hypothesis, that the static balance for single leg standing with eyes closed can be a predictor for slackline balance performance. There is no correlation to tandem stance balancing.



**Figure 7.5:** Scatter plot of balance time on the slackline and during the balance test for all beginner subjects. Spearman's rank correlation is given.

For evaluation of the slackline balance recordings, we trimmed the measurements to the time the subject was on the slackline. Since we wanted to prevent any bias from the getting up movement, the first 2 s were trimmed off the measurement. We refer to a cut recording as one trial. In the first part of the analysis we compared stable balancing and analyzed only trials that are longer than 8 s. Additionally, we removed the falling down part from the motion by cutting the last 2 s. Table 7.1 shows an overview of participants per group, number of recorded trials and trials that qualified for evaluation. Counts vary due to different number of participants per group and skill level.

For all groups, we find that single leg balancing shows the highest success rate and tandem stance is most difficult task. Beginner struggle to walk and to perform the tandem stance leading to a low percentage of trials that we can evaluate (23 % for walking and 13 % for the tandem stance). Professionals balanced for longer time and therefore showed fatigue, leading to fewer trials that were recorded per participant.

In the following we only evaluate single leg balancing and walking and follow the pipeline described above (see 7.3). Further, we analyze the falling off part of the motion separately using only the last 2 s of each trial in Section 7.6.

Group	N	Single Leg	%	Walking	%	Tandem Stance	%
Beginners	8	96 / 160	60	33 / 148	23	17 / 132	13
Sportive	6	76 / 85	90	56 / 83	67	35 / 70	50
Professional	6	43 / 43	100	34 / 36	94	24 / 30	80

**Table 7.1:** Overview of study participants. The number of evaluated and recorded trials is shown for standing and walking on the slackline.

For each subject we created a subject-specific rigid body model as described in Section 4.1. This model was fitted to all recorded marker data following the inverse kinematic method described in Section 5.1. The resulting joint angle trajectories were filtered using a 5<sup>th</sup>-order Butterworth low-pass filter with cut-off frequency of 9 Hz. Joint velocities and accelerations were computed using finite central differences. We computed all performance indicators that are suggested and discussed in the next section. Groups are compared by means a Wilcoxon Rank-Sum Test [162] and Cohen's-d [163]:

$$d = \frac{\mu_1 - \mu_2}{s} \quad (7.1)$$

$$s = \sqrt{\frac{(n_1 - 1)s_1^2 + (n_2 - 1)s_2^2}{n_1 + n_2 - 2}} \quad (7.2)$$

where  $\mu_{1/2}$  are the means,  $n_{1/2}$  are the number of trials and  $s_{1/2}$  are standard deviations. It normalizes the group difference by pooled standard deviation. Sawilowsky et al. [164] suggest consider  $d = 0.2$  as small effect,  $d = 0.5$  as medium effect and  $d > 0.8$  as large effect. We evaluate single leg balancing and walking separately.

## 7.3 Evaluation and Performance Indicators

In the following we propose kinematic performance indicators for slackline balancing and discuss how they relate to balance control. Most performance indicators can be computed for standing and walking. Additional analysis that requires a stance and a swing leg is only well defined for single leg balancing when there is no double support phase.

### Time

For slackline balancing, the time a person is able to maintain balance is a arguably the most evident performance indicator. The table on the right gives an idea of the expected times for the different skill levels. Experts are able to balance for more then 2 min. Talented beginners are expected to balance up to 1 min by the end of the first training session.

Skill Level	Time [s]
Expert	> 120
Advanced	60 - 120
Intermediate	40 - 60
Beginner	8 - 20
Trial excluded	< 8

Trials with less than 8 s are excluded from further analysis, as random and uncontrolled behavior should be excluded. The correlation between other metrics and the time in balance will also be evaluated.

### Center of Mass Dynamics

The CoM position  $\mathbf{c}$  of a  $N$ -body system with the total mass  $M$  can be computed via forward kinematics. For each body  $i$  we compute the CoM positions  $\mathbf{c}_i$  and use the body masses  $m_i$  in a weighted sum:

$$\mathbf{c} = \frac{1}{M} \sum_i^N \mathbf{c}_i m_i \quad (7.3)$$

accordingly, the CoM velocity  $\dot{\mathbf{c}}$  and CoM acceleration  $\ddot{\mathbf{c}}$  can be computed from the velocity of the body CoM  $\dot{\mathbf{c}}_i$  and acceleration  $\ddot{\mathbf{c}}_i$

$$\dot{\mathbf{c}} = \frac{1}{M} \sum_i^N \dot{\mathbf{c}}_i m_i \quad (7.4)$$

$$\ddot{\mathbf{c}} = \frac{1}{M} \sum_i^N \ddot{\mathbf{c}}_i m_i \quad (7.5)$$

The CoM is constantly accelerated by the changing external contact forces of the slackline. The subject, however, needs to maintain the CoM right above the slackline to prevent falling.

We suggest the following performance indicators related to the CoM dynamics:

- **Standard deviation of CoM acceleration**

The mean CoM acceleration is zero for stable balancing, hence, a lower standard deviation represents less overall acceleration. We analyze movement perpendicular to the slackline, along the slackline and in vertical direction separately. During the walking tasks, less standard deviation of CoM acceleration, results in a smoother walking motion. Overall we claim that this resembles better balance control.

- **Standard deviation of CoM support polygon projection**

Static balance requires the CoM ground projection to be within the support polygon. A larger distance to the edges of the support polygon throughout a movement is associated with better stability. Similar to the RDIST metric (Table 6.2) we can compute the standard deviation of the CoM position in the support polygon as performance indicator.

- **Mean of CoM velocity during walking**

Experts should be able to walk at a higher velocity when compared to beginners.

### Angular Momentum and Normalized Angular Momentum

The total angular momentum of a rigid body system about it's CoM is computed by:

$$\mathbf{L} = \sum_i^N ((\mathbf{c}_i - \mathbf{c}) \times m_i \dot{\mathbf{c}}_i + \mathbf{I}_i \boldsymbol{\omega}_i) \quad (7.6)$$

where  $\mathbf{I}_i$  is the moment of inertia and  $\boldsymbol{\omega}_i$  the angular velocity of body  $i$ . The resulting values are proportional to the total mass and dimensions of the rigid body system. We normalize the angular momentum to find the average angular velocity or normalized angular momentum as suggested by Essen [165].

$$\boldsymbol{\omega}(t) = \mathbf{I}(\mathbf{q}(t))^{-1} \mathbf{L}(\mathbf{q}(t), \dot{\mathbf{q}}(t)) \quad (7.7)$$

where  $\mathbf{I}(\mathbf{q})$  is the total inertia of the rigid body system for a given joint configuration that is calculated from all bodies using the parallel axis theorem [27, 166]:

$$\mathbf{I} = \sum_i^N \left( \mathbf{R}_i \mathbf{I}_i \mathbf{R}_i^T + m_i * (|\mathbf{c}_i - \mathbf{c}|^2 * \mathbb{1} - (\mathbf{c}_i - \mathbf{c}) * (\mathbf{c}_i - \mathbf{c})^T) \right) \quad (7.8)$$

with  $\mathbf{R}_i$  being the orientation of body  $i$ . In terms of balance performance indicators, the normalized angular momentum tells us how fast the subject is rotating around the specific axis. For stable balancing, the angular momentum is zero, and therefore we can use the standard deviation to quantify how much rotational movement is present during a given motion.

We can analyze the three different directions separately, as it is visualized in Figure 7.6:

- **Frontal Plane (Vertical Plane perpendicular to the slackline):**  
We expect the main balancing movement in this plane, as it is the main instability introduced by the slackline. Larger values represent more and greater recovery movement.
- **Sagittal Plane (Vertical Plane along the slackline):**  
We assume that experienced subjects are able to maintain an upright position and do not rotate in the sagittal plane. This should be the case for single leg balancing and walking.
- **Coronal Plane (Around the vertical axis):**  
Similarly to the sagittal plane, we expect experts to maintain an upper body orientation perpendicular to the slackline. Turning parallel to the slackline increases the difficulty dramatically and is therefore not desired. As discussed in Chapter 1, we find reduction of angular momentum around the vertical axis as a prerequisite for stable running.

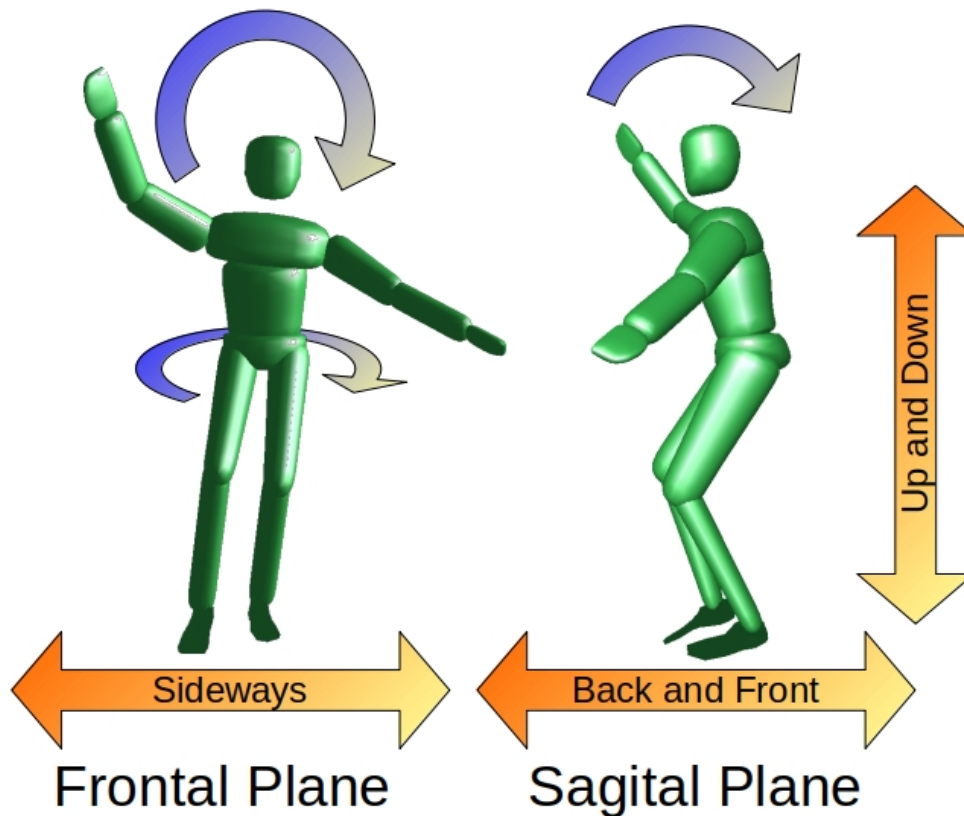


**Figure 7.6:** Illustration of CoM movement (orange) and average angular velocity (blue) in the different directions.

**Kinetic Energy**

The kinematic energy of a rigid body  $i$  is computed from the CoM velocity and angular velocity:

$$E_i = \frac{1}{2}m_i\dot{\mathbf{c}}_i^2 + \mathbf{I}_i\boldsymbol{\omega}_i^2 \quad (7.9)$$

Summing over all bodies results in the energy of the whole rigid body system. This quantifies the overall movement by combining CoM velocity and rotational angular velocity. However, this quantity is proportional to the total subject mass. We therefore propose the normalized kinematic energy:

$$E_{norm} = \frac{1}{M} \sum_i^N E_i \quad (7.10)$$

For single leg balancing we expect to find higher kinetic energy for beginner subjects as they are expected to perform more movement to maintain balance. We compute the mean of the kinetic energy over one trial as performance indicator.

**Balance Energy Ratio**

For slackline walking, we define the balance energy ratio that measures how much of the kinetic energy is due to translation and how much is used to maintain balance. We define the normalized translational kinetic energy by means of the CoM velocity squared at each point of the trajectory:

$$E_{trans}(t) \equiv \frac{1}{2}\mathbf{c}(\dot{\mathbf{t}})^2 \quad (7.11)$$

Unlike the famous Equation derived in [167] and similar to Equation 7.10, we do not take the subject mass into account and obtain a normalized value. We define the balance energy ratio as the fraction of the kinetic energy that is not in translational movement:

$$R_{balance} \equiv 1 - \frac{E_{trans}}{E_{norm}} \quad (7.12)$$

For standing tasks this value is ideally to one. For walking tasks we expect professional slackline athletes to walk more efficiently by means of a lower balance energy ratio. We compute the ration for every instance of the trial and take the mean as a performance measure.

**Movement Coordination**

We expect controlled and well coordinated hand movement as a sign of good balance control. Kodama et al. [92] showed difference in hand movement when comparing one beginner to one experienced slackline athlete. For each subject we compute the absolute velocity for both hands, and in the case of single leg balancing, for the swing foot. We assume that professional slackliners move both hands consistently at the same time, whereas beginners might use only one hand at a time. For single leg balancing, the swing foot might also be synchronized to the hand movement.

We compute the rolling window Pearson correlation between the two values, similar to algorithms developed by Tschacher et al. [168] or Choeng et al. [169]. We take a small subset of the whole trajectory of a given window length and compute the "local" Pearson correlation [161]. The window is then shifted by one data point and the correlation computed for the new subset. This is done for the entire trajectory. The performance indicator for movement coordination is defined as the mean of all correlation values. Since the window size, is somewhat arbitrary, we evaluate short term movements of 0.2 s and longer periods of 1 s.

A sample evaluation comparing two recordings from this study is shown in Figure 7.7. Well coordinated hand movement is shown in the left column and arbitrary movement in the right column. Hand velocities are plotted in the top row. We see overlapping trajectories at the left, as it is expected for good coordination, and independent hand movement at the right. The rolling window correlation for a 1 s window is plotted in the middle row and for a 0.2 s window in the bottom row. The mean values that we intend to use as performance indicator, are plotted for both measurements in red. The intended relationship between the mean value and the similarity of hand velocity trajectories can be observed.

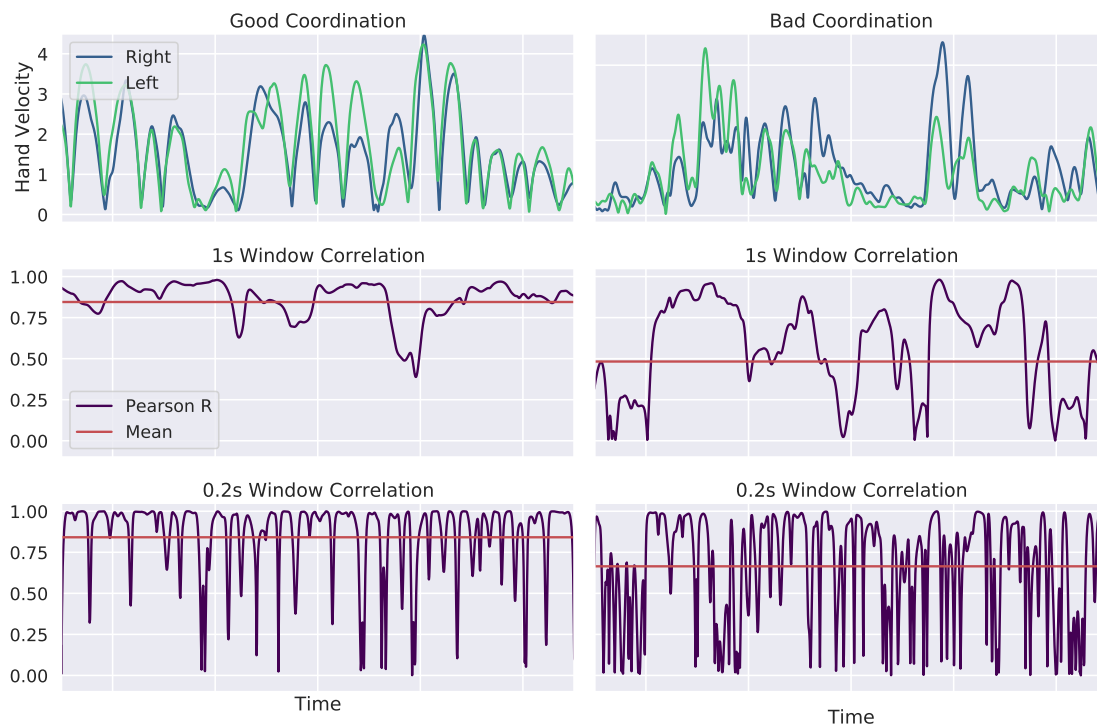


**Figure 7.7:** Hand velocities are shown at the top for well and badly coordinated movement. The rolling window correlation is plotted for a 1 s window in the middle row and for a 0.2 s in the bottom row. The intended relationship between the mean value and the similarity of hand velocity trajectories can be observed.

### **Mean Pose**

We can analyze each joint angle trajectory individually. We define the mean pose as the mean positions of all joints over the motion. For slackline balancing the shoulder and elbow angles are of great interest. Consistent behavior of the expert group could reveal strategies that then can be communicated to beginners.

### **Utilized Range of Motion - Variation of Joint Angle**

We define the utilized range of motion as the standard deviation of the joint angle trajectory. This can give us insights in which joints are mainly used for the balance task and which joints do not contribute. Serrien et al. [93] found significant changes in movement patterns when comparing beginners before and after a 6 weeks slackline training. For the arms and swing leg we expect a larger active range of motion in professional slackliners. They should be able to maintain balance while moving their swing leg in different directions. We expect them to exploit the whole range of motion of the shoulders. Beginners might only be stable in some poses and fall when it comes to more difficult situations.

### **Stance Foot vs CoM Acceleration and Variation of Knee Angle**

The foot contact with the slackline is able to swing sideways and vertically. Paoletti et al. [86] suggest a spring like behavior of the contact forces, where the restoring force changes with the deflection of the slackline. Hence, the contact forces of the slackline are constantly changing and the stance foot of the subject is being accelerated. We expect experts to be able to control these contact forces and therefore reduce their stance foot acceleration. Additionally, they might be able to decouple the external forces on the foot from the upper body. In this case, they could also show similar accelerations at the contact foot but smaller CoM acceleration. Variation in the knee angle can be a sign of stance leg compliance in vertical direction.

## Evaluation Pipeline

Summarizing the whole evaluation pipeline we followed these steps:

- **Recording:**  
Kinematic data and the static trial are recorded following the protocol of the study.
- **Modeling and Kinematic Fitting:**  
The subject-specific model is created from the static trial. This is fully automated in Python using the `c3d` package from the Embodied Cognition Lab (UT, Austin, USA) [170]. Joint angle trajectories are computed based on the inverse kinematics algorithm described in Chapter 5 using `Puppeteer` [143].
- **Computation of raw Performance Indicator Trajectory:**  
Before we can summarize the physical quantity into a single value, we need to compute the entire trajectory. All performance indicators were computed using the RBDL by Martin Felis [142]. The library already supports the computation of CoM dynamics, Angular Momentum and the ZMP position. We implemented functions that compute the inertia for a given joint position and the normalized angular momentum.
- **Summary and Statistics:**  
We summarize the trajectories using Python and the `Pandas` package [171]. Statistics are computed using `Pingouin` [172] and figures created using `Seaborn` [173].

Code snippets for inertia and normalized angular momentum computation using RBDL and computation of hand coordination can be found in Appendix A.4.

## 7.4 Single Leg Balancing

In this Section we compare successful balance trials of at least 8 s for single leg balancing.

### 7.4.1 Time and Overview

Figure 7.8 shows the time for all trials recorded. We see a clear progression between the groups. On average, beginners managed  $16 \pm 9$  s, sportive beginners  $46 \pm 19$  s and professionals  $71 \pm 25$  s.<sup>1</sup> The longest trials were 73 s, 133 s and 190 s, respectively. Overall, the short slackline setup was beginner friendly and all subjects managed to perform several valid trials. Experts had to adjust to the unusual short slackline and the static standing task, since they are used to longer setups and more challenging movements.

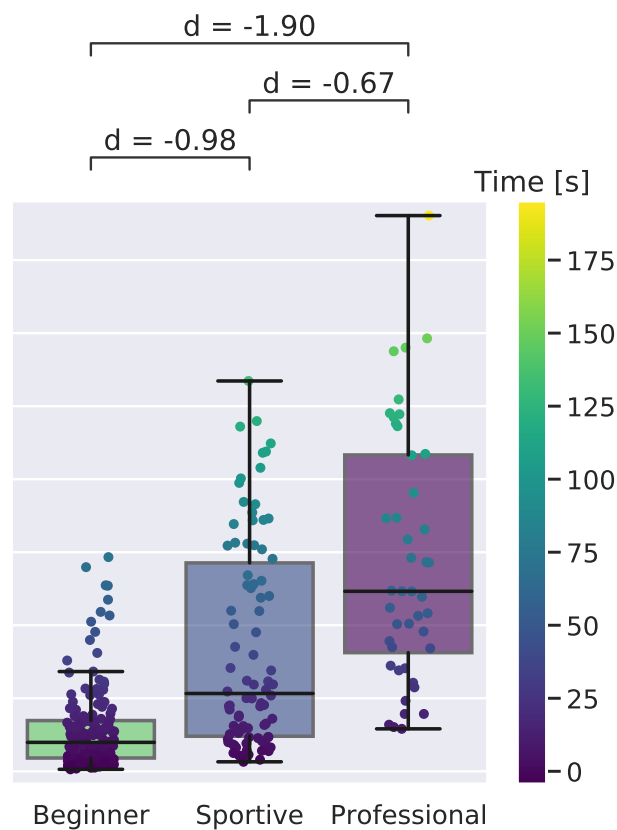


**Figure 7.8:** Boxplot of time in balance for single leg slackline balancing for the three subject groups. Boxes contain the inner 50% of the data and the median is shown. Whiskers are maximum 1.5 times the inner quartile range but end at the last data point which lays inside. Cohen's-d is given for comparison. All values are plotted in the color following the time, as visualized in the color bar.

<sup>1</sup>The boxplot shows the median and inner quartile range.

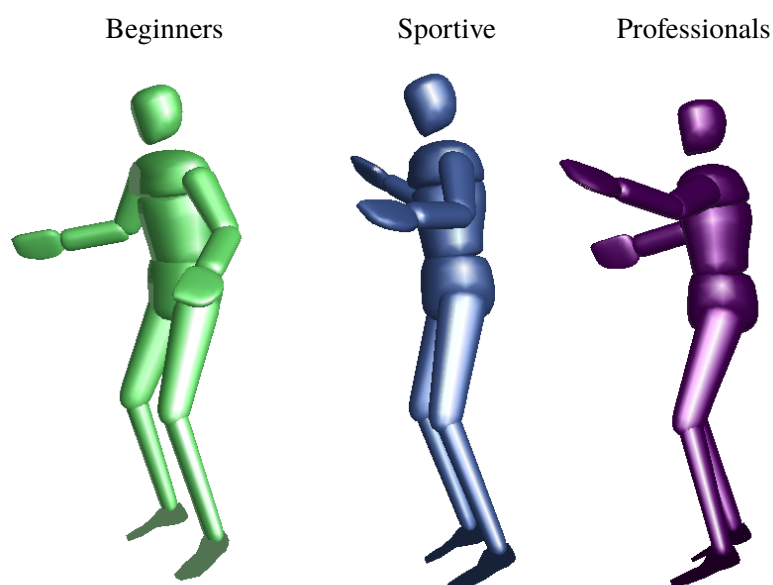
### 7.4.2 Movement and Strategy

We analyze movement and strategy by comparing the average posture and angular velocity around the three directions. We then analyze shoulder and elbow movement in the frontal plane in more detail and compare the overall hand and feet coordination.

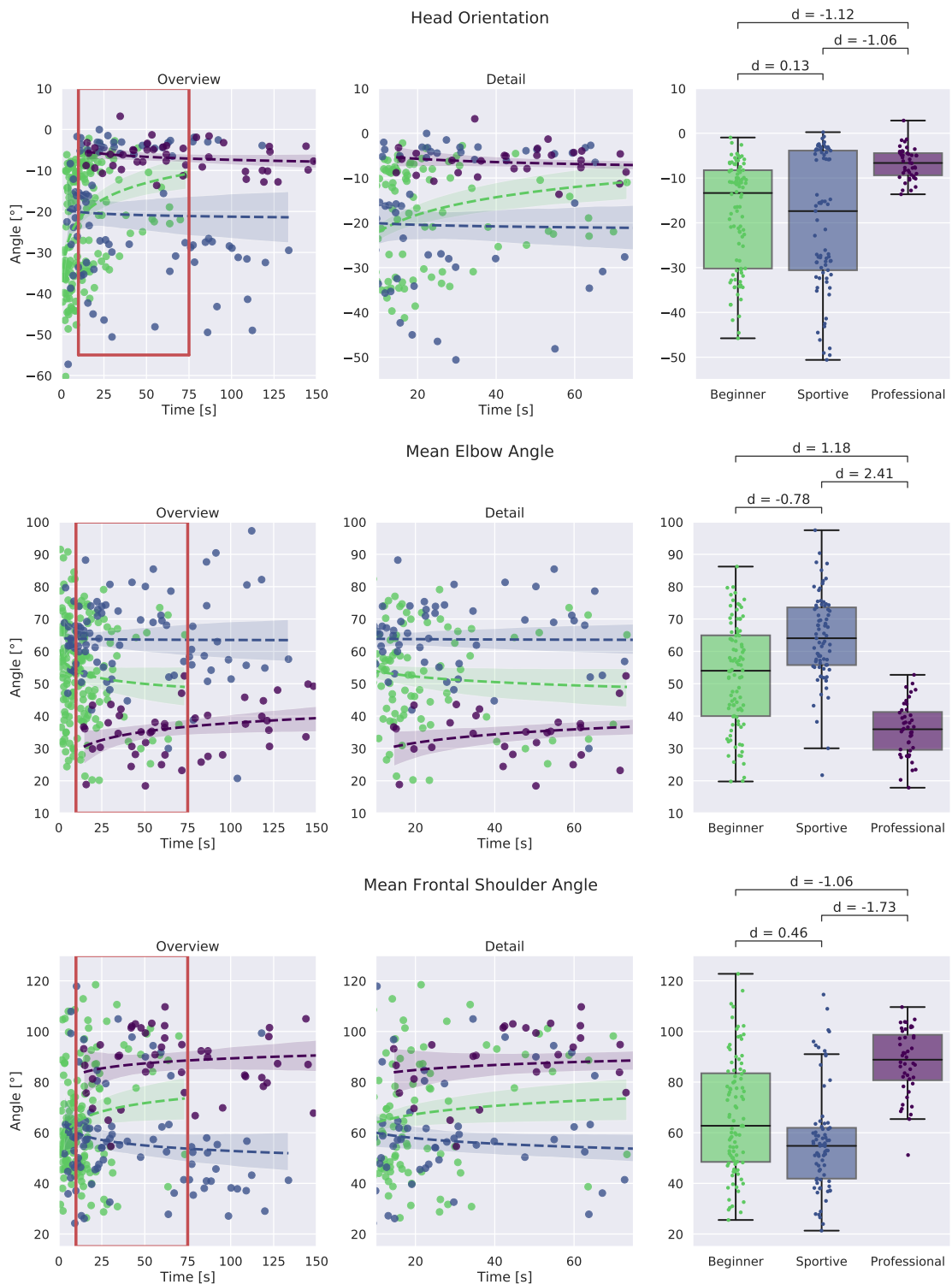
#### Posture and Utilized Joints

Figure 7.9 shows the mean posture for all groups. Leg and upper body configuration are similar, as it is expected, since all trials were cut to stable balancing and the stance leg alternated. Differences are visible for head orientation and arm angles. Exact values and trends with respect to balance time are plotted in Figure 7.10. Head orientation is shown at the top, elbow angle in the middle and frontal shoulder angle at the bottom. We plotted the mean of both arms.

Professionals show consistent, balance time independent behavior, while both beginner groups vary between trials and between subjects. For head orientation we find that beginners and sportive beginners look down at the end of the slackline, while professional slackline athletes look straight ahead. All professionals assume a similar head orientation of about  $-5^\circ$  with respect to the horizontal plane. Beginner subjects vary between  $0^\circ$  and  $-50^\circ$ . Similar observations are made for shoulder and elbow angles. Professional slackliners have their arms perpendicular to the upper body and elbows stretched, while both beginner groups tend to align their upper arm and bend their elbows more. We find  $90^\circ$  compared to  $60^\circ$  for the shoulder and  $35^\circ$  compared to  $60^\circ$  for elbow joint.



**Figure 7.9:** Mean posture for single leg slackline balancing. Beginners are shown at the left, sportive beginners in the middle and professional slackline athletes on the right.



**Figure 7.10:** Comparison of head orientation, frontal shoulder angle and elbow angle with respect to time in balance and between groups. An overview of all trials is shown at the left, more detail in the middle and box plots for successful trials longer than 8 s at the right. Beginners and sportive beginners show large variation. The professional group is more consistent and manages to maintain a horizontal head orientation.

In Figure 7.11 we compare the shoulder and elbow movement in the frontal plane, by means of variation around the mean pose. For both joints, we found that beginners and sportive beginners used less of their range of motion:  $12^\circ$  compared to  $16^\circ$  for the elbow and  $19^\circ$  compared to  $29^\circ$  for the shoulder.

We see that for longer trials, the professional group used more of the possible shoulder range of motion, suggesting that they are stable in a greater variety of poses. For example, they are able to point both arms in the same direction during a recovery movement and come back to the regular t-pose balancing, while beginners and sportive beginners are not able to perform this recovery movement and fall. The fact, that the elbow joint is more involved in the balancing suggests that the professional group also performs smaller adjustment movements instead of large shoulder movement. To follow up on this thought we compare the movement coordination.

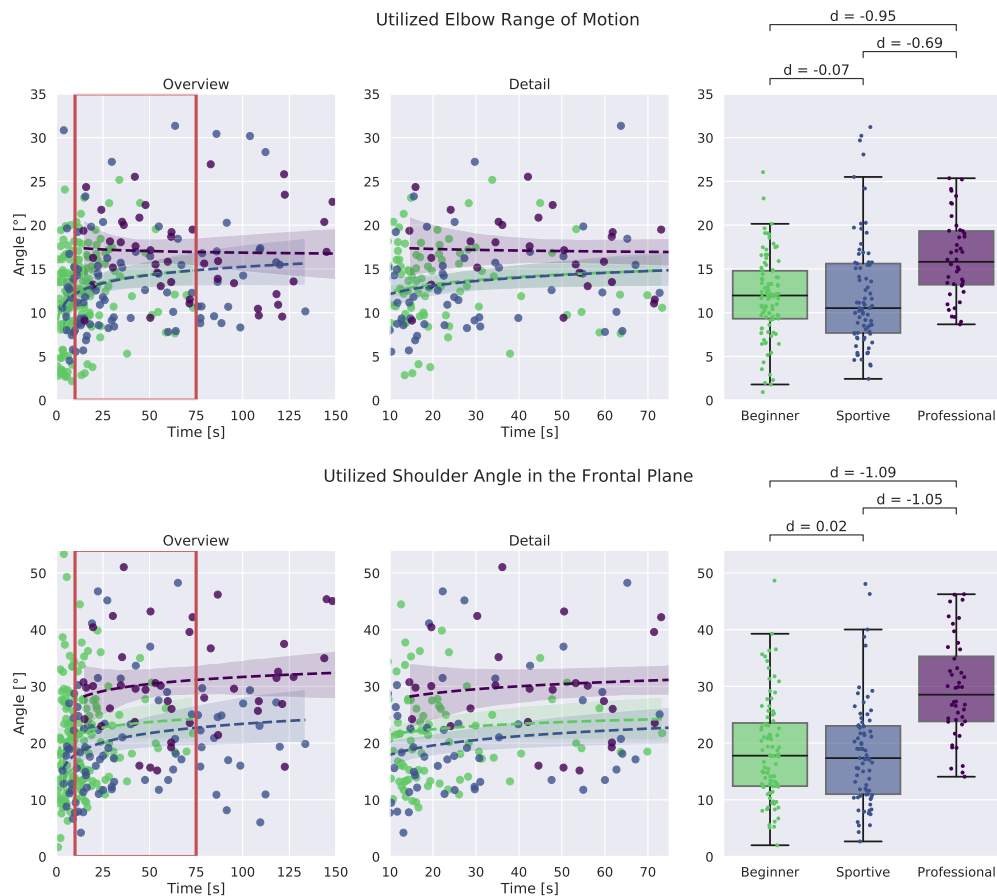


**Figure 7.11:** Comparison of utilized range of motion for frontal shoulder and elbow angle. An overview of all trials is shown at the left, more detail in the middle and box plots for successful trials longer than 8 s at the right. The professional group shows larger values for both joints. We suggest that they are able to balance in a greater variety of poses and also involve smaller recovery movements in the elbow joint.

### Movement Coordination

For comparison of movement coordination we compute the moving window correlation between the absolute velocity of the hands and the free foot. We consider a time window of 0.2 s and 1.0 s and take the mean of the three combinations. Figure 7.12 shows all movement coordination values for all trials. A larger value represents more coordinated arm and foot movement. Results are similar for both time windows. Beginner subjects were less coordinated than sportive beginners and professionals, especially for short and unsuccessful balance trials. Sportive beginners showed similar level of coordination as professional slackliners. For longer trials correlation values converge to about 0.75 for the 0.2 s window and 0.7 for the 1.0 s window.

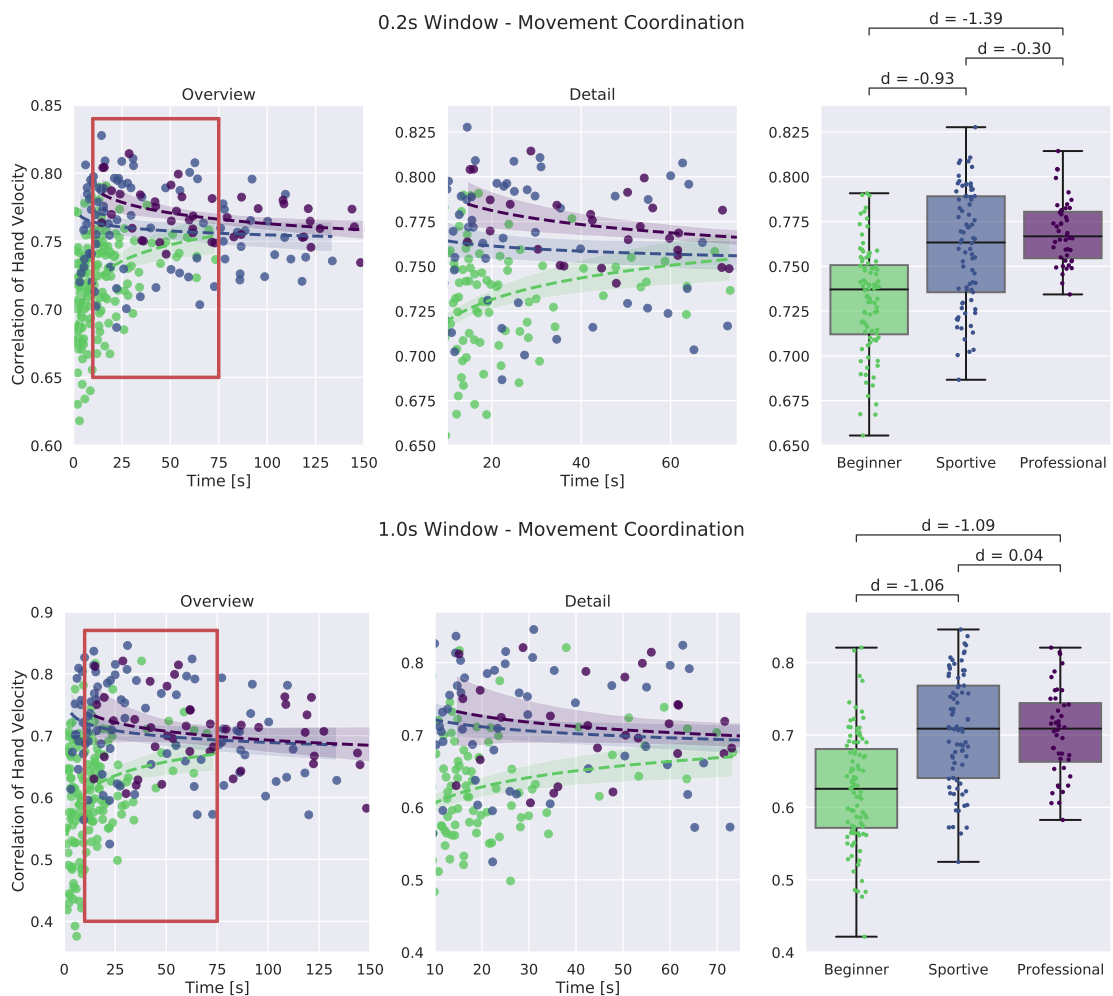


**Figure 7.12:** Comparison of movement coordination by means of rolling window correlation. We chose a 0.2 s at the top and a 1.0 s window at the bottom. An overview of all trials is shown at the left, more detail in the middle and box plots for successful trials longer than 8 s at the right.

### Normalized Angular Momentum

The normalized angular momentum or so-called average angular velocity summarizes the active movement and passive rotation of the whole subject. The lab coordinate system is shown in Figure 7.2. The X-Axis is aligned with the Slackline, the Y-Axis perpendicular and the Z-Axis points in the vertical direction. Figure 7.13 shows the time in balance plotted against the normalized angular momentum on the left and in more detail in the middle. Box plots for the subject groups are shown on the right. The frontal plane is shown at the top, sagittal plane in the middle row and vertical axis at the bottom. For all three directions we observe a decrease with longer balance trials. We make the following observations:

- The largest normalized angular momentum is observed in the **frontal plane** with  $\approx 20^\circ/\text{s}$ . It is the direction that coincides with the instability introduced by the slackline. Beginners show  $\approx 20\%$  larger values than sportive beginners and professionals. Values are especially large for shorter and unsuccessful trials. For successful balancing they converge to  $\approx 17^\circ/\text{s}$ . This is reasonable since we expect there to be longer stable balancing between recovery movements and smaller recovery movements in general.
- In the **sagittal plane**, all participants show similar and comparably small values of  $\approx 5^\circ/\text{s}$ . Again, short beginner trials show larger values as participants also tilt forward and backward. This direction becomes more relevant during the walking task when leaning forward is part of the gait motion.
- The largest difference between the professional slackline athletes and the other groups is found for movement around the **vertical axis** in the bottom row. Professional slackliners manage to maintain a perpendicular alignment with the slackline, such that their frontal shoulder joint can move in the frontal plane, while other participants also rotate around this axis. When looking at the whiskers of the box plot, we see that the variation between trials is much smaller for the professional group than for the two beginner groups. We found  $8.7 \pm 2.7^\circ/\text{s}$  compared to  $12.2 \pm 7.7^\circ/\text{s}$  and  $11.2 \pm 6.7^\circ/\text{s}$ , respectively. Values converge to less than  $10^\circ/\text{s}$  for successful trials.

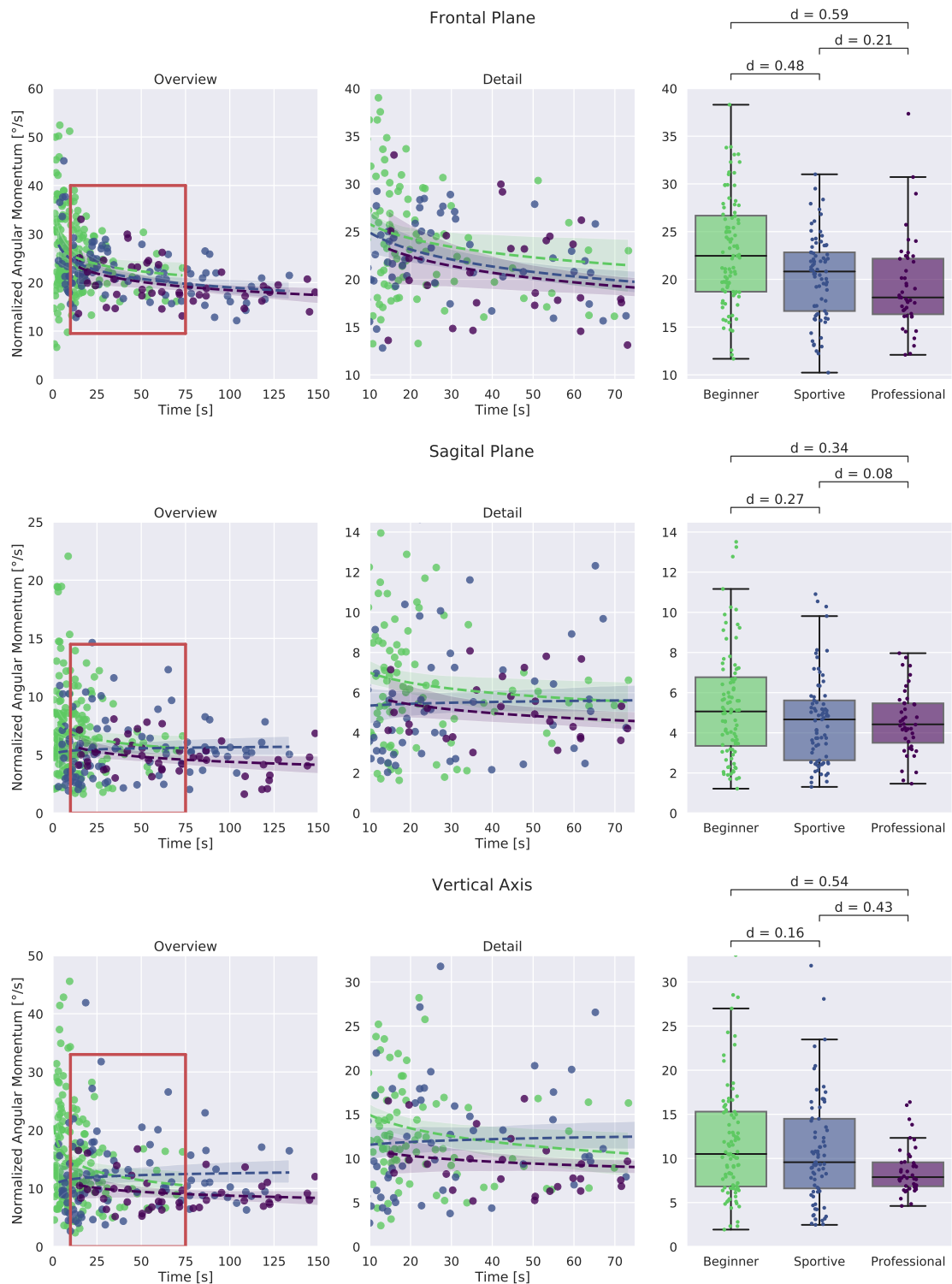


**Figure 7.13:** Normalized angular momentum around the three coordinate axis. An overview of all trials is shown at the left, more detail in the middle and box plots for successful trials longer than 8 s at the right. Short trials show larger values, especially in the beginner group. For longer trials minimization of normalized angular momentum around all three coordinate axis becomes important. The professional group shows the smallest variation around the vertical axis..

### 7.4.3 Slackline Interaction

The interaction force with the slackline is constantly changing and the stance foot is accelerated by the spring-like rubber band. We compare the stance foot acceleration between the subject groups and investigate how the subjects CoM is affected by this.

#### Stance Foot Acceleration

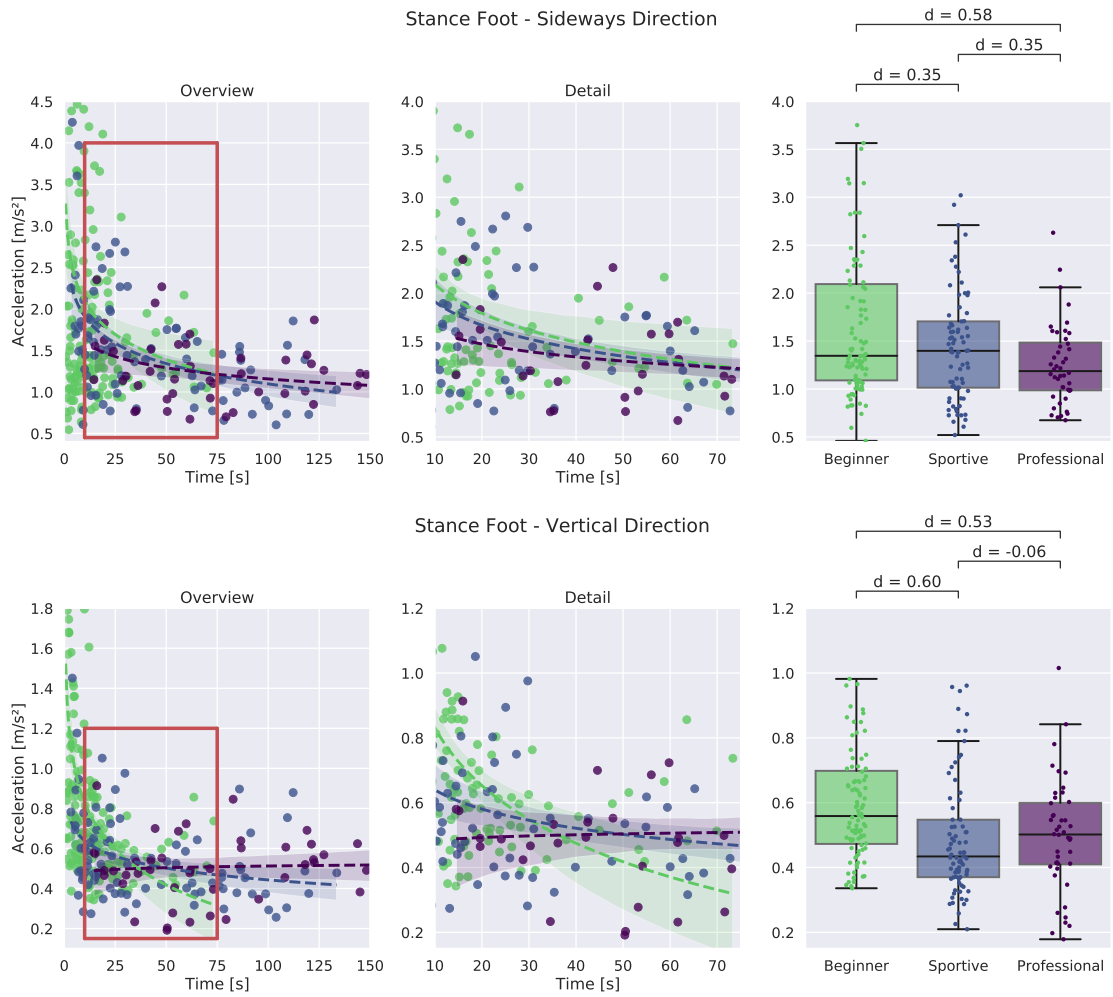
In Figure 7.14 the foot acceleration in sideways direction is shown at the top and in vertical direction at the bottom. Acceleration in sideways direction is much larger than in vertical direction due to the different masses that are accelerated. In up and down direction, the whole body weight needs to be accelerated by the slackline force, while in sideways direction mainly the leg and feet are accelerated. We elaborate more on this fact in the jump analysis in Chapter 11. For the sideways direction we see a clear tendency towards lower values with longer time in balance. Professional slackliners show smaller values when compared to the other groups. The stance foot of beginners is highly accelerated, especially for shorter trials. This is consistent with findings on reduced muscle reflexes by [91]. The shaking sideways leg motion that beginners experience on longer slacklines reduces with training and experience.

In vertical direction we find a similar trend with time. Beginners experience high accelerations during short and unsuccessful trials and acceleration is reduced for longer trials. In general, all groups show similarly large variation between trials. The foot of beginners is accelerated between  $0.35 \text{ m/s}^2$  and  $1.0 \text{ m/s}^2$ . The sportive group and the professional group show smaller mean values between  $0.2 \text{ m/s}^2$  and  $0.8 \text{ m/s}^2$  suggesting better contact force control.

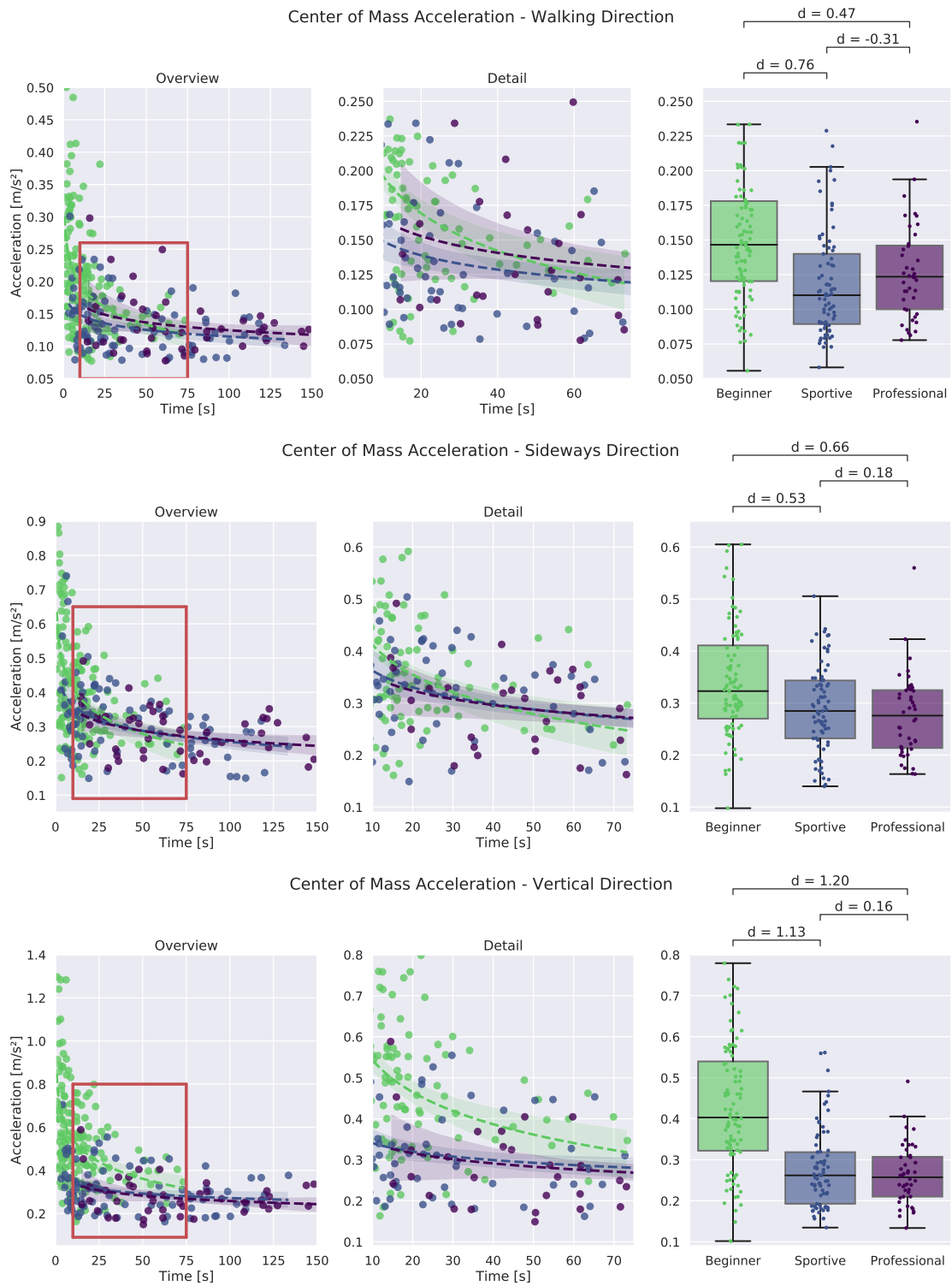
#### Center of Mass Acceleration

Figure 7.15 shows the CoM acceleration in the three directions following the coordinate system shown in Figure 7.2. In all directions we see smaller values with larger times in balance. Beginner show very high accelerations for short and unsuccessful trials. The walking direction will be more relevant during the walking task. In sideways direction we see the same findings as for the stance foot acceleration. Acceleration decreases with time and beginners show consistently higher values than professionals. Correlation between the two metrics is high:  $r = 0.83$  for beginners and sportive beginners and  $r = 0.64$  for professional slackliners. We suggest that professional slackliners are able to accelerate their CoM more independently from their stance foot when compared to the beginners.

In vertical direction, the professional group and the sportive beginners show similar and about 50% lower values than the beginners group. Correlation is lower than for the sideways direction ( $r = 0.6$  for all groups). Beginners show high variation for shorter balance trials with values up to  $0.8 \text{ m/s}^2$ , whereas the professional groups is consistent between  $0.2 \text{ m/s}^2$  and  $0.4 \text{ m/s}^2$ . We suggest that they are able to compensate the interaction force in their stance leg knee.



**Figure 7.14:** Comparison of stance foot acceleration in vertical and sideways direction. An overview of all trials is shown at the left, more detail in the middle and box plots for successful trials longer than 8 s at the right.



**Figure 7.15:** Comparison of Center of Mass acceleration. An overview of all trials is shown at the left, more detail in the middle and box plots for successful trials longer than 8 s at the right.

### Stance Leg Knee Angle Variation

Figure 7.16 shows the variation of knee angle. We see large values for short and unsuccessful beginner trials. For successful trials we see an increase with time in balance. Here, the beginner group shows less variation than the sportive and professional group. However, group mean differences are less than  $1^\circ$  which is in the range of accuracy for joint angles derived from motion capture data.

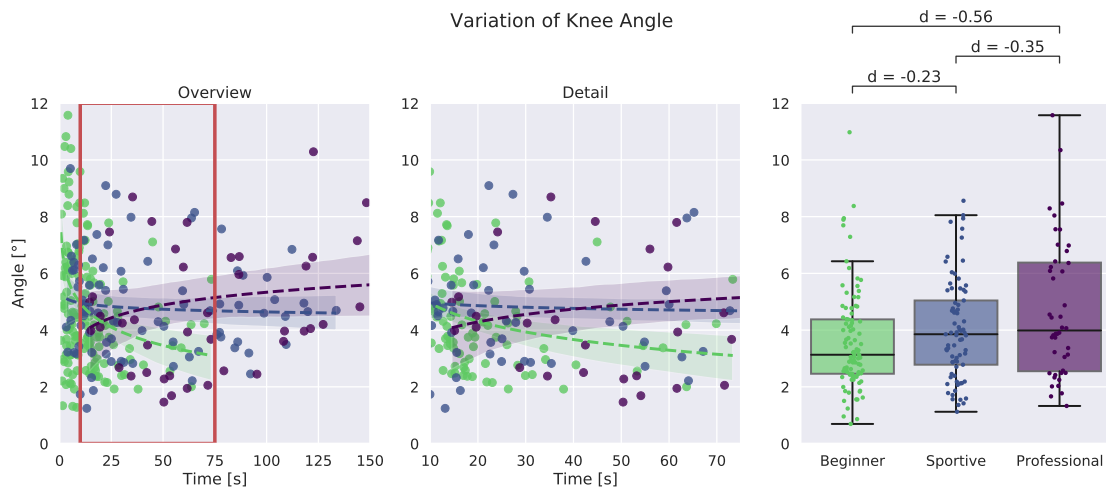


**Figure 7.16:** Comparison of stance leg knee angle variation. An overview of all trials is shown at the left, more detail in the middle and box plots for successful trials longer than 8 s at the right.

### Static Stability

In the publication of preliminary results [133] we found reduced variation of CoM position in the foot frame for professional slackliners. We were not able to generally confirm this observation with the larger data set. This is in part due to a more thorough evaluation and the fact, that short trials with less than 8 s in balance are now discarded. The standard deviation of sideways CoM position in the foot is plotted in Figure 7.17. For unsuccessful beginner trials shorter than 8 s we find a high variation, suggesting that they are not able to find a statically stable equilibrium. All participants converge to a variation of less than 1 cm, which is in the range of measurement and reconstruction accuracy.

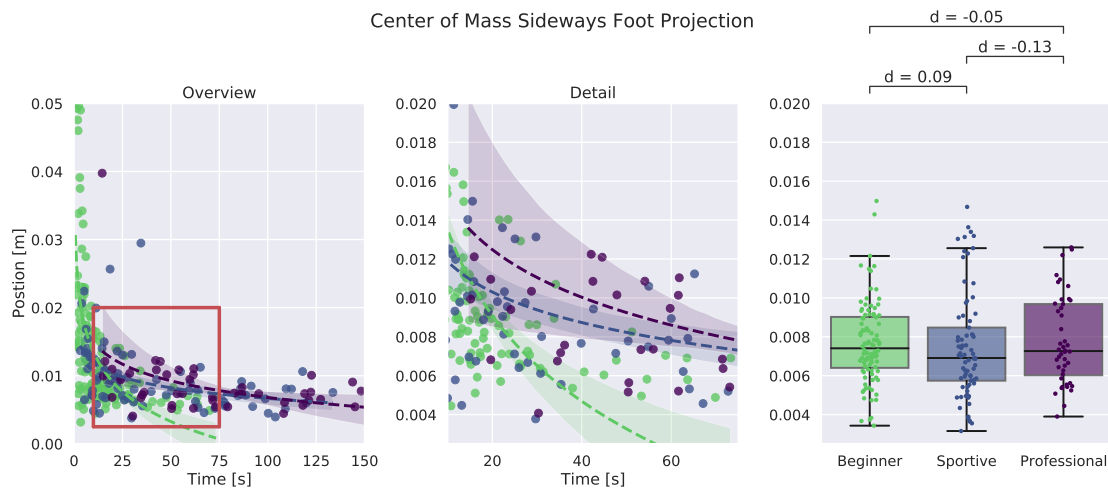


**Figure 7.17:** Comparison of CoM foot projection. An overview of all trials is shown at the left, more detail in the middle and box plots for successful trials longer than 8 s at the right.

#### 7.4.4 Summary

In Table 7.2 we listed all performance indicators for single leg balancing. For each group we list the mean value, standard deviation and range that was observed. We evaluate if the groups are significantly different using a ranked-sum-test [162] and compute the effect size using Cohen's-d [163]. The first column is color coded according to group differences.

Performance indicators in red showed differences between the three groups. These are the time in balance and the mean posture. There is was a clear progression in balance time between the groups and every group showed a different mean pose.

In yellow we find performance indicators that differed between professional slackliners and the two beginner groups. These are the utilized range of motion, where professionals use their elbow joints more and are able to balance in different shoulder configurations. They also maintain a horizontal head position. Further, professionals reduce their normalized angular momentum around the vertical axis allowing them to align their frontal shoulder and elbow joint in the frontal plane.

In green we marked all performance indicators where the balance-inexperienced beginners differ from the two balance-experienced groups. We find reduced hand coordination and increased CoM and vertical stance foot acceleration. They also show significantly larger normalized angular momentum in the frontal plane, meaning that they perform faster and more recovery movements.

Variable	Beginners			Sportive			Professional			Beg / Sport		Beg / Pro		Sport / Pro				
	Mean ± SD	Range	Mean ± SD	Range	Mean ± SD	Range	p-val	d	p-val	d	p-val	d						
Time [s]	14.27	14.15	0.67	73.53	42.32	35.44	3.25	133.62	72.31	42.51	14.53	190.23	<0.0001	-1.17	<0.0001	-2.47	<0.0001	-0.78
Head Orientation [°]	-18.00	11.80	-45.78	-0.96	-19.74	14.99	-50.60	0.24	-6.78	3.46	-13.63	2.84	0.80	0.12	<0.0001	-1.11	<0.001	-1.06
Mean Frontal Shoulder Angle [°]	66.56	22.57	25.54	122.76	56.67	20.27	21.32	114.57	87.96	12.94	51.19	109.64	0.006	0.46	<0.0001	-1.06	<0.0001	-1.73
Mean Elbow Angle [°]	52.54	16.07	19.79	86.21	64.18	13.25	21.73	97.45	35.85	8.12	17.86	52.75	<0.0001	-0.78	<0.0001	1.17	<0.0001	2.41
Utilized Elbow Angle [°]	11.84	4.66	0.92	26.06	12.21	6.36	2.43	31.21	16.25	4.57	8.66	25.36	0.52	-0.07	<0.0001	-0.94	<0.0001	-0.69
Utilized Frontal Shoulder Angle [°]	19.11	9.79	1.99	62.54	18.92	10.57	2.67	65.67	29.48	8.75	14.08	46.24	0.73	0.02	<0.0001	-1.09	<0.0001	-1.05
Hand Coordination (1.0s)	0.62	0.08	0.42	0.82	0.71	0.08	0.52	0.85	0.70	0.06	0.58	0.82	<0.0001	-1.06	<0.0001	-1.09	0.75	0.04
Hand Coordination (0.2s)	0.73	0.03	0.64	0.79	0.76	0.03	0.69	0.83	0.77	0.02	0.73	0.81	<0.0001	-0.93	<0.0001	-1.39	0.26	-0.30
Normalized Angular Momentum X [°/s]	23.26	7.12	6.24	61.06	20.31	4.34	10.23	31.01	19.38	4.85	12.09	37.35	0.006	0.48	0.0002	0.59	0.12	0.21
Normalized Angular Momentum Y [°/s]	5.54	3.22	1.22	20.31	4.74	2.46	1.31	14.66	4.57	1.57	1.47	7.96	0.12	0.27	0.22	0.34	0.82	0.08
Normalized Angular Momentum Z [°/s]	12.30	7.72	1.93	49.94	11.16	6.73	2.47	39.62	8.70	2.70	4.61	16.39	0.37	0.15	0.01	0.54	0.05	0.43
Stance Foot Acceleration Y [m/s <sup>2</sup> ]	1.70	0.88	0.46	4.36	1.44	0.57	0.52	3.02	1.26	0.42	0.67	2.63	0.17	0.34	0.005	0.59	0.08	0.35
Stance Foot Acceleration Z [m/s <sup>2</sup> ]	0.62	0.25	0.34	1.90	0.49	0.18	0.21	0.96	0.50	0.17	0.18	1.02	<0.0001	0.60	0.007	0.53	0.27	-0.06
COM Acceleration X [m/s <sup>2</sup> ]	0.16	0.06	0.06	0.41	0.12	0.04	0.06	0.23	0.13	0.05	0.08	0.34	<0.0001	0.76	0.003	0.47	0.07	-0.31
COM Acceleration Y [m/s <sup>2</sup> ]	0.34	0.11	0.10	0.73	0.29	0.08	0.14	0.51	0.28	0.08	0.16	0.56	0.003	0.53	0.0003	0.66	0.30	0.18
COM Acceleration Z [m/s <sup>2</sup> ]	0.43	0.16	0.10	0.93	0.28	0.10	0.13	0.56	0.26	0.07	0.13	0.49	<0.0001	1.13	<0.0001	1.20	0.88	0.16
Utilized Knee Angle [°]	3.60	1.76	0.69	10.98	4.02	1.76	1.12	8.56	4.72	2.41	1.33	11.58	0.08	-0.23	0.02	-0.56	0.21	-0.34

**Table 7.2:** Summary of all Performance Indicators for Single Leg Balancing. P-values are computed using a Wilcoxon Rank-Sum Test. We color-coded performance indicators according to group differences: red: all groups are different, orange: professionals are different from beginners and sportive beginners, green: beginners are different from the sportive and professional group.

## 7.5 Slackline Walking

### 7.5.1 Time and Overview

Figure 7.18 shows the time for all trials of slackline walking. We see that professional slackliners are able to maintain balance as long as for standing ( $72 \pm 27$  s), whereas beginners ( $6 \pm 3$  s) and sportive beginners ( $15 \pm 8$  s) only manage  $\frac{1}{3}$  of the time.<sup>2</sup> Beginners only managed short balance trials and as discussed for single leg balancing usually show high variation. For a meaningful and consistent evaluation we, again focus on trials that are longer than 8 s.

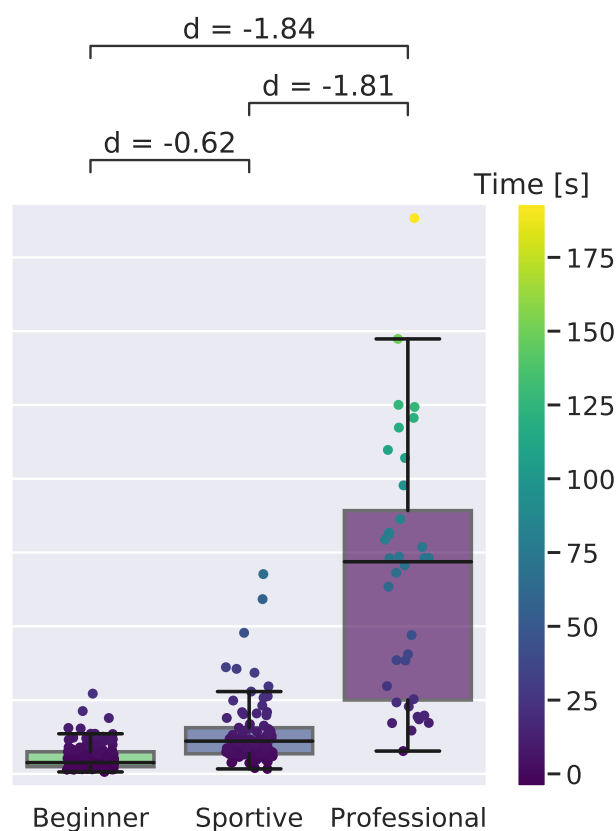


**Figure 7.18:** Box plot of time in balance for slackline walking for the three subject groups. Boxes contain the inner 50% of the data and the median is shown. Whiskers are maximum 1.5 times the inner quartile range but end at the last data point which lays inside. Cohen's-d is given for comparison and all values plotted on top with the color following the time, as visualized in the color bar.

<sup>2</sup>The boxplot shows the median and inner quartile range.

## 7.5.2 Movement and Strategy

### Posture and Utilized Joints

Mean head orientation, elbow and shoulder angle in the frontal plane are plotted in Figure 7.19. Overall the pose is very similar to single leg balancing as visualized in Figure 7.9. Except for one subject, all professional slackliners maintain a horizontal head orientation.

All beginner subjects look down at the slackline. We suggest that they are insecure about the slackline position and ensure correct foot placement. Sportive beginner subjects vary between looking at the feet ( $-45^\circ$ ), at the end of the slackline ( $-25^\circ$ ) and horizontally ( $-5^\circ$ ). Professionals are consistent in their posture, whereas the beginner groups are varying from trial to trial, especially for unsuccessful and short trials. Professionals stretch their arms perpendicularly whereas beginners have more aligned upper arms with larger elbow angle.

Figure 7.20 shows the utilized range of motion for shoulder and elbow joint in the frontal plane. As for single leg balancing, professionals show larger movement in the elbow joint. We see no difference in the shoulder joint when comparing all successful trials, however, for longer walking trials professionals require less joint range than sportive beginners, suggesting that their walk is more stable.

### Movement Coordination

For walking we evaluate movement coordination by comparing the absolute hand velocities. Since results for a 0.2 s and 1.0 s time window are similar, we only show the result for the 1.0 s window in Figure 7.12. Again we see high variation for beginners and short trials and a decrease in coordination for longer trials. For successful trials, we see increasing movement coordination between the groups. When compared to single leg balancing, where the professional and sportive group had similar values, we now find that professional slackline athletes show better coordination.

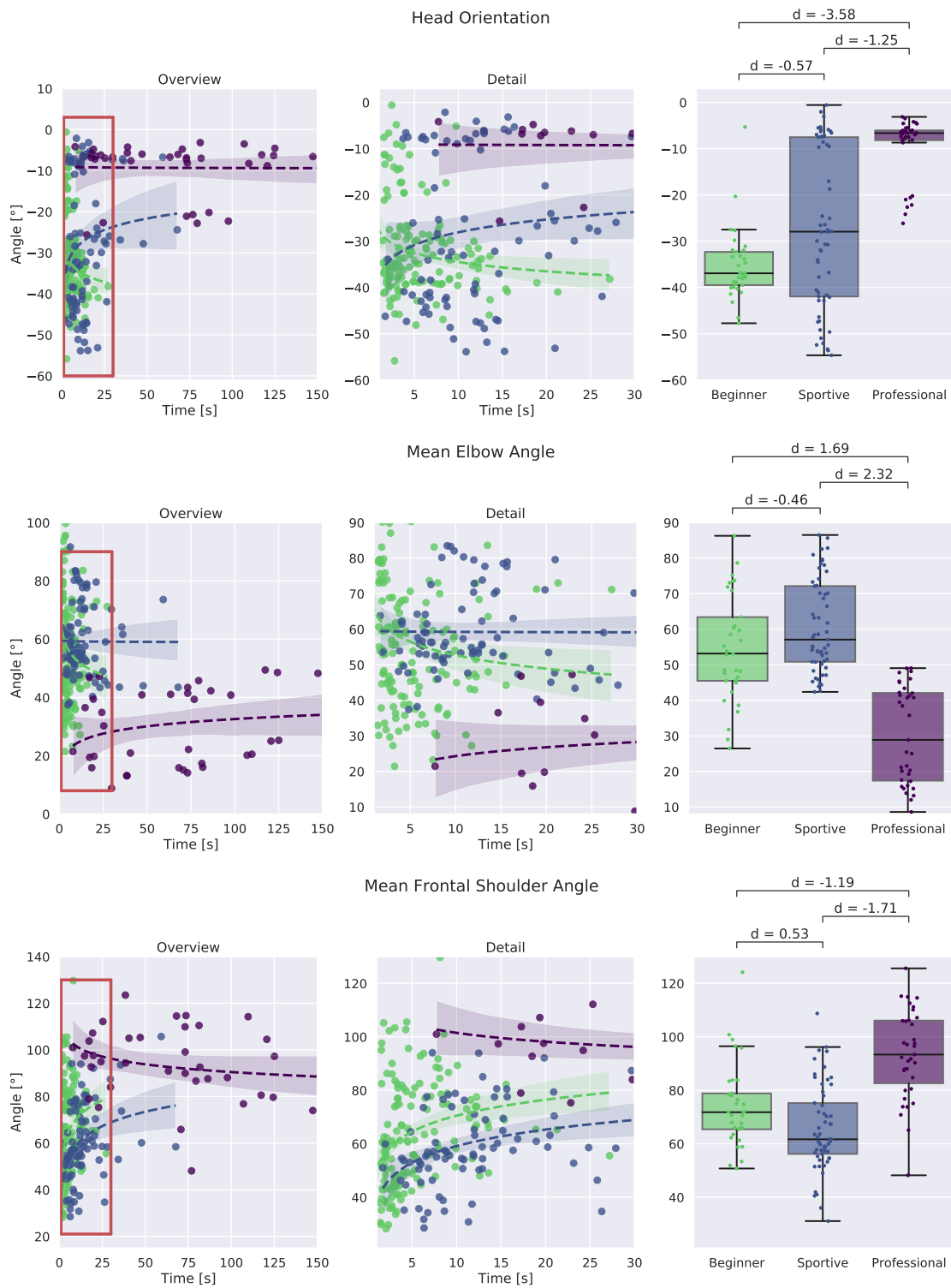


**Figure 7.19:** Comparison of head orientation, frontal shoulder angle and elbow angle with respect to time in balance and between groups. An overview of all trials is shown at the left, more detail in the middle and box plots for successful trials longer than 8 s at the right.

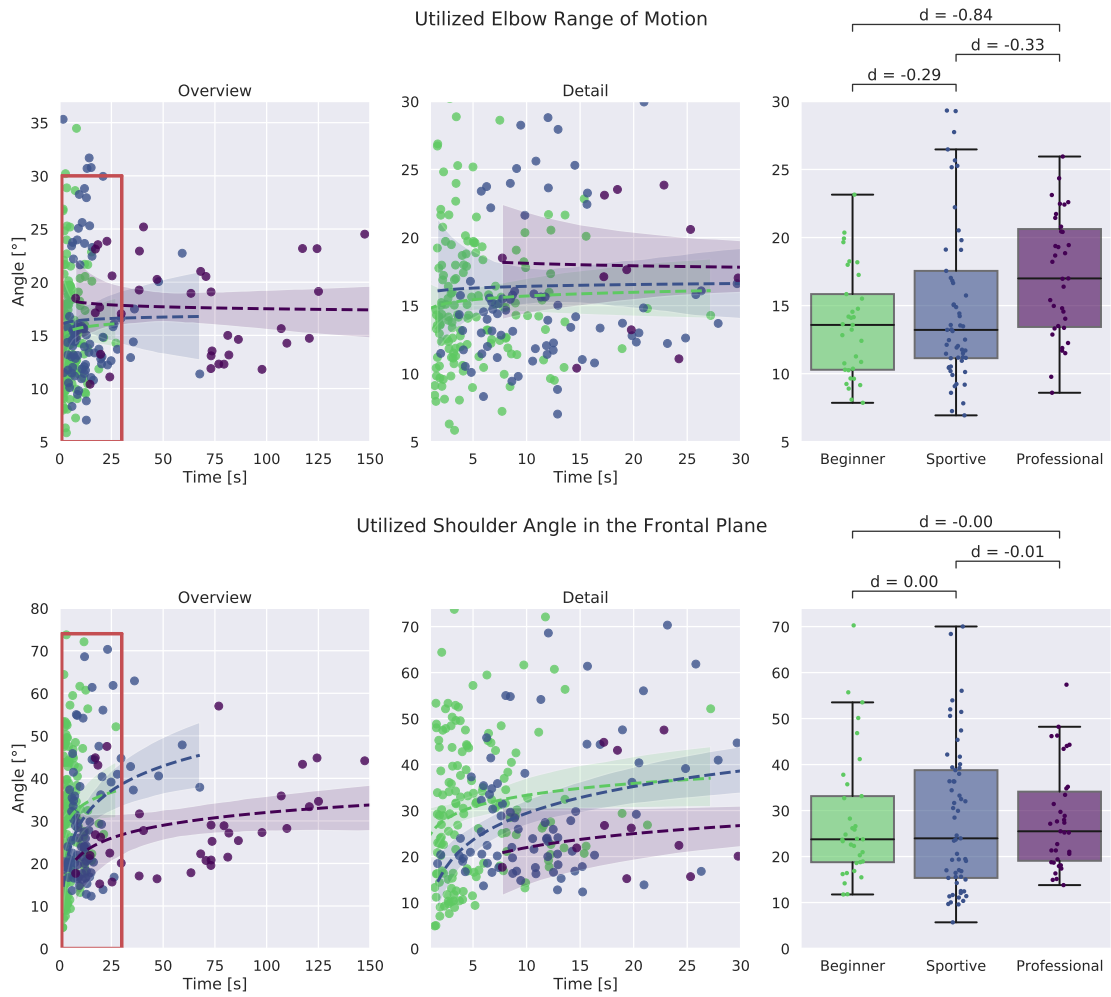


**Figure 7.20:** Comparison of utilized range of motion for frontal shoulder and elbow angle. An overview of all trials is shown at the left, more detail in the middle and box plots for successful trials longer than 8 s at the right. The professional group shows larger values for the elbow joints and groups show similar values in the frontal shoulder joint.



**Figure 7.21:** Comparison of movement coordination by means of rolling window correlation. An overview of all trials is shown at the left, more detail in the middle and box plots for successful trials longer than 8 s at the right.

### Walking Speed and Energy Ratio

Figure 7.22 shows the walking speed at the left, the normalized kinetic energy in the middle and the balance energy ratio at the right. We see that beginners attempt to walk faster (0.25 m/s) and do not focus on balance. Their balance energy ratio is lower than for the sportive beginners and professionals, but their normalized kinetic energy is about twice as large. Sportive beginners and professional slackliners walk at similar speeds of 0.15 m/s. Sportive beginners need to perform more balance related movement showing a larger energy ratio and larger normalized kinetic energy. Overall professionals are more consistent than the two beginner groups.

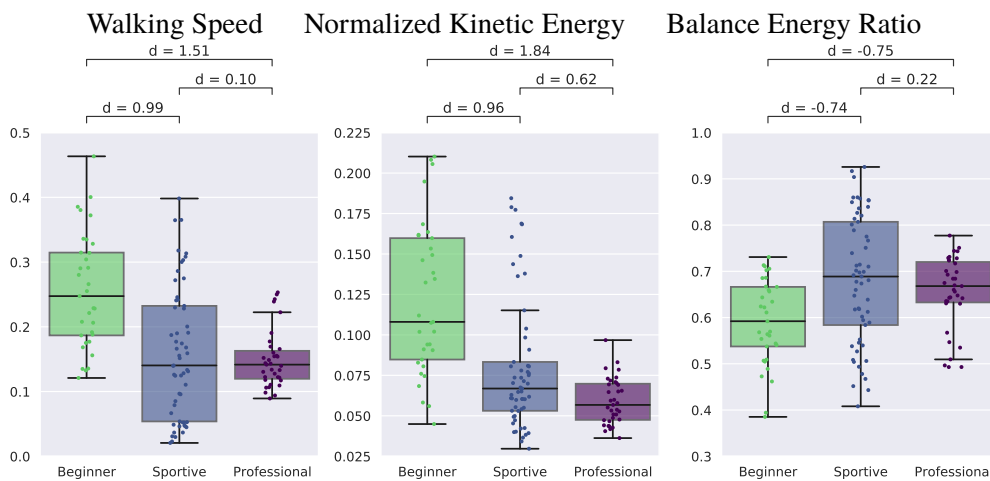


**Figure 7.22:** Comparison of walking speed, kinetic energy and balance energy ratio.

### **Normalized Angular Momentum**

In Figure 7.23 we plotted the normalized angular momentum around the three axes. Similar to single leg balancing we see a decrease from the beginner group to the professional slackliners in all three cases. The largest values are observed in the frontal plane, where all subjects need to perform balance related movement. Beginners show also large values around the vertical axis. No differences were found for the sagittal plane in single leg balancing. For walking this direction becomes important and we see, that beginners tilt forward and backward at a rate of  $14^\circ/\text{s}$ . Professionals maintain an upright posture and show about  $8^\circ/\text{s}$  of normalized angular momentum. Rotation around the vertical axis was a key factor in single leg balancing and is equally important for slackline walking. On average, beginners rotate at  $26^\circ/\text{s}$  and sportive beginners at  $21^\circ/\text{s}$ , whereas professionals maintain a posture where the arms are perpendicular to the slackline and rotate only at  $15^\circ/\text{s}$ .

### **Center of Mass Acceleration**

The CoM acceleration in all three directions is shown in Figure 7.24. Similar to single leg balancing, we see a reduction in all directions when comparing the groups, however values are generally larger. Sideways and vertical direction show the largest difference between the professional and beginner group.

### **7.5.3 Summary**

In Table 7.3 we listed all performance indicators for single leg balancing. For each group we list the mean value, standard deviation and range that was observed. We evaluate if the groups are significantly different using a ranked-sum-test [162] and compute the effect size using Cohen's-d [163]. The first column is color coded according to group differences. Performance indicators in red show differences between the three groups. We see that, unlike single leg balancing, where groups often showed similar behavior, walking exhibits more distinct differences. This can be explained by the task being more difficult and the fact that groups differed much more in their performance. All professional slackliners could easily walk on the slackline, most sportive beginners managed by the end of their recording session and barely any beginner trial was above the 8 s time limit. We see differences between all three groups for time, head orientation, movement coordination and kinetic energy.

We found a clear progression between groups for normalized angular momentum and CoM acceleration. In yellow, we show all performance indicators where the professional group differs from the two beginner groups and beginner groups show no difference between them. They are both related to the elbow joint. Professional slackliners use a different elbow angle and perform more movement. In green, we show all performance indicators where the beginner group differs from the balance-experienced groups, but no difference is found between the sportive and the professional group. For the Energy ratio we found that beginners walk faster than the other groups and use comparably less movement energy to balance. Further, beginners are not able to compensate the sideways acceleration of the slackline as well as the other groups leading to a larger CoM acceleration.

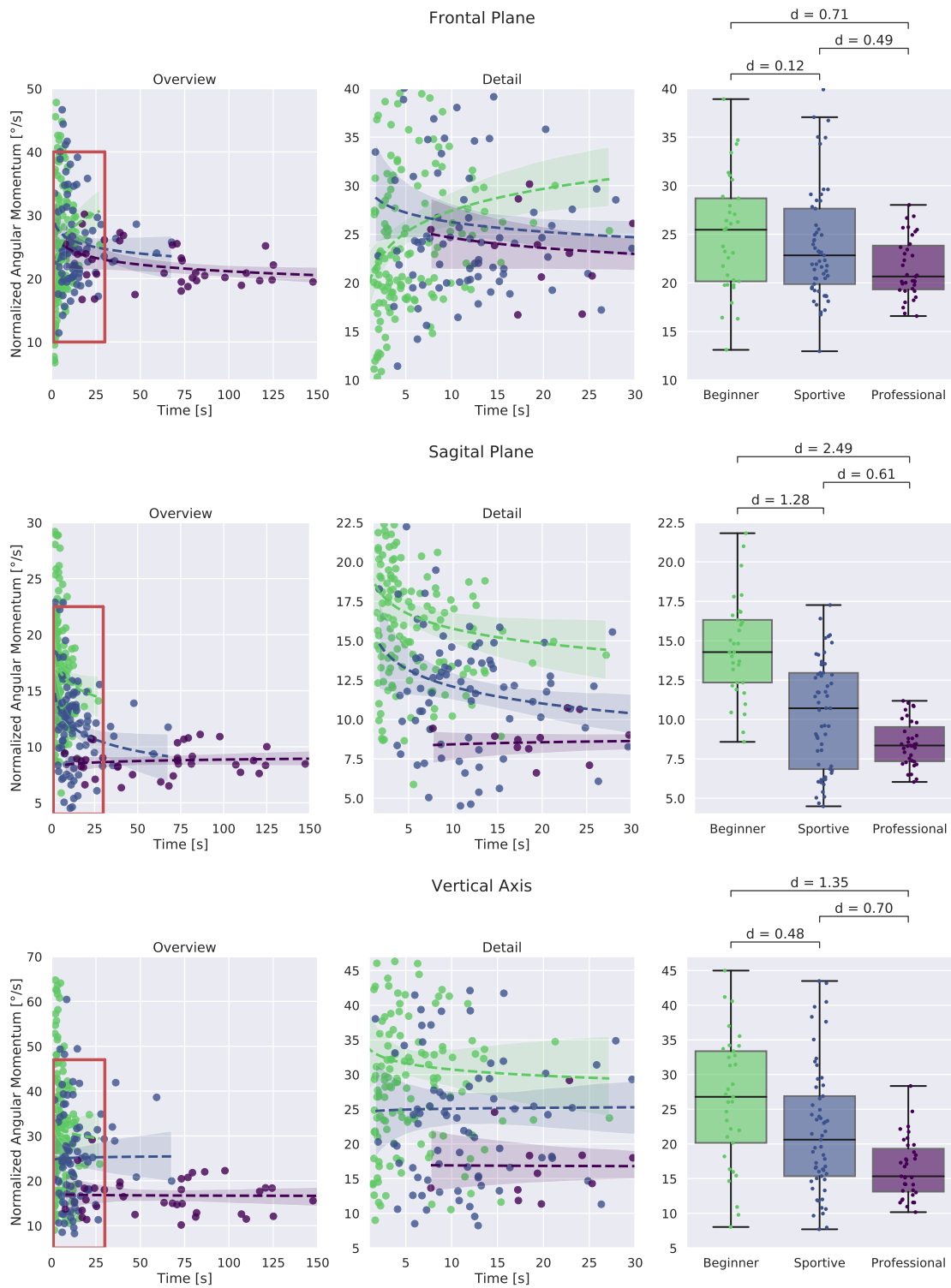


**Figure 7.23:** Normalized angular momentum around the three coordinate axis. An overview of all trials is shown at the left, more detail in the middle and box plots for successful trials longer than 8 s at the right. Short trials show larger values, especially in the beginner group. For longer trials minimization of normalized angular momentum around all three coordinate axis becomes important. The professional group shows the smallest variation between trials.

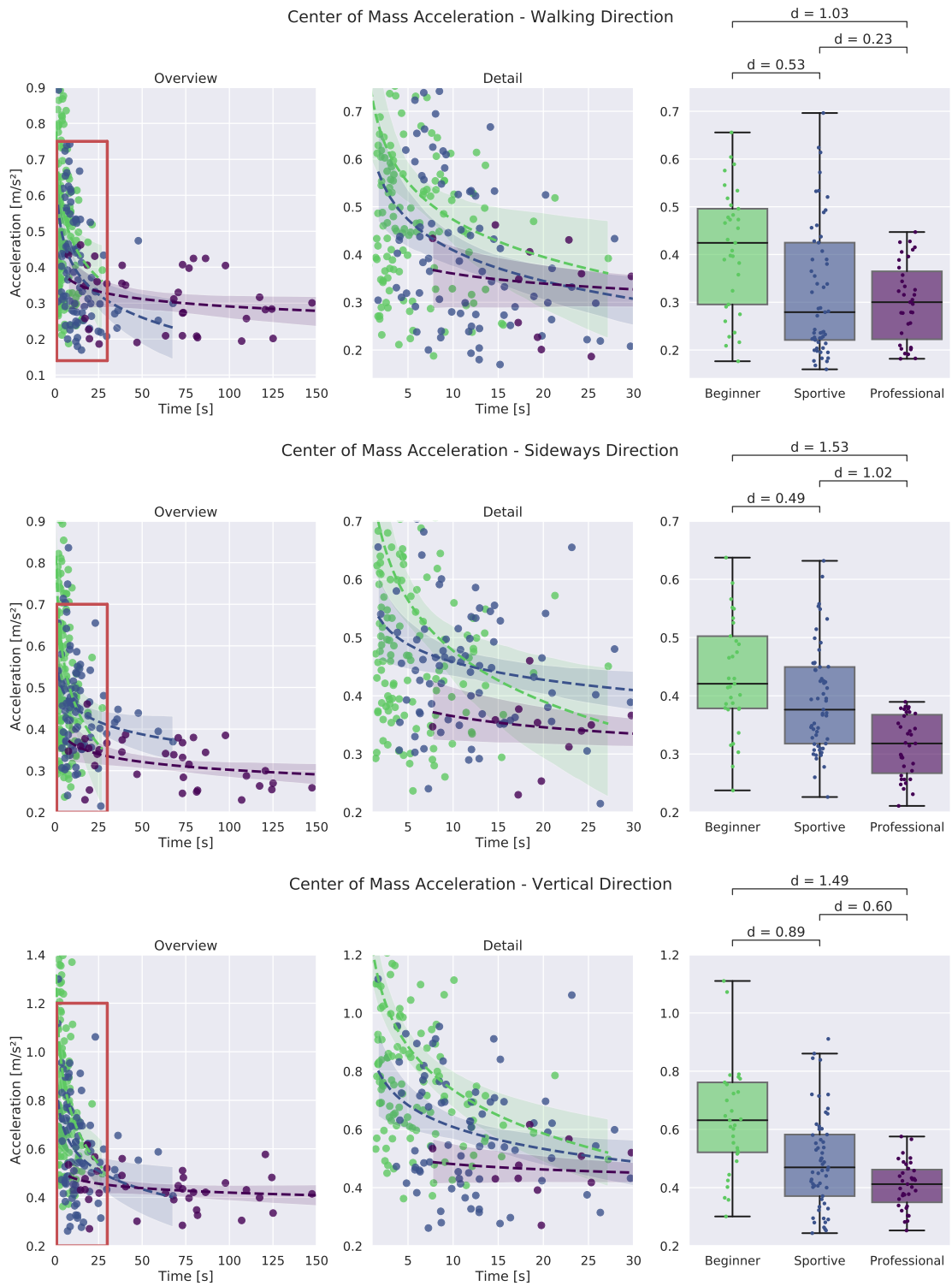


**Figure 7.24:** Comparison of Center of Mass acceleration. An overview of all trials is shown at the left, more detail in the middle and box plots for successful trials longer than 8 s at the right.

Variable	Beginners			Sportive			Professional			Beg / Sport			Beg / Pro			Sport / Pro		
	Mean ± SD	Range	Mean ± SD	Range	Mean ± SD	Range	Mean ± SD	Range	Mean ± SD	Range	p-val	d	p-val	d	p-val	d	p-val	d
Time	5.41	4.23	0.67	27.19	14.02	11.42	1.69	67.69	67.21	42.99	7.73	188.27	<0.0001	-1.12	<0.0001	-3.18	<0.0001	-2.08
Head Orientation [°]	-35.36	7.60	-47.73	-5.31	-27.13	17.05	-54.66	-0.56	-9.46	6.65	-26.14	-3.12	0.04	-0.57	<0.0001	-3.58	<0.0001	-1.25
Mean Frontal Shoulder Angle [°]	74.11	15.47	50.75	124.16	65.59	15.97	31.09	108.72	93.50	16.50	48.21	125.59	0.01	0.53	<0.0001	-1.20	<0.0001	-1.71
Mean Elbow Angle [°]	54.48	14.81	26.45	86.27	60.77	12.77	42.36	86.50	30.34	13.34	8.58	49.04	0.06	-0.46	<0.0001	1.69	<0.0001	2.32
Utilized Elbow Angle [°]	13.63	3.94	7.86	23.15	15.29	6.35	6.94	30.78	17.21	4.40	8.60	25.95	0.50	-0.29	0.002	-0.84	0.02	-0.33
Utilized Frontal Shoulder Angle [°]	28.14	13.73	11.76	70.26	28.09	15.62	5.70	70.02	28.19	11.10	13.79	57.37	0.73	0.00	0.68	0.00	0.51	-0.01
Hand Coordination (1.0s)	0.59	0.10	0.38	0.78	0.70	0.07	0.54	0.90	0.75	0.07	0.64	0.88	<0.0001	-1.32	<0.0001	-1.9	0.002	-0.73
Hand Coordination (0.2s)	0.73	0.05	0.59	0.80	0.76	0.03	0.68	0.85	0.78	0.02	0.75	0.84	0.008	-0.71	<0.0001	-1.49	<0.0001	-0.87
Normalized Kinetic Energy [J/kg]	0.12	0.05	0.04	0.21	0.08	0.04	0.03	0.18	0.06	0.01	0.04	0.10	<0.0001	0.96	<0.0001	1.84	0.03	0.62
Energy Ratio	0.59	0.09	0.39	0.73	0.68	0.14	0.41	0.93	0.85	0.08	0.49	0.78	0.003	-0.74	0.005	-0.75	0.37	0.22
Normalized Angular Momentum X [°/s]	24.92	5.89	13.11	38.91	24.19	6.21	12.96	44.16	21.57	3.05	16.58	28.02	0.39	0.11	0.01	0.71	0.07	0.49
Normalized Angular Momentum Y [°/s]	14.55	3.10	8.58	21.82	10.26	3.44	4.49	17.26	8.50	1.42	6.04	11.18	<0.0001	1.28	<0.0001	2.50	0.02	0.61
Normalized Angular Momentum Z [°/s]	26.30	9.25	8.03	44.98	21.89	9.10	7.71	43.48	16.51	4.25	10.17	28.35	0.02	0.48	<0.0001	1.35	0.005	0.70
CoM Acceleration X [m/s <sup>2</sup> ]	0.41	0.13	0.18	0.66	0.33	0.16	0.16	0.96	0.30	0.08	0.18	0.45	0.003	0.53	0.0002	1.03	0.83	0.23
CoM Acceleration Y [m/s <sup>2</sup> ]	0.44	0.10	0.24	0.71	0.39	0.09	0.23	0.63	0.31	0.05	0.21	0.39	0.03	0.49	<0.0001	1.53	<0.0001	1.02
CoM Acceleration Z [m/s <sup>2</sup> ]	0.66	0.23	0.30	1.23	0.49	0.16	0.24	0.91	0.41	0.08	0.25	0.58	0.0003	0.89	<0.0001	1.49	0.02	0.59

**Table 7.3:** Summary of all Performance Indicators for Slackline Walking. P-values are computed using a Wilcoxon Rank-Sum Test. We color-coded performance indicators according to group differences: red: all groups are different; orange: professionals are different from beginners and sportive beginners; green: beginners are different from the sportive and professional group.

## 7.6 Comparison Between Stable and Unstable Balancing

In this section we compare stable balancing, as analyzed in the sections above, to unstable balancing, shortly before the subject fell off the slackline. We define the stable part from 2 s after getting up until 2 s before losing contact with the slackline, as before. The unstable part of the movement is during the last 2 s. We computed all performance indicators for the two parts for single leg balancing and walking. For the short, unstable movements we expect higher variations between trials than for the stable, longer movement trajectories. We did not find any differences for posture, hand coordination, the energy ratio during walking and sideways stance foot acceleration during single leg balancing. Further findings are discussed in more detail.

### Center of Mass Acceleration

For CoM acceleration we plotted the results in Figure 7.25. Single leg balancing is shown in the left two columns and walking in the right two columns. We find larger values when comparing stable to unstable balancing for both beginner groups in all three directions and for both tasks. As derived earlier, they are not able to control and minimize their CoM acceleration. We see that the acceleration when falling after single leg balancing is similar or lower than the acceleration during stable walking. The professional group only shows increased values in the vertical direction for walking.

### Normalized Angular Momentum

We did not find differences in normalized angular momentum during single leg balancing. Also we found no differences in the frontal plane during walking. Results for the sagittal plane are plotted at the left and around the vertical axis at the right in Figure 7.26. Similar to the CoM acceleration, the professional group shows small mean values during the stable and unstable part and only a larger variance. We found larger values for the two beginner groups when being unstable. This supports the finding that the professional group is able to focus the balance movement in the frontal plane even shortly before falling. They do not lean forward or rotate around the vertical axis.

### Static Balance and Stance Foot Acceleration

The variance of CoM position in the stance foot frame in sideways direction is plotted on the left of Figure 7.27. We see comparably small and similar values for all groups during stable single leg balance, however a larger variance is observed before falling for the two beginner groups. They lose static balance and their CoM projection moves away from the support polygon. In the right two columns we plotted the vertical foot acceleration. We find larger values for all groups, which is consistent with the increased values of vertical CoM acceleration that we found previously.

## 7.6 Comparison Between Stable and Unstable Balancing

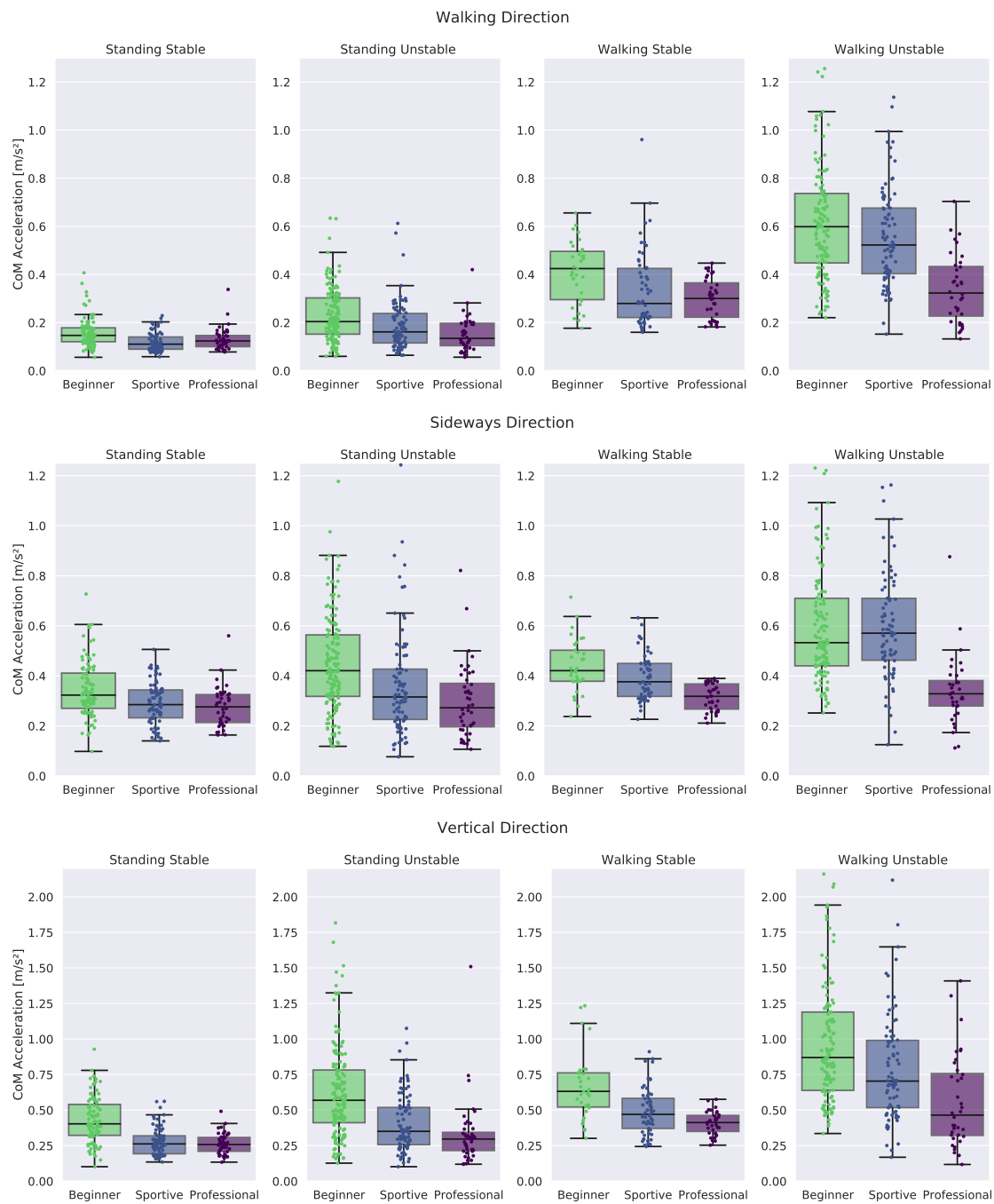


**Figure 7.25:** Center of Mass Acceleration for stable and unstable balancing. Stable balancing is shown in the first and third column, unstable balancing in the second and last column. The beginner and sportive group show increased values in all directions before falling. Professional Slackliners only show increased values in the vertical direction for walking.

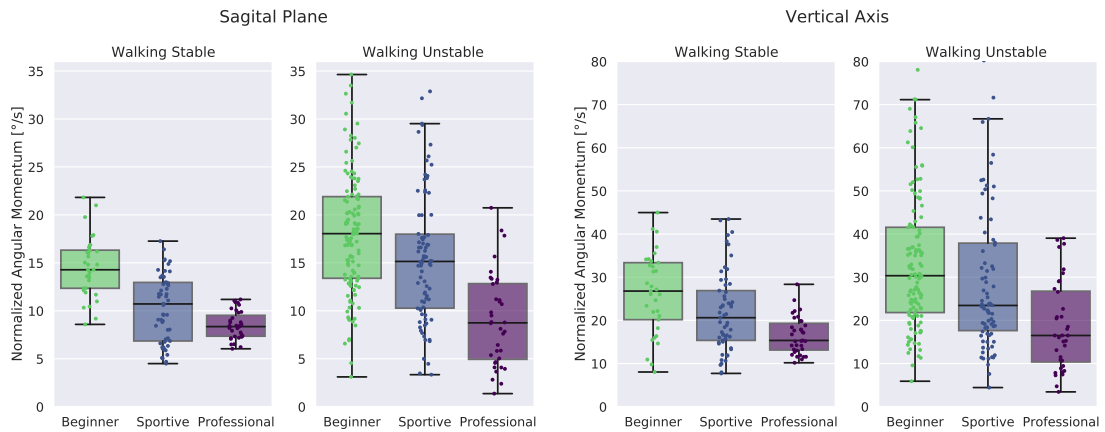


**Figure 7.26:** Group comparison of normalized angular momentum for stable and unstable walking.

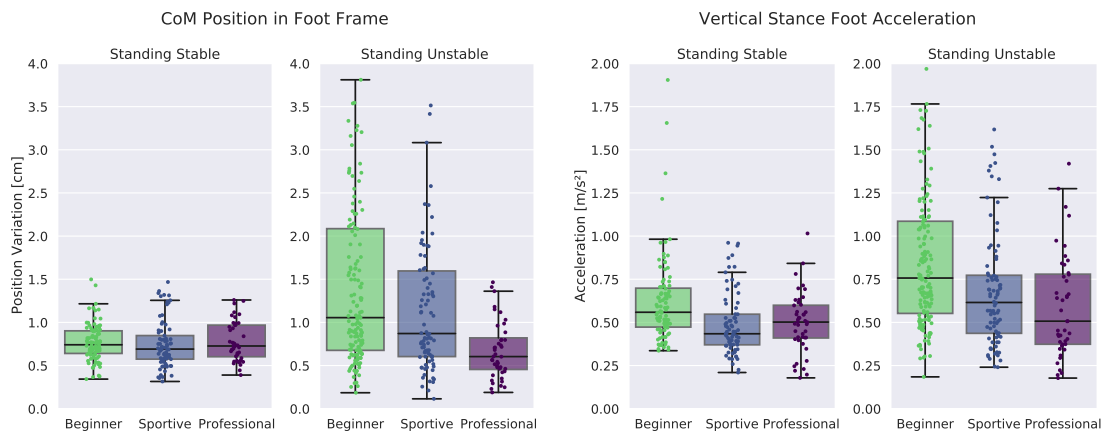


**Figure 7.27:** Center of Mass projection and stance foot acceleration for stable and unstable single leg slackline balancing.

### Summary

By comparing the stable to the unstable part of slackline balancing we were able to confirm the findings that CoM acceleration can be used as a measure of how stable and balanced a subject on the slackline is. We also found that beginners show larger values of angular momentum shortly before falling than the professional group, suggesting that they still try to somehow maintain balance, while the professional group realized that they will fall and do not increase angular momentum. This results in increased stance foot acceleration and loss of static balance.

## 7.7 Discussion

The static balance test was shown to be suitable to divide participants according to their balance expertise. Especially the single leg scenario with eyes closed allowed us to distinguish two groups based on whether the subject managed to maintain balance for 30 s. We found strong correlation between the time in balance with eyes closed and the time that a subject was able to balance on the slackline. The balance-experienced beginners group managed to maintain balance on the slackline about three times longer than the balance-inexperienced group.

Regarding performance indicators, we found reduced average angular velocity in all three directions and reduced CoM acceleration in sideways and vertical direction as suitable measures for how well a subject has mastered single leg slackline balancing and slackline walking. Reduced rotation around the vertical axis allows professional slackliners to maintain an upright posture and focus their movement on the frontal plane, whereas beginners and sportive beginners show larger movement in all three directions. Differences in pose strategy were found between the professional group and the beginners group. Professional slackline athletes perform most of the balance related movement in the elbow joint and maintain a perpendicular arm configuration.

We also found that, the professional group shows a 50 % larger utilized range of motion in the shoulder and elbow. We conclude that they are more versatile in performing balance movements and can maintain balance in a larger set of postures. Beginners are stable only in some postures, but fall in others, where professionals are still able to balance. We found adjusted stance leg compliance for the professional and sportive group. They show similar variation in vertical foot acceleration as the beginner group, but reduced vertical CoM acceleration.

In Chapter 1 we discussed proprioception, the vestibular system and visual feedback as key components that allow humans to balance. The balance test with eyes closed has been used in the literature to investigate lack of proprioception [20]. We suggest, that the sportive beginners group does have better proprioception than the balance-inexperienced beginners. Findings for hand coordination support this claim. Maintaining an upright head position with respect to gravity is crucial for the vestibular system to function properly [174]. Indeed, the professional group consistently maintains a horizontal head orientation. This can also be linked to visual feedback. We assume that their gaze is fixed to a point, as it was shown by Schärli et al. [126], whereas, especially during walking, beginners need to confirm their foot placement. When comparing stable to unstable balancing we were able to confirm that CoM acceleration can be used as a measure of how stable a subject's balances on the slackline is.



## 8 Static and Dynamic Balance in Schizophrenia Patients

In this chapter we analyze balance data from persons with schizophrenia and compare them to a healthy control group. The data recording was part of the "Schizophrenia and the Moving Body" project by Lily Martin [7].

A total of 20 subjects with schizophrenia referred to as the "Experimental Group" and 27 control subjects participated in the study. All participants were recruited by Lily Martin who also assessed demographic, psychiatric and movement data. At the motion capture lab of HCMR Lily Martin was assisted by the author of this thesis and other lab employees.

We recorded the following tasks: regular walking, a static balance test, tandem walking with eyes open and eyes closed and a star jump. In context of this thesis, static and dynamic balance capabilities were evaluated based on the recordings of the static balance test and the tandem walk.

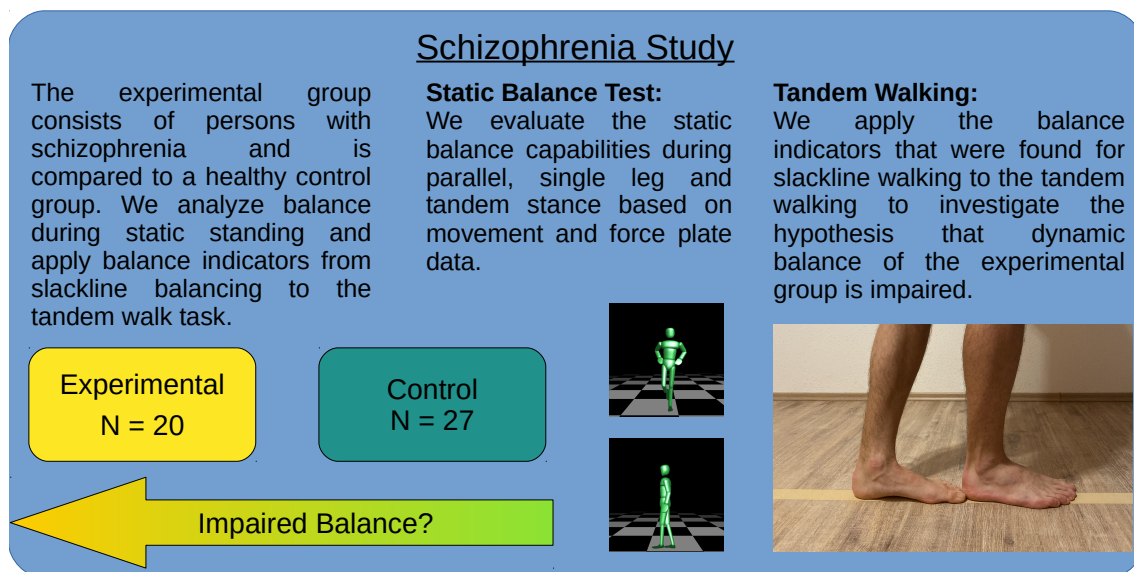


**Figure 8.1:** Overview of the Balance Study in the "Schizophrenia and the Moving Body" project

### Participant Overview

Table 8.1 shows an overview of the demographic and clinical characteristics. Subject groups match for age, sex and height. For weight, the experimental group on average weighs 14.6 kg more ( $p = 0.007$ ) resulting in a  $5.6 \text{ kg/m}^2$  higher BMI ( $p < 0.0001$ ). Only the Experimental group takes medication which is given in OPZ [175, 176].

Characteristics	Schizophrenia (n = 20)		Healthy Control (n = 27)	
	Median	Range	Median	Range
Age [a]	36.2	[19, 59]	39.0	[20, 59]
Sex [F/M]	14 / 6		18/9	
Height [cm]	178.3	[156.0, 196.6]	179.0	[165.0, 194.5]
Mass [kg]*	91.9	[60.9, 124.7]	77.5	[54.6, 122.1]
BMI [ $\text{kg/m}^2$ ] **	29.3	[23.2, 36.2]	23.7	[19.5, 35.3]
Medication [OPZ]	17.0	[5.0, 32.3]		

**Table 8.1:** Demographic and clinical characteristics of all participants. Groups match for age and height, but are significantly different for mass and BMI. \* ( $p < 0.01$ ) and \*\* ( $p < 0.0001$ )

## 8.1 Motion Capture Protocol

In the following we summarize the motion capture protocol. The motion assessment can be divided into five parts: the preparation of the subject, regular walking, the static balance test, tandem walking and the star jump.

### Subject Preparation

After obtaining written consent, all subjects were prepared with the Gait IOR marker set [128] described in Section 3.1.1. Unlike to the slackline study no additional markers were placed. The height and weight of the participant was measured and a static trial recorded. Afterwards the static markers were removed.

### Regular Walking

Subjects were asked to walk back and forth in their most comfortable speed in a marked corridor of  $10 \times 0.5 \text{ m}$ . After 2 min, it was assumed that the subject had adjusted to the situation and gait was *regular*. Then, 8 sequences of walking through the capture volume were recorded. Afterwards, subjects were asked to count down from 100 (dual task) and another 8 sequences were recorded. Evaluation of these recordings are not subject of this thesis.

### Balance Test

The balance test was instructed and recorded following the protocol in Section 6.1.

### Tandem Walking

Subjects were asked to perform a tandem walk of  $\approx 2$  m. Tape marks were used to indicate a straight line. Afterwards, subjects turned around and performed the same walk, but with eyes closed, without indications for direction.

### Star Jump

Subjects were asked to stand on the force plates and perform a star jump, starting in neutral position with arms aligned and feet closed. After a short demonstration of the task eight to ten repetitions were recorded.

## 8.2 Static Stability Evaluation

Analysis of the static balance test was divided into evaluation by means of success rate and time in balance and CoP sway analysis. We analyzed the CoP parameters introduced in Chapter 6: sway distance (RDIST), sway velocity (MVEL), sway frequency (MFREQ) and the RATIO between the AP and ML RDIST. We used a Wilcoxon Rank-Sum Test [162] to compare between the two groups, a Wilcoxon signed-rank test to compare the change between the eyes open and eyes closed condition and mixed model ANOVAs to quantify interaction effects. Effect sizes are quantified percentually and by means of Cohen's  $d$  [163]. As introduced in Chapter 2 we aimed to answer the following hypotheses with regards to static balance:

- **Static Balance Analysis:** We hypothesize that the experimental group shows impaired static balance capabilities and performs worse than the control group by means of success rate and time in balance.
- **Center of Pressure Sway Analysis:** We expect to find differences in CoP sway parameters even when comparing successful trials during static balance.
- **Eyes Open and Closed Condition:** We expect that removing visual perception has a larger effect on the experimental group.

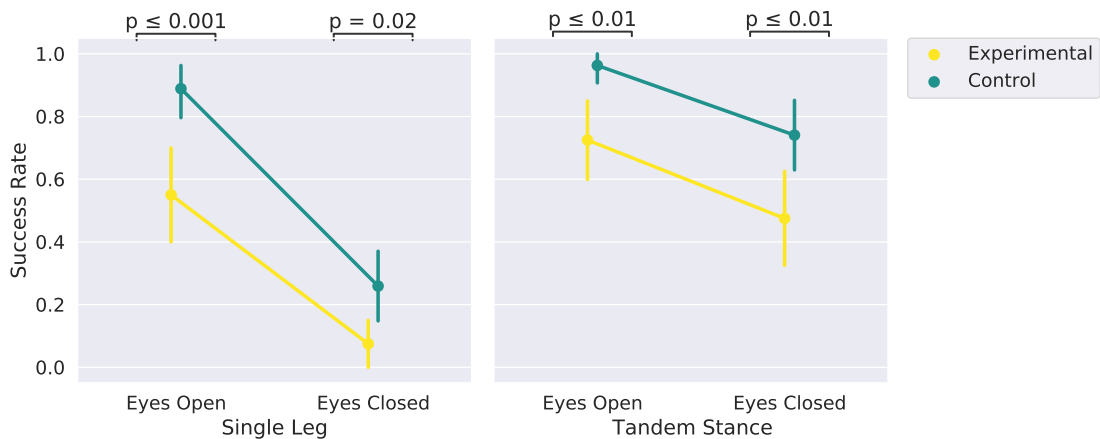
### 8.2.1 Success Rate and Time in Balance

Table 8.2 shows an overview of all tasks and the percentage of participants that were able to balance the full 30 s. We combined results of the different leg configurations for single leg and tandem stance trials. For healthy patients literature shows no difference between dominant and non-dominant leg [82, 177]. This is why we did not further analyze if this is indeed the case for the experimental group. As expected, the regular parallel stance was fulfilled successfully by all subjects. During all other scenarios, the control group had a significantly higher success rate: 89 % compared to 55 % for single leg balancing with eyes open ( $p \leq 0.001$ ,  $d = 0.83$ ), 26 % compared to 8 % for single leg balancing with eyes closed ( $p = 0.02$ ,  $d = 0.49$ ), 96 % compared to 73 % for tandem stance balancing with eyes open ( $p \leq 0.001$ ,  $d = 0.73$ ) and 74 % compared to 48 % for tandem stance balancing with eyes closed ( $p \leq 0.001$ ,  $d = 0.56$ ).

Findings show that standing on one leg was more difficult than the tandem stance, as was already observed in the slackline study in Chapter 7. Results are summarized in Table 8.3 and plotted in Figure 8.2.

Task \ Group	Eyes Open		Eyes Closed		Color Coding Percent [%]
	Experimental	Control	Experimental	Control	
Both Feet Parallel	100	100	100	100	≥ 75
Single Leg	55	89	8	26	≥ 50
Tandem Stance	73	96	48	74	≥ 25
Overall Average	65	94	28	50	< 25

**Table 8.2:** Balance test success rate for Experimental and Control for all balance test scenarios. A trial was counted as successful when the subject managed to balance the full 30 s. Cell entries are color coded by quartile.



**Figure 8.2:** Direct comparison of the two groups and the eyes open and eyes closed situation for single leg and tandem stance balancing by means of success rate. We plotted the group mean, the 95% confidence interval and the trend between the two conditions as straight line. The experimental group is shown in yellow, the control group in green. p-values were calculated using the Wilcoxon Rank-Sum Test and show that the groups differ significantly in all conditions.

Since the success rate is not able to differentiate between early falling and almost successful trials, we evaluated the time the subjects were able to maintain balance. Figure 8.3 shows the distribution for the two scenarios at the top and the group comparison at the bottom. We see that the control group shows a longer time in balance for all scenarios and that the majority of trials are close to 30 s, except for single leg standing with eyes closed. On average, healthy subjects managed to balance  $\approx 7$  s longer for single leg stance, both with eyes open ( $p < 0.0001$ ,  $d = 0.89$ ) and eyes closed ( $p < 0.001$ ,  $d = 0.71$ ). Further, they balanced  $\approx 4$  s longer for tandem stance with eyes open ( $p < 0.01$ ,  $d = 0.62$ ) and  $\approx 6$  s longer for tandem stance with eyes closed ( $p < 0.01$ ,  $d = 0.59$ ). Details are given in Table 8.3.

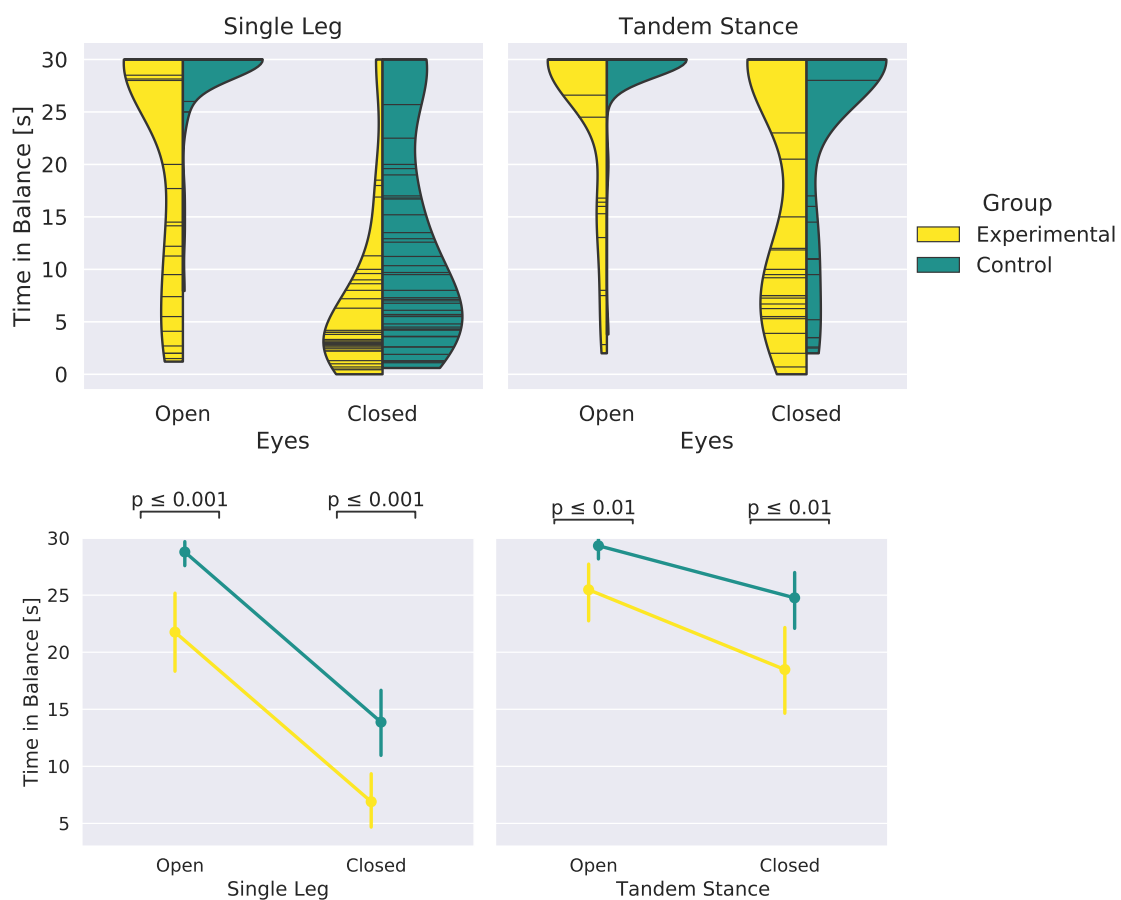


**Figure 8.3:** We plotted the time that the subject managed to maintain balance. Top Row: Violin Plot showing the distribution of all participants and scenarios. Bottom Row: Direct comparison of the two groups and scenarios. We plotted the group mean, the 95 % confidence interval and the trend between the two conditions as straight line. The experimental group is shown in yellow, the control group in green. P-values were calculated using the Wilcoxon Rank-Sum Test.

Task \ Variable	Eyes	Experimental (N = 20)			Control (N = 27)			p-val	Cohen's d
		Mean ± SD	95%CI	Success Rate [%]	Mean ± SD	95%CI	Success Rate [%]		
Single Leg	Open	55	50	[40, 70]	89	31	[79, 96]	<b>0.0002</b>	0.83
	Closed	8	26	[0, 18]	26	44	[15, 39]	<b>0.02</b>	0.49
Tandem	Open	73	45	[58, 85]	96	19	[91 100]	<b>0.001</b>	0.73
	Closed	48	50	[33, 63]	74	44	[61 85]	<b>0.01</b>	0.56
<b>Time in Balance [s]</b>									
Single Leg	Open	21.8	11.0	[18.2 25.1]	28.8	4.1	[27.6 29.7]	<b>0.0001</b>	0.89
	Closed	6.9	8.0	[4.6 9.5]	13.9	10.7	[11.1 16.8]	<b>0.0002</b>	0.71
Tandem	Open	25.5	8.4	[22.7 27.9]	29.3	3.6	[28.2 30.0]	<b>0.001</b>	0.62
	Closed	18.5	11.6	[14.8 22.2]	24.76	9.6	[22.1 27.2]	<b>0.007</b>	0.59

**Table 8.3:** Summary and statistics for evaluation of the balance test. The success rate of the experimental group is significantly lower than for the control group in all scenarios. Effect sizes are large to medium. The same observation is made for the time in balance. P-values were calculated using the Wilcoxon Rank-Sum Test.

### 8.2.2 Center of Pressure Sway Analysis

The CoP trajectory of the force plate data was recorded at a rate of 900 Hz and filtered using a 5<sup>th</sup> order Butterworth low-pass filter with cut-off frequency of 9 Hz [178]. To avoid any bias from stepping on and off the force plate, all trials were cut to 20 s by removing the first and last 5 s. For parallel stance, all trials were evaluated. Due to technical malfunction, we were only able to collect force plate data from 19 of 20 participants of the experimental group.

For standing on one leg and tandem stance, only successful trials, where the subject did not fall or move the stance foot were taken into account. Falling results in a large change in CoP position and stepping off the force plate leads to gaps in the trajectory, both biasing the result and therefore not leading to further insight. We combined the trials of the two single leg and tandem stance configurations. For the experimental group we evaluated 27 trials of single leg stance with eyes open and 27 trials of tandem stance with eyes open. For the control group we evaluated 50 and 52 trials respectively. The number of trials was not sufficient for the two eyes-closed conditions. Only 3 trials for single leg stance and 16 trials of tandem stance were successful, which is less than 50% of participants. Hence, we evaluate parallel stance with eyes open and closed and the single leg and tandem stance with eyes open.

We computed the balance metrics proposed and discussed in Chapter 6: RDIST, MVEL, MFREQ and the RATIO between the AP and ML RDIST. As derived in Section 6.3 and suggested by Chiari et al. [159], distance metrics were normalized by subject height.

**Sway Distance and Ratio**

Figure 8.4 shows boxplots of the RDIST in both directions and the RATIO for the four scenarios. Group differences are indicated. Findings for AP direction and the ratio are not consistent across the scenarios. The ML direction shows large discrimination between the two groups in all four scenarios. The experimental group consistently shows  $\approx 30\%$  larger sway ( $p < 0.01$ ,  $d > 0.77$ ). As expected, sway values are generally smaller for parallel stance, since subjects can actively use both feet to control this direction. Differences in AP direction are only found for single leg balancing ( $p = 0.04$ ,  $d = 0.57$ ). Subject groups differ in sway ratio during parallel stance. This is a consequence of the increased sway for the experimental group in ML direction. Table 8.4 summarizes all findings.

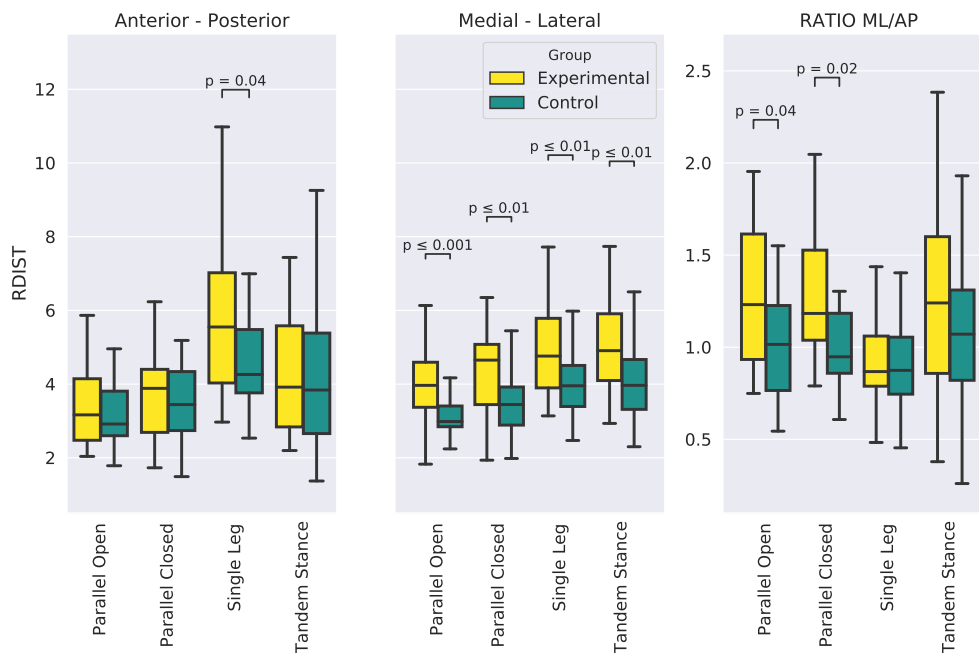


**Figure 8.4:** Evaluation of CoP data: sway distance (RDIST) in ML and AP direction and ratio. Box plots indicate median and interquartile range. Whiskers are extended till values within 1.5 times the innerquartile range. The experimental group shows significantly larger sway in ML direction for all tasks. P-values were calculated using the Wilcoxon Rank-Sum Test.

### Mean Velocity and Mean Frequency

Figure 8.5 shows the evaluation of MVEL and MFREQ. There is a clear increase between parallel stance and the more difficult single leg balancing and tandem stance. Differences between the groups are found for the AP velocity during eyes open parallel stance (30 %,  $p = 0.01$ ,  $d = 0.78$ ) and in the ML mean frequency during eyes closed parallel stance (21 %,  $p = 0.01$ ,  $d = -0.64$ ), single leg balancing (19 %,  $p = 0.02$ ,  $d = -0.6$ ) and tandem stance (25 %,  $p \leq 0.01$ ,  $d = -0.69$ ). The difference in frequency is a consequence of larger sway in ML direction since it is defined as the fraction between velocity and sway. Exact values are given in Table 8.5.

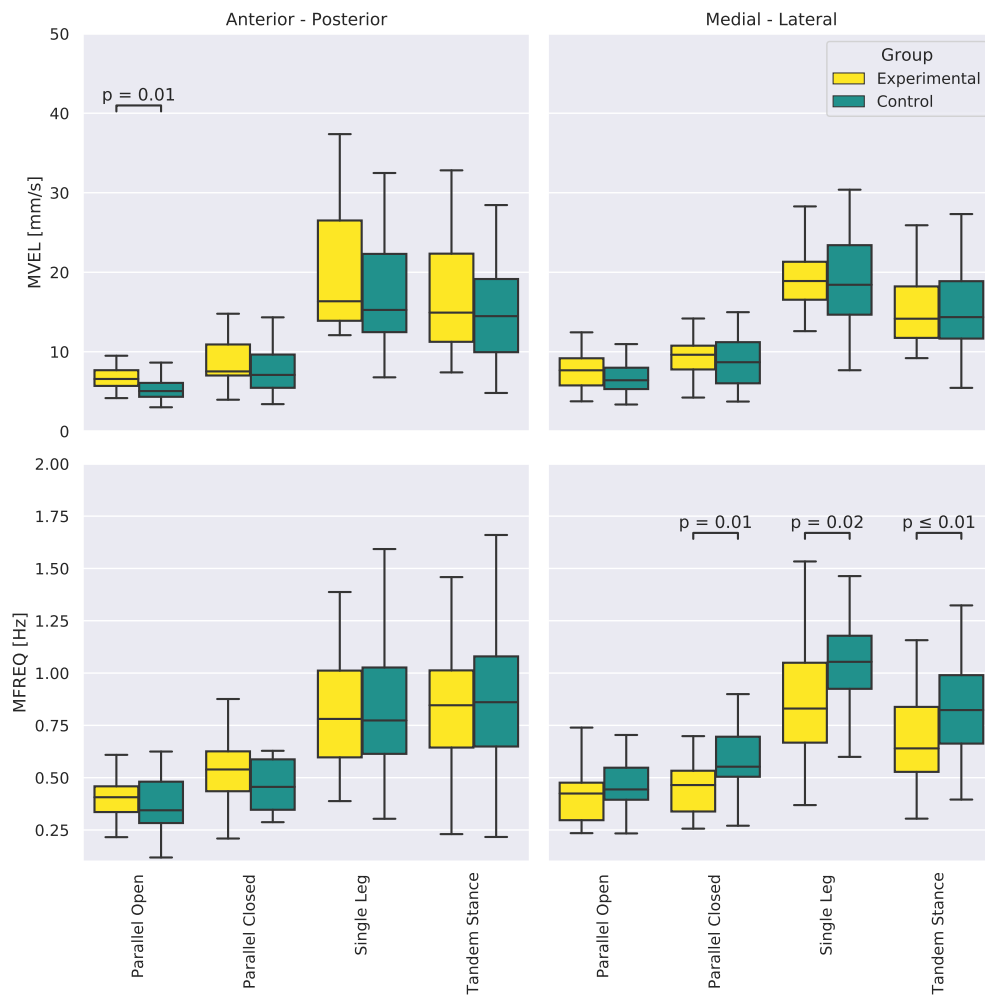


**Figure 8.5:** Evaluation of CoP data for sway velocity (MVEL) and sway frequency (MFREQ) in ML and AP direction. Box plots indicate median and interquartile range. Whiskers are extended till values within 1.5 times the innerquartile range. The experimental group shows significantly smaller sway frequency in ML direction for parallel stance with eyes closed, single leg stance and tandem stance. P-values were calculated using the Wilcoxon Rank-Sum Test.

Task \ Variable	Direction	Experimental				Control				p-val	Cohen's d
		N	M	SD	Range	N	M	SD	Range		
<b>RDIST [mm] (normalized to subject height)</b>											
Parallel Open	ML	19	4.19	1.21	[1.83, 6.75]	27	3.23	0.90	[1.88, 6.63]	<b>0.0009</b>	0.90
	AP	19	3.50	1.14	[2.04, 5.86]	27	3.38	1.38	[1.78, 8.55]	0.69	0.09
Parallel Closed	ML	19	4.49	1.31	[1.93, 7.76]	27	3.50	0.96	[1.98, 6.09]	<b>0.006</b>	0.87
	AP	19	3.68	1.24	[1.73, 6.23]	27	3.51	0.96	[1.49, 5.18]	0.74	0.15
Single Leg	ML	27	5.11	1.64	[3.14, 9.43]	50	4.04	0.99	[2.47, 7.40]	<b>0.002</b>	0.84
	AP	27	5.72	2.03	[2.97, 10.98]	50	4.74	1.50	[2.53, 9.48]	<b>0.04</b>	0.57
Tandem Stance	ML	27	5.17	1.53	[2.93, 9.26]	52	4.15	1.17	[2.30, 8.87]	<b>0.002</b>	0.77
	AP	27	4.92	2.97	[2.20, 12.64]	52	4.48	2.49	[1.37, 16.28]	0.80	0.16
<b>RATIO</b>											
Parallel Open		19	1.27	0.39	[0.75, 1.95]	27	1.02	0.28	[0.54, 1.55]	<b>0.04</b>	0.73
Parallel Closed		19	1.28	0.35	[0.79, 2.05]	27	1.03	0.29	[0.61, 2.18]	<b>0.015</b>	0.78
Single Leg		27	0.94	0.26	[0.48, 1.49]	50	0.90	0.23	[0.45, 1.52]	0.67	0.20
Tandem Stance		27	1.32	0.64	[0.38, 3.33]	52	1.10	0.44	[0.26, 2.41]	0.18	0.41

**Table 8.4:** Sway distance (RDIST) and sway ratio (RATIO) evaluation of CoP data for successful balance trials. Less trials are available for the experimental group as they succeeded at a lower rate. The experimental group shows significantly higher sway distance in the medial-lateral direction in all four scenarios. Differences in anterior-posterior direction are only significant for single leg stance. Sway ratio is significantly different for parallel stance. P-values were calculated using the Wilcoxon Rank-Sum Test.

Task \ Variable	Direction	Experimental				Control				p-val	Cohen's d
		N	M	SD	Range	N	M	SD	Range		
<b>MVEL [mm/s] (normalized to subject height)</b>											
Parallel Open	ML	19	7.64	2.43	[3.77, 12.44]	27	6.75	1.77	[3.37, 10.96]	0.18	0.42
	AP	19	7.01	2.08	[4.17, 11.73]	27	5.54	1.67	[3.02, 9.70]	<b>0.012</b>	0.78
Parallel Closed	ML	19	9.79	4.81	[3.10, 26.79]	27	9.35	3.82	[3.74, 20.45]	0.81	0.10
	AP	19	9.25	4.51	[3.97, 24.53]	27	8.08	3.94	[3.41, 22.63]	0.24	0.27
Single Leg	ML	27	19.52	4.25	[12.59, 28.28]	50	19.48	6.69	[7.68, 38.88]	0.59	0.01
	AP	27	20.61	8.76	[12.09, 46.07]	50	17.64	6.89	[6.78, 32.48]	0.21	0.38
Tandem Stance	ML	27	15.90	6.51	[9.20, 41.46]	52	16.14	6.54	[5.46, 38.98]	0.93	-0.04
	AP	27	17.58	9.12	[7.41, 47.39]	52	16.53	8.54	[4.82, 39.28]	0.65	0.12
<b>MFREQ [Hz]</b>											
Parallel Open	ML	19	0.41	0.13	[0.23, 0.74]	27	0.46	0.11	[0.23, 0.70]	0.20	-0.41
	AP	19	0.46	0.23	[0.22, 1.25]	27	0.38	0.13	[0.12, 0.62]	0.25	0.47
Parallel Closed	ML	19	0.47	0.16	[0.26, 0.90]	27	0.57	0.15	[0.27, 0.90]	<b>0.014</b>	-0.64
	AP	19	0.55	0.17	[0.21, 0.88]	27	0.49	0.18	[0.29, 1.00]	0.18809	0.32
Single Leg	ML	27	0.88	0.28	[0.37, 1.53]	50	1.05	0.27	[0.48, 1.79]	<b>0.018</b>	-0.60
	AP	27	0.84	0.32	[0.39, 1.87]	50	0.84	0.30	[0.30, 1.59]	0.90229	-0.00
Tandem Stance	ML	27	0.68	0.21	[0.30, 1.16]	52	0.85	0.25	[0.40, 1.54]	<b>0.006</b>	-0.69
	AP	27	0.87	0.35	[0.23, 1.71]	52	0.88	0.36	[0.22, 2.10]	0.95	-0.02

**Table 8.5:** Sway velocity (MVEL) and frequency (MFREQ) evaluation of CoP data. Group differences are found for the AP MVEL during eyes open parallel stance and in the ML MFREQ during eyes closed parallel stance, single leg balancing and tandem stance. P-values were calculated using the Wilcoxon Rank-Sum Test.

### 8.2.3 Difference Between Eyes Open and Eyes Closed Condition

We want to answer the hypothesis that closing the eyes has a stronger effect on the balance performance of the experimental group. We can evaluate success rate and time in balance for single leg and tandem stance and CoP data for the parallel stance. When comparing the results of the visual evaluation, all subjects performed significantly worse with their eyes closed. Success rate and time in balance relatively dropped by more than 50 % ( $p < 0.0001$ ) for single leg balancing and  $\approx 20$  % for tandem stance balancing ( $p = 0.005$ ). We find slightly larger changes for the experimental group in all cases except the absolute change for single leg balancing.

Looking at the CoP parameters, we find no change in sway distance ( $< 10$  %  $p \gg 0.05$ ), but significant increase in velocity ( $\approx 35$  %  $p < 0.001$ ) for both groups. Consequently the sway frequency increases ( $\approx 20$  %  $p = 0.05$ ). Changes are larger in the control group. Table 8.7 shows the relative and absolute change of all analyzed variables. Computing a two-way mixed model ANOVA [172] did not show any interaction effect between the groups and eye condition for any variable.

Variable	Single Leg			Tandem Stance		
	Absolute	Relative [%]	p-val <sup>1</sup>	Absolute	Relative [%]	p-val <sup>1</sup>
<b>Success Rate [%]</b>						
Experimental	-48	-86	<0.0001	-25	-34	0.005
Control	-63	-71	<0.0001	-22	-23	0.002
<b>Time in Balance [s]</b>						
Experimental	-14.9	-68	<0.0001	-7.0	-27	<0.0001
Control	-14.9	-52	<0.0001	-4.6	-16	0.002

**Table 8.6:** Effect of change in eye condition for single leg and tandem stance. Evaluation of change in success rate and time in balance. <sup>1</sup>Wilcoxon signed-rank test.

Variable	Medial - Lateral			Anterior - Posterior		
	Absolute	Relative [%]	p-val <sup>1</sup>	Absolute	Relative [%]	p-val <sup>1</sup>
<b>RDIST [cm]</b>						
Experimental	0.30	7	0.46	0.19	5	0.73
Control	0.27	8	0.41	0.13	4	0.58
<b>MVEL [cm/s]</b>						
Experimental	2.15	28	0.0004	2.23	32	<0.0001
Control	2.59	38	0.0001	2.54	46	<0.0001
<b>MFREQ [Hz]</b>						
Experimental	0.06	16	0.02	0.08	18	0.05
Control	0.11	25	<0.0001	0.11	30	0.0007

**Table 8.7:** Effect of change in eye condition on CoP parameters during parallel stance. <sup>1</sup>Wilcoxon signed-rank test.

### **8.2.4 Summary of Static Balance Analysis**

We revisit the three hypotheses from the beginning of the section.

#### **Static Balancing**

We can confirm the hypothesis that the experimental group is not able to maintain balance as well as the control group for single leg balancing and tandem stance, both with eyes open and with eyes closed. A significantly larger fraction failed to achieve 30 s in balance and mean time in balance was significantly lower.

#### **CoP Sway Analysis**

Findings of CoP sway analysis can be condensed into sway distance and velocity. The ratio and frequency metrics can be derived from them. We showed significantly higher ML CoP (sideways) sway in all four tasks and larger AP CoP sway during single leg stance for the experimental group. Sway velocity was increased in AP direction during parallel stance with eyes open.

Accordingly, CoP mean frequency is significantly larger in ML direction for the healthy control group during parallel stance with eyes closed, single leg stance and tandem stance. We suspect, that reduced CoP control in ML direction by means of larger RDIST and lower MFREQ is a reason for the lower success rate in single leg and tandem stance. Findings in AP direction are not consistent between the tasks. The ratio between sway distances is different for both parallel stance tasks.

#### **Effect of Eyes Closed Condition and Visual Perception**

Both groups are affected similarly by the eyes closing condition and show decrease in success rate and time in balance. CoP parameters show a similar change in all participants. Sway distance does not depend on eye condition, however sway velocity and the sway frequency increase when the eyes are closed. We can not confirm the hypothesis that the experimental group is influenced differently by removal of visual perception since changes are similar for all participants and a mixed-model ANOVA did not show any significant interaction between groups and the eyes open and closed condition.

### 8.3 Performance Indicators for Tandem Walking

For evaluation of tandem walking, we adopted many of the performance indicators defined for slackline walking and define further measures that can only be evaluated for flat ground walking.

#### Center of Mass Dynamics

We can compute the CoM position, velocity and acceleration based on Equation 7.3. We evaluate:

- **Standard deviation of CoM acceleration**

We analyze the three directions indicated in Figure 8.7 separately. Smaller variation values in horizontal directions, represent a smoother walking motion. Larger values in walking direction indicate slowing down, stopping and accelerating again. In the sideways direction, the variation indicates how well the subject was able to follow the straight line. Overall we claim that smaller values resemble better balance control. One example is shown in Figure 8.6 where we compare smooth walking at the left to interrupted walking at the right. The performance indicator for interrupted walking is about four times larger as the one for smooth walking.

- **Mean of CoM velocity**

We expect subjects to adapt the walking velocity to their balance. Unstable subjects are expected to slow down and focus on the task, rather than walking at a high velocity and failing the task.

- **Walking angle**

Subjects are supposed to walk on a straight line. This is rather easy with eyes open but significantly harder with eyes closed. We compute the angle  $\alpha$  that the subject deviated from a straight line from the lateral displacement of the CoM position  $(\Delta x, \Delta y)$  at the start and end of the walk.

$$\alpha = \tan^{-1} \left( \frac{\Delta y}{\Delta x} \right) \quad (8.1)$$

Good proprioception and better balance should enable the subject to follow a straight path accurately, even with eyes closed.

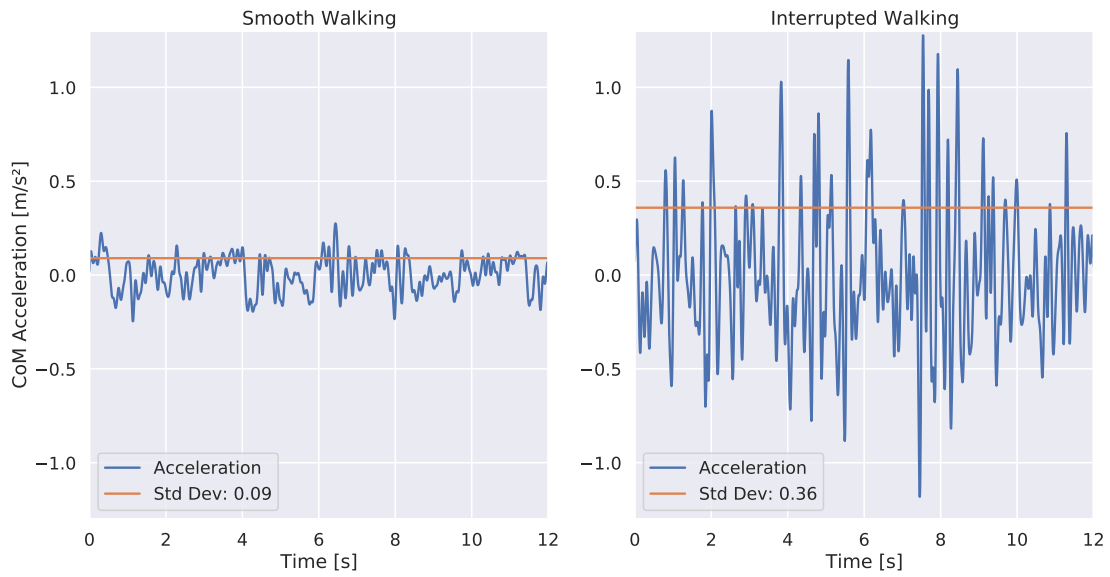


**Figure 8.6:** Comparison of CoM acceleration during two tandem walks. Smooth walking is shown at the left, interrupted walking at the right. In both cases the standard deviation is indicated in orange. A larger value is found for interrupted walking.

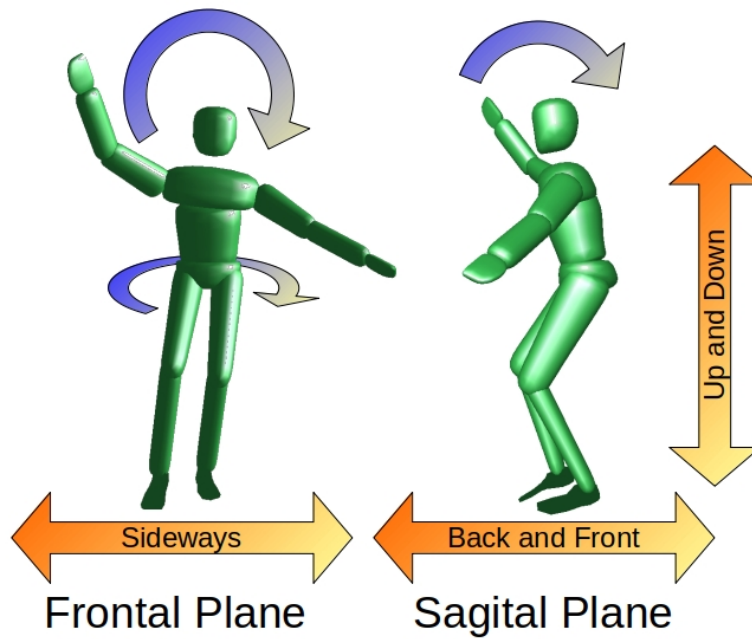


**Figure 8.7:** Illustration of CoM movement (orange) and normalized angular momentum (blue) in the different directions. The same reasoning holds for many other performance indicators.

### Angular Momentum and Normalized Angular Momentum

The total angular momentum of a rigid body system about its CoM is computed by Equation 7.6 and normalized by the subject inertia as in Equation 7.7. In terms of balance performance indicators, the normalized angular momentum tells us how fast the subject is rotating around the specific axis. For stable balancing, the angular momentum is zero, and therefore we can use the standard deviation to quantify how much rotational movement is present during a given motion. Variations in angular momentum in the frontal plane and around the vertical axis are a measure for active recovery movement to maintain balance. We can analyze the three different directions separately, as it is visualized in Figure 8.7:

- **Frontal Plane (Vertical plane, perpendicular to the walking direction):**  
We expect the main balancing movement in this plane, as it is the main instability introduced by the tandem walk.
- **Sagittal Plane (Vertical Plane along the walking direction):**  
We assume that experienced subjects are able to maintain an upright position and do not lean back and forth in the sagittal plane.
- **Coronal Plane (Around the vertical axis):**  
Similar to the sagittal plane, we expect experts to maintain an upper body orientation perpendicular to the walking direction such that the arms are aligned with the frontal plane.

### Zero Moment Point

The ZMP is a measure for dynamic stability and mainly applied in robotic gait stabilization [29, 30]. If the ZMP is inside or at the edge of the support polygon it coincides with the CoP. Similar to the CoM ground projection in static balance, the ZMP is maintained close to the center of the support polygon to ensure dynamic stability in robotic walking. For a rigid multi-body system we can compute the ZMP as derived by Sardain and Bessonnet [179]:

$$p_x = \frac{mgc_x - \dot{L}_y}{m(g + \ddot{c}_z)} \quad (8.2)$$

$$p_y = \frac{mgc_y - \dot{L}_x}{m(g + \ddot{c}_z)} \quad (8.3)$$

where  $g$  is the gravity and  $\dot{L}$  the change of angular momentum. We can compute the standard deviation of the ZMP location as a measure of stability. To obtain a meaningful result, we removed the linear trend due to walking from the data to obtain the local ZMP position in the moving frame.

### Balance Energy Ratio

The balance energy ratio evaluates how much kinetic energy comes from balance related movement. We assume that all rotational movement is performed to maintain balance and all directed movement is from the tandem walk task. A larger balance energy ratio parameter represents more recovery movement and less stability. The equations and derivation can be found in Section 7.3.

### Hand Coordination

We compute the hand coordination as described in Section 7.3. We expect controlled and well coordinated hand movement as a sign of good balance control.

### Mean Shoulder Pose

When confronted with a balancing task, one of the first reactions by subjects is to spread the arms out sideways to increase the moment of inertia [153]. Mechanically, this decreases the rotational velocity when falling and increases the time the subject has to react. In context of the tandem walk it gives us insight on whether the subjects see the task as a balance task that requires additional stability, or more as regular walking. In the latter the arms would stay aligned to the upper body.

### Utilized Range of Motion - Variation of Joint Angle

Similar to slackline balancing, we use this performance indicator to analyze which joints are involved in maintaining balance.

### Step Accuracy

We record the position of foot placement during the tandem walk. We define the sideways (y-direction) step accuracy  $\sigma_y$  as the standard deviation of all foot placement position  $p^{foot}$  in the lateral direction.

$$\sigma_y = std(p_x^{foot}) \quad (8.4)$$

If the feet are placed on a straight line, this value should be small. As there are indications where to step, this performance indicator only becomes relevant in the eyes closed scenario. In walking direction, the tandem walk requires the toes and heel to be in contact. We compute the distance between steps  $d_{step}$  using

$$d_{step} = \frac{d}{n_{steps}} - l_{foot} \quad (8.5)$$

where  $l_{foot}$  is the foot segment length,  $n_{steps}$  the number of steps and  $d$  the distance walked during the tandem walk. This parameter should be  $\approx 0$  if the tandem walk was performed correctly and larger if there is a significant gap between steps.

### Recovery Steps

This performance indicator counts the number of additional steps that the subject takes during the task. As we intend to evaluate 8 correct steps, every additional step is taken to maintain balance and therefore a recovery movement. A larger number of recovery steps can be associated with worse balance.

## 8.4 Dynamic Stability Analysis

Motion capture recordings were cut to start and end time of the tandem walk. The start time is **after** the first step was taken, when the subject has assumed a tandem stance pose. We want to analyze only steps during the tandem walk and avoid bias from an arbitrary starting position. The end time is when the subject had managed 8 successful steps. Any additional sideways steps that were taken to maintain balance are included into the recording. Afterwards, the subject specific model as described in Chapter 4 was fitted using the algorithm described in Chapter 5. We compute the metrics proposed above based on the resulting kinematics to discuss the following hypothesis:

- **Quality of Task Execution:** We expect that the experimental group is not able to fulfill the task as well as the control group.
- **Dynamic Balance Capabilities:** We hypothesize that the experimental group shows lack of balance control and stability when applying the balance metrics.
- **Strategy Adaptation:** We expect to find lack of adaptability in schizophrenia patients when comparing the tandem walk with eyes closed to the one with eyes open.

### 8.4.1 Quality of Task Execution

To evaluate the quality of task execution, we analyzed if participants managed to do the task without recovery steps and compute the step accuracy and the distance between steps.

#### Successful Tandem Walk

All control group participants and 90 % of the experimental group managed to do 8 steps of the tandem walk without losing balance and needing a recovery step. For the eyes closed situation the numbers drop to 70 % and 25 %, respectively.

#### Recovery Steps

In the left top plot of Figure 8.8 the average number of recovery steps per group is shown. The control group did not take any additional step with eyes open. Two out of 20 participants from the experimental group did take one additional step ( $p = 0.1$ ,  $d = 0.5$ ). Both groups needed to take additional steps with eyes closed. On average the control group took 0.7 steps and the experimental group 1.3 steps ( $p = 0.02$ ,  $d = 0.7$ ). Differences are not significant with eyes open, however more data should be considered for further analysis.

#### Distance between Steps

The top right plot shows the average distance between consecutive steps. We did not find differences between groups, however all subjects seemed to neglect the instructions to place the feet in contact when performing the tandem walk with eyes closed. With eyes open the distance is  $\approx 1$  cm which is in the order of model accuracy. With eyes closed, however, there is an average distance of  $\approx 7$  cm for both groups.

### Step Accuracy

The bottom left plot shows the step accuracy in sideways direction. A larger value for step accuracy represents less consistent foot placement. We find similar values with eyes open, as it was expected since there had been visual guidance for foot placement during the task. With eyes closed, the experimental group shows significantly higher values and more inaccurate step placement ( $p = 0.02$ ,  $d = 0.84$ ). The bottom right plot shows the distribution of step accuracy plotted against the number of additional steps and the eyes open/closed condition for all participants and trials. They are uncorrelated for the eyes open condition ( $r = 0.15$ ) [180].

We see a general trend towards less accurate stepping when subjects took three or more recovery steps during the eyes closed condition. However, for subjects that took 2 or less steps, the step accuracy is not correlated to the number of additional steps ( $r = 0.14$ ). In fact, the largest value for step accuracy was observed for a subject, that did not take recovery steps.

All findings concerning the quality of task execution are summarized in Table 8.8 and differences between groups highlighted. No differences were found for the tandem walk with eyes open and for step distance in general. With eyes closed, the success rate, the number of recovery steps and the step accuracy are different, all suggesting that the experimental group was not able to fulfill the tandem walk as well as the control group with eyes closed.

Task	Eyes Open		Eyes Closed	
	Experimental	Control	Experimental	Control
N	20	27	20	27
Success Rate [%]	90	100	25	70
Recovery Steps	0.1 (0.3)	0.0 (0.0)	1.35 (1.1)	0.66 (1.1)
Step Distance [cm]	1.6 (1.4)	1.0 (0.8)	7.7 (1.8)	7.3 (1.6)
Step Accuracy [cm]	0.83 (0.45)	0.65 (0.24)	3.9 (2.4)	2.3 (1.1)

**Table 8.8:** Group comparison for tandem walk quality by means of success rate, additional recovery steps, distance between steps and step accuracy. Significant differences ( $p < 0.05$ ) are highlighted. Explanatory bar and box plots can be found in Figure 8.8.

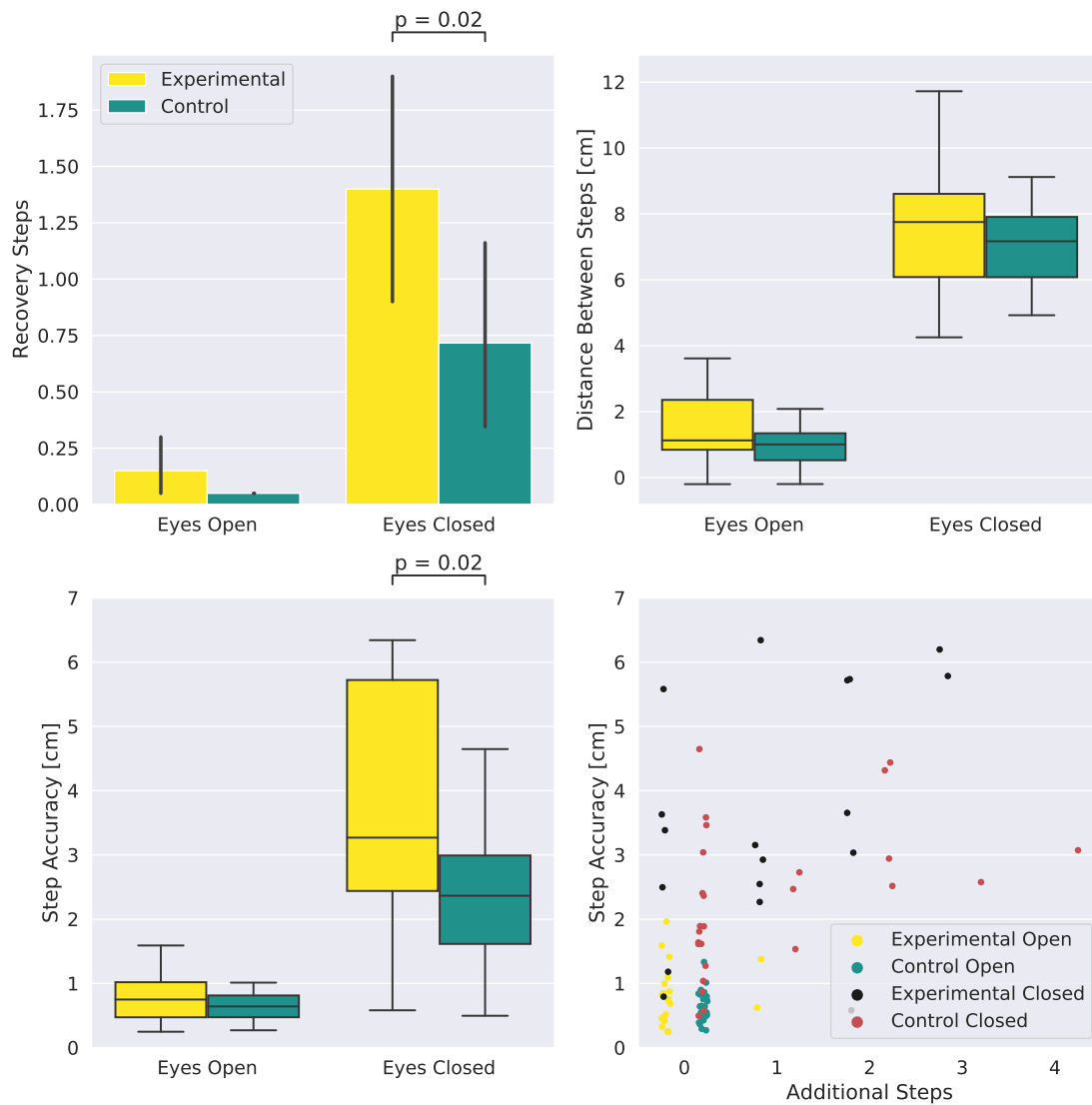


**Figure 8.8:** Top Left: Additional steps during the tandem walk. Group means are shown as bar height and the 95 % confidence interval is shown as vertical line. Top Right: Distance between consecutive steps of the tandem walk. Participants take larger steps with eyes closed. Bottom Left: Accuracy of sideways Foot Placement in cm in as box plot. Steps become less accurate with eyes closed. Bottom Right: Step accuracy plotted against the number of additional steps. Correlation between the metrics is not given for 2 or less additional steps.

### 8.4.2 Dynamic Balance Capabilities

In this section we compute the CoM dynamics and look at the average angular velocity as these metrics were able to quantify balance capabilities for slackline walking in Chapter 7. Further we evaluate the ZMP position and compare the shoulder and pelvis movement as a measure for posture control in more detail.

#### Center of Mass Acceleration

As suggested in Section 8.3, we associate smoother and more stable walking with lower variation in the CoM acceleration. Figure 8.9 shows box plots for the two tandem walk scenarios. The walking direction is shown at the left, the sideways direction in the middle and the vertical direction at the right.

We find no differences in walking direction, however, the experimental group shows 31% and 22% larger sideways acceleration with eyes open and closed ( $p < 0.01$ ,  $d = 0.87$  and  $p = 0.04$ ,  $d = 0.6$ ). They are effected more by the instability introduced by the tandem walk and show larger changes in their sideways CoM velocity. Similar differences are found for the vertical direction (+27%,  $p = 0.02$ ,  $d = 0.82$  and  $p < 0.01$ ,  $d = 0.60$ ).

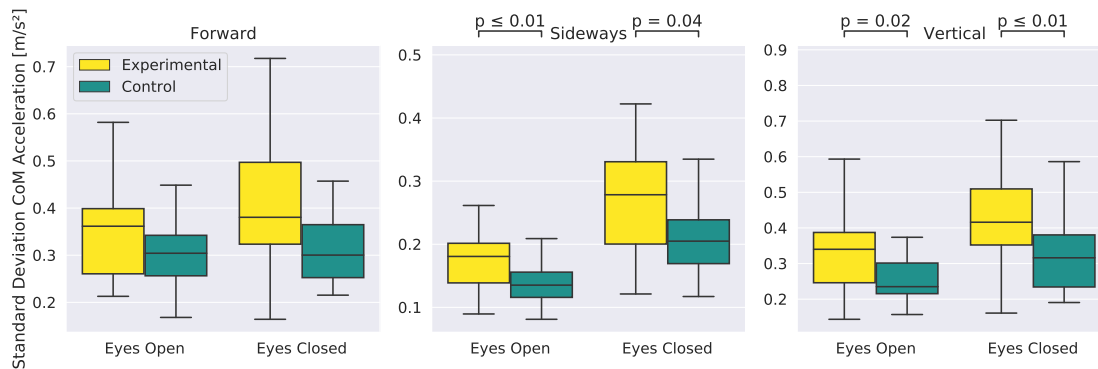


**Figure 8.9:** Standard deviation of CoM acceleration in walking, sideways and vertical direction during tandem walking.

### Zero Moment Point

Figure 8.10 shows the standard deviation of the ZMP position in walking and sideways direction. The experimental group shows larger values in both directions and for both scenarios. Differences are significant in the sideways direction with eyes open ( $\approx 18\%$   $p = 0.01$ ,  $d = 0.81$ ) and especially with eyes closed ( $\approx 48\%$   $p < 0.01$   $d = 1.02$ ).

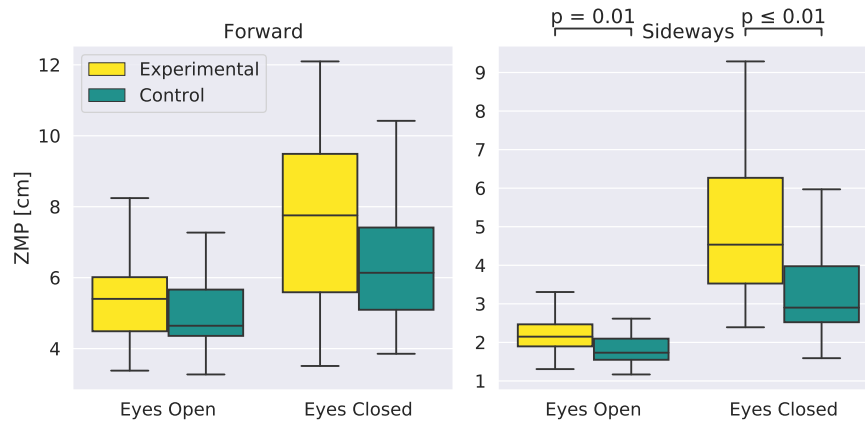


**Figure 8.10:** Standard deviation of ZMP position for tandem walking.

### Normalized Angular Momentum

The normalized angular momentum summarizes all rotational movement. This includes arm movement as well as rotation and tilting of the upper body. The instability is mainly in the frontal plane and we found that, for example, slackline athletes show most movement in this plane to balance but manage to not tilt with their upper body. All other planes should not be affected if the subject is well balanced and performs the correct and task-specific recovering arm movements.

Figure 8.11 shows the standard deviation of normalized angular momentum for the tandem walk. No difference is seen in the sagittal plane (along the walking direction). For the eyes open tandem walk the experimental group shows a 31% larger value in the frontal plane ( $p < 0.001$ ,  $d = 1.23$ ) and 19% larger value around the vertical axis ( $p = 0.02$ ,  $d = 0.73$ ). This suggests that there is already a lot of recovery movement during the eyes open task.

With eyes closed the control group also shows larger values in the frontal plane, but they reduce the angular velocity around the vertical axis while the experimental group remains at the same value. Groups are now similar in the frontal plane, but differ by 31% ( $p < 0.01$ ,  $d = 0.83$ ) around the vertical axis, suggesting that the control group performs task-specific movement whereas the experimental group does not manage to maintain an aligned posture.

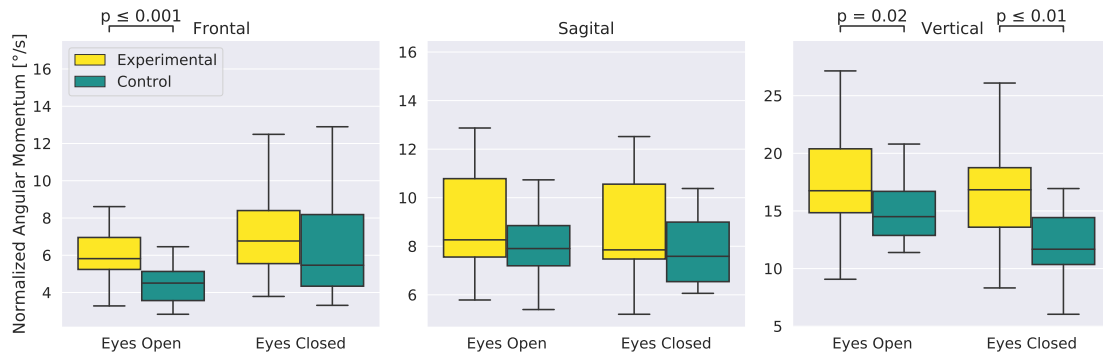


**Figure 8.11:** Standard deviation of normalized angular momentum in the frontal and sagittal plane and around the vertical axis.

### Movement Parameters

To quantify the source of angular momentum, we look at the shoulder joints that are actively used to maintain balance and the resulting passive pelvis movement. Figure 8.12 shows the utilized range of motion in degrees of the shoulder joint in the frontal and sagittal plane and the ratio between the two directions.

We see that the experimental group moved about twice as much in the frontal and sagittal plane with eyes open compared to the control group ( $p < 0.05$ ,  $d = 0.9$  /  $p = 0.014$ ,  $d = 0.98$ ). With eyes closed both groups used their shoulder joints to maintain balance, however, the experimental group moves the shoulders equally in both directions, whereas the control group performs a greater portion of the movement in the frontal plane. The ratios are significantly different ( $p = 0.01$ ,  $d = 0.83$ ). The resulting stability of the balance task can be evaluated by the amount of passive rotational movement of the pelvis.

Figure 8.13 shows the standard deviation of pelvis orientation in the frontal plane and around the vertical axis. The control group shows significantly less rotational pelvis movement and better orientation control with eyes open. They tilt 50% ( $p < 0.01$ ,  $d = 0.99$ ) less in the frontal plane and rotate 50% less around the vertical axis ( $p < 0.01$ ,  $d = 1.04$ ). Groups show similar tilt values with eyes closed in the frontal plane. Around the vertical axis, the experimental group maintains the same rotational velocity while the control group decreases.

### Effect of Eyes Open and Closed Condition

We computed mixed model ANOVAs to investigate if the experimental group shows a stronger change in balance parameters than the control group. We analyzed the number of recovery steps, step accuracy, step distance, CoM acceleration, normalized angular momentum and ZMP sway. Significant interaction effects were found for step accuracy ( $F = 7.3$ ,  $p = 0.01$ ,  $\eta^2 = 0.14$ ) and sideways ZMP sway ( $F = 8.0$ ,  $p = 0.007$ ,  $\eta^2 = 0.15$ ). Subject groups showed similar changes for all other parameters.

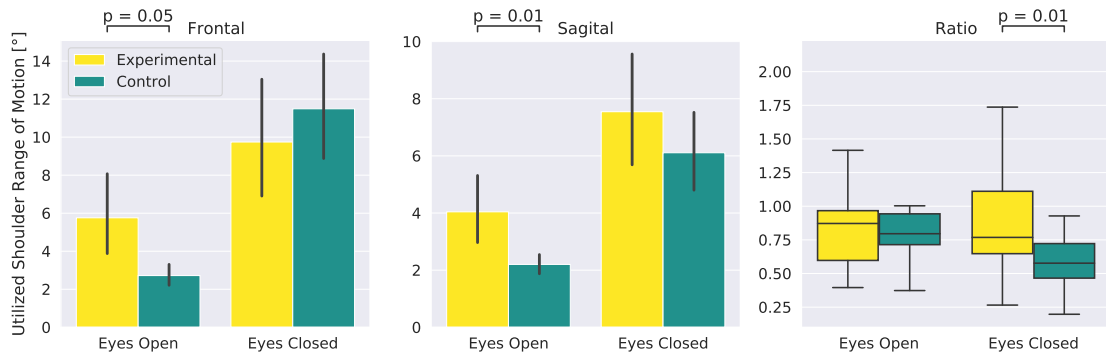


**Figure 8.12:** Utilized range of motion of the shoulder joint in the frontal and sagittal plane and the ratio between the two directions.

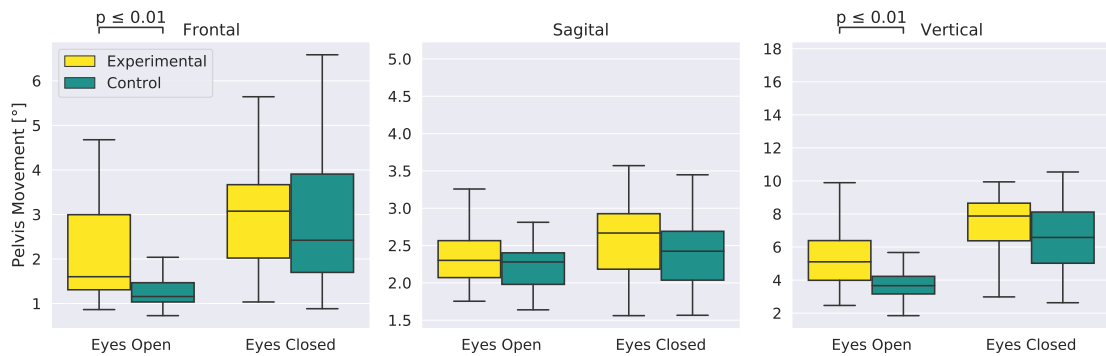


**Figure 8.13:** Quantification of motion of the pelvis.

### Summary

Summarizing we can confirm the hypothesis that the experimental group was not able to balance as well as the control group during the tandem walk test. They showed larger sideways ZMP sway and larger CoM acceleration both with eyes open and eyes closed. Already with eyes open, they performed many more recovery movements resulting in a larger utilized range of motion of the shoulder joints and larger normalized angular momentum. The pelvis orientation showed higher variation with larger sideways tilt and around the vertical axis.

With eyes closed both groups were more unstable and we only found limited evidence that the experimental group is more affected. Both groups performed recovery movements in the frontal plane. We found that the control group managed to perform these movements mainly in the frontal plane, specific to the instability introduced by the balance task, whereas the experimental group showed larger movement also in the sagittal plane. The ratios were significantly different. We investigate this further in the next section. Analysis of kinetic energy and balance energy ratio did not show any difference between groups. Hand coordination showed large variation within groups but did not show any group difference. More information on the evaluation can be found in the inter study comparison in Chapter 9.

### 8.4.3 Balance Strategy

There are different balance strategies and recovery movements available to succeed in the tandem walk test. The task requires the feet to be placed on a narrow line and in contact with each other. As discussed, taking a recovery step outside the line and therefore applying a stepping strategy to balance is not allowed. However, using an arm strategy to balance, is perfectly valid. In this section, we compare the different strategies used by the two groups and discuss the hypothesis that subjects with diagnosed schizophrenia lack adaptability to different tasks.

The tandem walk was performed once with eyes open and immediately afterwards with eyes closed. Findings where the control group changed behavior and applied a different strategy while the experimental group did not adapt would support the hypothesis. We therefore evaluate the strategy, the mean posture during the walks, the active range of motion of the arms and compare walking speed.

In Figure 8.14 we plotted histograms for the two tandem walks and the strategies applied by the participants. With eyes open a balance strategy was rarely necessary and both groups were mostly stable. With eyes closed we find similar percentages of stable walking and the unstable situation, where both, arms and legs, were used for recovery movements. The key difference was the fact, that 40 % of the control group were able to pass the tandem walk successfully by using their arms to balance, while 45 % of the experimental group took a recovery step without performing any arm movement. Employing the arms to maintain balance is significantly rarer in the experimental group than in the control group ( $\chi^2 = 14.36$ ,  $df = 4$ ,  $p = 0.0060$ , [181]). We investigate this further by looking at the mean posture and the shoulder and elbow movement in the next section.

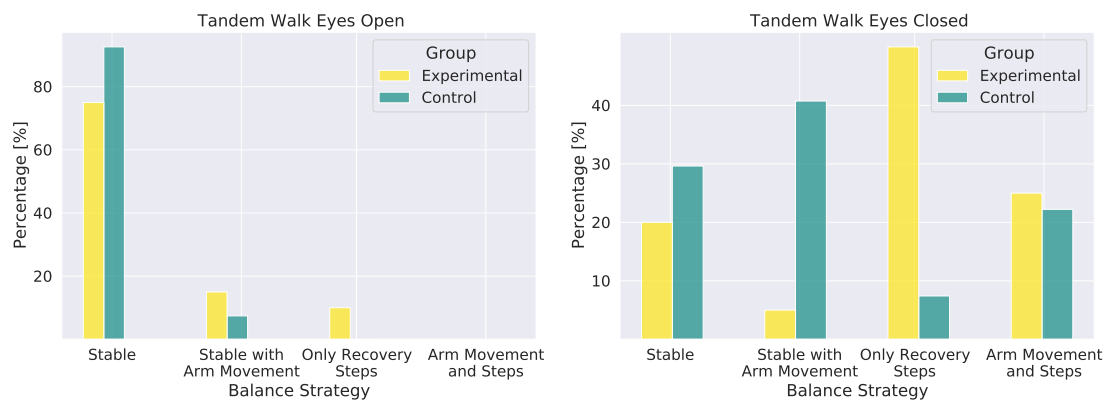


**Figure 8.14:** Different balance strategies during the tandem walk. Participants rarely used their arms or took a step with eyes open and most participants performed a stable tandem walk. With eyes closed, stable walking and use of arms and steps occur at similar percentages. Groups differ by how often they use their arms to fulfill the task successfully and by how often they directly take a recovery step without involving the arms to balance.

### **Posture and Movement**

A visualization and detailed plots of the mean posture for the two groups and eye conditions are shown in Figure 8.15. Arm and shoulder configurations were similar with eyes open, as most subjects were stable. When closing the eyes, the control group did spread the arms wider and showed a larger mean elbow angle, resulting in a more stable overall position since the inertia in the frontal plane is larger. Shoulder angle in the frontal plane changed by  $23^\circ$  for the control group and by  $6^\circ$  for the experimental group. Elbow angle changed is  $12^\circ$  compared to  $4^\circ$ . A mixed model ANOVA shows a significant interaction between mean posture and eye open/closed condition ( $p = 0.05$ ,  $\eta^2 = 0.09$  for elbow angles and  $p = 0.006$ ,  $\eta^2 = 0.14$  for frontal shoulder angles).

Figure 8.16 shows the utilized joint angles for the frontal shoulder joint and the elbow. As discussed above, we find lower values in the control group for the eyes open condition and similar values when walking with eyes closed. Therefore, the increase in movement and adaptation in arm movement to the eyes closed task is larger. Shoulder joint movement increases by  $9^\circ$  for the control group compared to  $4^\circ$  for the experimental group. Elbow movement increases by  $5^\circ$  and  $3.5^\circ$ , respectively. A mixed model ANOVA confirms a significant interaction for utilized frontal shoulder angle between groups and eye open/closed condition ( $p = 0.02$ ,  $\eta^2 = 0.11$ ). No interaction effect is observed for the elbow joints.

In Figure 8.17 we plotted only successful tandem walks that did not require additional recovery steps. These are the stable trials and the trials using arm movement to pass the test successfully. We find the same results as the histogram of Figure 8.14. Many participants of the control group changed their shoulder angle and movement to perform successful balance with eyes closed, while successful trials of the experimental group did not involve any arm strategy. However, the number of trials is insufficient for further statistical analysis since only five successful tandem walks with eyes closed were performed by the experimental group.

Summarizing, we can confirm the hypothesis that the experimental group did not employ different, task specific balance strategies and did not adapt to the eyes closed tandem walk in the same way as the control group. We found greater changes in mean shoulder and elbow angles in the control group when analyzing all trials. They assumed a different posture and spread their arms wider whereas the experimental group maintained a similar posture and kept the arms aligned, relying mostly on a step strategy.

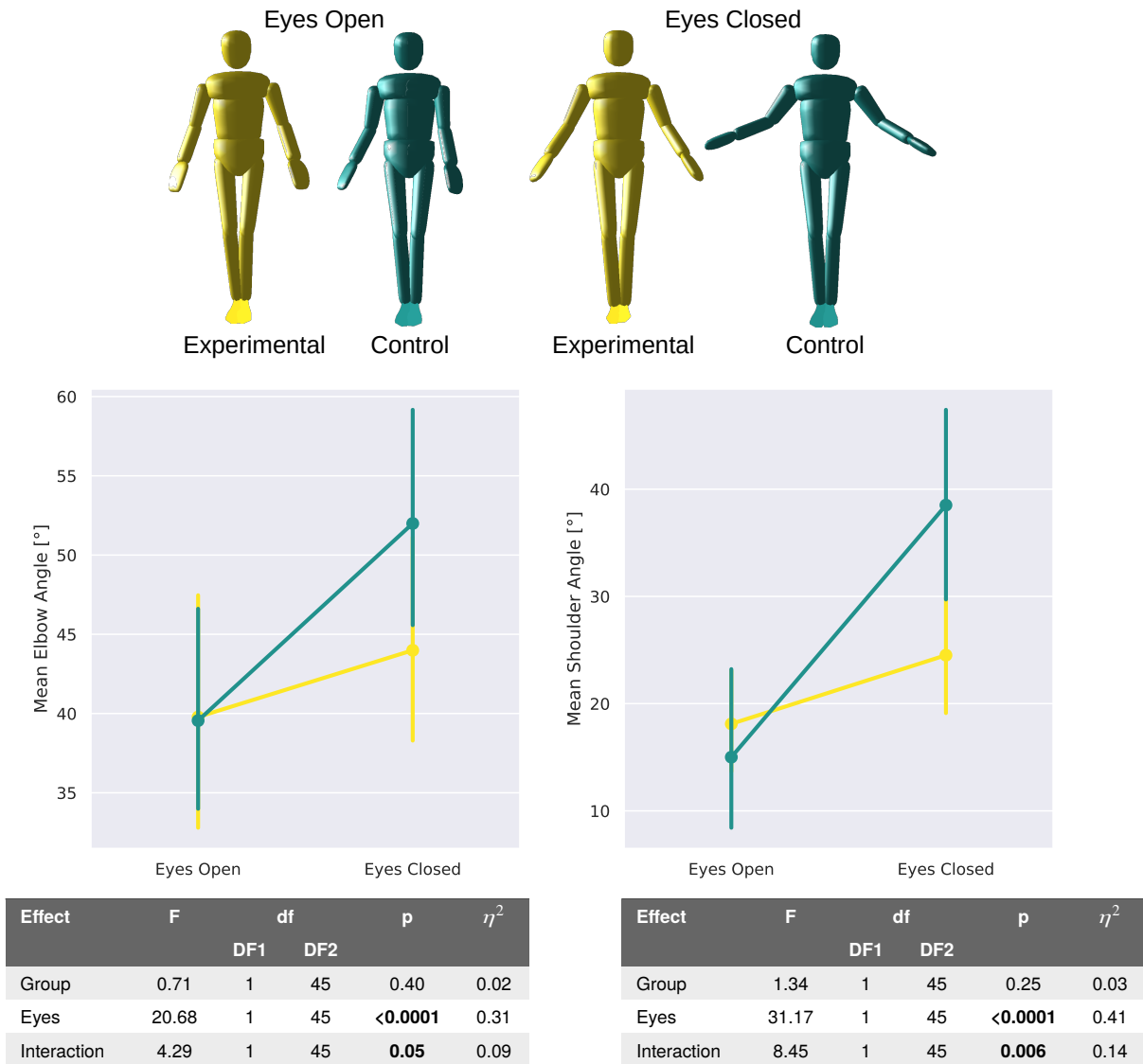


**Figure 8.15:** Top: Visualization of the mean posture of both groups and the eyes open and closed condition. Middle: Details on pose change. Bottom: Mixed Model ANOVA showing an interaction effect between group and eyes open/closed condition for the mean posture.

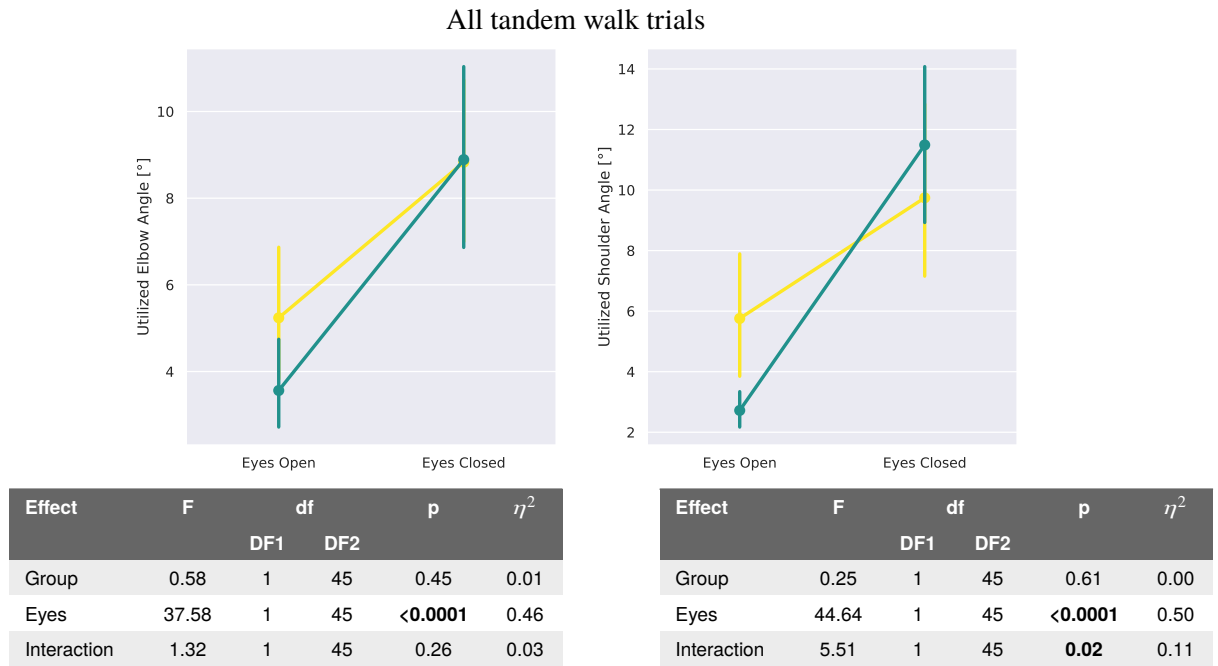


**Figure 8.16:** Top: Details on change of utilized joint angles. Bottom: Mixed Model ANOVA showing an interaction effect between group and eyes open/closed for utilized shoulder angle and no interaction for utilized elbow angle.

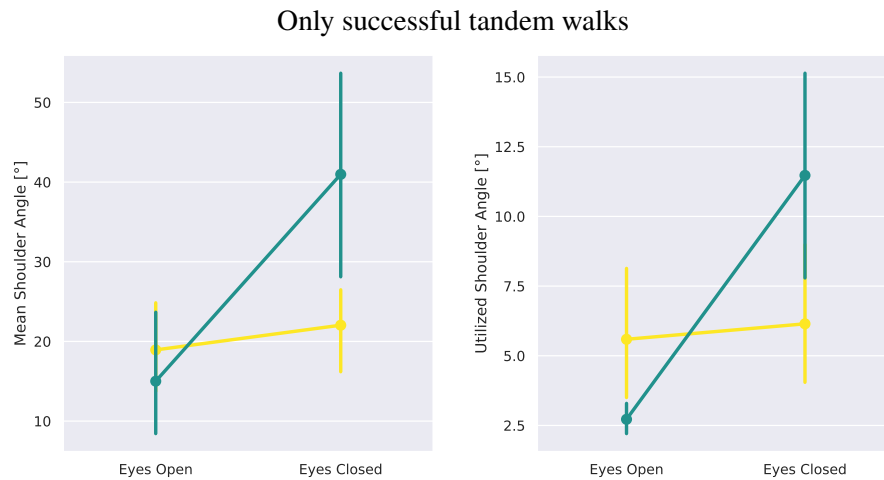


**Figure 8.17:** Shoulder angles for successful tandem walking. Left: Mean frontal shoulder angle, Right: Utilized range of motion. We only plotted successful tandem walks that did not require recovery steps. For the control group these are 27 with eyes open and 14 with eyes closed. For the experimental group these are 16 with eyes open and 5 with eyes closed. We see adaption to the task by the control group and no adaptation by the experimental group, however there are insufficient trials for a statistical analysis.

### Walking Speed

Figure 8.18 shows the average walking speed in m/s. When comparing all trials, groups are not different ( $p = 0.3$ ). Both groups decrease the speed when closing the eyes and adapt to the new situation. When we compare only the successful trials we see that the control group maintained the same walking speed while the experimental group slightly increased their speed.

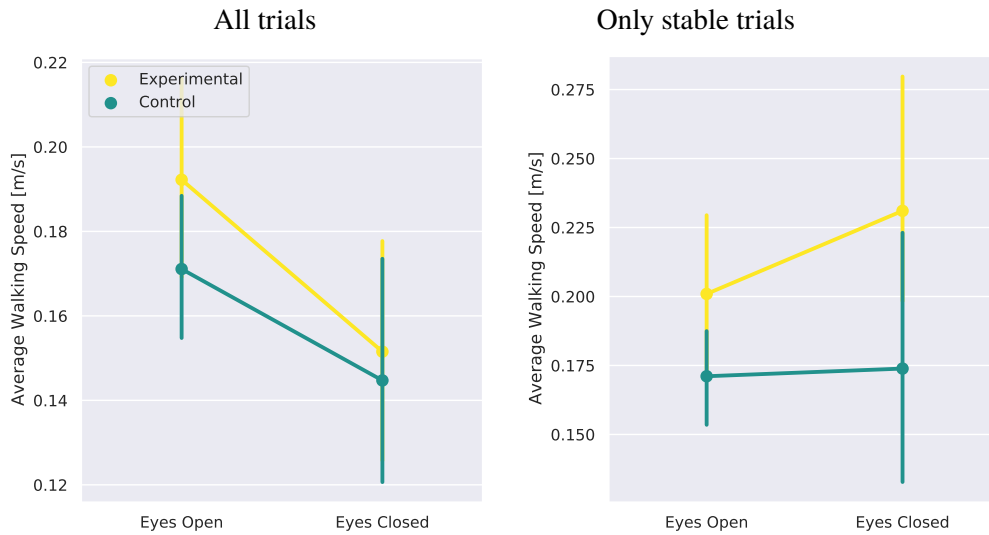


**Figure 8.18:** Walking speed for the two groups and eye conditions.

#### **8.4.4 Summary and Discussion of Dynamic Balance**

##### **Quality of Task Execution**

We found no differences in the quality of task execution with eyes open. With eyes closed, however, the experimental group did not perform the tandem walk test as well as the control group. The number of additional recovery steps was larger and step accuracy significantly worse. In a different study, Jeon et al. [70] found a larger number of additional steps for both scenarios.

##### **Dynamic Balance Capabilities**

Many balance indicators that were found for slackline balancing show, that the participants with schizophrenia lack balance capabilities and actively need to maintain balance already with eyes open, whereas the control group only performed balance related movement in the frontal plane with eyes closed.

We found a larger standard deviation of CoM acceleration in sideways and vertical direction for both tandem walks. The gait is more interrupted and less smooth. A larger normalized angular momentum around the vertical axis suggests that the upper body is less involved to control this stability criterion. Specific movement analysis for the eyes closed task suggests, that the experimental group balances in forward **and** sideways direction, while the control group mainly performs arm movement related to the sideways direction and therefore is specific to the instability introduced by the tandem walk. Analysis of the ZMP shows a larger sway in sideways direction for both scenarios hereby confirming lack in medial-lateral balance control that was found during the static balance test.

##### **Strategy Adaptation**

Analysis of strategy adjustment showed that both groups change their walking speed with the eyes closed condition, but no interaction between groups and eye closed condition was found. Comparison of posture showed significant changes in both groups, however, the adjustment in pose was about 3 to 4 times larger in the control group by means of joint angle. Interaction effects were found for mean frontal shoulder and elbow angle as well as the utilized range of motion of the frontal shoulder joint. With eyes closed, the control group prioritized an arm strategy and only took a step when falling, whereas the experimental group solely relied on a step strategy and the arms were only involved in a reflexive manner.

A summary of all performance indicators is listed in Table 8.9 and 8.10.

Variable	Experimental		Control		p-val	Cohen's d				
	Mean $\pm$ SD	Range	Mean $\pm$ SD	Range						
Additional Steps	0.10	0.30	0	0	0.10	0.50				
Step Accuracy [cm]	0.83	0.45	0.25	1.96	0.65	0.24	0.272	1.33	0.30	0.50
CoM Acceleration X [ $m/s^2$ ]	0.35	0.09	0.21	0.58	0.31	0.08	0.17	0.48	0.18	0.44
CoM Acceleration Y [ $m/s^2$ ]	0.18	0.06	0.09	0.36	0.14	0.04	0.08	0.26	<b>0.005</b>	0.87
CoM Acceleration Z [ $m/s^2$ ]	0.33	0.11	0.14	0.59	0.26	0.06	0.16	0.37	<b>0.02</b>	0.82
Angular Velocity X [ $^\circ/s$ ]	6.01	1.43	3.28	8.61	4.48	1.03	2.83	6.46	<b>0.0004</b>	1.23
Angular Velocity Y [ $^\circ/s$ ]	8.91	1.90	5.79	12.87	8.00	1.25	5.39	10.74	0.13	0.57
Angular Velocity Z [ $^\circ/s$ ]	17.78	4.47	9.07	27.15	14.90	3.28	6.75	23.51	<b>0.02</b>	0.73
Utilized Frontal Shoulder Angle [ $^\circ$ ]	5.76	4.71	1.35	19.69	2.72	1.56	0.72	8.21	<b>0.05</b>	0.90
Utilized Sagittal Shoulder Angle [ $^\circ$ ]	4.04	2.60	1.23	9.77	2.20	0.91	1.10	4.52	<b>0.014</b>	0.98
Ratio	0.84	0.32	0.40	1.72	0.94	0.43	0.37	2.14	0.67	-0.24
Pelvis Rotation X [ $^\circ$ ]	2.12	1.10	0.87	4.68	1.30	0.47	0.73	2.69	<b>0.005</b>	0.99
Pelvis Rotation Y [ $^\circ$ ]	2.41	0.59	1.75	4.35	2.25	0.30	1.64	2.81	0.57	0.35
Pelvis Rotation Z [ $^\circ$ ]	5.60	2.28	2.47	10.82	3.82	1.04	1.85	6.75	<b>0.004</b>	1.04
ZMP Variation sagittal [cm]	5.56	1.52	3.34	9.87	5.04	1.17	3.27	8.41	0.17	0.38
ZMP Variation frontal [cm]	2.14	0.46	1.31	3.31	1.81	0.35	1.17	2.62	<b>0.013</b>	0.81
Walking Speed [m/s]	0.19	0.06	0.12	0.32	0.17	0.05	0.09	0.26	0.31	0.41
Mean Frontal Shoulder Angle [ $^\circ$ ]	18.11	10.64	2.45	41.95	15.01	20.46	1.26	88.03	<b>0.01</b>	0.18
Mean Elbow Angle [ $^\circ$ ]	39.78	15.69	16.27	79.69	39.55	16.60	22.62	99.50	0.72	0.01
Utilized Elbow Angle [ $^\circ$ ]	5.24	3.31	1.12	13.94	3.56	2.77	1.34	16.13	0.07	0.54

**Table 8.9:** Summary table with all performance indicators for tandem walking with eyes open. P-values were calculated using the Wilcoxon Rank-Sum Test.

Variable	Experimental			Control			p-val	Cohen's d		
	Mean $\pm$ SD	Range	Range	Mean $\pm$ SD	Range	Range				
Additional Steps	1.35	1.10	0	3	0.67	1.08	0	4	<b>0.02</b>	0.60
Step Accuracy [cm]	3.86	2.44	0.58	10.6	2.31	1.10	0.50	4.65	<b>0.02</b>	0.84
CoM Acceleration X [ $\text{m}/\text{s}^2$ ]	0.39	0.13	0.16	0.72	0.32	0.09	0.22	0.56	0.06	0.62
CoM Acceleration Y [ $\text{m}/\text{s}^2$ ]	0.27	0.08	0.12	0.42	0.22	0.08	0.12	0.49	<b>0.04</b>	0.60
CoM Acceleration Z [ $\text{m}/\text{s}^2$ ]	0.45	0.16	0.16	0.85	0.35	0.16	0.19	0.88	<b>0.007</b>	0.60
Angular Velocity X [ $^\circ/\text{s}$ ]	7.04	2.15	3.79	12.49	6.76	3.28	3.31	16.84	0.32	0.10
Angular Velocity Y [ $^\circ/\text{s}$ ]	8.73	2.00	5.20	12.52	8.26	2.28	6.06	15.94	0.23	0.21
Angular Velocity Z [ $^\circ/\text{s}$ ]	16.97	4.69	8.32	28.21	12.91	4.85	6.04	28.67	<b>0.003</b>	0.83
Utilized Frontal Shoulder Angle [ $^\circ$ ]	9.74	6.98	2.55	28.83	11.49	6.96	2.36	24.85	0.37	-0.25
Utilized Sagittal Shoulder Angle [ $^\circ$ ]	7.55	4.63	2.35	19.65	6.11	3.65	1.41	15.87	0.36	0.34
Ratio	0.89	0.42	0.27	1.94	0.60	0.26	0.20	1.40	<b>0.01</b>	0.83
Pelvis Rotation X [ $^\circ$ ]	3.07	1.22	1.04	5.64	2.91	1.51	0.88	6.59	0.47	0.11
Pelvis Rotation Y [ $^\circ$ ]	2.78	0.82	1.56	5.01	2.48	0.67	1.57	5.06	0.15	0.40
Pelvis Rotation Z [ $^\circ$ ]	7.86	2.53	2.98	14.20	6.91	2.96	2.63	17.63	0.12	0.33
ZMP Variation sagittal [m]	7.78	2.53	3.51	12.10	6.50	1.86	3.86	10.42	0.08	0.57
ZMP Variation frontal [m]	4.90	1.90	2.39	9.29	3.31	1.16	1.59	5.97	<b>0.003</b>	1.02
Walking Speed [m/s]	0.15	0.06	0.08	0.32	0.14	0.07	0.07	0.38	0.57	0.10
Mean Frontal Shoulder Angle [ $^\circ$ ]	24.52	12.30	6.93	47.92	38.51	23.76	7.57	101.5	<b>0.04</b>	-0.69
Mean Elbow Angle [ $^\circ$ ]	43.99	15.03	19.10	88.91	51.99	18.30	24.80	99.22	0.07	-0.46
Utilized Elbow Angle [ $^\circ$ ]	8.83	4.39	2.38	18.47	8.89	5.90	1.31	24.20	0.77	-0.01

**Table 8.10:** Summary table with all performance indicators for tandem walking with eyes closed. P-values were calculated using the Wilcoxon Rank-Sum Test.

## 8.5 Correlation with Medication and PANSS

In this section we evaluate how the findings correlate with medication and symptoms. We consider the variables that showed differences in the static balance test: time in balance, ML sway distance and mean frequency. Dynamic balance variables for the tandem walk are step accuracy, additional steps, walking speed, the standard deviation of CoM acceleration, normalized angular momentum and sideways ZMP position as well as the utilized shoulder angle. We correlate with medication by means of OPZ and PANSS [2] as introduced in Chapter 2. In all cases we compute Spearman's rank correlation  $r_s$  [161] which can be used if the data is not necessarily normally distributed. We follow Mukaka's guidelines and consider  $|r_s| < 0.3$  as negligible,  $0.3 < |r_s| < 0.5$  as a low correlation,  $0.5 < |r_s| < 0.7$  as a moderate correlation and  $|r_s| > 0.7$  as highly correlated [180].

### Static Balance Test

We analyzed all scenarios individually and did not find correlation between medication and the time in balance or any of the CoP sway parameters. We found a low negative correlation between PANSS scores and ML sway frequency for parallel stance with eyes open, single leg stance and tandem stance. As derived in Section 8.2 there is not sufficient CoP data available for single leg and tandem stance with eyes closed. The correlation values are shown and plotted in Figure 8.19 and Table 8.11. We find a low negative correlation for three of the four scenarios, meaning that the sway frequency reduces with increasing symptom load.

Configuration	Positive	Negative	Global	Total
Parallel Open	-0.37	-0.46	-0.34	-0.40
Parallel Closed	-0.01	-0.05	-0.10	-0.08
Single Leg Stance	-0.48	-0.42	-0.40	-0.43
Tandem Stance	-0.37	-0.26	-0.30	-0.28

**Table 8.11:** Spearman's rank correlation between PANSS and ML sway frequency for the different stance configuration.

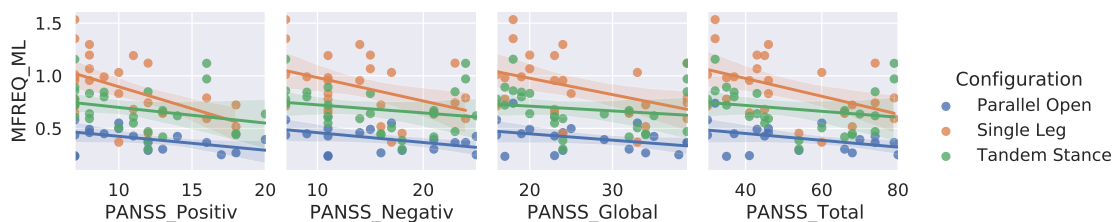


**Figure 8.19:** Scatter plot with linear regression for mean sway frequency in ML direction and PANSS scores.

**Tandem Walk**

For the tandem walk with eyes open we found a low correlation ( $r = 0.48$ ) between OPZ and sideways ZMP sway. No other correlation between medication and balance performance indicators was found. PANSS scores were positively correlated to sideways step accuracy during tandem walk with eyes open meaning that participants with larger symptom load showed more inaccurate stepping. Additionally we found a negative correlation between PANSS and normalized angular momentum around the vertical axis.

Variable	Positive	Negative	Global	Total
Sideways Step Accuracy Eyes Open	0.34	0.36	0.30	0.35
Normalized AM Eyes Open	-0.62	-0.51	-0.45	-0.53
Normalized AM Eyes Closed	-0.63	-0.69	-0.66	-0.70

**Table 8.12:** Spearman’s rank correlation between PANSS, sideways step accuracy and normalized angular momentum during the tandem walk.

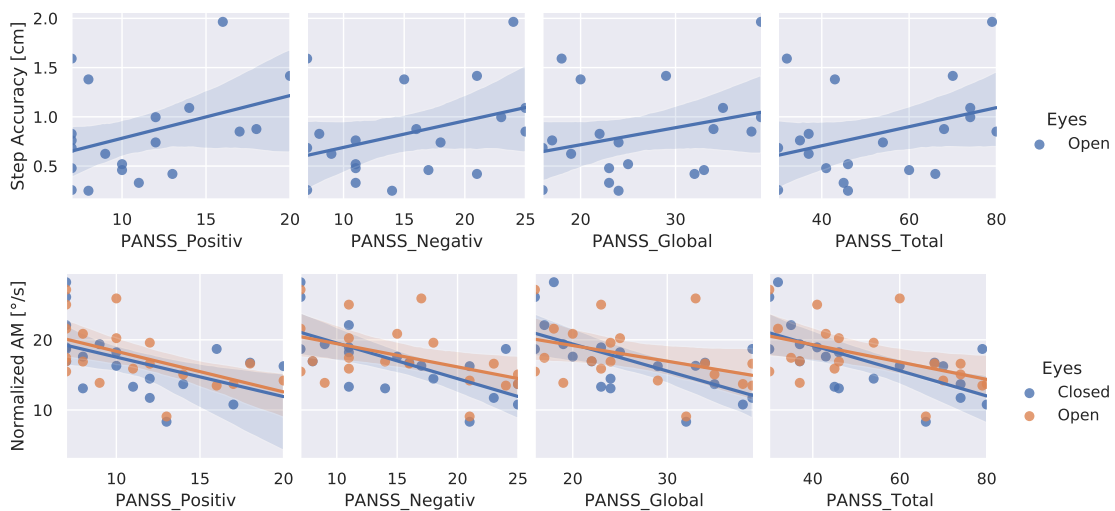


**Figure 8.20:** Scatter plot with linear regression for PANSS scores and sideways step accuracy at the top and normalized angular momentum at the bottom.

**Summary**

In the explorative analysis of correlation between balance metrics, medication and PANSS, we found only few significant correlations. Medication only correlates to sideways ZMP sway. Other than this, no further indications on the influence of medication on balance were found. Symptom load was correlated to a lower CoP sway frequency in sideways direction during three out of four tasks of the static balance test and to a larger inaccuracy in sideways step placement during the tandem walk with eyes open. We also found smaller normalized angular momentum around the vertical axis with increased symptom load.

While the first two findings suggest that larger PANSS scores correlate to worse balance and stepping coordination, the last finding is contradictory as we showed that an increased normalized angular momentum around the vertical axis is an indicator for reduced balance control.

## 8.6 Discussion

We discuss the findings by revisiting the research questions posed in Chapter 2.

### Static Balance

We confirm the hypothesis that persons with schizophrenia have impaired static balance. They showed a lower success rate throughout the different balance tasks and managed to balance for a shorter time when compared with the control group. CoP sway analysis revealed a larger ML sway distance and lower sway frequency. We found that the sway frequency correlates with the symptom load by means of PANSS score.

### Dynamic Balance

Many of the balance metrics we analyzed showed that the experimental group is less stable during the tandem walk. They require recovery arm movement and additional recovery step out of the line of the tandem walk already with eyes open. The control group is able to perform this task accurately and without recovery steps. Both groups struggle to perform the tandem walk with eyes closed, however the experimental group showed significantly larger sideways CoM and ZMP sway. We can confirm the hypothesis that the experimental group has worse dynamic balance capabilities than the control group.

### Visual Condition During Static Stance

Both groups showed significantly worse balance performance with eyes closed. We did not find evidence that they are affected differently and did not find confirmation of the hypothesis.

### Visual Condition During Tandem Walk

Out of the many parameters analyzed, only two showed a significant interaction effect between group and eye condition. We therefore suggest further research and can not yet confirm the hypothesis that the experimental group is affected more strongly by the eyes closed condition.

### Balance Strategy and Adaptability

We investigated the change in posture between the eyes open and eyes closed task and found that the control group showed significant adaptation by means of shoulder and elbow angle. They spread their arms to increase their inertia in the frontal plane and became more stable during the eyes closed condition. In the experimental group, the upper arms stayed aligned to the upper body and amount of shoulder movement remained similar to the eyes open task.

In summary, many of the findings fit the global picture of schizophrenia in the literature and also support the disembodiment approach. We found larger CoM acceleration suggesting that the movement is more fragmented, less smooth and often interrupted. The experimental group only uses the necessary body parts during the tandem walk and the upper body is not integrated into the movement. Stabilizing, rhythmic arm movement is not present, resulting in larger normalized angular momentum around the vertical axis. The strategy analysis showed that the option of using arms to balance is rarely chosen. Instead, since the movement focuses on taking precise steps, only taking recovery steps is considered.

We suggest that explicit training of balance with focus on arm movements can increase whole body awareness and counteract disembodiment. The balance parameters and the respective values established in this work can function as a baseline to provide objective measures for therapy. We suggest to perform a systematic analysis that monitors the change over time of balance parameters during different tasks in combination with movement therapy. In general there is great need for objective parameters to support the diagnosis of schizophrenia. PANSS and NSS are widely used, however they rely on subjective evaluation. Motion capture and standardized movement analysis can help understanding the connections between body movement and schizophrenia.

## 9 Interstudy comparison of Balance Metrics

In this chapter we compare results from both studies and all participants. We aim to give an overall picture of the balance metrics that were defined and used throughout this work. For the balance test we combine all participants, divide them into balance-experienced and balance-inexperienced based on the time in balance and evaluate the force plate data. We compare flat ground tandem walking to slackline walking using the established performance indicators.

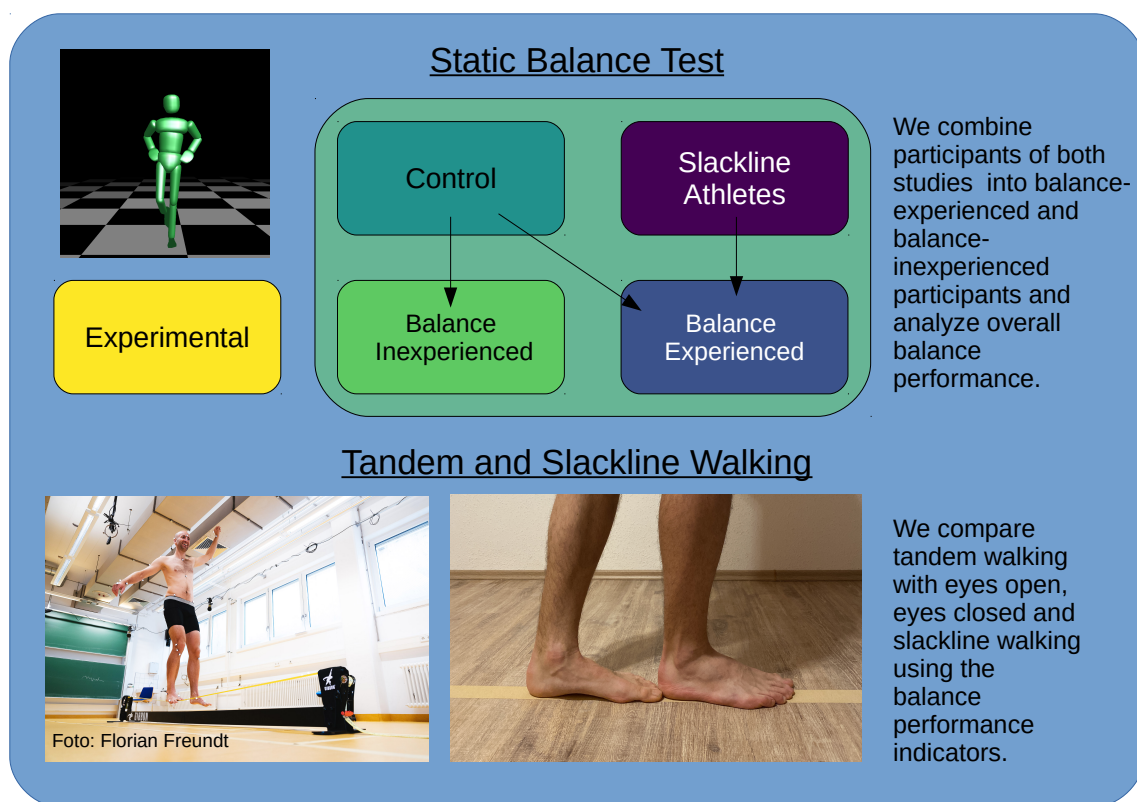


**Figure 9.1:** Chapter overview of the interstudy comparison.

## 9.1 Balance Performance in the Balance Test

For analysis of the CoP force plate data, we combine the control subjects of the "Schizophrenia and the Moving Body" study with the slackline study and set 260 s of total time in balance as threshold to divide them into balance-experienced and inexperienced participants. The same value was chosen in Chapter 7. The experimental group remains the same.

Distributions of the time in balance is shown in Figure 9.2. They are similar for single leg balancing with eyes open and the tandem stance. Balance-experienced subjects manage to also balance on one leg with eyes closed, whereas the other two groups fail to achieve this task. For the force plate analysis only successful trials, where the subject did not fall or move the stance foot, can be evaluated. Table 9.1 shows how many measurements per scenario were available for evaluation. We evaluated all scenarios except single leg balancing with eyes closed. In Chapter 8 we also excluded the tandem stance with eyes closed, as less than 50 % of participants manages the task. However, as the focus in this chapter lies on balance in general, we find the number of trials sufficient.

Group \ Eyes	Parallel Stance		Single Leg		Tandem Stance	
	Open	Closed	Open	Closed	Open	Closed
Experimental	19	19	27	3	27	18
Control <sup>1</sup>	25	25	46	4	44	40
Sportive <sup>1</sup>	22	22	46	33	44	40

**Table 9.1:** Number of successful trials per group and scenario.

The force plate data was filtered using a 5<sup>th</sup>-order Butterworth low-pass filter with cut-off frequency of 9 Hz. To avoid any bias, we cut all trials to 20 s by removing the first and last 5 s. CoP metrics were computed as introduced in Chapter 6. We employ a Kruskal-Wallis-Test [182] to find balance metrics that are able to distinguish between the three groups for all scenarios. Again, this is a non parametric ranked-based test for not necessarily normally distributed data. Resulting p-values are given in Table 9.2. CoP sway distance in ML direction and velocity in AP direction show significance ( $p \leq 0.001$ ) for all five scenarios.

<sup>1</sup>Combined group from both studies

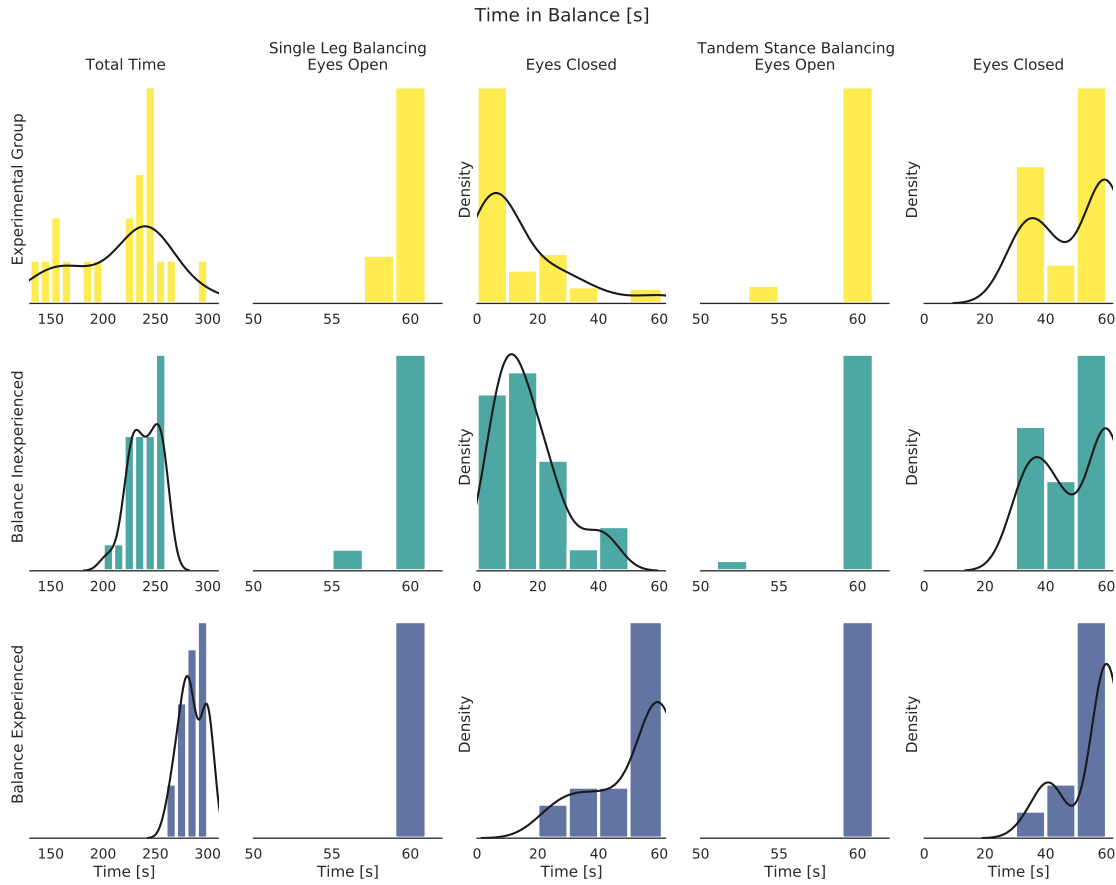


**Figure 9.2:** Time in Balance for all participants of the two studies. The experimental group remains unchanged. All other subjects were divided into balance-experienced and inexperienced following a 260 s threshold for the summed total time in balance for all 5 scenarios.

Variable \ Eyes	Parallel Stance		Single Leg	Tandem Stance	
	Open	Closed	Open	Open	Closed
RDIST ML	0.0005	0.0002	<0.0001	<0.0001	<0.0001
RDIST AP	0.93	0.31	0.015	0.1	0.001
MVEL ML	0.023	0.16	0.0001	0.0014	0.0032
MVEL AP	0.0003	0.006	<0.0001	<0.0001	<0.0001
RATIO	0.015	0.0027	0.74	0.1	0.016
MFREQ ML	0.61	0.017	0.002	0.002	0.02
MFREQ AP	0.021	0.046	<0.0001	0.014	0.5

**Table 9.2:** P values of Kruskal-Wallis-Test for all CoP Variables. P-Values smaller than 0.01 are highlighted.

Figure 9.3 shows box plots for the sway distance in ML direction and velocity in AP direction. In Chapter 8 the sway distance parameter was significantly different between the control group and the experimental group. We found smaller values in the control group. The trend towards smaller sway distance values continues with the balance-experienced group. They show consistently about 30 % lower values than the experimental group for all scenarios and about 15 % lower values than the balance-inexperienced group. We conclude, that sway distance in ML direction, where the foot area is limited, indeed is a suitable performance indicator for static balance.

For sway velocity in AP direction we found differences only during parallel stance with eyes open in Chapter 8. No differences were found for the other standing configurations. Balance experienced beginners, however, show about 30 % lower values than the experimental group for all scenarios. Again, this is a suitable parameter to quantify balance capabilities. We found that balance training decreases the two parameters. In further research it could be analyzed whether this is also the case for the experimental group and if the low values of the balance-experienced groups are within the range of trainability.

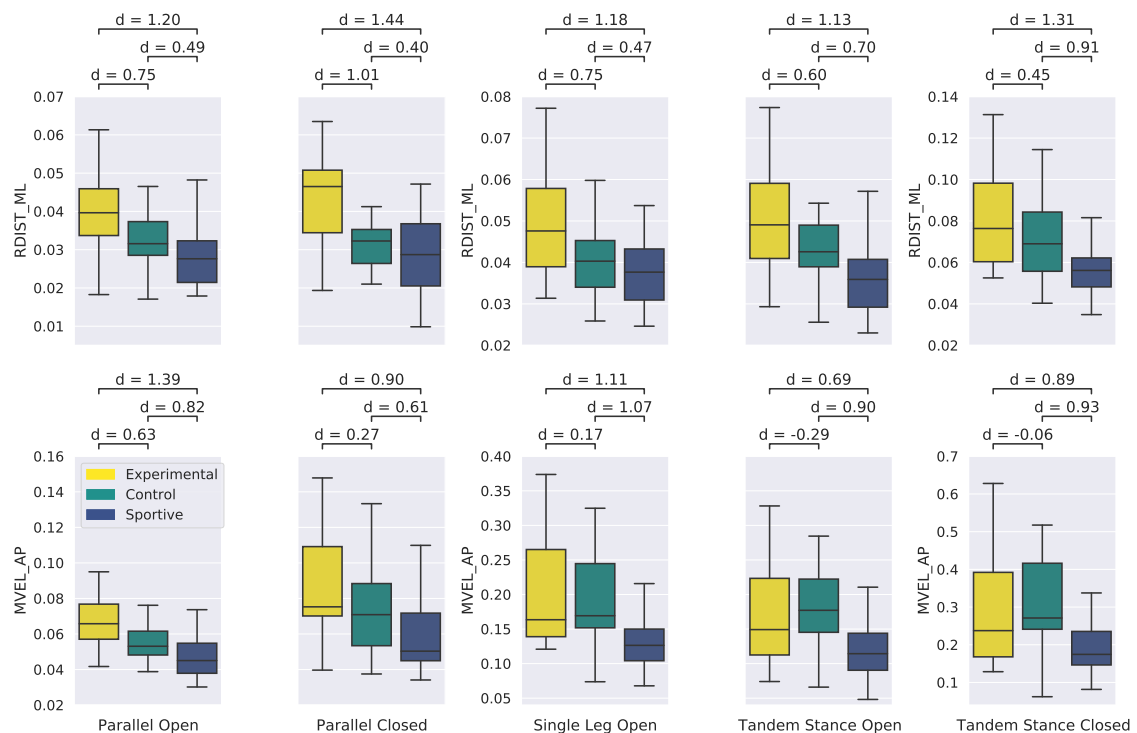


**Figure 9.3:** Sway distance in ML direction and velocity in AP direction for the three groups and five scenarios. Cohen's-d is given to quantify differences.

## 9.2 Comparison of Tandem and Slackline Walking

In this Section we compare all balance metrics that were available for tandem and slackline walking: CoM acceleration, normalized angular momentum, normalized kinetic energy, energy ratio, mean pose, joint angle variation and hand coordination. Different to Chapter 8 we only evaluate successful tandem walking, where no recovery steps were taken. We assume an increasing difficulty throughout the tasks with tandem walking with eyes open being the least challenging and slackline walking being the most difficult scenario. As evaluated in Chapter 8, the control group performs the tandem walk without difficulties and without additional balance movement of the shoulders and arms. We can therefore assume this scenario as the baseline case.

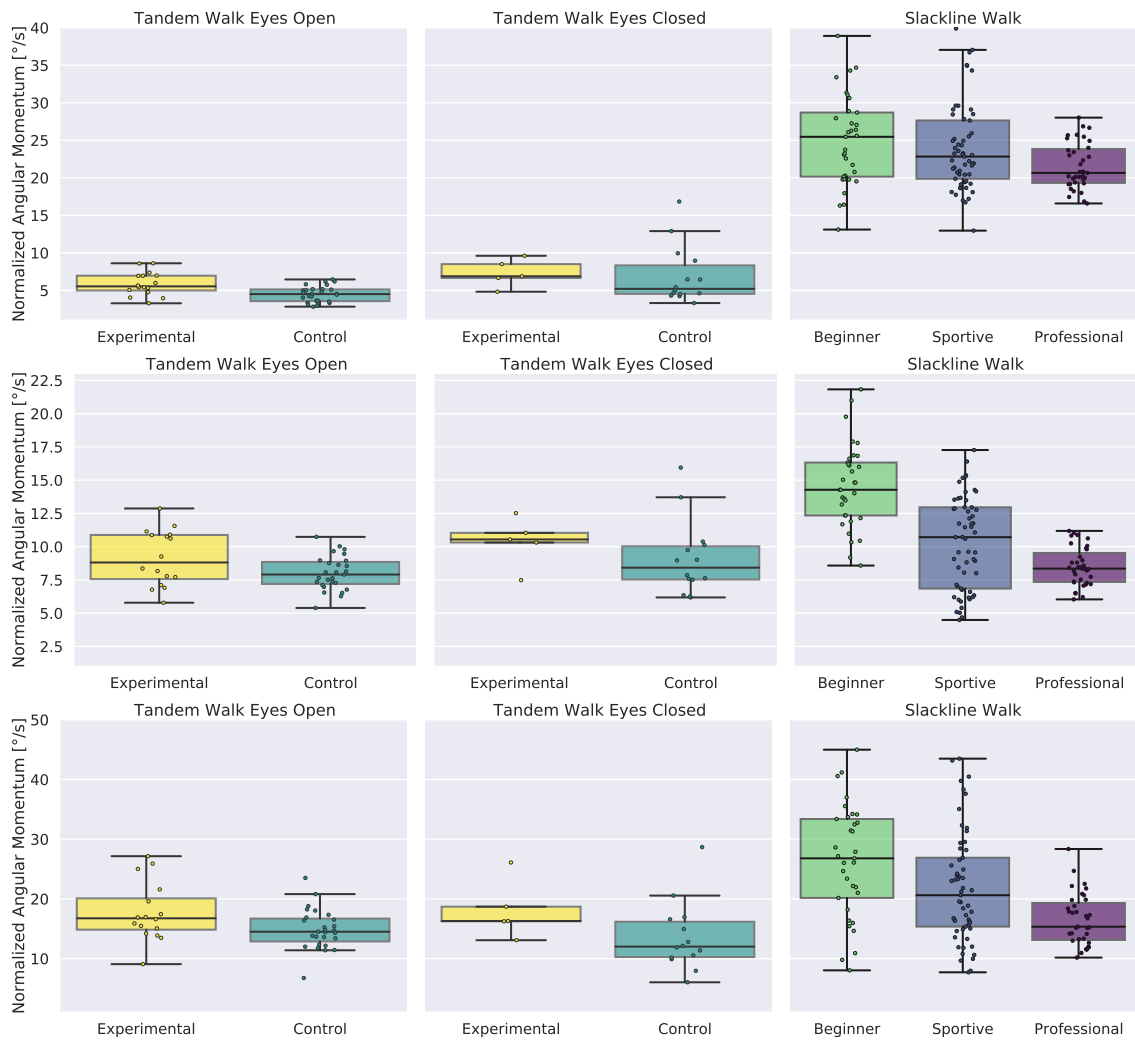
### Normalized Angular Momentum

Figure 9.4 shows the normalized angular momentum in all three directions. We see a clear increase with difficulty and the necessary amount of balance recovery movement. In the frontal plane, almost no balance movements are required during the tandem walk with eyes open. Only the experimental group needs to balance. On the slackline, all participants are constantly performing arm movement and the normalized angular momentum is about five to six times larger.

In the sagittal plane, values are smaller in general and only the beginner group on the slackline shows about twice as much movement as the other groups. The professional slackliners manage to reduce their momentum to the same values that were observed for regular tandem walking. The same is true for normalized angular momentum around the vertical axis. Again, the professional group shows the same values as the control group during regular walking. We conclude that experienced slackline athletes have almost "normalized" their gait and only perform additional movement in the frontal plane, specific to the slackline instability.

### Center of Mass Acceleration

Figure 9.5 shows the CoM acceleration in all three directions. We see similar values in walking direction for slackline and tandem walking in the top row. Professional slackliners manage to reduce their acceleration values to the level of the control group during both tandem walks. The experimental group and the balance-inexperienced beginner group show about 50 % larger values. In sideways and vertical direction, the slackline is accelerating the subject and we see higher values for slackline walking than for the tandem walk. Compared to the balance-inexperienced beginner group, the professional group manages to reduce the acceleration values to about half the level of regular walking.



**Figure 9.4:** Comparison of normalized angular momentum about the CoM for tandem and slackline walking. The sagittal plane is plotted at the top, the frontal plane in the middle and normalized angular momentum around the vertical axis at the bottom.

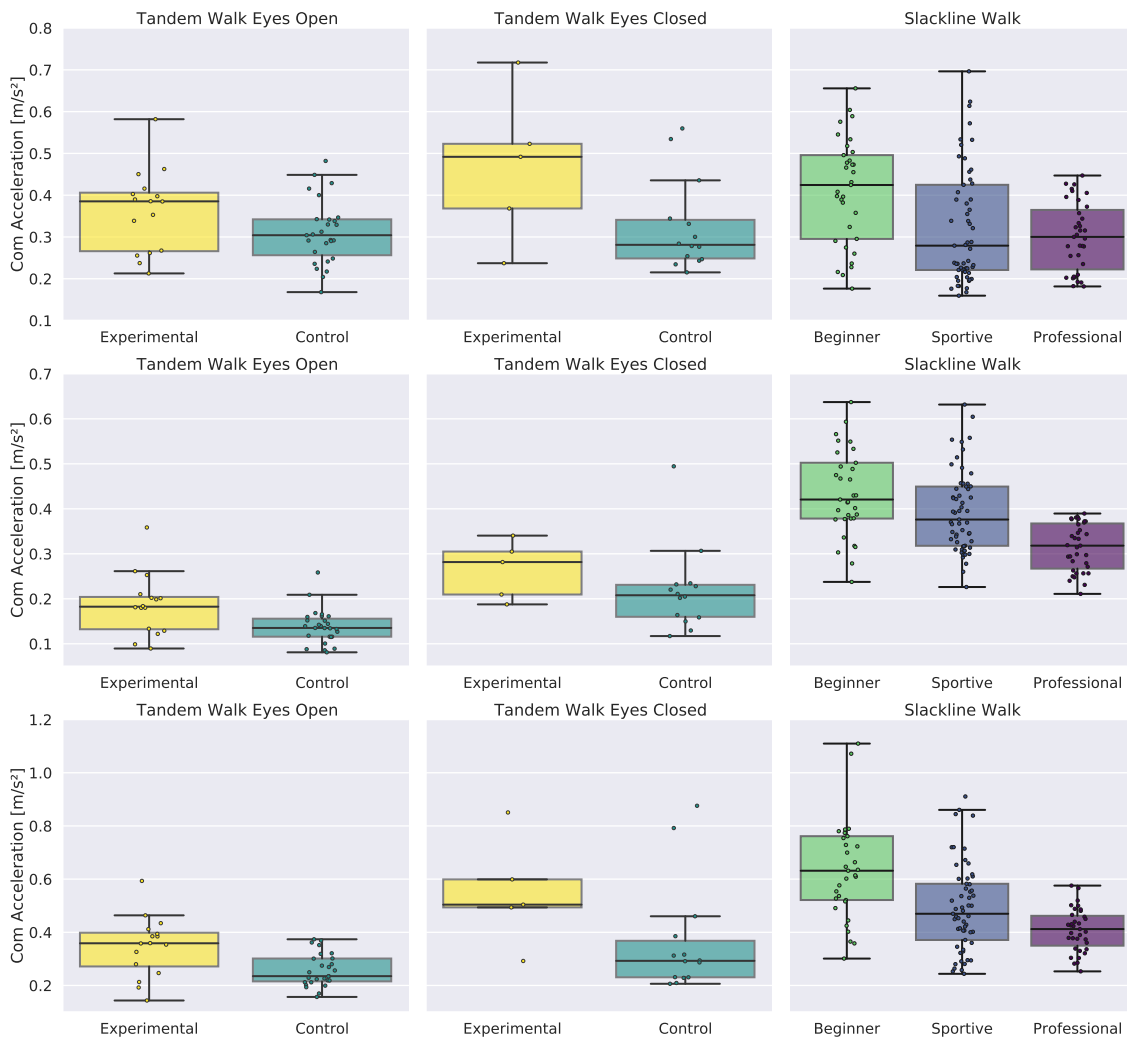


**Figure 9.5:** Comparison of Center of Mass acceleration for tandem and slackline walking. The walking direction is plotted at the top, the sideways direction in the middle and the vertical direction at the bottom.

### Kinetic Energy and Energy Ratio

Figure 9.6 shows the normalized kinetic energy and the energy ratio. We see larger kinetic energy for slackline balancing as expected due to additional balance movement and continuous acceleration. Similar to the findings for acceleration and normalized angular momentum, the professional group and the sportive group managed to reduce the value to about half way the value of regular walking.

The balance energy ratio between rotational energy and linear movement energy increases with difficulty and is a well defined measure of how much effort is required to maintain balance. We see that the experimental group does not change between the eyes open and eyes closed task, while the control group does perform balance related movement. All successful tandem walks with eyes closed of the experimental group were performed without active balancing arm movement as evaluated already in Chapter 8. On the slackline, we see that the balance-inexperienced group does balance, but not as much as the sportive and professional group.

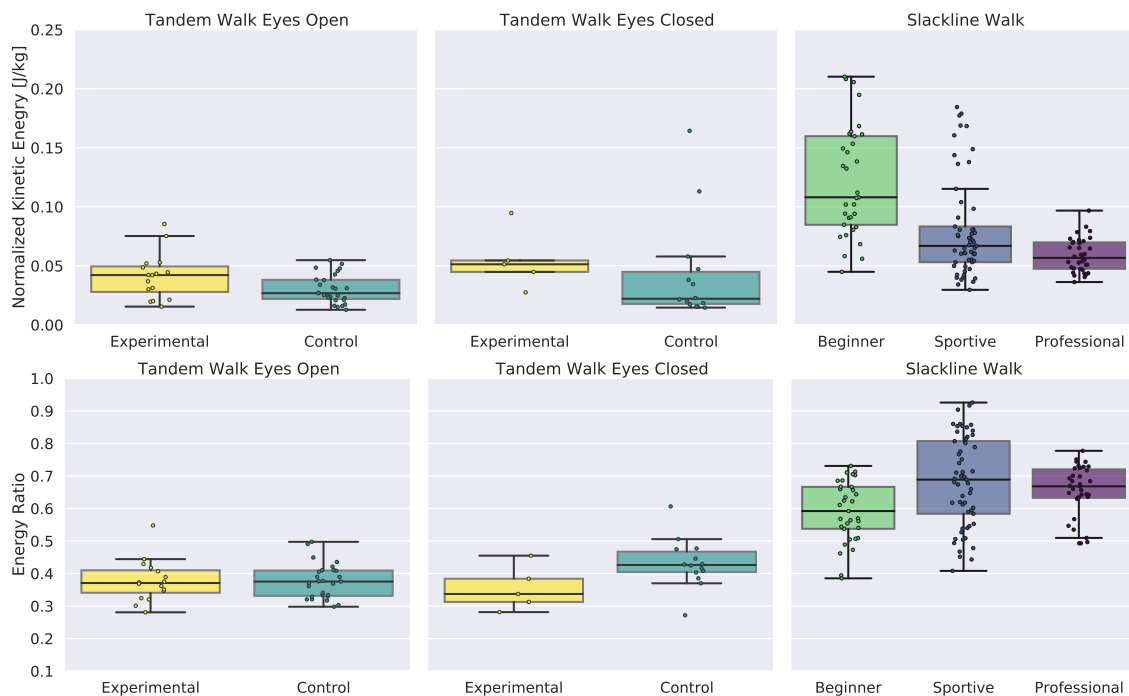


**Figure 9.6:** Comparison of walking speed (top), normalized kinetic energy (middle) and energy ratio (bottom) for tandem and slackline walking.

**Utilized Range of Motion**

Figure 9.7 shows the angle variation of elbow, frontal shoulder and knee angle. We see increasing upper body movement with difficulty and less movement in the knee joints. Subjects become more rigid and less compliant in their stance legs, when under a challenging balance situation.

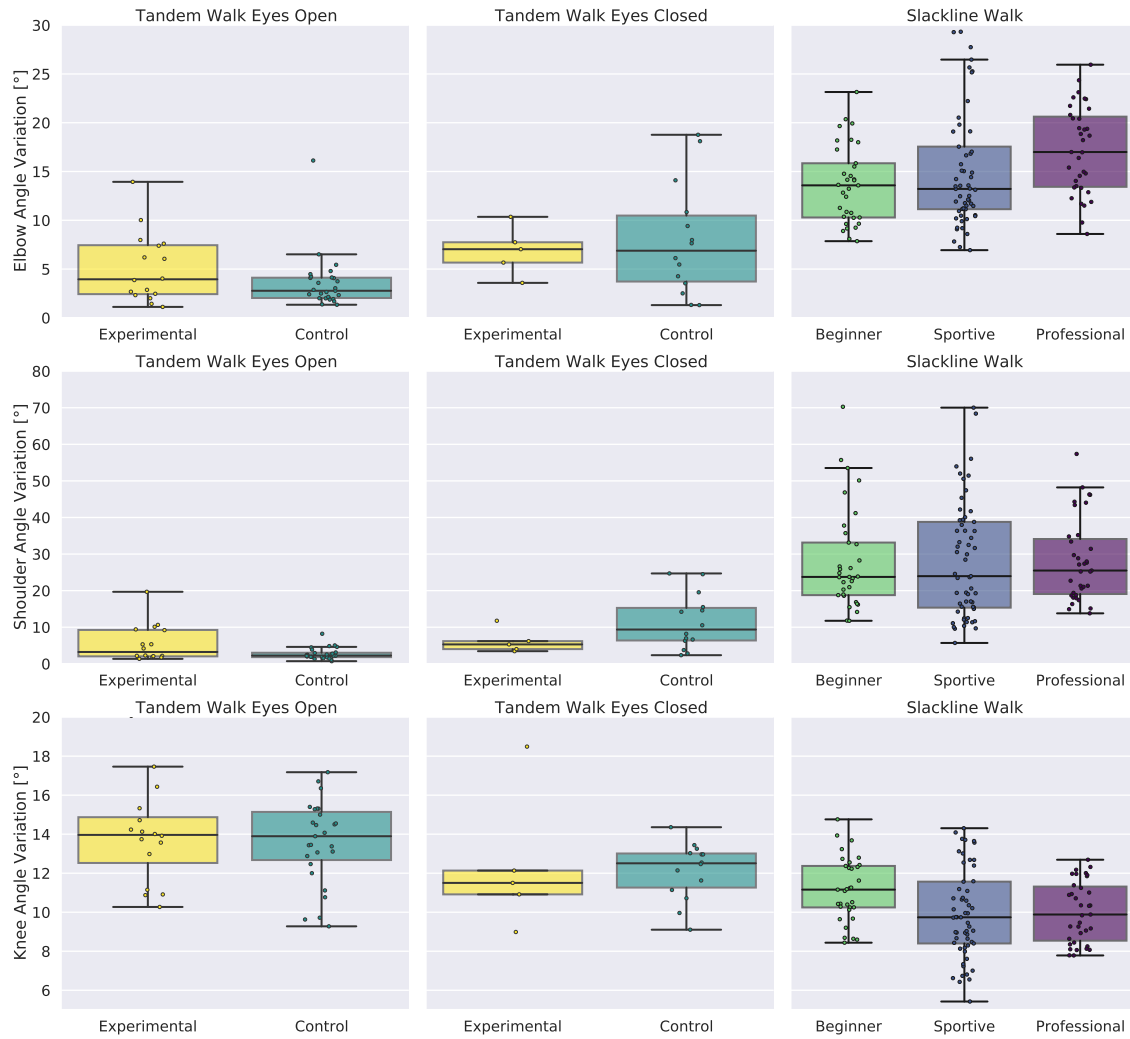


**Figure 9.7:** Comparison of joint angle variation of elbow, frontal shoulder and knee joint.

**Mean Pose**

Figure 9.8 shows the mean head orientation and mean angle of frontal shoulder and elbow joint. We see that subjects look down during the tandem walk with eyes open as well as beginners during slackline walking. Experienced slackliners and subjects during the tandem walk with eyes closed prefer an upright head orientation. All subjects raise their upper arms in a more perpendicular configuration with increasing difficulty. Stretching the elbows seems a specific pose of slackline athletes.

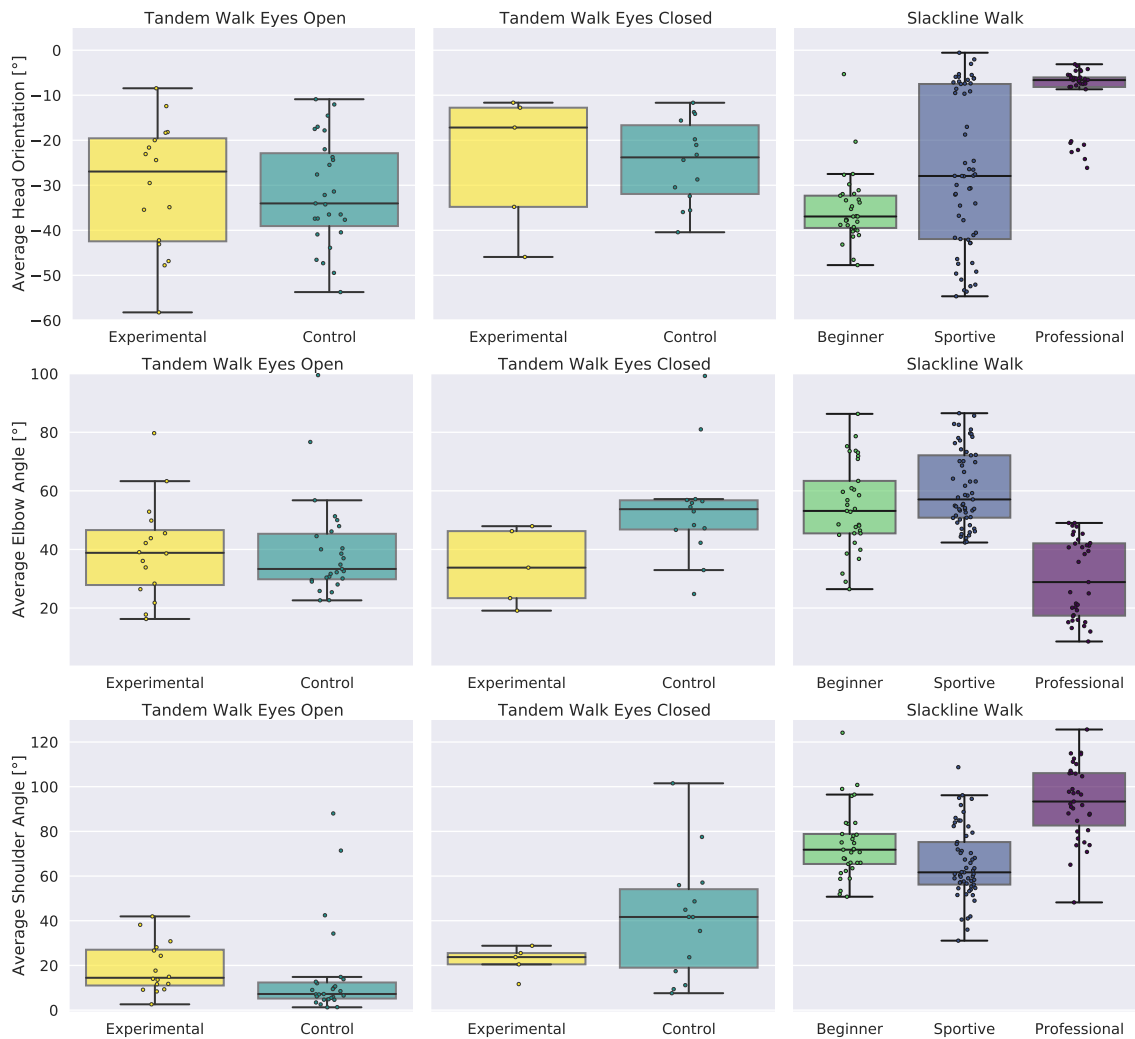


**Figure 9.8:** Comparison of head orientation, elbow and shoulder angle.

### Hand Coordination

In Figure 9.9 we plotted the hand coordination for the three tasks. We find values of 0.5 for the 1 s window and 0.75 for the 1 s window in regular tandem walking. Short term coordination decreases with eyes closed, whereas the 1 s window correlation stays at a similar value. For both time windows we see higher values for slackline balancing, and with increasing skill level. This supports the claim that good movement coordination is a desired skill in more challenging balance situation.

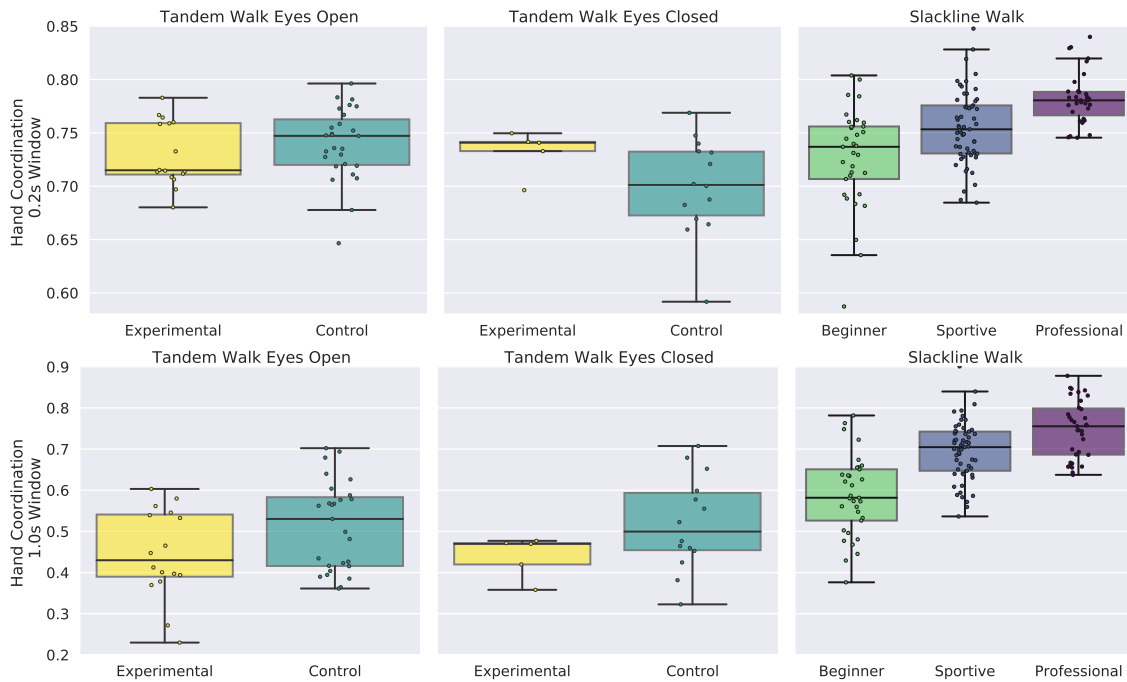


**Figure 9.9:** Comparison of hand coordination.

### 9.3 Summary and Discussion

We analyzed force plate data of all 66 participants of the two studies for parallel stance and tandem stance with eyes open and eyes closed and for single leg stance with eyes open. Not enough data was available for the single leg scenario with eyes closed.

We found that sway distance in ML direction and sway velocity in AP direction were able to distinguish between the three groups in all five scenarios. Balance experienced subjects generally show lower values. As already discussed in Chapter 8 we found impaired balance in the experimental group. Based on the findings of this chapter we can quantify that the effect of balance training in the control group is about as large as the lack of balance capabilities in the experimental group. The difference between the experimental group and the balance-inexperienced group was about as large as the difference between the balance-inexperienced and balance-experienced group. We conclude that the balance parameters can be used to monitor balance training and to objectively quantify static balance capabilities.

We evaluated the proposed balance metrics for tandem and slackline walking. Findings from previous chapters that average angular velocity and CoM acceleration are suitable performance indicators were confirmed. Professional slackline athletes manage to reduce many of the metrics to the baseline level of flat ground tandem walking. The energy ratio proved to be a reliable indicator for the difficulty of a walking task with balance related constraints. Looking at the posture, it was found that subjects prefer horizontal head orientation when possible. This supports the importance of the vestibular system during balance tasks. Hand coordination is a key skill to master slackline balancing, but was not necessarily required for tandem walking.

## **Part IV**

# **Technical and Computational Studies of Slackline Motions**



## 10 Towards a first contact interaction measurement on the slackline

In this chapter we discuss the possibility of measuring and modeling the CoP dynamics between the subject and the slackline directly. One possibility is using pressure-sensitive insoles, however, they require the subject to wear shoes. Ideally the sensor is attached directly to the slackline and allows the subject to balance bare foot. To the author's knowledge and by the time of this reserach, there are only tension measurement sensors available for slackline balancing [183, 184]. The Heidelberg InnovationLab (iL) develops printed electronics and flexible pressure sensitive sensors. In context of this thesis one of their sensors was tested to measure slackline balancing.

### Pressure Sensor Matrix

The Pressure Sensor Matrix (PSM) consists of three components: the sensor matrix layout, a flexible connection circuit and the read-out electronics. They are shown in Figure 10.1. The printed matrix layout is a 2D array of pressure sensitive elements. It consists of two layers that contain parallel lines, one representing the matrix rows, the other the matrix columns. They are turned by 90° with respect to each other. In our case the matrix has 20 × 65 cells. Each cell covers ≈ 4 × 4 mm. The distance between neighboring cells is ≈ 1 mm in each direction. Hence, 64 % of the area is equally covered. The distance between neighboring pixels is 5 mm. The multiplexing of rows and columns by the read-out electronics allows us to measure the output signal of every sensor pixel  $i, j$  of the PSM. The logarithm of the resulting values  $s_{ij}$  is proportional to the pressure  $p_{i,j}$  on the corresponding cell [185, 186].

$$p_{i,j} \propto \log(s_{ij}) \quad (10.1)$$

To compute the actual pressure in N/m<sup>2</sup> a calibration with known weight has to be performed. However, we can calculate the CoP position without knowledge about the calibration. The pixel position of the CoP can be computed as average over all elements.

$$x = \frac{1}{\sum_{i,j} \log(s_{ij})} \sum_{i=0}^{65} \sum_{j=0}^{65} i * \log(s_{ij}) \quad (10.2)$$

$$y = \frac{1}{\sum_{i,j} \log(s_{ij})} \sum_{i=0}^{65} \sum_{j=0}^{65} j * \log(s_{ij}) \quad (10.3)$$

With a conversion factor of 5 mm/px we get the CoP position in coordinates of the sensor matrix. A sample measurement of a foot on the floor is shown in Figure 10.2. We see that the sensor is about 1 cm too narrow to cover the whole area, however the sensor is wide enough for the slackline.



**Figure 10.1:** The InnovationLab Pressure Sensor Matrix. The sensor layout is shown at the bottom, the connection circuit in the middle and the read-out electronics at the top.

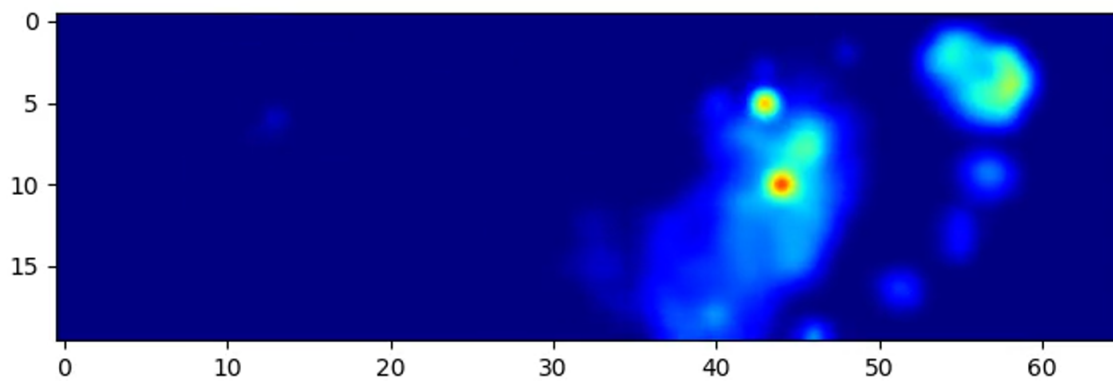


**Figure 10.2:** Foot measurement on the Pressure Sensor Matrix. The Center of Pressure was computed using Equation 10.3 and is visualized in red.

## 10.1 Validation of the Sensor Matrix

We validate the resulting CoP measurements against two other systems and in two situations. First, we mount the PSM on the Bertec force plates and, second, we install the sensor on the slackline and use Moticon pressure insoles as a comparison. Both systems were introduced in Section 3.4.

### 10.1.1 Validation with Force Plates

The PSM was taped on the force plate and single leg balancing was recorded. The force plate directly reports the CoP position. For the PSM data we applied Equation 10.3 to compute the CoP position. The recordings were cut to the time of foot contact and aligned using cross correlation. We subtracted the mean position for both measurements to account for the spatial offset of the two coordinate systems.

Figure 10.3 shows a sample measurement. We see similar trajectories for ML and AP direction, however the amplitude of the force plate is larger. For the ML direction this is reasonable, since the PSM does not cover the entire foot width and a great part of the pressure distribution is not detected. For the AP direction we found that the heel area is measured accurately. Towards the toes, the foot becomes wider and part of the area is not on the sensor. In the left plot in Figure 10.3, we see that positive values are followed accurately, but negative values seem to be limited to a value of  $-30$  mm.

At the bottom of Figure 10.3 a scatter plot for the two directions of the same measurement is presented. We see high correlation between the two systems, however the slope of the linear fit is significantly lower than 1. This represents the observation from Figure 10.3 that the extreme points of the trajectory are not fully recognized. In AP direction we observe a bending, which represents the fact that the heel is measured accurately, but not the distal part of the foot. However, when balancing on the slackline, the matrix layout is wide enough to cover the entire contact area and should be more accurate.

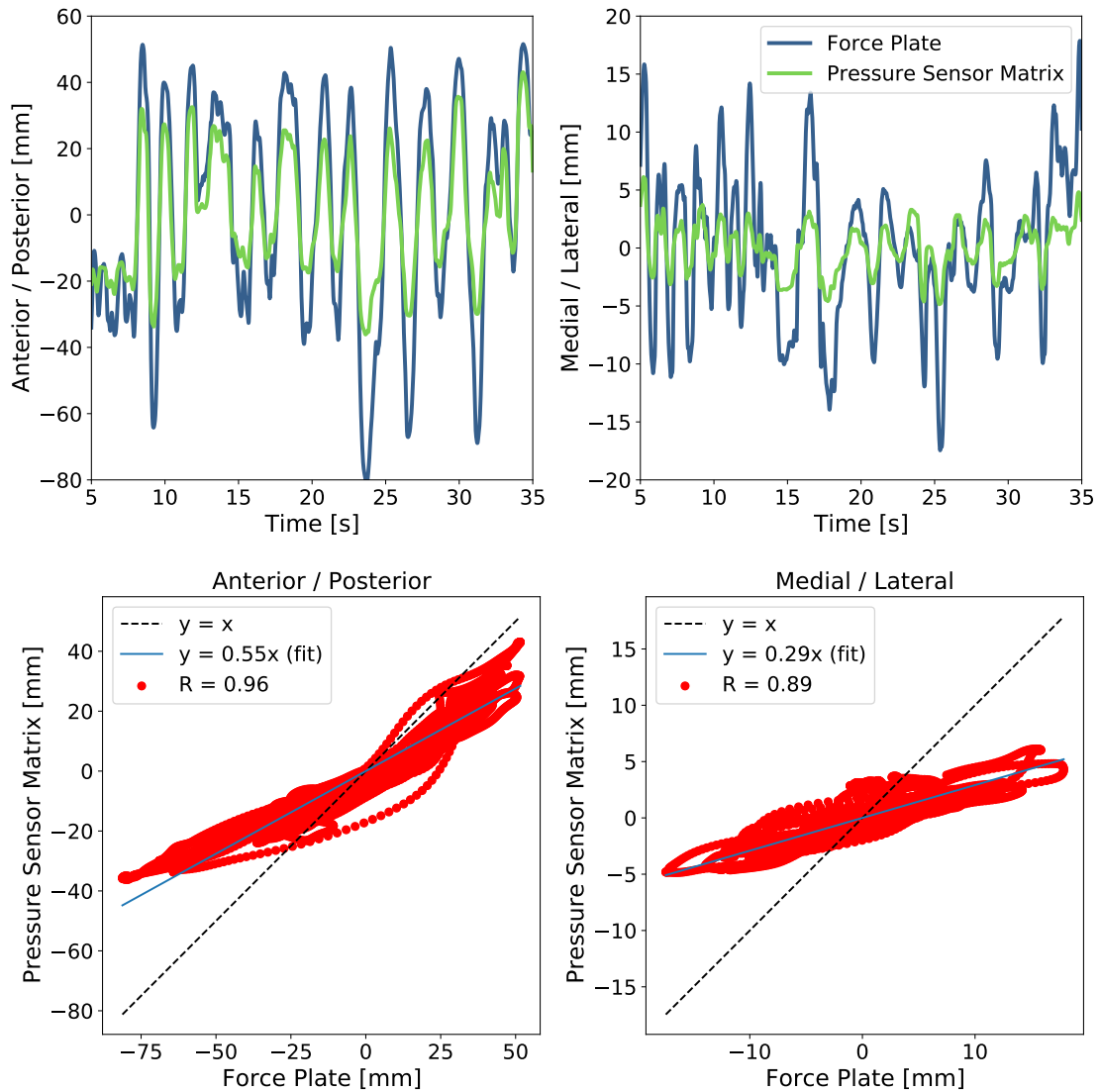


**Figure 10.3:** Synchronized CoP measurements on the force plate. Top: Blue: force plate measurement, Green: Pressure Sensor Matrix. Results are shown for AP and ML direction. Bottom: Scatter plots of the same measurement.

### 10.1.2 Measurements on the Slackline

The matrix sensor was attached to the slackline using double sided tape at the bottom and higher friction tape at the top as shown in Figure 10.4. We performed synchronized measurements using the sensor matrix and pressure sensitive insoles from Moticon. Figure 10.5 shows the results from a measurement with the two systems. The insole data is plotted in blue, the data from the PSM in green. The left plot shows the AP direction along the slackline. We see consistent curves for the two systems and a range of motion of about 80 mm. The PSM shows a slightly larger amplitude and a faster response to sudden changes in the CoP position. This is due to the fact that the PSM captures the entire contact area, while the insoles do not have sensors all the way to the heel and tip of the foot. The right plot shows the perpendicular ML direction. The same scale is applied. No variation is seen for the PSM and also the Moticon insole shows more noise. We will discuss the nature of this curiosity in Section 10.2.1. For now we further evaluate the AP direction.



**Figure 10.4:** The matrix sensor layout mounted on the slackline.

Figure 10.6 shows a scatter plot at the left and a Bland-Altman plot [187] at the right. A linear fit was added to the scatter plot and the correlation computed. We find good agreement between the methods. The larger amplitudes measured by the matrix sensor leads to a linear fit that is about 10% larger with respect to the insole measurement. The Bland-Altman plot shows no systematic difference between the methods.

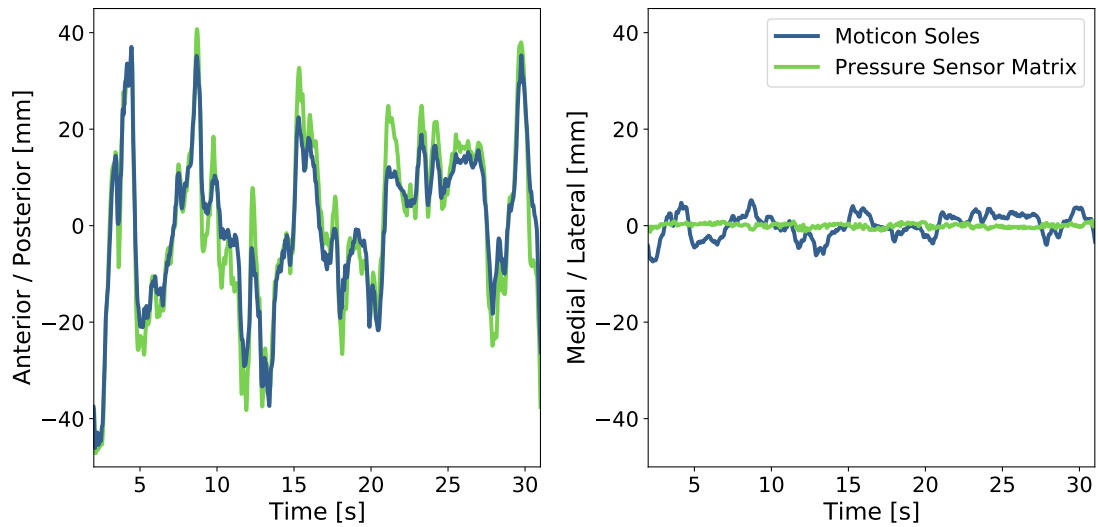


**Figure 10.5:** Synchronized CoP measurements on the slackline. Blue: Moticon Sensor Insoles, Green: Pressure Sensor Matrix. Results are shown along and perpendicular to the slackline.

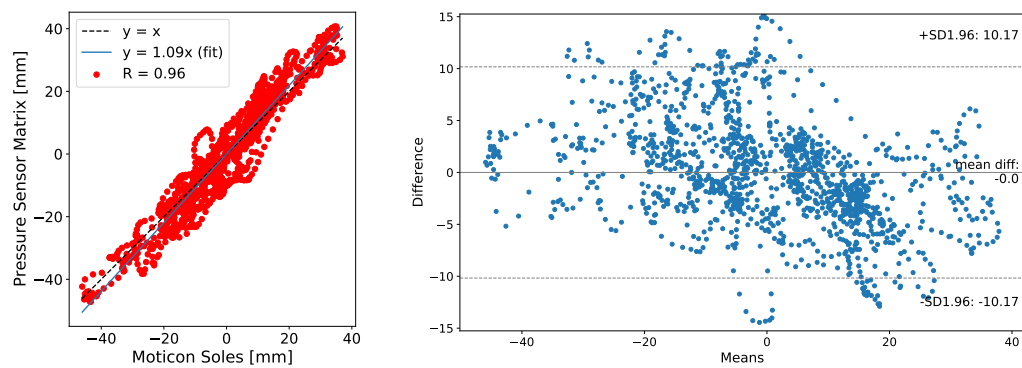


**Figure 10.6:** Scatter and Bland-Altman plot to compare the two measurement systems. We find good agreement and no systematic deviation.

## 10.2 Foot Contact Analysis and Modeling

Since we did not see any dynamic perpendicular to the slackline in the CoP position measurement presented in Figure 10.6, we performed further measurements using Moticon Pressure Insoles to gain additional insight. The absence of any movement in ML direction contradicts the findings for regular ground balancing from the balance test in Section 1.3.2. We recorded standing on one leg in three different situations and for each foot individually. The following results are visualized in Figure 10.7 and have already been published in [188]:

- **Left:** Single leg balancing on regular surface
- **Middle:** Balancing on the slackline with aligned stance foot
- **Right:** Balancing on the slackline with turned stance foot

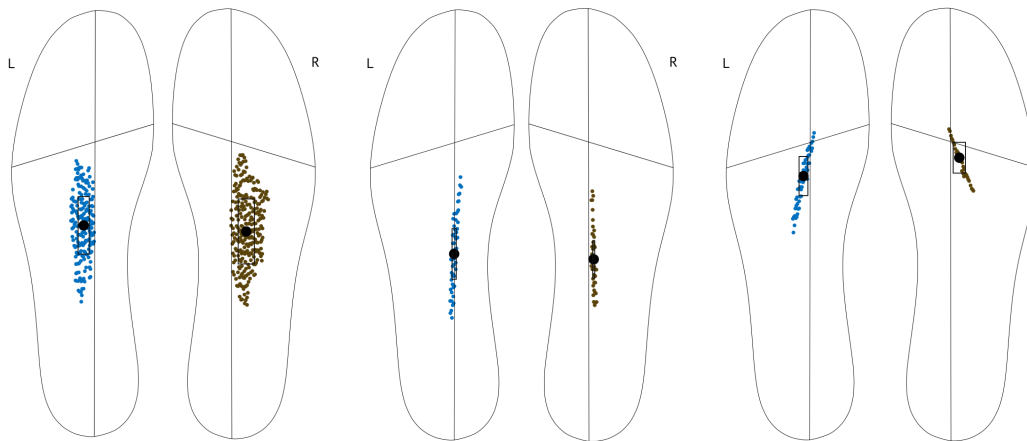


**Figure 10.7:** Center of Pressure recording of different single leg balancing tasks. We recorded both legs individually using Moticon Pressure Insoles. Left: Single leg balancing on regular surface. The CoP is moving in the anterior-posterior and in medial-lateral direction. Middle: Balancing on the slackline with aligned stance foot. Right: Balancing on the slackline with turned stance foot. The CoP is constrained by the direction of the slackline and to a single line.

We see a clear difference between three cases: On flat ground the CoP moves in medial-lateral and in anterior-posterior direction, as is established in Chapter 1.3.2. It is different on the slackline: we observe that the CoP does not move within the whole contact plane, but only on a single line. From the aligned and turned foot positioning we can conclude that the direction of this line is determined by the direction of the slackline. Even though the slackline measures 5 cm in width, we see from the measurement data that the CoP does not deviate from the very center of the slackline. The same can be said from the sensor matrix measurement that is directly performed in the frame of the slackline. No movement of the CoP perpendicular to the slackline is recorded, also for a turned stance foot.

We explain this with the fact that the ribbon band of the slackline is able to freely rotate around the center axis between the anchor points. This rotation is barely damped and therefore highly sensitive to shifting the CoP away from the slackline center. Rotating a contact surface, however, greatly reduces the normal force and therefore reduces the non slipping threshold. We conclude that a small shift of the CoP away from the center of the slackline can already lead to the contact foot slipping off. The very narrow constraints on the CoP together with the continuous vertical and sideways movement of the stance foot explains the difficulty of slackline balancing especially in contrast to walking on a beam.

### 10.2.1 Slackline Contact Modeling

A foot contact model is required to perform a dynamic motion analysis. A regular planar, non slipping contact can be described using a total of 8 variables [189]: The contact force  $\mathbf{F}$  acting in three directions, two variables for the CoP position  $\mathbf{p}$  in the contact plane and three contact torques  $\mathbf{M}$ . The forces are constrained by the friction cone to prevent slipping. Taking the measurements presented in Section 10.2 into account, we propose a new contact model for slackline balancing that includes 6 variables. Based on the slackline coordinate system shown in Figure 7.2 they are:

$$\mathbf{F} = [F_x, F_y, F_z]: \text{ The contact forces} \quad (10.4)$$

$$\mathbf{p} = [p_x, 0]: \text{ The CoP position in along the slackline} \quad (10.5)$$

$$\mathbf{M} = [0, M_y, M_z]: \text{ The contact torques in the slackline coordinate system} \quad (10.6)$$

Zeros are placed where the regular contact model would have had an additional variable. The contact force can still act in all three directions and is still subject to the friction cone. As a consequence of the measurements presented in Figure 10.7, the CoP position is described by only one free variable instead of two. The Y-coordinate is always zero. The position can no longer be defined in the local coordinate system of the foot, but has to be transformed in the coordinate system of the slackline. Furthermore, we allow only two instead of three contact torques. Again these are defined by the global position of the slackline and can not be modeled locally. They act around the vertical axis and are perpendicular to the slackline. As described before, the slackline can freely rotate around the X-Axis and therefore no torque can be applied around this axis.

## 11 Whole Body Dynamic Analysis of Challenging Slackline Jumping

In this chapter we analyze a more advanced slackline jumping motion. The motion of interest can be seen in Figure 11.1. The subject balances with both feet aligned to the slackline, then bends their knees, goes down to increase the tension of the slackline and prepares the jump. While in the air, a 180° rotation is performed. The subject lands with both feet simultaneously.

After obtaining written consent by the subject, we recorded the motion using Qualisys and the marker set described in Section 3.1.1. We utilize the optimization approach described in Section 5.2 and include the contact model developed in Section 10.2.1. The subject-specific model from Section 4.1 is slightly adjusted by means of the DoF. We show the advantages of this analysis when compared to the inverse kinematics analysis (see Table 5.1) and to the commercial motion analysis software Visual3d (C-Motion, Germantown, Maryland, USA). A part of the results from this analysis have been published in the Journal of Applied Sciences [188].

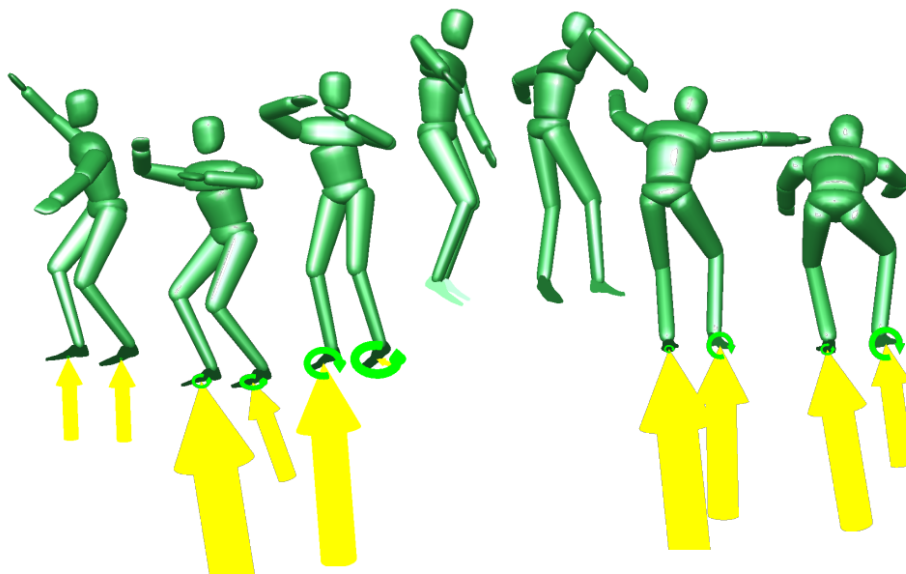


**Figure 11.1:** A dynamic reconstruction of a jumping motion with rotation on the slackline. The contact forces and torques are visualized.

### Adjusted Subject Model

The subject-specific dynamic model is the same as described in Section 4.1, only the DoF are slightly reduced. DoF that are not essential to performing the jump motion were removed from the model to decrease the complexity of the resulting OCP. These are two DoF each at the neck and ankle joint. Table 11.1 shows the new DoF. Changes compared to the model described in Section 4.1 are highlighted. The segment length and joint center positions remain unchanged. The subject weight 86 kg and was 1.9 m tall. The right column shows the mass for each segment.

Segment	Joint	Degrees of Freedom	Mass [kg]
Pelvis	3d Floating Base	TX, TY, TZ, RX, RY, RZ	5.9
Middle Trunk	Lumbar Spine	RY,RZ	15.5
Upper Trunk	Thorax Spine	RX, RY	12.5
Head	Neck	RZ	6.5
Upper Arm	Shoulder	RX, RY, RZ	2.3
Fore Arm	Elbow	RY, RZ	1.4
Hand	Wrist	Fixed	0.4
Thigh	Hip	RX, RY, RZ	13.5
Shank	Knee	RY	3.9
Foot	Ankle	RY	1.2

**Table 11.1:** Details of the subject specific model. DoF were reduced compared to the model described in Section 4.1

### Slackline Coordinate System

As shown in Figure 11.2 on the right, the coordinate system for this work is the same as in Chapter 7. The X direction is aligned with the slackline, the Y direction perpendicular in the horizontal plane and the Z direction represents the vertical axis.

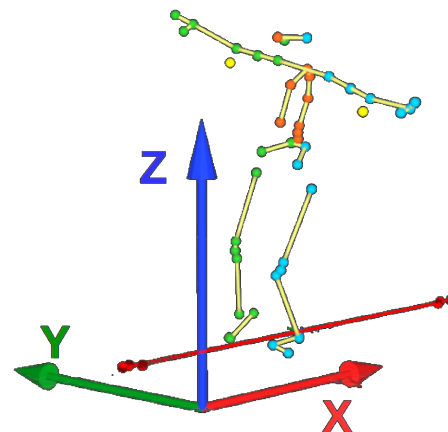


**Figure 11.2:** The coordinate system of the study.

## 11.1 Optimal Control Problem Formulation

We formulate the dynamic reconstruction of the recorded motion as an OCP following what is described in Section 5.2. Unlike previous work by Emonds et al. [15] or Stein et al. [16] that tracked joint trajectories that were computed beforehand using inverse kinematics, we formulate an OCP that tracks the marker positions directly. In the cost function we minimize the distance between the positions  $\vec{m}_i$  of the virtual markers on the model and the 45 recorded marker trajectories  $\vec{m}_i^*$  over the time  $t \in [0, T]$  of the motion, similar to Equation 5.9a:

$$\min_{\mathbf{x}, \mathbf{u}} \int_0^T \sum_{i=0}^{45} \|\mathbf{m}_i(\mathbf{q}(t)) - \mathbf{m}_i^*(t)\|^2 dt \quad (11.1)$$

We did not use a regularization term, unlike in [16], where additionally  $\mathbf{u}^2$  is minimized. This can be useful to account for possible redundancies in the contact forces during the double support phases, but was not in this example. The state vector consists of joint angles and joint velocities:

$$\mathbf{x}(t) = [\mathbf{q}, \dot{\mathbf{q}}] \quad (11.2)$$

The control vector represents the torques  $\boldsymbol{\tau}$  of all actuated joints and all variables of the slackline contact model that was derived in Chapter 10.

$$\mathbf{u}(t) = [\boldsymbol{\tau}(t), \boldsymbol{\lambda}_L, \boldsymbol{\lambda}_R] \quad (11.3)$$

There are six additional controls per foot contact: three forces, two torques and the CoP position. All are given in the coordinate system of the slackline.

$$\boldsymbol{\lambda}_{R/L} = [F_x, F_y, F_z, M_y, M_z, p] \quad (11.4)$$

The slackline jumping motion can be divided into three phases: the initiation of the jump, the flight phase and the landing phase. During the two contact phases the dynamics of the system are described by Equation 4.9. While the subject is airborne Equation 4.6 must hold. We reformulate the forward dynamic equations as first order ODE of the state vector:

$$\dot{\mathbf{x}}(t) = [\mathbf{q}, \mathbf{FD}_i(t, \mathbf{x}(t), \boldsymbol{\tau}(t))] \quad (11.5)$$

where  $i = [1, 2, 3]$  is the phase index. We implemented two formulations: In the first implementation, we used the foot position trajectories of the inverse kinematics fit to determine if the feet are in contact with the slackline. Figure 11.3 shows the height of the feet above the ground during the jump motion. The slackline is mounted at a rest height of 31 cm. Therefore, we can define a flight phase whenever both feet are above this height. This is indicated in red. Accordingly, phases 1 and 3 are contact phases and subject to Equation 4.9 and Phase 2 is a flight phase and subject to Equation 4.6. The phase switching times are fixed to be  $t_1 = 1.06$  s and  $t_2 = 1.44$  s. The take-off and landing are modeled to be continuous. There is no hard impact that would lead to a jump in joint velocities and therefore no phase change function  $h$  is needed.

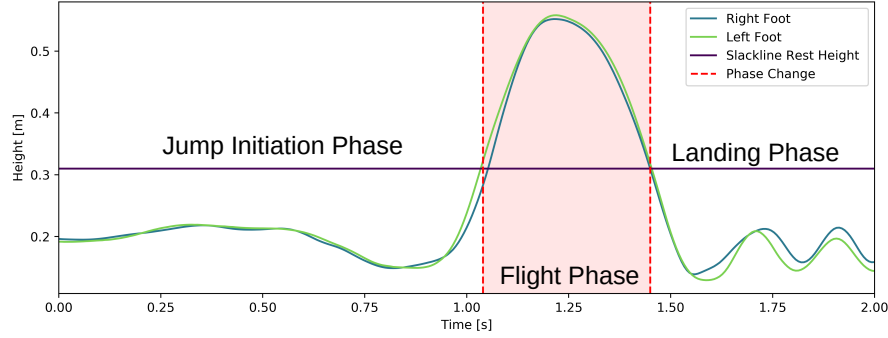


**Figure 11.3:** Feet positions are plotted against time for a slackline jumping motion. The rest height of the slackline is at 31 cm. The flight phase is indicated in red, when both feet are higher than the slackline.

In the second implementation, we defined the whole motion as one phase that is subject to the contact dynamics (Equation 4.9). We formulated the following discontinuous path constraint throughout the motion:

$$r^{eq}(\mathbf{u}(0), \dots, \mathbf{u}(T)) = \begin{cases} \lambda_R, & \text{if Right Foot Height} > 0.31 \text{ m} \\ \lambda_L, & \text{if Left Foot Height} > 0.31 \text{ m} \neq 0 \\ 0, & \text{otherwise} \end{cases} \quad (11.6)$$

Whenever a foot is above the slackline height, no interaction force can act. We achieve this by constraining the controls to be zero. This allows the optimizer to determine the exact timing of the foot contact which is fixed within the other implementation. Additionally this formulation allows for different contact timings, such as jumping or landing with one foot after the other. This should enable for slightly better marker positions tracking. On the other hand, such a formulation introduces non-differentiabilities in the model which might cause numerical problems. We expect the first implementation to show better convergence, since discontinuities in the dynamics are supposed to be formulated explicitly as phase changes and constraints should be differentiable throughout one phase. However, in practical tests we observed that formulating phase changes as constraints also works in the present case.

In both implementations, further boundary constraints  $g(\cdot)$  are implemented for joint angles, velocities and torques and have to be respected throughout the motion. The friction cone is implemented as an inequality constraint that requires the normal force to be larger than the horizontal forces. To determine reasonable upper limits for contact forces and torques, we performed a similar jumping motion on two force plates (Bertec, Columbus, OH) and recorded the acting GRF and Moments.

We set the following limits:

$$F_x[\text{N}] = F_y[\text{N}] = [-400, 400] \quad (11.7)$$

$$F_z[\text{N}] = [0, 1500] \quad (11.8)$$

$$M_y[\text{N/m}] = [-30, 30] \quad (11.9)$$

$$M_z[\text{N/m}] = [-30, 30] \quad (11.10)$$

$$p[\text{cm}] = [-10, 10] \quad (11.11)$$

Both implementations converged with a computation time of approximately 24 h. Due to the problem's complexity, we were numerically limited to  $\approx 80$  shooting nodes. We chose 40 multiple shooting intervals per 1 second of motion and reconstructed around 2 seconds of motion. Other choices are possible, but we found that the computation time drastically increases with more shooting nodes and that the solver is not always able to find solutions for less shooting nodes per second of motion. The single phase implementation resulted in a slightly lower tracking error, however the difference is marginal. Therefore we present and analyze only the results for the single phase implementation.

The resulting motion and the interaction forces (visualized as yellow arrows) are shown in Figure 11.1. Contact and flight phases are clearly distinguished. We see that the subject equally used both feet to initiate and land the jump and that contact torques were acting to build the necessary angular momentum for the rotation. The feet were aligned with the Slackline during the first contact phase and were turned perpendicularly for landing.

## 11.2 Method Comparison

In this section we want to compare the results of three methods: the single phase OCP-based analysis, the inverse kinematics analysis and the commercial software Visual3d. The first two use the same subject model, described above, while Visual3d uses a model with different properties. It consists of 15 segments, having only one trunk segment. All other segments are identical for the two models. It is based on Dempster's regression equations [190]. By default, there are no kinematic constraints to the joints in Visual3d and each segment is fitted to the marker data individually having 6 DoF.

### 11.2.1 Fitting Error

Figure 11.4 shows the deviation between the marker measurement and the virtual markers of the subject model for the OCP solution. The average residuum per marker is shown on the top and the frame by frame error on the bottom. Overall we achieved an average tracking error of 3 cm per marker. This accuracy is similar to the least squares inverse kinematic fit. In both cases, the largest deviations occur for the two shoulder markers (L\_SAE and R\_SAE). One reason for this is that the arms were aligned to the upper body during the static pose on which the model is based. During the jump, however, the arms are mainly turned  $90^\circ$  compared to this pose and parallel to the ground which results in skin and marker movement relative to the bone and shoulder joint. The markers are moved closer to the spine. This offset is visible throughout the motion.

Additionally, the shoulder is modeled as a spherical joint with only three DoF. In reality this joint is much more complex and also has translational DoF. This currently limits the tracking accuracy, however a more precise kinematic shoulder model could be used.

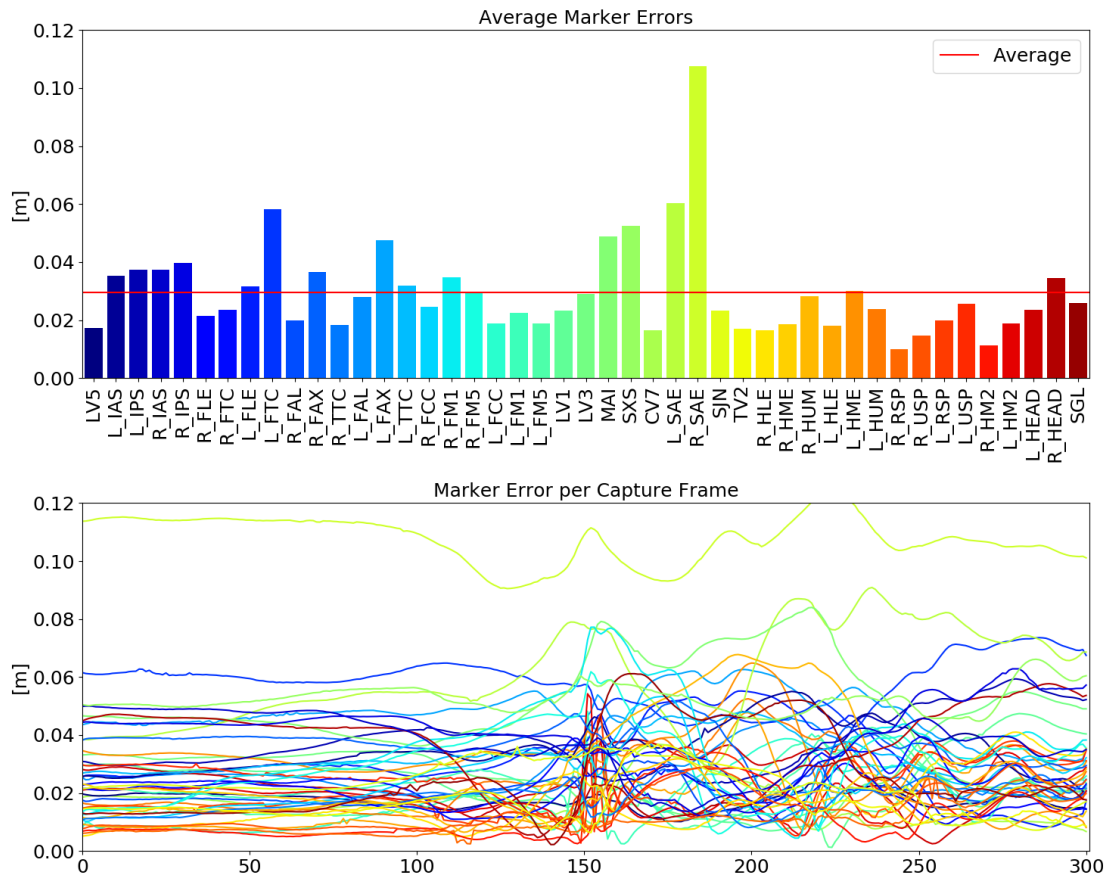


**Figure 11.4:** Marker deviation between the recording and the virtual markers on the model for the OCP solution. Top: Average marker error for all 45 markers. Largest deviations occur for the shoulder markers. This is due to the fact that the model is based on a N-Pose capture and the slackline motion mainly had a T-Pose like arm positioning. Bottom: Frame by frame marker error.

### 11.2.2 Dynamics Analysis

For the mechanical system at hand Newton's EoM [191] can be reformulated as:

$$\ddot{\mathbf{c}} * m = \sum_{\lambda_{L/R}} \mathbf{F} \quad (11.12)$$

$$\dot{\mathbf{L}} = \sum_{\lambda_{L/R}} (\mathbf{M} + (\mathbf{p}_i - \mathbf{c}) \times \mathbf{F}) \quad (11.13)$$

where the change of momentum is equal to the CoM acceleration  $\ddot{\mathbf{c}}$  times the subject mass  $m$ ,  $\dot{\mathbf{L}}$  is the change of angular momentum and  $\mathbf{p}$  is the point where the force is acting on the system. During all phases, Equation 11.12 and 11.13 must hold. For the contact phases we can compute the left hand side of Equation 11.12 and Equation 11.13 using the `CalcCenterOfMass` function of RBDL and the right hand side from the result values of  $\lambda_{L/R}$  of the OCP. Hence, when looking at the motion analysis the following mechanical properties of the overall system need to be satisfied:

- Horizontal momentum is conserved during the flight phase
- Gravity is the only acceleration acting on the CoM during the flight phase
- Angular momentum is conserved during the flight phase
- The change of momentum is proportional to the sum of external forces
- The change of angular momentum is equal to the sum of all acting torques.

We validate the OCP method by showing that these mechanical properties of the overall system are, in fact, satisfied since Newton's EoM have been formulated as constraints. During the flight phase of the motion all external are zero. Here we can check the requirements also for the inverse kinematic fit and the Visual3d analysis.

Figure 11.5 shows the CoM position throughout the motion. The inverse kinematic based motion analysis is plotted in purple, the OCP result in light green and the evaluation by Visual3d in blue. Phase changes are indicated in red. We see that the OCP and the inverse kinematics solution follow similar trajectories as they use the same dynamic model. The Visual3d result is similar for X (along the Slackline) and Z (vertical) direction, however it differs drastically perpendicular to the slackline. We see an offset at the beginning of the motion, that suggests that the CoM location of the Visual3d model is different due to the difference in trunk segments. It is shifted approximately 7 cm upwards and 4 cm in horizontal direction.

In the vertical direction we see the largest range of motion with 80 cm. During the motion the subject jumps approximately 15 cm forward, along the slackline. Not much movement is possible in Y direction, perpendicular to the slackline. The jump has to be performed precisely and movement in this direction would lead to a fall. A total range of motion of 4 cm is observed. The fact, that the CoM position of the two models differs about as much as the total movement in this direction makes further analysis ambiguous.

This becomes more evident when looking at derived quantities such as the CoM and angular momentum dynamics. Figure 11.6 shows the CoM velocity and Figure 11.7 the CoM acceleration. We added scatter plots that compare the three methods. The contact phases are plotted in blue, the flight phase in red and the correlation between the methods shown in the legend. The diagonal indicates the expectation when both methods measure the same value.

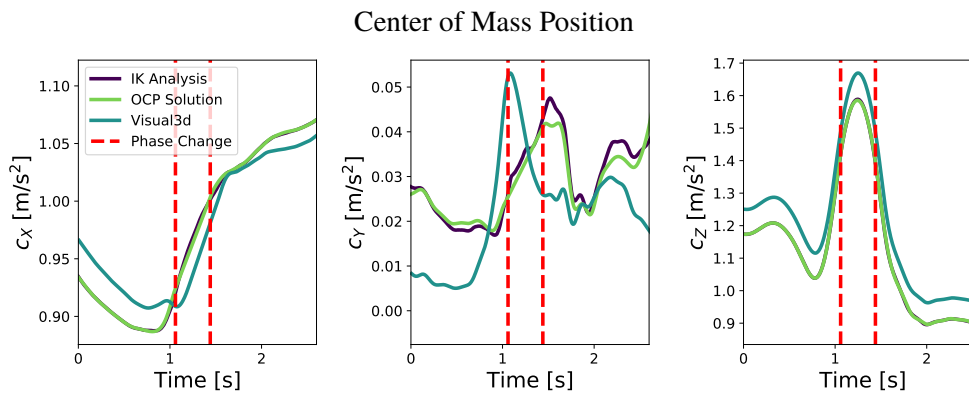


**Figure 11.5:** Center of Mass position throughout the jumping motion. Analysis methods are consistent in the forward and upward direction. There is only little CoM movement in the sideways direction and the measurements show different trajectories. This is due to the different dynamic model used by Visual3d.

### Contact Phase

In both plots, we see good agreement for the vertical direction during the contact phases in the bottom row. The difference in the model CoM position does not play a role when looking at the derivative, since there is no rotation in the sagittal plane and the range of motion is comparably large. This is different in the horizontal direction. We still find agreement in the velocity during the contact phases, when using the same model as it is shown in the second left column of Figure 11.6. As already suggested from the CoM position analysis, the derived CoM velocity and acceleration measurements are not consistent when fitting different models to the marker, since the range of motion is small. Looking at the CoM acceleration in Figure 11.7 no agreement is found in the X direction along the slackline. Values in Y direction show better agreement.

### Flight Phase

During the flight phase, the methods only agree in the vertical velocity, where gravity is acting. The OCP solution shows constant values and conservation of momentum, while a frame by frame, kinematic analysis shows a change in momentum of up to 50%. Newton's EoM are clearly violated.

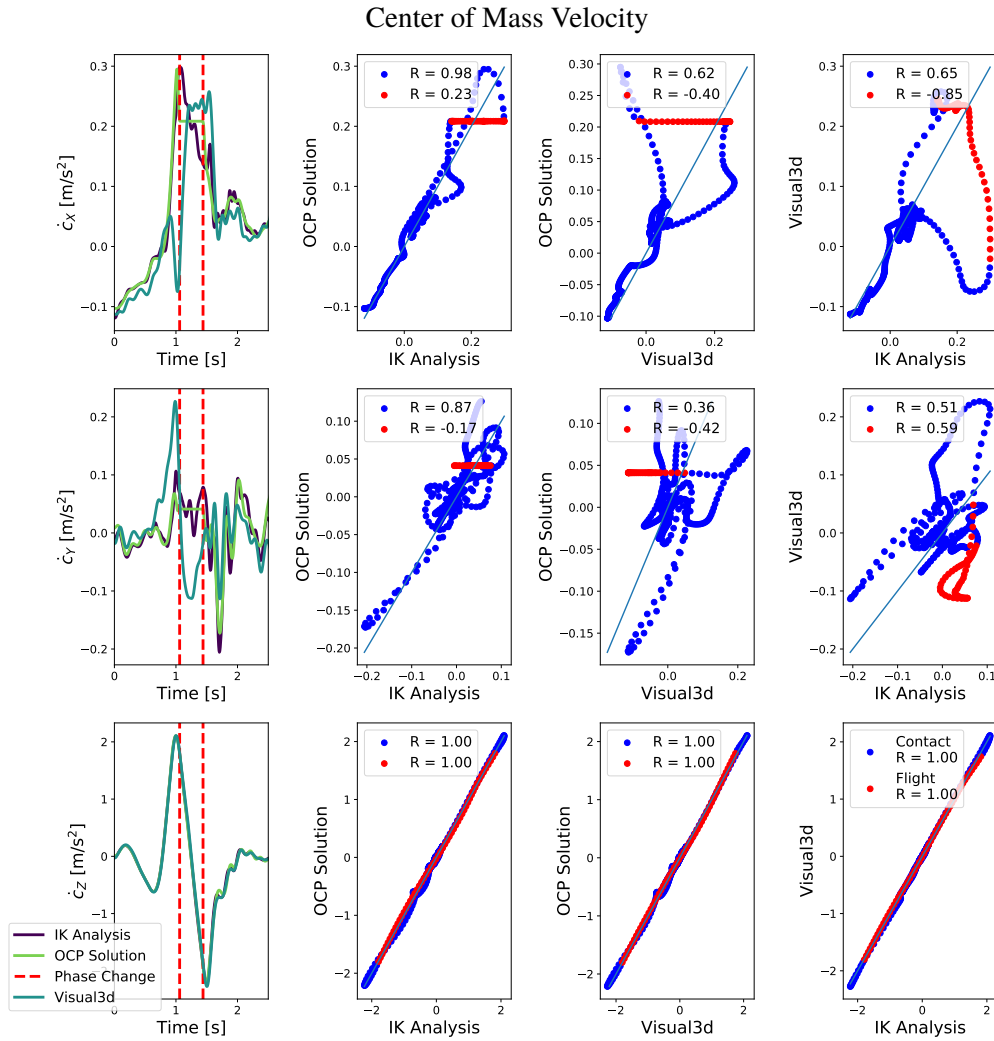


**Figure 11.6:** CoM velocity and scatter plots that compare the three methods. Contact phases are plotted in blue, the flight phase in red. We see good agreement in vertical direction and for the contact phases, when using the same model. Visual3d uses a different model and is not consistent with the other two methods. This suggests that the modeling error is larger than the measurement.

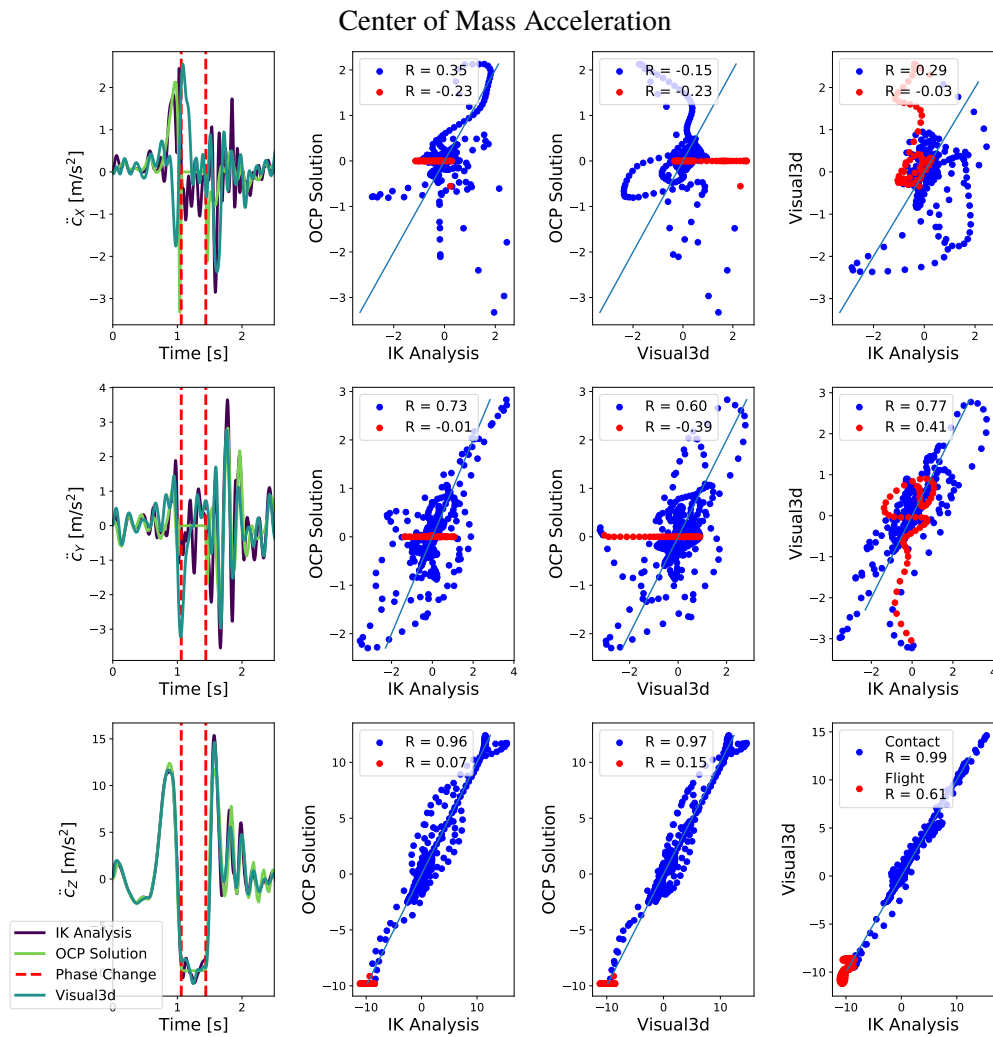


**Figure 11.7:** CoM acceleration and scatter plots that compare the three methods. Contact phases are plotted in blue, the flight phase in red. We see good agreement in vertical direction during the contact phases. The methods are not consistent during the flight phases and in horizontal direction, even when using the same model. A least squares fit on a frame by frame bases clearly violates Newton's EoM.

### Angular Momentum

Angular momentum is plotted in Figure 11.8. It should be conserved during the flight phase and the change should be equal to zero when no external torques are acting. Again, we observe the desired properties for the optimized motion. The other two methods show high variability during the flight phase and changes of up to 100% in the horizontal plane. Methods agree during the contact phases when there is less dynamic movement. The difference in mass distribution between the models becomes apparent in the bottom row. The Visual3d model shows significantly less momentum which suggests, that the mass of the arms is lower.

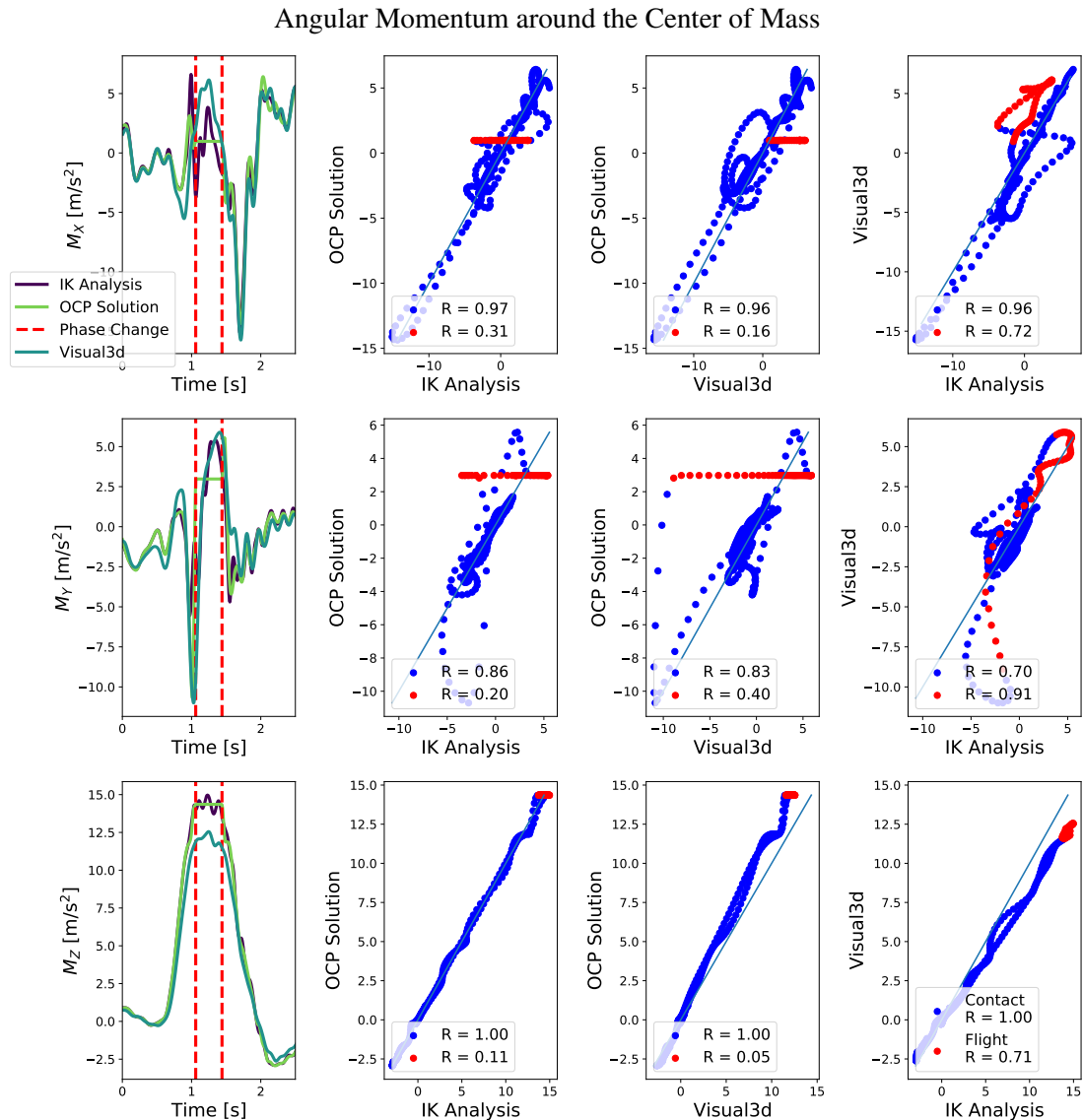


**Figure 11.8:** Angular Momentum during the motion. The main rotation takes place around the vertical Z-axis. Momentum conservation is violated during the flight phase, especially in around the horizontal axis.

When we analyze the change of angular momentum we see similarities to the CoM acceleration. We find high variability between the methods and only see agreement around the vertical axis for the contact phases, where the motion is smooth. Fast dynamic balancing in the horizontal plane leads to different results depending on the model and fitting method. The optimized motion is dynamically consistent during the flight phase.

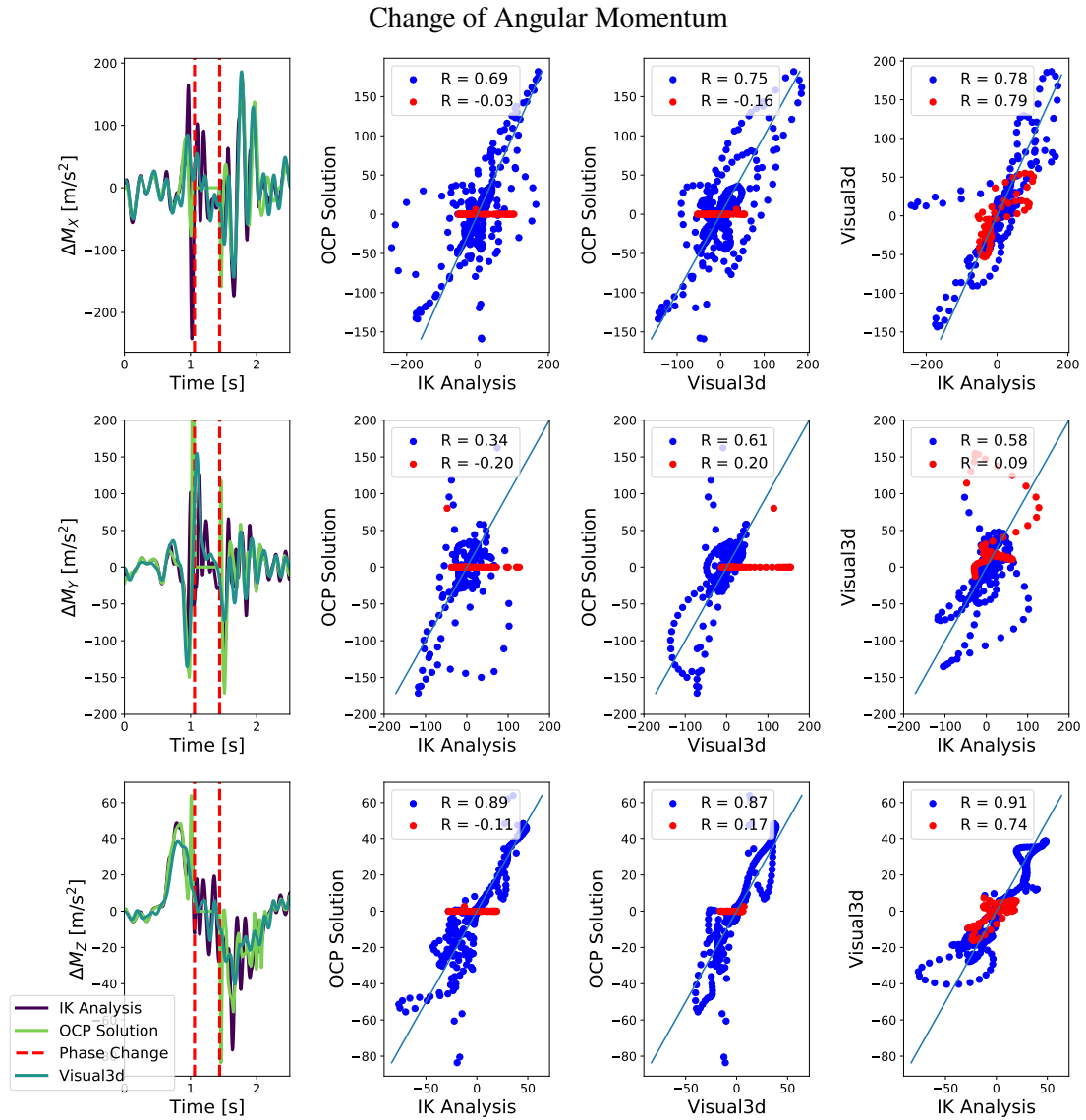


**Figure 11.9:** Change of angular momentum around the three axis. Methods only agree around the vertical axis, where the motion is smooth. For fast dynamic balancing in the horizontal plane results differ depending on the model and fitting method.

### Contact Dynamics

During the contact phases all external forces must add up to the CoM acceleration and all external torques must produce the change of angular momentum. This is plotted in Figure 11.10. On the left we plotted the contact forces of the slackline for each foot stacked on top of each other and the CoM acceleration times the subject mass as dashed line. We can see that they exactly match and that Equation 11.12 holds.

On the right we have the same result for the contact torques. The top right plot shows the resulting torques due to the contact forces as described on the right hand side of Equation 11.13. There are no contact torques around this axis and the change of angular momentum is solely based on the foot position and the contact forces. In the lower right plot the contact torque at the feet is plotted in green and the torque resulting from the forces in purple. We see that Equation 11.13 is satisfied throughout the motion. This shows that the optimization result follows Newton's EOM also during the contact phases.

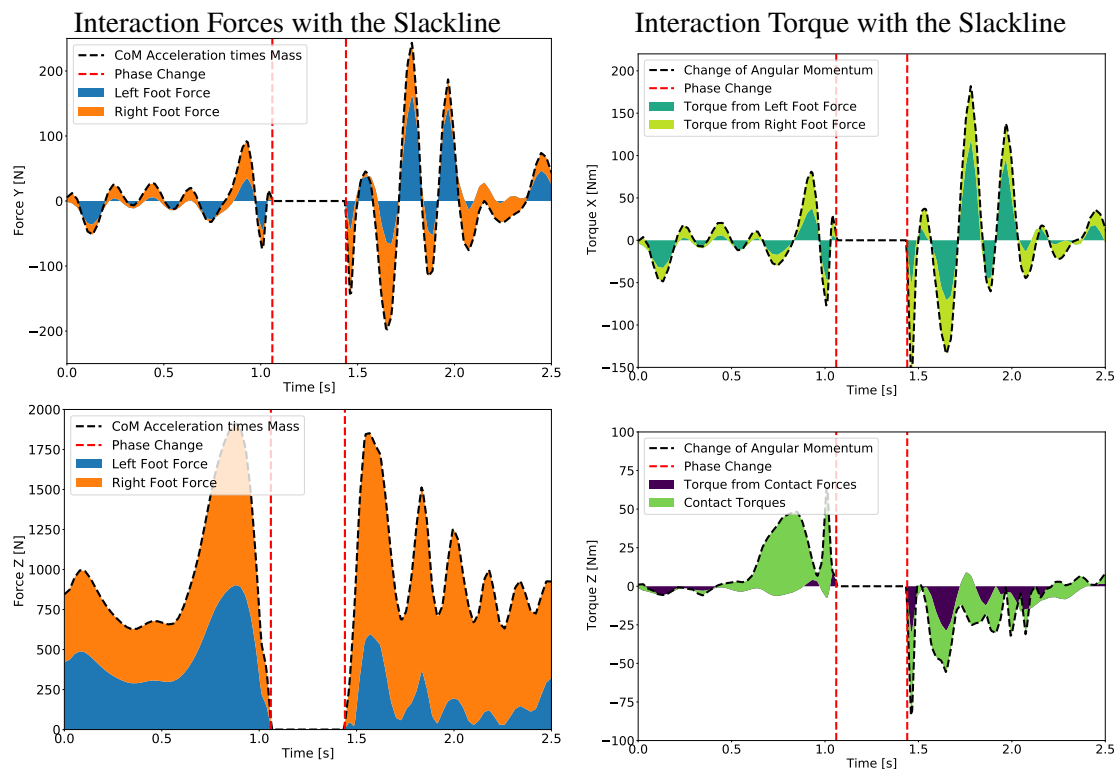


**Figure 11.10:** Left: Sum of contact forces and Center of Mass acceleration times subject mass. Right: Sum of contact torques and torques produced by the contact forces plotted against the change of angular momentum. Equation 11.12 and Equation 11.13 are satisfied throughout the motion.

### 11.3 Slackline Spring Model

By the time of this work, we found two papers that suggest control strategies of tightrope and slackline balancing by Paoletti et al. [86] and by Athanasiadis et al. [87]. They propose to model the slackline as a spring with the restoring force pointing towards the rest position.

However, their model is oversimplified as it does not take the whole range of motion of the slackline into account. They only consider the horizontal direction, when linearizing their model. In this section we want to further analyze the contact forces, model the slackline as a spring and compute the stiffness parameters for the horizontal and vertical direction. With the spring model we analyze the different phases of the jump motion.

#### 11.3.1 Stiffness Estimation

We estimate the stiffness of the slackline in vertical and in horizontal direction. In Figure 11.11 we plotted the mean height of the feet and the vertical contact force at the upper left. The mean horizontal position and horizontal force are plotted at the lower left. For both plots, the average foot position correlates with contact force as expected for a spring. Forces and amplitudes are small before the jump and larger when landing. The flight phase is indicated in red, when the feet are above the rest height of the slackline.

The right plots show the force plotted against the displacement for the corresponding direction. Larger amplitudes are observed in vertical direction. Here, we see an almost linear relationship. The main balancing happens with a deflection larger than 10 cm. Smaller values are only observed shortly before and after the jump. We fitted two linear functions that compute the stiffness in N/m for the two regions. The slackline has a low stiffness of  $\approx 5700$  N/m for the first 10 cm and then becomes stiffer for larger displacement ( $\approx 14\,600$  N/m). Based on this observation we define two regimes of low and high tension of the slackline. They are indicated for the two plots at the left in light green. The jump initiation and landing mainly happens in the high tension regime. Only few data points are available for the low tension part of the motion. Compared to the vertical direction the horizontal displacement is smaller and we are only able to compute meaningful results for the high tension part of the motion. The evaluation before and after the jump agree with a stiffness of  $\approx 4700$  N/m.

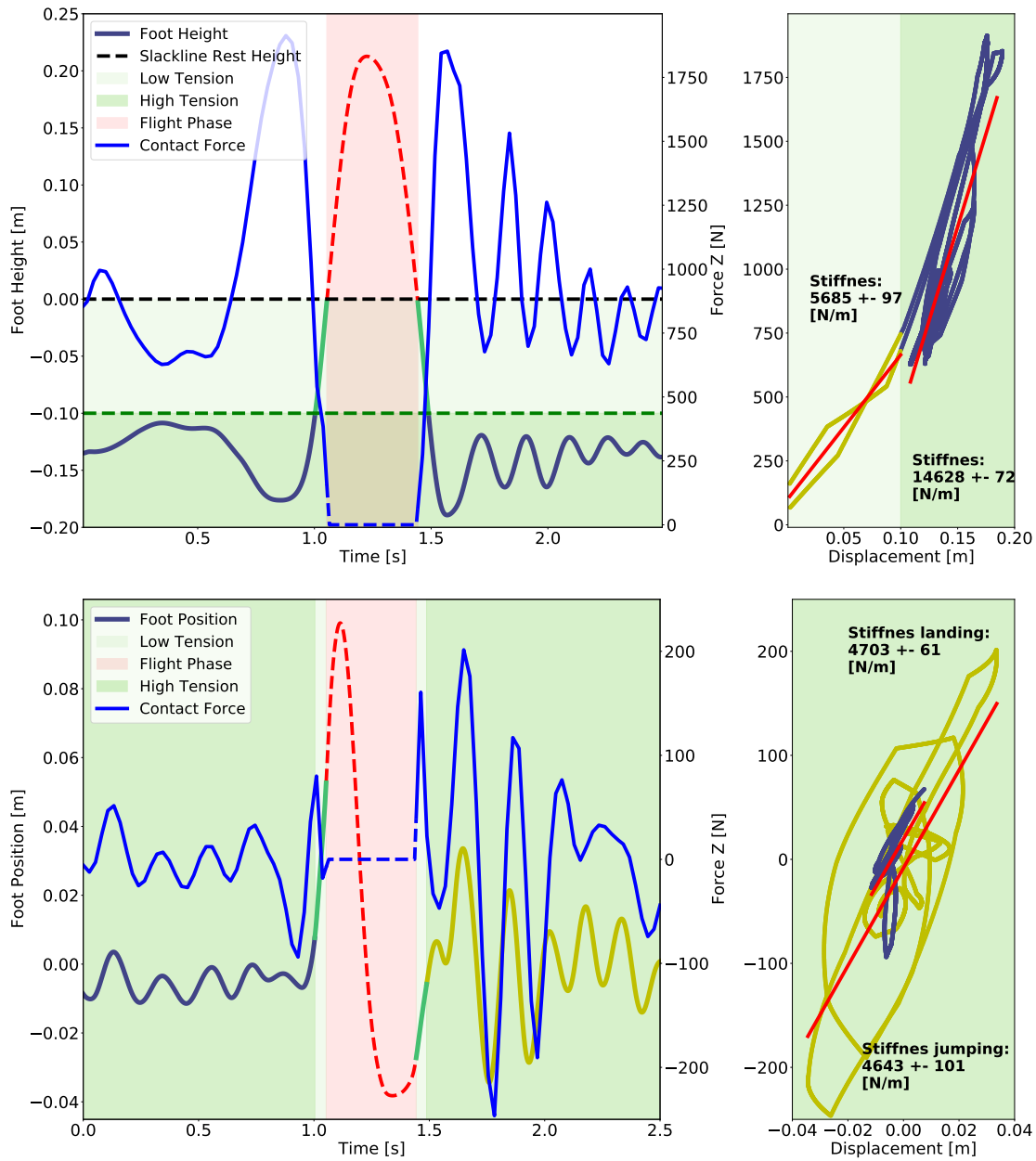


**Figure 11.11:** The top left plot shows the vertical contact force and mean height of the two feet. The lower left plot shows the vertical contact force and mean position of the two feet. The flight phase is indicated in red. The right plots show the force plotted over the displacement and linear fits that estimate the stiffness. We see that the slackline is loose for the first 10 cm of vertical deflection with a stiffness of  $\approx 5700$  N/m and then becomes stiffer for larger displacement. The high and low tension region are indicated in the plot at the left. We estimate the horizontal stiffness of  $\approx 4700$  N/m.

### 11.3.2 Interaction Analysis

Looking at feet positions in Figure 11.11 we see harmonic oscillation of the feet. The frequency  $f$  of an harmonic oscillator depends on the mass  $m$  and the stiffness  $D$  of the spring.

$$f = \frac{1}{2\pi} \sqrt{\frac{D}{m}} \quad (11.14)$$

We can estimate the frequency of the foot position movement for different phases of the motion. From this we can determine the mass that takes part in the oscillation by rearranging Equation 11.14 and using the previously obtained stiffness values:

$$m = \frac{D}{(2\pi f)^2} \quad (11.15)$$

Figure 11.12 shows the foot position throughout the motion. For the horizontal part before the jump and the last part of the landing we fitted the EoM of a damped harmonic oscillator to estimate the oscillation frequency. The amplitude  $A$  over time is given by:

$$A(t) = A_0 e^{-\beta t} \sin(\omega t + \phi_0) \quad (11.16)$$

In vertical direction the same function was used for the landing part. We adjusted the fit function for the initiation part of the jumping such that the amplitude increases over time.

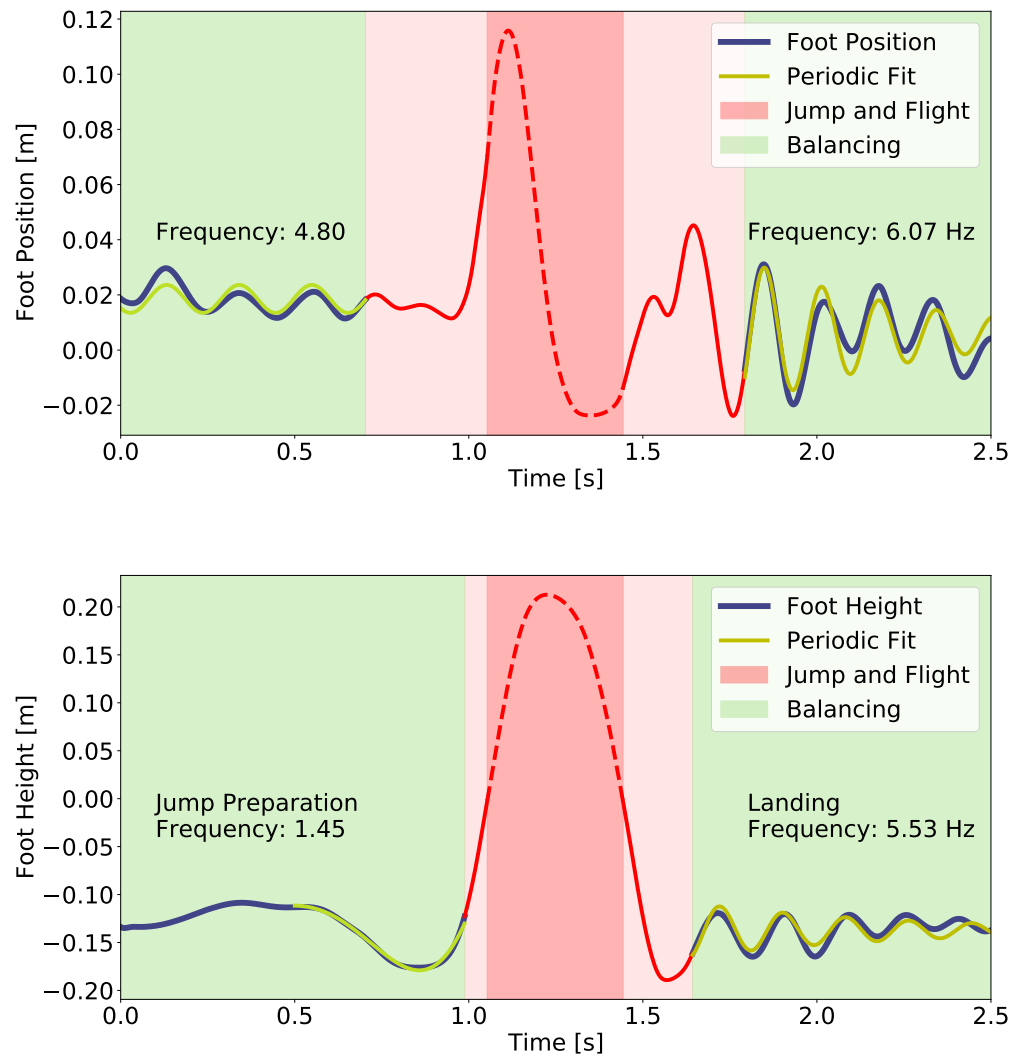
$$A(t) = A_0(1 + e^{\beta t}) \sin(\omega t + \phi_0) \quad (11.17)$$

Table 11.2 shows the four phases of the motion with the corresponding frequency, stiffness and the computed swinging mass. In horizontal direction we find a frequency of 4.8 Hz before and 6.1 Hz after the jump. Using Equation 11.15 we get a swinging mass 5.2 kg and 3.2 kg, respectively. Looking at the segment mass distribution in Table 11.1 we find that this corresponds to the mass of the feet and parts of the shank. This is plausible, since it is mainly the foot segment moving in this direction.

Before the jump, the subject is almost aligned to the slackline as can be seen in Figure 11.1. The foot and knee axis only allow movement in the perpendicular direction. Therefore, also the thighs are involved in the movement. Looking at the position when landing the jump, we see that the subject is turned  $90^\circ$  with respect to the slackline and can now absorb the oscillation in the knee joints.

For the landing, we find a frequency of 5.6 Hz in the vertical direction which corresponds to a swinging mass of 11.8 kg when considering the higher stiffness of the slackline in this direction. Again, this matches the segment weight of the feet and shank and parts of the thighs. The rotation takes place in the hip joint. In this direction the whole shank and foot segment move in up and down direction, therefore the swinging mass is larger than in sideways direction. In all three cases, the subject is clearly able to decouple the slackline motion from the upper body. The oscillation occurs passively without a driving force.

This is different before the jump, where the subject is actively putting energy into the slackline. We find a frequency of 1.5 Hz that corresponds to a swinging mass of 176 kg. This is consistent with the vertical force of about 1800 N.



**Figure 11.12:** Top: Feet position and with a periodic function fit. We find a frequency of 4.8 Hz before and 6.1 Hz after the jump. Bottom: We find a frequency of 1.5 Hz before and 5.5 Hz after the jump.

Phase and Direction	Stiffness [N/kg]	Frequency [Hz]	Swinging Mass [kg]
Horizontal Balancing	4700	4.8	5.2
Vertical Jump Initiation	14600	1.5	175.9
Horizontal Landing	4700	6.1	3.2
Vertical Landing	14600	5.5	12.1

**Table 11.2:** The table shows the four phases of the motion with the corresponding frequency, stiffness and the computed swinging mass.

## **11.4 Discussion**

We formulated and solved an OCP that allows us to reconstruct dynamic slackline jumping motions. The previously derived contact model from interaction measurements was successfully implemented and we were able to obtain meaningful and interpretable results for the slackline interaction forces. We implemented a multi-phase and a single-phase formulation leading to almost equivalent results.

When comparing the OCP method to two inverse kinematics based analysis, we found that the resulting motions have similar fitting error to the markers. The optimized motion is dynamically consistent following Newton's EoM, whereas the two other movement reconstructions show large variations and violate Newton's EoM. The advantage of the OCP approach becomes apparent during the flight phase of the motion and when comparing the CoM and angular momentum dynamics. We found variations of up to 30 % for the conventional method.

Due to numeric complexity and the high amount of variables necessary to formulate the OCP, this method is limited to a few seconds of motion. This might limit the application to compare longer slackline motions of beginners and experts as initially intended. However, we can apply it to interesting parts of motion and analyze specific movements connected to balance recovery. For example, we were able to reconstruct the variable stiffness of the slackline in the different directions and show that the subject is modulating the compliance of the stance leg to initiate the jump.

## 12 Summary and Outlook

In this work we analyzed human balancing in static and dynamic balance tasks based on motion capture data. For evaluation of static balance, we designed a static balance test consisting of five different standing configurations: parallel stance, single leg stance on each leg, and tandem stance with each leg in front. All configurations were performed for 30 s with eyes open and 30 s with eyes closed and CoP data was collected using force plates. The data was analyzed by means of existing performance metrics from the literature. Since we found high correlation between many of the metrics, we decided to evaluate sway distance, velocity and frequency in ML and AP direction as well as the ratio between the sway in both directions. Analysis of dynamic balance was based on slackline balancing and the tandem walk test. We gathered data from over 60 participants in two studies.

Participants of the slackline study performed the static balance test and slackline balancing on one leg and walking. We analyzed beginners that had never balanced on a slackline before and compared them to professional slackline athletes. As a first result we found that trained slackliners also performed very well in the static balance test, whereas the beginner group showed a larger variance in the time they managed to balance. We therefore decided to divide the beginner group into a balance-experienced, sportive group that performed similarly to the professional group and a balance-inexperienced, beginner group using the static balance test. By comparing the balance times for each task with the professional group, we defined a threshold of 260 s of total time in the static balance test as the cutoff. Single leg balancing with eyes closed was the task in which the beginner group showed the largest variation. It was successfully performed by 80 % of the professional group. Comparing the average time per beginner subject on the slackline during their first session to the time in balance during the eyes closed single leg balance of the balance test we found large correlation, suggesting that slackline performance can be predicted by this task.

We then defined performance indicators for slackline balancing and analyzed over 300 balancing trials of 20 participants. Normalized angular momentum or CoM acceleration allow us to quantify how stable and controlled a subject is while balancing and how many recovery (arm) movements occur. We found a clear progression from large values of the beginner group to consistently small values in the professional group. Posture and movement were similar for the beginner and sportive beginner groups. Professional slackliners consistently maintain a horizontal head orientation, also during walking, whereas beginners either struggle to maintain upright posture or need to look down to secure foot placement.

Furthermore, professionals have a mean shoulder angle of  $90^\circ$ , that maximizes their inertia in the frontal plane and maintain straightened elbows. Beginners tend to align their upper arms more and show bent elbow angles. For single leg balancing professionals are able to balance in a greater variation of poses using a greater part of their shoulder and elbow range of motion. We found that overall, their hand movement is more coordinated when computing a rolling window correlation

between the absolute velocity of the hands. Differences were found in the interaction with the slackline by means of stance foot acceleration. In horizontal direction professional slackliners show reduced values confirming findings in the literature of adjusted muscle reflexes. In vertical direction the sportive group and the professional group show reduced values when compared to short beginner trials. Both findings suggest, that control of the stance foot acceleration is a key factor to successful slackline balancing.

In the study of the "Schizophrenia and the Moving Body" project we compared the balance capabilities of the experimental group consisting of persons with schizophrenia against a healthy control group. Participants performed the static balance test and twice the tandem walk, once with eyes open and once with eyes closed. For the static balance test we found that the experimental group was not able to balance as well as the control group showing a significantly lower success rate and time in balance for all tasks with eyes open and eyes closed. Further analysis of force plate data of successful trials revealed a larger ML CoP sway during all tasks for the experimental group. For the tandem walk test groups performed equally well with eyes open. Analyzing the quality of task execution by means of success rate, step accuracy and recovery steps did not show a difference.

The situation was different for the eyes closed tandem walk. Here, the experimental group took significantly more recovery steps, placed steps more inaccurately and only 25 % managed to perform the required number of steps without losing balance, compared to 75 % of the control group. When analyzing the strategy employed by the two groups, we found that 40 % of the control group successfully used their arms to balance and place correct steps. The experimental group used this balance strategy significantly less and mainly relied on recovery steps. When applying the balance performance indicators, we found significant differences in sideways and vertical CoM acceleration and sideways ZMP sway, suggesting that the experimental group is less stable during both tandem walks. Increased normalized angular momentum in the frontal plane during the eyes open walk shows that they perform balance related movements and are not able to maintain an upright posture. We found increased variation of sideways pelvis tilt and more variable frontal shoulder angle.

We then compared the static balance test for all participants of both studies. They were divided into the experimental group, a balance-experienced and a balance-inexperienced group using the 260 s threshold. Again, the balance task with the largest variance was the single leg stance with eyes closed. We analyzed the CoP data and found, similar to the analysis in the "Schizophrenia and the Moving Body" study, that sway distance in the ML is an indicator for more stable balancing. We see a clear progression from the experimental group to the balance-experienced group. Further, the balance-experienced group showed reduced AP sway velocity compared to the other groups. We conclude that these two parameters are suitable to measure stability in static balance using force plate data.

Further, we compared flat ground tandem walking to slackline walking based on the balance performance indicators. For normalized angular momentum and CoM acceleration we found that professional slackline athletes are able to reduce most of the values to the range of regular tandem walking. They only show larger normalized angular momentum in the frontal plane and increased sideways CoM acceleration, which are both a direct consequence of the instability introduced by the slackline. Movement outside the frontal plane is not affected. Further, we found that their pose

---

and movement strategy is specific to slackline balancing and not used by other participants neither in tandem walking nor slackline walking of beginners.

In the last part of this thesis we prototyped a pressure sensor for the slackline and showed that we can reliably measure CoP data. Based on the findings we developed a contact interaction model specific to slackline balancing. Different to a regular foot contact, the CoP position is constrained to a single line determined by the direction of the slackline and the number of possible contact torques is reduced by the tilting of the freely rotating slackline band. We used this contact model inside an optimal control problem formulation to perform a fully dynamic reconstruction of slackline jumping. As a result of this optimization based analysis, we obtained joint torques of the subject and all interaction forces between the feet and the slackline. We were able to reconstruct the stiffness of the slackline and set up a spring model. From this model we computed the swing mass of the system and found that the slackline athletes actively modulated the stance leg compliance to balance the jump.

Based on the slackline balance research presented in this work there are many possible future studies. The balance indicators for slackline balancing are by no means complete and different metrics can reveal additional skills that allow professional athletes to balance. The effect of balance training has also not been analyzed. It is interesting to understand how the performance indicators change over the course of a training program. So far, the pressure sensor for the slackline was only validated. A study that involves measurements of beginners and experts is yet to be done. The optimal control-based analysis was only applied to one motion so far. Thorough analysis of different jumping motions and the analysis of specific recovery movements based on the method is now possible. One could analyze and compare the efficiency of different recovery movements and compute optimal strategies.

In interdisciplinary collaboration we showed that research on schizophrenia can greatly benefit from objective measures and motion analysis. Many findings support the disembodiment approach. Application of balance and movement parameters on other motions can further improve our understanding of the disease. The evaluation of gait data was not part of this work and results will be published in the near future in collaboration with Lily Martin.



# A Appendix

## A.1 List of Figures

1.1	Slackline balancing. . . . .	16
3.1	Motion Capture Equipment . . . . .	27
3.2	The three video mods of the Qualisys Oqus 500 cameras. . . . .	28
3.3	Marker position reconstruction. . . . .	29
3.4	The front of the upper body part of the marker set. . . . .	30
3.5	The back and leg part of the marker set . . . . .	31
3.6	IMU measurement schematic . . . . .	32
3.7	The Xsens model and the IMU placement. . . . .	32
3.8	The subject with markers and Xsens IMU sensors. . . . .	36
3.9	Foot height during walking on a slackline and on flat ground. . . . .	38
3.10	Foot position for standing on a slackline and on flat ground. . . . .	39
3.11	Foot position during tandem walking on flat ground. . . . .	40
3.12	Schematic of a force plate. . . . .	41
3.13	Moticon Pressure Soles. . . . .	42
4.1	A generic rigid body model of a human. . . . .	43
4.2	The model with joint positions and DoF. . . . .	45
4.3	The static marker recording and the subject-specific model. . . . .	46
6.1	Overview of the Static Balance Test . . . . .	61
6.2	The inverted pendulum model. . . . .	67
6.3	Correlation between stability metrics. . . . .	68
6.4	Sample measurements and evaluation. . . . .	69
7.1	Overview of the Slackline Study . . . . .	71
7.2	Slackline Study Setup . . . . .	72
7.3	The Gibbon Slack Rack 300 . . . . .	73
7.4	Time in balance during the static balance test for the slackline study. . . . .	74
7.5	Scatter plot of balance time on the slackline and during the balance test. . . . .	75
7.6	Illustration of CoM movement and average angular velocity. . . . .	79
7.7	Moving window correlation as a measure for hand coordination . . . . .	81
7.8	Time in balance for single leg slackline balancing. . . . .	84
7.9	Mean posture during slackline balancing . . . . .	85
7.10	Comparison of head orientation, frontal shoulder angle and elbow angle. . . . .	86
7.11	Utilized range of motion for frontal shoulder angle and elbow joint. . . . .	87
7.12	Comparison of movement coordination . . . . .	88

7.13	Normalized angular momentum around the three coordinate axis. . . . .	90
7.14	Comparison of stance foot acceleration . . . . .	92
7.15	Comparison of Center of Mass acceleration. . . . .	93
7.16	Comparison of stance leg knee angle variation. . . . .	94
7.17	Comparison of static balance. . . . .	95
7.18	Time in balance for walking on the slackline. . . . .	97
7.19	Comparison of head orientation, frontal shoulder angle and elbow angle. . . . .	99
7.20	Utilized range of motion of shoulder and elbow joint in the frontal plane. . . . .	100
7.21	Comparison of movement coordination . . . . .	101
7.22	Comparison of walking speed, kinetic energy and balance energy ratio. . . . .	101
7.23	Average angular velocity around the three coordinate axis. . . . .	103
7.24	Comparison of Center of Mass Acceleration during Slackline Walking . . . . .	104
7.25	Center of Mass Acceleration for stable and unstable balancing . . . . .	107
7.26	Normalized angular momentum for stable and unstable walking . . . . .	108
7.27	Center of Mass projection and stance foot acceleration . . . . .	108
8.1	Overview of the Balance Study in the "Schizophrenia and the Moving Body" project	111
8.2	Balance Test Success Rate Comparison between Experimental and Control Group	114
8.3	Balance Test Comparison: Time in Balance . . . . .	115
8.4	RDIST and RATIO evaluation of CoP data . . . . .	118
8.5	MVEL and MFREQ evaluation of CoP data . . . . .	119
8.6	Example KPI . . . . .	125
8.7	Illustration of CoM movement and normalized angular momentum. . . . .	125
8.8	Additional steps and step accuracy during tandem walk. . . . .	130
8.9	Standard deviation of CoM acceleration for tandem walking . . . . .	131
8.10	Standard deviation of ZMP position for tandem walking . . . . .	132
8.11	Standard deviation of normalized angular momentum for tandem walking . . . . .	133
8.12	Utilized range of motion of the shoulder joint. . . . .	134
8.13	Quantification of motion of the pelvis. . . . .	134
8.14	Balance strategy during the tandem walk. . . . .	135
8.15	Mean posture for tandem walking. . . . .	137
8.16	Movement range for tandem walking. . . . .	138
8.17	Shoulder angles for successful tandem walking. . . . .	138
8.18	Walking speed during the tandem walk. . . . .	139
8.19	Scatter plot with linear regression for MFREQ and PANSS scores. . . . .	143
8.20	Scatter plot with linear regression for MFREQ and PANSS scores. . . . .	144
9.1	Chapter overview: Comparison of results between the studies. . . . .	147
9.2	Time in Balance for all participants. . . . .	149
9.3	Sway distance in ML direction and velocity in AP direction . . . . .	150
9.4	Normalized angular momentum for tandem and slackline walking. . . . .	152
9.5	Center of Mass acceleration for tandem and slackline walking. . . . .	153
9.6	Walking speed, normalized kinetic energy and energy ratio for tandem and slackline walking. . . . .	154
9.7	Joint angle variation of elbow, frontal shoulder and knee joint. . . . .	155

9.8	Comparison of head orientation, elbow and shoulder angle. . . . .	156
9.9	Comparison of hand coordination. . . . .	157
10.1	Pressure Sensor Matrix. . . . .	162
10.2	Foot measurement on the Pressure Sensor Matrix . . . . .	162
10.3	Synchronized CoP measurements on the force plate. . . . .	164
10.4	The matrix sensor layout mounted on the slackline . . . . .	165
10.5	Synchronized CoP measurements on the slackline . . . . .	166
10.6	Slackline CoP measurements: Scatter and Bland-Altman for system comparison. . . . .	166
10.7	Center of Pressure recording of different single leg balancing tasks. . . . .	167
11.1	Dynamic reconstruction of a jumping motion with rotation on the slackline. . . . .	169
11.2	The coordinate system of the study. . . . .	170
11.3	Phase time estimation for the optimal control problem. . . . .	172
11.4	Marker residuum for the optimal control problem based analysis . . . . .	174
11.5	Center of mass acceleration position for the three methods. . . . .	176
11.6	Center of mass velocity comparison for the three methods. . . . .	177
11.7	Center of mass acceleration comparison for the three methods. . . . .	178
11.8	Angular momentum comparison for the three methods. . . . .	179
11.9	Change of angular momentum comparison for the three methods. . . . .	180
11.10	Computed contact forces and contact torques. . . . .	181
11.11	Stiffness estimation of the slackline in vertical and horizontal direction. . . . .	183
11.12	Feet position and with a periodic function fit. . . . .	185

## A.2 List of Tables

3.1	Body measurements of Xsens. . . . .	33
3.2	Comparison of the two motion capture systems. . . . .	35
3.3	Measurement difference for position and orientation between Qualisys and Xsens. . . . .	37
4.1	Definition of segment lengths. . . . .	44
4.2	Definition of joint center locations. . . . .	45
5.1	Comparison of motion analysis approaches. . . . .	58
6.1	Possible outcomes of a balance task . . . . .	63
6.2	CoP Distance Measures . . . . .	65
6.3	CoP Frequency Measures . . . . .	66
7.1	Overview of study participants . . . . .	76
7.2	Summary of all Performance Indicators for Single Leg Balancing . . . . .	96
7.3	Summary of all Performance Indicators for Slackline Walking . . . . .	105
8.1	Demographic and clinical data of all participants. . . . .	112
8.2	Balance test success rate for Experimental and Control. . . . .	114
8.3	Summary and statistics for visual evaluation of the balance test . . . . .	116

8.4	RDIST and RATIO evaluation of CoP data . . . . .	120
8.5	MVEL and MFREQ evaluation of CoP data . . . . .	121
8.6	Static balance test evaluation for changing eye condition. . . . .	122
8.7	Effect of change in eye condition on CoP parameters during parallel stance. . . . .	122
8.8	Tandem walk quality evaluation for Experimental and Control. . . . .	129
8.9	Tandem Walk Summary - Eyes Open . . . . .	141
8.10	Tandem Walk Summary - Eyes Closed . . . . .	142
8.11	Correlation between PANSS and ML sway frequency. . . . .	143
8.12	Correlation between PANSS and Tandem Walk Parameters. . . . .	144
9.1	Overview of balance data measurements . . . . .	148
9.2	Kruskal-Wallis-Test for all CoP Variables . . . . .	149
11.1	Details of the subject specific model. . . . .	170

### A.3 List of Acronyms

<b>AP</b>	Anterior-Posterior . . . . .	62
<b>BMI</b>	Body Mass Index . . . . .	22
<b>CoM</b>	Center of Mass . . . . .	8
<b>CoP</b>	Center of Pressure . . . . .	xii
<b>CP</b>	Capture Point . . . . .	9
<b>DoF</b>	Degrees of Freedom . . . . .	10
<b>EASE</b>	Examination of Self-Experience . . . . .	21
<b>EoM</b>	Equations of Motion . . . . .	54
<b>EPS</b>	Extrapyramidal symptoms . . . . .	21
<b>FD</b>	Fractal Dimension . . . . .	66
<b>GRF</b>	Ground Reaction Forces . . . . .	9
<b>HCMR</b>	Heidelberg Center for Motion Research . . . . .	1
<b>IMU</b>	Inertial Measurement Unit . . . . .	27
<b>IVP</b>	Initial Value Problem . . . . .	56
<b>MDIST</b>	Mean Absolute Distance . . . . .	64
<b>MFREQ</b>	Mean Frequency . . . . .	66
<b>MVEL</b>	Mean Velocity . . . . .	64
<b>ML</b>	Medial-Lateral . . . . .	62
<b>NLP</b>	Nonlinear Program . . . . .	55
<b>NSS</b>	Neurological Soft Signs . . . . .	20
<b>OCP</b>	Optimal Control Problem . . . . .	54

<b>ODE</b>	Ordinary Differential Equations .....	54
<b>OPZ</b>	Olanzapine Equivalents .....	23
<b>PANSS</b>	Positive and Negative Syndrome Scale.....	xii
<b>QP</b>	Quadratic Programming.....	57
<b>PSM</b>	Pressure Sensor Matrix .....	161
<b>RBDL</b>	Rigid Body Dynamics Library .....	49
<b>RDIST</b>	Standard Deviation of the Trajectory .....	64
<b>RD</b>	Resultant Distance.....	64
<b>SQP</b>	Sequential Quadratic Programming.....	55
<b>TOTEX</b>	Total Excursion .....	64
<b>VOR</b>	Vestibulo-Ocular Reflex .....	7
<b>VPP</b>	Virtual Pivot Point.....	9
<b>xCoM</b>	Extrapolated Center of Mass.....	9
<b>ZMP</b>	Zero Moment Point .....	9
<b>ZRAM</b>	Zero Rate of Change of Angular Momentum .....	10

## A.4 Code

```
#!/usr/bin/python

import numpy as np
import c3d
from numpy.linalg import norm as norm

# based on subject height and weight
def calcSegLen(filename, directory, height, weight):
    reader = c3d.Reader(open(filename, 'rb'))
    labels = [s.strip() for s in reader.point_labels]

    #Define Variables
    Height = float(height)/100
    Weight = float(weight)
    Foot_R = 0
    Foot_L = 0
    Thigh_R = 0
    Thigh_L = 0
    Shank_L = 0
    Shank_R = 0
    MiddleTrunk = 0
    UpperTrunk = 0
    UpperArm_L = 0
    UpperArm_R = 0
    LowerArm_L = 0
    LowerArm_R = 0
    Hand_R = 0
    Hand_L = 0
    Head = 0
    Pelvis = 0
    AsisDist = 0

    #Calculate Pelvis Dist and Shoulder Width by averaging over all frames
    j = 0
    for i, p, analog in reader.read_frames():
        j = j+1
        points = {s:p[labels.index(s)] for s in labels}
        AsisDist += norm((points['R_IAS'] - points['L_IAS'])[0:3])
        L5 += points['LV5'][2] - 0.5*(points['R_IAS'][2] + points['L_IAS'][2])
        ShoulderWidth += norm((points['R_SAE'] - points['L_SAE'])[0:3])

    #Normalize by number of frames
```

```

L5 = L5/j
ShoulderWidth = ShoulderWidth / j
AsisDist = AsisDist / j
#Pelvis Model
Pelvis = L5 + 0.3 * AsisDist

#Same for all other segments
j = 0
for i, p, analog in reader.read_frames():
    points = {s:p[labels.index(s)] for s in labels}

    #Shoulder Joint
    S_offset = norm((points['CV7'] - 0.5*(points['R_SAE'] + points['L_SAE'])))[2]) + 0.17*ShoulderWidth
    ShoulderNeckOffset += S_offset

    Foot_R += 5 / 4 * norm((points['R_FCC'] - points['R_FM1'])[0:3])
    Foot_L += 5 / 4 * norm((points['L_FCC'] - points['L_FM1'])[0:3])

    MiddleTrunk += norm((points['MAI'] - points['LV5'])[2])
    UpperTrunk += norm((points['MAI'] - points['CV7'])[2])

    Thigh_R += norm((points['LV5'] - points['R_FLE'])[2]) - Pelvis
    Thigh_L += norm((points['LV5'] - points['L_FLE'])[2]) - Pelvis
    Shank_L += norm((points['R_FAL'] - points['R_FLE'])[0:3])
    Shank_R += norm((points['L_FAL'] - points['L_FLE'])[0:3])

    #Distance to Shoulder Joint
    UpperArm_L += norm((points['L_SAE'] - points['L_HLE'])[0:3]) - 0.17*ShoulderWidth
    UpperArm_R += norm((points['R_SAE'] - points['R_HLE'])[0:3]) - 0.17*ShoulderWidth

    LowerArm_L += norm((points['L_HLE'] - points['L_USP'])[0:3])
    LowerArm_R += norm((points['R_HLE'] - points['R_USP'])[0:3])
    Hand_R += 2*norm((points['R_HM2'] - points['R_RSP'])[0:3])
    Hand_L += 2*norm((points['L_HM2'] - points['L_RSP'])[0:3])
    Head += Height * 1000 - points['CV7'][2]
    j = j + 1

#Normalize by number of frames and convert into meter (c3d in mm)
normalize = 1000 * j

#Save to file
f = open(directory + "/SegmentLengths.txt", "w")
f.write('Pelvis, ' + str(Pelvis / 1000) + "\n")
f.write('Thigh_R, ' + str(Thigh_R / normalize) + "\n")
f.write('Thigh_L, ' + str(Thigh_L / normalize) + "\n")
f.write('Shank_R, ' + str(Shank_R / normalize) + "\n")
f.write('Shank_L, ' + str(Shank_L / normalize) + "\n")
f.write('Foot_R, ' + str(Foot_R / normalize) + "\n")
f.write('Foot_L, ' + str(Foot_L / normalize) + "\n")
f.write('MiddleTrunk, ' + str(MiddleTrunk / normalize) + "\n")
f.write('UpperTrunk, ' + str(UpperTrunk / normalize) + "\n")
f.write('UpperArm_R, ' + str(UpperArm_R / normalize) + "\n")
f.write('UpperArm_L, ' + str(UpperArm_L / normalize) + "\n")
f.write('LowerArm_R, ' + str(LowerArm_R / normalize) + "\n")
f.write('LowerArm_L, ' + str(LowerArm_L / normalize) + "\n")
f.write('Hand_R, ' + str(Hand_R / normalize) + "\n")
f.write('Hand_L, ' + str(Hand / normalize) + "\n")
f.write('Head, ' + str(Head / normalize) + "\n")
f.close()

```

Listing A.1: Python Code that calculates the segment length from the static c3d file

```

#!/usr/bin/python

import numpy as np
import c3d
from numpy.linalg import norm as norm

# based on subject height and weight
def calcAntro(filename, directory, height, weight):
    reader = c3d.Reader(open(filename, 'rb'))

    labels = [s.strip() for s in reader.point_labels]

    #Define Variables
    Height = float(height)/100
    Weight = float(weight)
    ShoulderWidth = 0
    ShoulderNeckOffset = 0
    HipCenterWidth = 0
    FootWidth_R = 0
    FootWidth_L = 0
    AnkleHeight_L = 0
    AnkleHeight_R = 0
    KneeDist_R = 0
    KneeDist_L = 0
    AnkleDist_R = 0
    AnkleDist_L = 0
    ElbowDist_R = 0
    ElbowDist_L = 0
    AsisDist = 0

    j = 0
    for i, p, analog in reader.read_frames():
        j = j+1
        points = {s:p[labels.index(s)] for s in labels}
        AsisDist += norm((points['R_IAS'] - points['L_IAS'])[0:3])
        ShoulderWidth += norm((points['R_SAE'] - points['L_SAE'])[0:3])

    ShoulderWidth = ShoulderWidth / j
    AsisDist = AsisDist / j
    Pelvis = L5 + 0.3 * AsisDist

    j = 0
    for i, p, analog in reader.read_frames():
        points = {s:p[labels.index(s)] for s in labels}
        S_offset = norm((points['CV7'] - 0.5*(points['R_SAE'] + points['L_SAE']))[2]) + 0.17*ShoulderWidth

    #Shoulder Joints
    ShoulderNeckOffset += S_offset

    FootWidth_R += norm((points['R_FM5'] - points['R_FM1'])[0:3])
    FootWidth_L += norm((points['L_FM5'] - points['L_FM1'])[0:3])

    KneeDist_R += norm((points['R_FME'] - points['R_FLE'])[0:3])
    KneeDist_L += norm((points['L_FME'] - points['L_FLE'])[0:3])
    AnkleDist_R += norm((points['R_FAL'] - points['R_TAM'])[0:3])
    AnkleDist_L += norm((points['L_FAL'] - points['L_TAM'])[0:3])
    ElbowDist_R += norm((points['R_USP'] - points['R_RSP'])[0:3])
    ElbowDist_L += norm((points['L_USP'] - points['L_RSP'])[0:3])

    AnkleHeight_L += (points['L_FAL'])[2]
    AnkleHeight_R += (points['R_FAL'])[2]
    j = j + 1

#Normalize by number of frames and convert into meter (c3d in mm)
normalize = 1000 * j

#Average left/right
FootWidth = (FootWidth_R + FootWidth_L)/2.
AnkleHeight = (AnkleHeight_L + AnkleHeight_R)/2
KneeDist = (KneeDist_R + KneeDist_L)/2
AnkleDist = (AnkleDist_R + AnkleDist_L)/2
ElbowDist = (ElbowDist_R + ElbowDist_L)/2
WristDist = (ElbowDist);

#Save to file
g = open(directory + "/Anthropometry.txt", "w")
g.write('Height, ' + str(Height) + "\n")
g.write('Weight, ' + str(Weight) + "\n")
g.write('ShoulderWidth, ' + str(ShoulderWidth / 1000) + "\n")
g.write('ShoulderNeckOffset, ' + str(ShoulderNeckOffset / normalize) + "\n")
g.write('HipCenterWidth, ' + str(AsisDist / 1000) + "\n")
g.write('FootWidth, ' + str(FootWidth / normalize) + "\n")
g.write('AnkleHeight, ' + str(AnkleHeight / normalize) + "\n")
g.write('KneeDist, ' + str(KneeDist / normalize) + "\n")
g.write('AnkleDist, ' + str(AnkleDist / normalize) + "\n")

```

## A Appendix

```
g.write('ElbowDist, ' + str(ElbowDist / normalize) + "\n")
g.write('WristDist, ' + str(WristDist / normalize) + "\n")
g.close()
```

**Listing A.2:** Python Code that calculates the antropomorphy from the static c3d file

```
Vector3d calcOmega(Model& model, const VectorNd& Q, const VectorNd& QDot)
{
    // Variables
    double mass = 0, mi = 0, rTr = 0;
    unsigned int i = 0;

    //3d Quantities
    Vector3d r_c = Vector3dZero; //CoM pos
    Vector3d H_c = Vector3dZero; //CoM local angular momentum
    Vector3d r_ci = Vector3dZero; //body to CoM vector
    Vector3d w_c = Vector3dZero; //avg angular velocity
    Vector3d riCi = Vector3dZero;
    Matrix3d J_c = Matrix3dZero; //CoM inertia
    Matrix3d J_ci = Matrix3dZero; //body com inertia
    Matrix3d J_i = Matrix3dZero; //body inertia
    Matrix3d R_i = Matrix3dZero; //body rotation

    //compute CoM position and velocity and angular momentum with RBDL function
    UpdateKinematics(model,Q,QDot,VectorNd::Zero(model.dof_count));
    RigidBodyDynamics::Utils::CalcCenterOfMass(model, Q, QDot, NULL, mass, r_c, NULL, NULL, &H_c);

    //compute total interia around CoM and
    for(std::map<std::string, unsigned int>::iterator it=model.mBodyNameMap.begin();
        it != model.mBodyNameMap.end(); it++){
        i = it->second;

        if (model.IsFixedBodyId(i)){
            continue;
        }
        else{
            mi = model.mBodies[i].mMass;
            riCi = model.mBodies[i].mCenterOfMass;
            J_i = model.mBodies[i].mInertia;
        }

        r_ci = CalcBodyToBaseCoordinates(model,Q,i,riCi,false) - r_c;
        R_i = CalcBodyWorldOrientation(model,Q,i,false).transpose();

        rTr = r_ci.transpose() * r_ci;
        Matrix3d rrT = r_ci * r_ci.transpose();
        Matrix3d ji0 = R_i * J_i * R_i.transpose();
        J_ci = (ji0 + mi * (rTr * Matrix3dIdentity - rrT));
        J_c += J_ci;
    }
    //avg angular velocity
    w_c = J_c.inverse()*H_c;

    return w_c;
}
```

**Listing A.3:** RBDL Code for calculation of the average angular velocity

```

Matrix3d calcTotalInertia(Model& model, const VectorNd& Q)
{
    // variables
    double mass = 0, mi = 0, rTr = 0;
    unsigned int i = 0;

    //3d Quantities
    Vector3d r_c = Vector3dZero; //CoM pos
    Vector3d r_ci = Vector3dZero; //body to CoM vector
    Vector3d riCi = Vector3dZero;
    Matrix3d J_c = Matrix3dZero; //CoM inertia
    Matrix3d J_ci = Matrix3dZero; //body com inertia
    Matrix3d J_i = Matrix3dZero; //body inertia
    Matrix3d R_i = Matrix3dZero; //body rotation

    //compute CoM position with RBDL function
    UpdateKinematics(model,Q,VectorNd::Zero(model.dof_count),VectorNd::Zero(model.dof_count));
    RigidBodyDynamics::Utils::CalcCenterOfMass(model, Q, NULL, NULL, mass, r_c, NULL, NULL);

    //compute total inertia around CoM
    for(std::map<std::string, unsigned int>::iterator it=model.mBodyNameMap.begin();
        it != model.mBodyNameMap.end(); it++){

        i =it->second;
        if (model.IsFixedBodyId(i)){
            continue;
        }
        else{
            mi = model.mBodies[i].mMass;
            riCi = model.mBodies[i].mCenterOfMass;
            J_i = model.mBodies[i].mInertia;
        }

        r_ci = CalcBodyToBaseCoordinates(model,Q,i,riCi,false) - r_c;
        R_i = CalcBodyWorldOrientation(model,Q,i,false).transpose();

        rTr = r_ci.transpose() * r_ci;
        Matrix3d rrT = r_ci * r_ci.transpose();
        Matrix3d ji0 = R_i * J_i * R_i.transpose();
        J_c = (ji0 + mi * (rTr * Matrix3dIdentity - rrT));
        J_c += J_ci;
    }
    return J_c;
}

```

Listing A.4: RBDL Code for calculation of the whole body inertia

```
import numpy as np
import pandas as pd

def MovingWindowCorrWalking(folder):
    file = folder + '/Coordination.csv'
    Hand_Vel = np.genfromtxt(file, delimiter=',', dtype=float, unpack = True)

    #Moving Window Correlation for 150 Frame Window (1s)
    df = pd.DataFrame(Hand_Vel.T, index = None, columns=None)
    roll_corr = df[1].rolling(150).corr(df[2])
    roll_corr = roll_corr.abs()
    Corr_150 = roll_corr.mean()

    #Moving Window Correlation for 30 Frame Window (0.2s)
    roll_corr = df[1].rolling(30).corr(df[2])
    roll_corr = roll_corr.abs()
    Corr_30 = roll_corr.mean()

    return {'hand_Correlation_1sWindow': Corr_150,
            'hand_Correlation_02sWindow': Corr_30}
```

**Listing A.5:** Python Code that calculates the hand coordination performance indicator from the hand velocities

## B Bibliography

- [1] Spencer L James, Degu Abate, Kalkidan Hassen Abate, Solomon M Abay, Cristiana Abbafati, Nooshin Abbasi, Hedayat Abbastabar, Foad Abd-Allah, Jemal Abdela, Ahmed Abdelalim, et al. Global, regional, and national incidence, prevalence, and years lived with disability for 354 diseases and injuries for 195 countries and territories, 1990–2017: a systematic analysis for the global burden of disease study 2017. *The Lancet*, 392(10159):1789–1858, 2018.
- [2] Stanley R Kay, Abraham Fiszbein, and Lewis A Opler. The positive and negative syndrome scale (panss) for schizophrenia. *Schizophrenia bulletin*, 13(2):261–276, 1987.
- [3] World Health Organization (WHO). Schizophrenia fact sheet. <https://www.who.int/news-room/fact-sheets/detail/schizophrenia>, 2020.
- [4] Lily AL Martin, Sabine C Koch, Dusan Hirjak, and Thomas Fuchs. Overcoming disembodiment: The effect of movement therapy on negative symptoms in schizophrenia—a multicenter randomized controlled trial. *Frontiers in psychology*, 7:483, 2016.
- [5] Heidelberg Center for Motion Research. URL <http://orb.iwr.uni-heidelberg.de/hcmr/>.
- [6] InnovationLab GmbH. User guide read-out electronics for pressure sensor matrix and “passivematrixui” software, 2019.
- [7] Lily Martin, Kevin Stein, Sabine Koch, Alexander Schubert, Leonardo Zapata-Fonseca, Wolfgang Tschacher, Katja Mombaur, and Thomas Fuchs. Schizophrenia and the moving body - an experiment on disembodiment and disembodied interaction. *Unpublished Study Protocoll of the Ethics Proposal. S-629/2018*, 2018.
- [8] SM Bruijn, OG Meijer, PJ Beek, and JH Van Dieën. Assessing the stability of human locomotion: a review of current measures. *Journal of the Royal Society Interface*, 10(83): 20120999, 2013.
- [9] Andre Seyfarth, Sten Grimmer, Daniel Häufle, and Karl Kalveram. Can robots help to understand human locomotion? *at - Automatisierungstechnik*, 60:653–661, 11 2012. doi: 10.1524/auto.2012.1040.
- [10] Kevin Stein. Walking Control Framework for the Humanoid Robot HeiCub - Implementation and Experimental Validation. *Optimization, Robotics and Biomechanics group, Interdisciplinary Center for Scientific Computing, Heidelberg*, 2016.
- [11] Yue Hu, Jorhabib Eljaik, Kevin Stein, Francesco Nori, and Katja Mombaur. Walking of the icub humanoid robot in different scenarios: implementation and performance analysis. In *2016 IEEE-RAS 16th International Conference on Humanoid Robots (Humanoids)*, pages 690–696. IEEE, 2016.

- [12] Fred Etoc, Jakob Metzger, Albert Ruzo, Christoph Kirst, Anna Yoney, M Zeeshan Ozair, Ali H Brivanlou, and Eric D Siggia. A balance between secreted inhibitors and edge sensing controls gastruloid self-organization. *Developmental cell*, 39(3):302–315, 2016.
- [13] Meir Plotnik, Nir Giladi, and Jeffrey M Hausdorff. A new measure for quantifying the bilateral coordination of human gait: effects of aging and parkinson’s disease. *Experimental brain research*, 181(4):561–570, 2007.
- [14] Christian Urbanek, Viola Gokel, Anton Safer, Heiko Becher, Armin J Grau, Florian Buggle, and Frederick Palm. Low self-reported sports activity before stroke predicts poor one-year-functional outcome after first-ever ischemic stroke in a population-based stroke register. *BMC neurology*, 18(1):181, 2018.
- [15] Anna Lena Emonds, Johannes Funken, Wolfgang Potthast, and Katja Mombaur. Comparison of sprinting with and without running-specific prostheses using optimal control techniques. *Robotica*, 37(12):2176–2194, 2019. doi: 10.1017/S0263574719000936.
- [16] K. Stein and K. Mombaur. Optimization-based analysis of a cartwheel. In *2018 7th IEEE International Conference on Biomedical Robotics and Biomechatronics (Biorob)*, pages 909–915, 08 2018. doi: 10.1109/BIOROB.2018.8488778.
- [17] K. Mombaur and H. Vallery. Stability and robustness of bipedal walking. In M. Sharbafi and A. Seyfarth, editors, *Bio-inspired legged locomotion: concepts, control and implementation*. Elsevier, 2017.
- [18] Eva Hansson, Anders Beckman, and Anders håkansson. Effect of vision, proprioception, and the position of the vestibular organ on postural sway. *Acta oto-laryngologica*, 130:1358–63, 12 2010. doi: 10.3109/00016489.2010.498024.
- [19] Fabrice Ango and Raphael Dos Reis. Sensing how to balance. *Elife*, 8, 2019.
- [20] Douglas J. Lanska and Christopher G. Goetz. Romberg’s sign. *Neurology*, 55(8):1201–1206, 2000. ISSN 0028-3878. doi: 10.1212/WNL.55.8.1201. URL <https://n.neurology.org/content/55/8/1201>.
- [21] Marcieli Bellé, Sílvia do Amaral Sartori, and Angela Garcia Rossi. Alcoholism: effects on the cochleo-vestibular apparatus. *Brazilian Journal of Otorhinolaryngology*, 73(1):110 – 116, 2007. ISSN 1808-8694. doi: [https://doi.org/10.1016/S1808-8694\(15\)31132-0](https://doi.org/10.1016/S1808-8694(15)31132-0). URL <http://www.sciencedirect.com/science/article/pii/S1808869415311320>.
- [22] Sarah Khan and Richard Chang. Anatomy of the vestibular system: a review. *NeuroRehabilitation*, 32(3):437—443, 2013. ISSN 1053-8135. doi: 10.3233/nre-130866. URL <https://doi.org/10.3233/NRE-130866>.
- [23] Mary Grace Gaerlan. The role of visual, vestibular, and somatosensory systems in postural balance. 2010.
- [24] Michael G Wade and Graeme Jones. The role of vision and spatial orientation in the maintenance of posture. *Physical therapy*, 77(6):619–628, 1997.

- [25] Marko Nardini and Dorothy Cowie. The development of multisensory balance, locomotion, orientation, and navigation. 2012.
- [26] John C. Tuthill and Eiman Azim. Proprioception. *Current Biology*, 28(5):R194 – R203, 2018. ISSN 0960-9822. doi: <https://doi.org/10.1016/j.cub.2018.01.064>. URL <http://www.sciencedirect.com/science/article/pii/S0960982218300976>.
- [27] DA Winter. Human balance and posture control during standing and walking. *Gait & Posture*, 3(4):193 – 214, 1995. ISSN 0966-6362. doi: 10.1016/0966-6362(96)82849-9. URL <http://www.sciencedirect.com/science/article/pii/0966636296828499>.
- [28] Lizeth Sloot, Matthew Millard, Christian Werner, and Katja Mombaur. Slow but steady: similar sit-to-stand balance at seat-off in older versus younger adults. *Frontiers in Sports and Active Living*, 2020.
- [29] Miomir Vukobratović and Branislav Borovac. Zero-moment point—thirty five years of its life. *International journal of humanoid robotics*, 1(01):157–173, 2004.
- [30] Shuuji Kajita, Fumio Kanehiro, Kenji Kaneko, Kiyoshi Fujiwara, Kensuke Harada, Kazuhito Yokoi, and Hirohisa Hirukawa. Biped walking pattern generation by using preview control of zero-moment point. In *Robotics and Automation, 2003. Proceedings. ICRA'03. IEEE International Conference on*, volume 2, pages 1620–1626. IEEE, 2003.
- [31] Ludovic Hoyet, Franck Multon, Katja Mombaur, and Eiichi Yoshida. Balance in dynamic situations: role of the underlying model. *Computer Methods in Biomechanics and Biomedical Engineering*, 12(S1):147–149, 2009.
- [32] Jerry Pratt, John Carff, Sergey Drakunov, and Ambarish Goswami. Capture point: A step toward humanoid push recovery. In *2006 6th IEEE-RAS international conference on humanoid robots*, pages 200–207. IEEE, 2006.
- [33] AL Hof, MGJ Gazendam, and WE Sinke. The condition for dynamic stability. *Journal of biomechanics*, 38(1):1–8, 2005.
- [34] Johannes Engelsberger, Christian Ott, Máximo A Roa, Alin Albu-Schäffer, and Gerhard Hirzinger. Bipedal walking control based on capture point dynamics. In *2011 IEEE/RSJ International Conference on Intelligent Robots and Systems*, pages 4420–4427. IEEE, 2011.
- [35] Patricia M McAndrew Young, Jason M Wilken, and Jonathan B Dingwell. Dynamic margins of stability during human walking in destabilizing environments. *Journal of biomechanics*, 45(6):1053–1059, 2012.
- [36] Vipul Lugade, Victor Lin, and Li-Shan Chou. Center of mass and base of support interaction during gait. *Gait & posture*, 33(3):406–411, 2011.
- [37] HM Maus, SW Lipfert, M Gross, J Rummel, and A Seyfarth. Upright human gait did not provide a major mechanical challenge for our ancestors. *Nature communications*, 1(6):70, 2010.

- [38] Charlotte Paiman, Daniel Lemus, Débora Short, and Heike Vallery. Observing the state of balance with a single upper-body sensor. *Frontiers in Robotics and AI*, 3:11, 2016. ISSN 2296-9144. doi: 10.3389/frobt.2016.00011. URL <http://journal.frontiersin.org/article/10.3389/frobt.2016.00011>.
- [39] Martin L Felis and Katja Mombaur. Synthesis of full-body 3-d human gait using optimal control methods. In *2016 IEEE International Conference on Robotics and Automation (ICRA)*, pages 1560–1566. IEEE, 2016.
- [40] Ambarish Goswami and Vinutha Kallem. Rate of change of angular momentum and balance maintenance of biped robot. volume 2004, pages 3785 – 3790 Vol.4, 01 2004. ISBN 0-7803-8232-3. doi: 10.1109/ROBOT.2004.1308858.
- [41] Aleksandr Mikhailovich Lyapunov. The general problem of the stability of motion. *International journal of control*, 55(3):531–534, 1992.
- [42] Jane Cronin. *Ordinary differential equations: introduction and qualitative theory*. CRC Press, 2007.
- [43] Steve Collins, Andy Ruina, Russ Tedrake, and Martijn Wisse. Efficient bipedal robots based on passive-dynamic walkers. *Science*, 307(5712):1082–1085, 2005.
- [44] Katja D Mombaur, Hans Georg Bock, Johannes P Schlöder, and Richard W Longman. Open-loop stable solutions of periodic optimal control problems in robotics. *ZAMM-Journal of Applied Mathematics and Mechanics/Zeitschrift für Angewandte Mathematik und Mechanik: Applied Mathematics and Mechanics*, 85(7):499–515, 2005.
- [45] Katja Mombaur. Using optimization to create self-stable human-like running. *Robotica*, 27(3):321–330, 2009.
- [46] Bryan L. Riemann, Joseph B. Myers, and Scott M. Lephart. Comparison of the ankle, knee, hip, and trunk corrective action shown during single-leg stance on firm, foam, and multiaxial surfaces. *Archives of Physical Medicine and Rehabilitation*, 84(1):90 – 95, 2003. ISSN 0003-9993. doi: <https://doi.org/10.1053/apmr.2003.50004>. URL <http://www.sciencedirect.com/science/article/pii/S0003999302048220>.
- [47] Lewis M Nashner and Gin McCollum. The organization of human postural movements: a formal basis and experimental synthesis. *Behavioral and brain sciences*, 8(1):135–150, 1985.
- [48] Kuangyou B. Cheng, Kuan-Mao Wang, and Shih-Yu Kuo. Role of arm motion in feet-in-place balance recovery. *Journal of Biomechanics*, 48(12):3155 – 3162, 2015. ISSN 0021-9290. doi: <https://doi.org/10.1016/j.jbiomech.2015.07.008>. URL <http://www.sciencedirect.com/science/article/pii/S0021929015003851>.
- [49] Mirjam Pijnappels, Idsart Kingma, Daphne Wezenberg, Guus Reurink, and Jaap H Van Dieën. Armed against falls: the contribution of arm movements to balance recovery after tripping. *Experimental brain research*, 201(4):689–699, 2010.

- [50] Alexander CH Geurts, Mirjam de Haart, Ilse JW van Nes, and Jaak Duysens. A review of standing balance recovery from stroke. *Gait & posture*, 22(3):267–281, 2005.
- [51] Yasuharu Tabara, Yoko Okada, Maya Ohara, Eri Uetani, Tomoko Kido, Namiko Ochi, Tokihisa Nagai, Michiya Igase, Tetsuro Miki, Fumihiko Matsuda, et al. Association of postural instability with asymptomatic cerebrovascular damage and cognitive decline: the japan shimanami health promoting program study. *Stroke*, 46(1):16–22, 2015.
- [52] AK Topper, BE Maki, and Pamela J Holliday. Are activity-based assessments of balance and gait in the elderly predictive of risk of falling and/or type of fall? *Journal of the American Geriatrics Society*, 41(5):479–487, 1993.
- [53] Andrea Trombetti, Mélanie Hars, François R Herrmann, Reto W Kressig, Serge Ferrari, and René Rizzoli. Effect of music-based multitask training on gait, balance, and fall risk in elderly people: a randomized controlled trial. *Archives of internal medicine*, 171(6):525–533, 2011.
- [54] Katherine Berg, Sharon Wood-Dauphine, JI Williams, and David Gayton. Measuring balance in the elderly: preliminary development of an instrument. *Physiotherapy Canada*, 41(6):304–311, 1989.
- [55] Lara Thompson, Mehdi Badache, Steven Cale, Lonika Behera, and Nian Zhang. Balance performance as observed by center-of-pressure parameter characteristics in male soccer athletes and non-athletes. *Sports*, 5(4):86, 2017.
- [56] Ya-Ling Teng, Chiung-Ling Chen, Shu-Zon Lou, Wei-Tsan Wang, Jui-Yen Wu, Hui-Ing Ma, and Vincent Chin-Hung Chen. Postural stability of patients with schizophrenia during challenging sensory conditions: Implication of sensory integration for postural control. *PLoS one*, 11(6):e0158219, 2016.
- [57] Cherie L Marvel, Barbara L Schwartz, and Richard B Rosse. A quantitative measure of postural sway deficits in schizophrenia. *Schizophrenia Research*, 68(2-3):363–372, 2004.
- [58] Alexander Ruhe, René Fejer, and Bruce Walker. Center of pressure excursion as a measure of balance performance in patients with non-specific low back pain compared to healthy controls: a systematic review of the literature. *European Spine Journal*, 20(3):358–368, 2011.
- [59] Hai Qiu and Shuping Xiong. Center-of-pressure based postural sway measures: reliability and ability to distinguish between age, fear of falling and fall history. *International Journal of Industrial Ergonomics*, 47:37–44, 03 2015. doi: 10.1016/j.ergon.2015.02.004.
- [60] David R Bell, Kevin M Guskiewicz, Micheal A Clark, and Darin A Padua. Systematic review of the balance error scoring system. *Sports health*, 3(3):287–295, 2011.
- [61] Grant L Iverson and Michael S Koehle. Normative data for the balance error scoring system in adults. *Rehabilitation research and practice*, 2013, 2013.
- [62] Pamela W Duncan, Stephanie Studenski, Julie Chandler, and Barbara Prescott. Functional reach: predictive validity in a sample of elderly male veterans. *Journal of gerontology*, 47(3):M93–M98, 1992.

- [63] Margaret Schenkman, Terry Ellis, Cory Christiansen, Anna E Barón, Linda Tickle-Degnen, Deborah A Hall, and Robert Wagenaar. Profile of functional limitations and task performance among people with early-and middle-stage parkinson disease. *Physical therapy*, 91(9): 1339–1354, 2011.
- [64] Teresa M Steffen, Timothy A Hacker, and Louise Mollinger. Age-and gender-related test performance in community-dwelling elderly people: Six-minute walk test, berg balance scale, timed up & go test, and gait speeds. *Physical therapy*, 82(2):128–137, 2002.
- [65] Teresa Steffen and Megan Seney. Test-retest reliability and minimal detectable change on balance and ambulation tests, the 36-item short-form health survey, and the unified parkinson disease rating scale in people with parkinsonism. *Physical therapy*, 88(6):733–746, 2008.
- [66] S Mathias, US Nayak, and Bernard Isaacs. Balance in elderly patients: the " get-up and go" test. *Archives of physical medicine and rehabilitation*, 67(6):387–389, 1986.
- [67] Diane Podsiadlo and Sandra Richardson. The timed “up & go”: a test of basic functional mobility for frail elderly persons. *Journal of the American geriatrics Society*, 39(2):142–148, 1991.
- [68] D Theisen and G Wydra. Untersuchung der gleichgewichtsfähigkeit. *B&G Bewegungstherapie und Gesundheitssport*, 27(06):231–239, 2011.
- [69] Standardized field sobriety testing procedures.
- [70] Hong Jin Jeon, Maeng Je Cho, Seong-Jin Cho, Seon-Uk Kim, Soo-Kyung Park, Jun Soo Kwon, Jae Yong Jeon, and Bong-Jin Hahm. Quantitative analysis of ataxic gait in patients with schizophrenia: the influence of age and visual control. *Psychiatry research*, 152(2-3): 155–164, 2007.
- [71] Amy J. Bastian, Jonathan W. Mink, Bruce A. Kaufman, and W. Thomas Thach. Posterior vermal split syndrome. *Annals of Neurology*, 44(4):601–610, 1998. doi: 10.1002/ana.410440405. URL <https://onlinelibrary.wiley.com/doi/abs/10.1002/ana.410440405>.
- [72] Sally D. Lark and Sowjanya Pasupuleti. Validity of a functional dynamic walking test for the elderly. *Archives of Physical Medicine and Rehabilitation*, 90(3):470 – 474, 2009. ISSN 0003-9993. doi: <https://doi.org/10.1016/j.apmr.2008.08.221>. URL <http://www.sciencedirect.com/science/article/pii/S0003999308016997>.
- [73] Helen S Cohen, Ajitkumar P Mulavara, Brian T Peters, Haleh Sangi-Haghpeykar, Doris H Kung, Dennis R Mosier, and Jacob J Bloomberg. Sharpening the tandem walking test for screening peripheral neuropathy. *Southern medical journal*, 106(10):565, 2013.
- [74] Fay B Horak, Diane M Wrisley, and James Frank. The balance evaluation systems test (bestest) to differentiate balance deficits. *Physical therapy*, 89(5):484–498, 2009.
- [75] JA Raymakers, MM Samson, and HJJ Verhaar. The assessment of body sway and the choice of the stability parameter (s). *Gait & posture*, 21(1):48–58, 2005.

- [76] Melvyn Roerdink, Claudine JC Lamoth, Peter J Beek, et al. Online gait event detection using a large force platform embedded in a treadmill. *Journal of biomechanics*, 41(12):2628–2632, 2008.
- [77] Hiroyuki Shimada, Shuichi Obuchi, Taketo Furuna, and Takao Suzuki. New intervention program for preventing falls among frail elderly people: the effects of perturbed walking exercise using a bilateral separated treadmill. *American journal of physical medicine & rehabilitation*, 83(7):493–499, 2004.
- [78] Ross A Clark, Adam L Bryant, Yonghao Pua, Paul McCrory, Kim Bennell, and Michael Hunt. Validity and reliability of the nintendo wii balance board for assessment of standing balance. *Gait & posture*, 31(3):307–310, 2010.
- [79] Kelly J Bower, Jennifer L McGinley, Kimberly J Miller, and Ross A Clark. Instrumented static and dynamic balance assessment after stroke using wii balance boards: Reliability and association with clinical tests. *PloS one*, 9(12):e115282, 2014.
- [80] Marcos Duarte, Sandra Freitas, and Vladimir Zatsiorsky. Control of equilibrium in humans: Sway over sway. *Motor control*, pages 219–242, 01 2011. doi: 10.1093/acprof:oso/9780195395273.003.0010.
- [81] Tomohisa Yamamoto, Charles E Smith, Yasuyuki Suzuki, Ken Kiyono, Takao Tanahashi, Saburo Sakoda, Pietro Morasso, and Taishin Nomura. Universal and individual characteristics of postural sway during quiet standing in healthy young adults. *Physiological reports*, 3(3): e12329, 2015.
- [82] Eadric Bressel, Joshua C Yonker, John Kras, and Edward M Heath. Comparison of static and dynamic balance in female collegiate soccer, basketball, and gymnastics athletes. *Journal of athletic training*, 42(1):42, 2007.
- [83] C Hrysomallis, P McLaughlin, and C Goodman. Relationship between static and dynamic balance tests among elite australian footballers. *Journal of science and medicine in sport*, 9(4):288–291, 2006.
- [84] Lakshdeep Gill, Andrew H Huntley, and Avril Mansfield. Does the margin of stability measure predict medio-lateral stability of gait with a constrained-width base of support? *Journal of biomechanics*, 95:109317, 2019.
- [85] Kyoung Jae Kim, Yoav Gimmon, Jennifer Millar, and Michael C Schubert. Using inertial sensors to quantify postural sway and gait performance during the tandem walking test. *Sensors*, 19(4):751, 2019.
- [86] Paolo Paoletti and Lakshminarayanan Mahadevan. Balancing on tigtropes and slacklines. *Journal of the Royal Society, Interface / the Royal Society*, 9:2097–108, 04 2012. doi: 10.1098/rsif.2012.0077.
- [87] Panos J Athanasiadis. Slackline dynamics and the helmholtz–duffing oscillator. *European Journal of Physics*, 39(1):014002, 2017.

- [88] Guinness World Records. Longest slackline walk over water. <https://www.guinnessworldrecords.com/world-records/468388-longest-slackline-walk-over-water>, May 2017.
- [89] Lars Donath, Ralf Roth, A Ruegge, M Groppa, Lukas Zahner, and Oliver Faude. Effects of slackline training on balance, jump performance & muscle activity in young children. *International journal of sports medicine*, 34, 05 2013. doi: 10.1055/s-0033-1337949.
- [90] Lars Donath, Ralf Roth, Lukas Zahner, and Oliver Faude. Slackline training and neuromuscular performance in seniors: A randomized controlled trial. *Scandinavian journal of medicine & science in sports*, 26, 03 2015. doi: 10.1111/sms.12423.
- [91] Martin Keller, Juergen Pfusterschmied, Michael Buchecker, Erich Mueller, and Wolfgang Taube. Improved postural control after slackline training is accompanied by reduced h-reflexes. *Scandinavian journal of medicine & science in sports*, 22:471–7, 03 2011. doi: 10.1111/j.1600-0838.2010.01268.x.
- [92] Kentaro Kodama, Yusuke Kikuchi, and Hideo Yamagiwa. Whole-body coordination skill for dynamic balancing on a slackline. In *JSAI International Symposium on Artificial Intelligence*, pages 528–546. Springer, 2015.
- [93] Ben Serrien, Erich Hohenauer, Ron Clijsen, Jean-Pierre Baeyens, and Ursula Küng. Balance coordination strategies on slackline: Analysis by means of self-organizing maps. 09 2016.
- [94] Ben Serrien, Erich Hohenauer, Ron Clijsen, Wolfgang Taube, Jean-Pierre Baeyens, and Ursula Küng. Changes in balance coordination and transfer to an unlearned balance task after slackline training: a self-organizing map analysis. *Experimental brain research*, 235 (11):3427–3436, 2017.
- [95] Lars Donath, Ralf Roth, Lukas Zahner, and Oliver Faude. Slackline training (balancing over narrow nylon ribbons) and balance performance: a meta-analytical review. *Sports Medicine*, 47(6):1075–1086, 2017.
- [96] Thomas Laursen, Merete Nordentoft, and Per Brøbech. Excess early mortality in schizophrenia. *Annual review of clinical psychology*, 10, 12 2013. doi: 10.1146/annurev-clinpsy-032813-153657.
- [97] Mark Olfson, Tobias Gerhard, Cecilia Huang, Stephen Crystal, and T Stroup. Premature mortality among adults with schizophrenia in the united states. *JAMA psychiatry*, 72:1–10, 10 2015. doi: 10.1001/jamapsychiatry.2015.1737.
- [98] World Health Organization et al. *The ICD-10 classification of mental and behavioural disorders: diagnostic criteria for research*, volume 2. World Health Organization, 1993.
- [99] World Health Organization. International statistical classification of diseases and related health problems. <https://icd.who.int/browse10/2014/en#!/F20-F29>, 2014.
- [100] Johannes Schröder, Rainer Niethammer, Franz-Josef Geider, Christoph Reitz, Michael Binkert, Marek Jauss, and Heinrich Sauer. Neurological soft signs in schizophrenia. *Schizophrenia Research*, 6(1):25–30, 1991.

- [101] Robert W Buchanan and Douglas W Heinrichs. The neurological evaluation scale (nes): a structured instrument for the assessment of neurological signs in schizophrenia. *Psychiatry research*, 27(3):335–350, 1989.
- [102] Stefan Fritze, Fabio Sambataro, Katharina M Kubera, Alina L Bertolino, Cristina E Topor, Robert C Wolf, and Dusan Hirjak. Neurological soft signs in schizophrenia spectrum disorders are not confounded by current antipsychotic dosage. *European Neuropsychopharmacology*, 31:47–57, 2020.
- [103] D Hirjak, G Northoff, PA Thomann, KM Kubera, and RC Wolf. Genuine motorische phänomene bei schizophrener psychosen. *Der Nervenarzt*, 89(1):27–43, 2018.
- [104] George L Engel. The biopsychosocial model and the education of health professionals. *Annals of the New York Academy of Sciences*, 310(1):169–181, 1978.
- [105] Rikke Hilker, Dorte Helenius, Birgitte Fagerlund, Axel Skytthe, Kaare Christensen, Thomas M. Werge, Merete Nordentoft, and Birte Glenthøj. Heritability of schizophrenia and schizophrenia spectrum based on the nationwide danish twin register. *Biological Psychiatry*, 83(6):492–498, 2018. ISSN 0006-3223. doi: <https://doi.org/10.1016/j.biopsych.2017.08.017>. URL <http://www.sciencedirect.com/science/article/pii/S0006322317319054>. Novel Mechanisms in Schizophrenia Pathophysiology.
- [106] Sukanta Saha, David Chant, Joy Welham, and John McGrath. A systematic review of the prevalence of schizophrenia. *PLoS medicine*, 2:e141, 06 2005. doi: 10.1371/journal.pmed.0020141.
- [107] Kenneth S Kendler, Mary McGuire, Alan M Gruenberg, Aileen O’hare, Mary Spellman, and Dermot Walsh. The roscommon family study: I. methods, diagnosis of probands, and risk of schizophrenia in relatives. *Archives of general psychiatry*, 50(7):527–540, 1993.
- [108] Alastair G Cardno, E Jane Marshall, Bina Coid, Alison M Macdonald, Tracy R Ribchester, Nadia J Davies, Piero Venturi, Lisa A Jones, Shôn W Lewis, Pak C Sham, et al. Heritability estimates for psychotic disorders: the maudsley twin psychosis series. *Archives of general psychiatry*, 56(2):162–168, 1999.
- [109] Christos Pantelis, Murat Yücel, Stephen J Wood, Dennis Velakoulis, Daqiang Sun, Gregor Berger, Geoff W Stuart, Alison Yung, Lisa Phillips, and Patrick D McGorry. Structural Brain Imaging Evidence for Multiple Pathological Processes at Different Stages of Brain Development in Schizophrenia. *Schizophrenia Bulletin*, 31(3):672–696, 01 2005. ISSN 0586-7614. doi: 10.1093/schbul/sbi034. URL <https://doi.org/10.1093/schbul/sbi034>.
- [110] Shitij Kapur and Gary Remington. Serotonin-dopamine interaction and its relevance to schizophrenia. *American Journal of Psychiatry*, 153(4):466–476, 1996.
- [111] Monte S. Buchsbaum and Richard J. Haier. Functional and Anatomical Brain Imaging: Impact on Schizophrenia Research. *Schizophrenia Bulletin*, 13(1):115–132, 01 1987.
- [112] Raquel E. Gur and Godfrey D. Pearlson. Neuroimaging in Schizophrenia Research. *Schizophrenia Bulletin*, 19(2):337–353, 01 1993.

- [113] Christian Gaser, Hans-Peter Volz, Stefan Kiebel, Stefan Riehemann, and Heinrich Sauer. Detecting structural changes in whole brain based on nonlinear deformations—application to schizophrenia research. *NeuroImage*, 10(2):107 – 113, 1999. ISSN 1053-8119. doi: <https://doi.org/10.1006/nimg.1999.0458>. URL <http://www.sciencedirect.com/science/article/pii/S1053811999904585>.
- [114] Joseph Ventura, Keith H Nuechterlein, Kenneth L Subotnik, Jean Pederson Hardesty, and Jim Mintz. Life events can trigger depressive exacerbation in the early course of schizophrenia. *Journal of Abnormal Psychology*, 109(1):139, 2000.
- [115] Elizabeth Kuipers, Amina Yesufu-Udechuku, Clare Taylor, and Tim Kendall. Management of psychosis and schizophrenia in adults: summary of updated nice guidance. *Bmj*, 348: g1173, 2014.
- [116] Kenneth S Koblan, Justine Kent, Seth C Hopkins, John H Krystal, Hailong Cheng, Robert Goldman, and Antony Loebel. A non-d2-receptor-binding drug for the treatment of schizophrenia. *New England Journal of Medicine*, 382(16):1497–1506, 2020.
- [117] Brian Kirkpatrick, Wayne S Fenton, William T Carpenter, and Stephen R Marder. The nimh-matrices consensus statement on negative symptoms. *Schizophrenia bulletin*, 32(2): 214–219, 2006.
- [118] F Röhricht and N Papadopoulos. A treatment manual: Body oriented psychological therapy for chronic schizophrenia. *London: Newham Centre for Mental Health*, 2010.
- [119] Thomas Fuchs and Sabine C Koch. Embodied affectivity: on moving and being moved. *Frontiers in psychology*, 5:508, 2014.
- [120] Thomas Fuchs. Selbst und schizoprenie. *Deutsche Zeitschrift für Philosophie*, 60(6): 887–901, 2012.
- [121] FRANK Rohricht and Stefan Priebe. Effect of body-oriented psychological therapy on negative symptoms in schizophrenia: a randomized controlled trial. *Psychol Med*, 2006.
- [122] Josef Parnas, Paul Møller, Tilo Kircher, Jørgen Thalbitzer, Lennart Jansson, Peter Handest, and Dan Zahavi. Ease-scale (examination of anomalous self-experience). *Psychopathology*, 38:236–58, 09 2005. doi: 10.1159/000088441.
- [123] Qualisys AB. Qualisys - The Swedish Motion Capture Company, 2020. URL <http://www.qualisys.com>.
- [124] Daniel Roetenberg, Henk Luinge, and Per Slycke. Xsens mvn: full 6dof human motion tracking using miniature inertial sensors. xsens motion technologies bv. Technical report, Xsens Motion Technologies BV: Enschede, the Netherlands, 2009.
- [125] Andrew D. Vigotsky, Israel Halperin, Gregory J. Lehman, Gabriel S. Trajano, and Taian M. Vieira. Interpreting signal amplitudes in surface electromyography studies in sport and rehabilitation sciences. *Frontiers in Physiology*, 8:985, 2018. ISSN 1664-042X. doi: 10.3389/fphys.2017.00985. URL <https://www.frontiersin.org/article/10.3389/fphys.2017.00985>.

- [126] Andrea Schaerli, Melanie Keller, S Lorenzetti, Kurt Murer, and Rolf Langenberg, van de. Balancing on a slackline: 8-year-olds vs. adults. *Frontiers in psychology*, 4:208, 04 2013. doi: 10.3389/fpsyg.2013.00208.
- [127] George T Rab, Kyria Petuskey, and Anita Bagley. A method for determination of upper extremity kinematics. *Gait and Posture*, 15(2):113–119, 2002. ISSN 0966-6362. doi: 10.1016/S0966-6362(01)00155-2.
- [128] Alberto Leardini, Fabio Biagi, Andrea Merlo, Claudio Belvedere, and Maria Grazia Benedetti. Multi-segment trunk kinematics during locomotion and elementary exercises. *Clinical Biomechanics*, 26:562–71, 03 2011. doi: 10.1016/j.clinbiomech.2011.01.015.
- [129] A Cappozzo, F Catani, U Della Croce, and A Leardini. Position and orientation in space of bones during movement: anatomical frame definition and determination. *Clinical Biomechanics*, 10(4):171 – 178, 1995. ISSN 0268-0033. doi: 10.1016/0268-0033(95)91394-T. URL <http://www.sciencedirect.com/science/article/pii/S026800339591394T>.
- [130] S. Van Sint Jan and P. Allard. *Color Atlas of Skeletal Landmark Definitions: Guidelines for Reproducible Manual and Virtual Palpations*. Churchill Livingstone/Elsevier, 2007. ISBN 9780443103155. URL [https://books.google.de/books?id=fK\\_ZAQAACAAJ](https://books.google.de/books?id=fK_ZAQAACAAJ).
- [131] Martin Schepers, Matteo Giuberti, and G. Bellusci. Xsens mvn: Consistent tracking of human motion using inertial sensing. Technical report, 03 2018.
- [132] Xsens. *Xsens MVN User Manual*. Xsens, November 2017. URL [documentation.xsens.com/MVN-User-Manual-4](http://documentation.xsens.com/MVN-User-Manual-4). Document MV0319P, Revision U.
- [133] K. Stein and K. Mombaur. Performance indicators for stability of slackline balancing. In *IEEE/RAS International Conference on Humanoid Robots (Humanoids 2019)*, 2019.
- [134] Daniel Dinu, Martin Fayolas, Marine Jacquet, Elsa Leguy, Jean Slavinski, and Nicolas Houel. Accuracy of postural human-motion tracking using miniature inertial sensors. *Procedia Engineering*, 147:655 – 658, 2016. ISSN 1877-7058. doi: <http://dx.doi.org/10.1016/j.proeng.2016.06.266>. URL <http://www.sciencedirect.com/science/article/pii/S1877705816307135>. The Engineering of Sport 11.
- [135] D.H Sutherland. The evolution of clinical gait analysis: Part II kinematics. *Gait & Posture*, 16(2):159 – 179, 2002. ISSN 0966-6362. doi: 10.1016/S0966-6362(02)00004-8. URL <http://www.sciencedirect.com/science/article/pii/S0966636202000048>.
- [136] Necip Berme. Multi-component force and moment measuring platform and load transducer, March 12 2002. US Patent 6,354,155.
- [137] Maximilian Müller. Moticon–knowledge integrated sports equipment. *CiDaD News*, (Januar 2009–Jahrgang 06–Nr. 01), 2009.
- [138] Thomas Stöggel and Alex Martiner. Validation of moticon’s opengo sensor insoles during gait, jumps, balance and cross-country skiing specific imitation movements. In *Journal of sports sciences*, 2017.

- [139] Paolo De Leva. Adjustments to Zatsiorsky-Seluyanov's segment inertia parameters. *Journal of Biomechanics*, 29(9):1223–1230, 1996.
- [140] Alexander L Bell, Richard A Brand, and Douglas R Pedersen. Prediction of hip joint centre location from external landmarks. *Human movement science*, 8(1):3–16, 1989.
- [141] Roy Featherstone. *Rigid Body Dynamics Algorithms*. 01 2008. ISBN 978-0-387-74314-1. doi: 10.1007/978-1-4899-7560-7.
- [142] Martin L. Felis. RBDL: an efficient rigid-body dynamics library using recursive algorithms. *Autonomous Robots*, pages 1–17, 2016. ISSN 1573-7527. doi: 10.1007/s10514-016-9574-0. URL <http://dx.doi.org/10.1007/s10514-016-9574-0>.
- [143] Martin Felis. *Modeling Emotional Aspects in Human Locomotion*. PhD thesis, Heidelberg University, 2015. URL <https://github.com/ORB-HD/puppeteer>.
- [144] Kenneth Levenberg. A method for the solution of certain non-linear problems in least squares. *Quarterly of Applied Mathematics*, 2(2):164–168, 1944. ISSN 0033569X, 15524485. URL <http://www.jstor.org/stable/43633451>.
- [145] T. Sugihara. Solvability-Unconcerned Inverse Kinematics by the Levenberg- Marquardt Method. *IEEE Transactions on Robotics*, 27:984–991, 2011.
- [146] Sander Schreven, Peter J. Beek, and Jeroen B.J. Smeets. Optimising filtering parameters for a 3d motion analysis system. *Journal of Electromyography and Kinesiology*, 25(5):808 – 814, 2015. ISSN 1050-6411. doi: <https://doi.org/10.1016/j.jelekin.2015.06.004>. URL <http://www.sciencedirect.com/science/article/pii/S1050641115001182>.
- [147] Eline van der Kruk and Marco M. Reijne. Accuracy of human motion capture systems for sport applications; state-of-the-art review. *European Journal of Sport Science*, 18(6): 806–819, 2018. doi: 10.1080/17461391.2018.1463397. PMID: 29741985.
- [148] Katja Mombaur. Using optimization to create self-stable human-like running. *Robotica*, 27(3):321–330, 2009. doi: 10.1017/S0263574708004724.
- [149] D. Leinweber, I. Bauer, H. Bock, and J. Schloeder. An efficient multiple shooting based reduced SQP strategy for large-scale dynamic process optimization. part I: Theoretical aspects. *Computers and Chemical Engineering*, 27:157–166, 2003.
- [150] Peter Kuhl, Joachim Ferreau, Jan Albersmeyer, Christian Kirches, Leonard Wirsching, Sebastian Sager, Andreas Potschka, Gerrit Schulz, Moritz Diehl, Daniel Leinweber, and Andreas Schafer. *MUSCOD-II Users' Manual*. IWR, 01 2001.
- [151] H.G. Bock and K.J. Plitt. A multiple shooting algorithm for direct solution of optimal control problems. pages 243–247. Pergamon Press, 1984.
- [152] Martina Mancini and Fay B Horak. The relevance of clinical balance assessment tools to differentiate balance deficits. *European journal of physical and rehabilitation medicine*, 46(2):239, 2010.

- 
- [153] Caroline Ribeiro de Souza, Marina Torres Betelli, Patrícia Sayuri Takazono, Julia Ávila de Oliveira, Daniel Boari Coelho, Jacques Duysens, and Luis Augusto Teixeira. Evaluation of balance recovery stability from unpredictable perturbations through the compensatory arm and leg movements (calm) scale. *PLoS one*, 14(8):e0221398, 2019.
- [154] Thomas E Prieto, Joel B Myklebust, Raymond G Hoffmann, Eric G Lovett, and Barbara M Myklebust. Measures of postural steadiness: differences between healthy young and elderly adults. *IEEE Transactions on biomedical engineering*, 43(9):956–966, 1996.
- [155] Peter Welch. The use of fast fourier transform for the estimation of power spectra: a method based on time averaging over short, modified periodograms. *IEEE Transactions on audio and electroacoustics*, 15(2):70–73, 1967.
- [156] Maurice S Bartlett. Periodogram analysis and continuous spectra. *Biometrika*, 37(1/2):1–16, 1950.
- [157] M. Duarte. psd2: A python module for estimation of power spectral density characteristics using welch’s method. <https://github.com/demotu/psd2>, 2020.
- [158] Damiana A Santos and Marcos Duarte. A public data set of human balance evaluations. *PeerJ*, 4:e2648, 2016.
- [159] Lorenzo Chiari, Laura Rocchi, and Angelo Cappello. Stabilometric parameters are affected by anthropometry and foot placement. *Clinical biomechanics*, 17(9-10):666–677, 2002.
- [160] Shuuji Kajita, Mitsuharu Morisawa, K. Miura, Shin’ichiro Nakaoka, Kensuke Harada, K. Kaneko, Fumio Kanehiro, and Kazuhito Yokoi. Biped walking stabilization based on linear inverted pendulum tracking. pages 4489 – 4496, 11 2010. doi: 10.1109/IROS.2010.5651082.
- [161] Wilhelm Kirch, editor. *Pearson’s Correlation Coefficient*, pages 1090–1091. Springer Netherlands, Dordrecht, 2008. ISBN 978-1-4020-5614-7. doi: 10.1007/978-1-4020-5614-7\_2569. URL [https://doi.org/10.1007/978-1-4020-5614-7\\_2569](https://doi.org/10.1007/978-1-4020-5614-7_2569).
- [162] Henry B Mann and Donald R Whitney. On a test of whether one of two random variables is stochastically larger than the other. *The annals of mathematical statistics*, pages 50–60, 1947.
- [163] Jacob Cohen. *Statistical power analysis for the behavioral sciences*. Academic press, 2013.
- [164] Shlomo S Sawilowsky. New effect size rules of thumb. *Journal of Modern Applied Statistical Methods*, 8(2):26, 2009.
- [165] Hanno Essén. Average angular velocity. *European journal of physics*, 14(5):201, 1993.
- [166] Torsten Fließbach. *Lehrbuch zur theoretischen Physik*. Springer, 2003.
- [167] Albert Einstein. Ist die Trägheit eines Körpers von seinem Energieinhalt abhängig? *Annalen der Physik*, 323(13):639–641, 1905.
- [168] Wolfgang Tschacher and Deborah Meier. Physiological synchrony in psychotherapy sessions. *Psychotherapy Research*, 30(5):558–573, 2020.

- [169] Jin Hyun Cheong, Zainab Molani, Sushmita Sadhukha, and Luke J Chang. Synchronized affect in shared experiences strengthens social connection. 2020.
- [170] Embodied Cognition Lab @ UT Austin. Python c3d processing. <https://github.com/EmbodiedCognition/py-c3d>, 2020.
- [171] The pandas development team. pandas-dev/pandas: Pandas, February 2020. URL <https://doi.org/10.5281/zenodo.3509134>.
- [172] Raphael Vallat. Pingouin: statistics in python. *The Journal of Open Source Software*, 3(31): 1026, November 2018.
- [173] Michael Waskom and the seaborn development team. mwaskom/seaborn, September 2020. URL <https://doi.org/10.5281/zenodo.592845>.
- [174] Jay M Goldberg and Cesar Fernandez. The vestibular system. *Handbook of physiology*, 3: 977–1021, 1984.
- [175] Stefan Leucht, Myrto Samara, Stephan Heres, Maxine X. Patel, Toshi Furukawa, Andrea Cipriani, John Geddes, and John M. Davis. Dose equivalents for second-generation antipsychotic drugs: The classical mean dose method. *Schizophrenia Bulletin*, 41(6): 1397–1402, 04 2015.
- [176] Stefan Leucht, Myrto Samara, Stephan Heres, and John M. Davis. Dose equivalents for antipsychotic drugs: The ddd method. *Schizophrenia Bulletin*, 42:S90–S94, 07 2016.
- [177] Wei-Hsiu Lin, Ying-Fang Liu, City Chin-Cheng Hsieh, and Alex JY Lee. Ankle eversion to inversion strength ratio and static balance control in the dominant and non-dominant limbs of young adults. *Journal of Science and Medicine in Sport*, 12(1):42–49, 2009.
- [178] Thomas W Parks and C Sidney Burrus. *Digital filter design*. Wiley-Interscience, 1987.
- [179] Philippe Sardain and Guy Bessonnet. Forces acting on a biped robot. center of pressure-zero moment point. *IEEE Transactions on Systems, Man, and Cybernetics-Part A: Systems and Humans*, 34(5):630–637, 2004.
- [180] Mavuto M Mukaka. A guide to appropriate use of correlation coefficient in medical research. *Malawi medical journal*, 24(3):69–71, 2012.
- [181] Karl Pearson. X. on the criterion that a given system of deviations from the probable in the case of a correlated system of variables is such that it can be reasonably supposed to have arisen from random sampling. *The London, Edinburgh, and Dublin Philosophical Magazine and Journal of Science*, 50(302):157–175, 1900.
- [182] William H. Kruskal and W. Allen Wallis. Use of ranks in one-criterion variance analysis. *Journal of the American Statistical Association*, 47(260):583–621, 1952. doi: 10.1080/01621459.1952.10483441.
- [183] Christian Katlein and Patrick Engel. Force measurement in slacklines – application report. [https://www.lorenz-messtechnik.de/english/company/force-measurement\\_slacklines.php](https://www.lorenz-messtechnik.de/english/company/force-measurement_slacklines.php), 2008.

- [184] Slacktivity Slacklines Benelux. Forces in slacklining. <https://www.slacktivity.com/slackline-infos/forces-in-slacklining>, 2020.
- [185] Wilfried Plassmann and Detlef Schulz. *Handbuch Elektrotechnik Grundlagen und Anwendungen fuer Elektrotechniker*. 6. Auflage. Springer Vieweg, 2013.
- [186] Elmar Schrüfer, Leonhard Reindl, and Bernhard Zagar. *Elektrische Messtechnik Messung elektrischer und nichtelektrischer Grössen*. Hanser, 2014.
- [187] Douglas G Altman and J Martin Bland. Measurement in medicine: the analysis of method comparison studies. *Journal of the Royal Statistical Society: Series D (The Statistician)*, 32(3):307–317, 1983.
- [188] Kevin Stein and Katja Mombaur. Whole-body dynamic analysis of challenging slackline jumping. *Applied Sciences*, 10(3):1094, 2020.
- [189] Herbert Elftman. Forces and energy changes in the leg during walking. *American Journal of Physiology*, 125(2):339–356, 1939. doi: 10.1152/ajplegacy.1939.125.2.339.
- [190] Wilfred Taylor Dempster. Space requirements of the seated operator, geometrical, kinematic, and mechanical aspects of the body with special reference to the limbs. Technical report, Michigan State Univ East Lansing, 1955.
- [191] Isaac Newton. *Philosophiæ naturalis principia mathematica* (mathematical principles of natural philosophy). *London (1687)*, 1687, 1987.



## **Eigenständigkeitserklärung / Declaration of Authorship**

Hiermit versichere ich, die vorliegende Arbeit selbstständig verfasst und keine anderen als die angegebenen Quellen und Hilfsmittel benutzt sowie die Zitate deutlich kenntlich gemacht zu haben.

I hereby declare that the thesis submitted is my own unaided work. All direct or indirect sources used are acknowledged as references.

Heidelberg, den 9. Februar 2021

Kevin Stein

